A FUNCTIONAL ANALYSIS OF HETEROCHROMATIN PROTEIN 1 (HP1) IN *XENOPUS LAEVIS*

Cheng-Fu Kao
高承福

A thesis submitted for the degree of Doctor of Philosophy

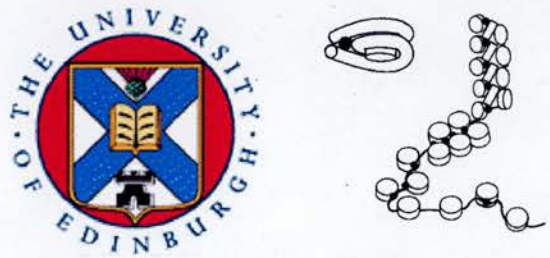

THE UNIVERSITY OF EDINBURGH
2002

DECLARATION OF ORIGINALITY

I declare that the composition of this thesis and the work presented herein is my own. Work performed by others as a part of collaboration is indicated in the text.

Cheng-Fu Kao 高承福

Table of Contents

Abstract
Acknowledgements

Chapter **Page**

Chapter 1 Introduction *1-1*
1.1 Background 1-1
1.1.1 Aneuploidy 1-1
1.1.2 An Introduction to chromatin structure 1-5
1.2 Heterochromatin 1-8
1.2.1 The heterochromatic state 1-9
1.2.2 Heterochromatin formation 1-11
1.2.3 Long-range heterochromatic interactions 1-12
1.3 Heterochromatin and centeomere 1-13
1.4 Heterochromatin and Position effect variegation 1-15
1.4.1 Position effect and heterochromatin 1-16
1.4.2 Mechanisms of position effect variegation 1-19
1.4.3 Modifier of Position Effect Variegation 1-20
1.5 Chromo domain proteins and chromatin organisation 1-24
1.5.1 Identification of the chromo domain 1-24
1.5.2 The three-dimensional structure of the chromo domains 1-24
1.5.3 Chromo domain proteins modulate chromatin organisation 1-32
1.6 HP1 protein and the chromo domains 1-34
1.6.1 Identification of HP1 1-34
1.6.2 HP1 proteins and the chromo domains 1-35
1.7 HP1 function in chromatin organisation and gene expression 1-37
1.7.1 HP1 function in gene silencing 1-37
1.7.2 HP1 and Nuclear assembly 1-38
1.7.3 HP1 mediates transcription regulation 1-40
1.7.4 Phosphorylation of HP1 and the regulation of heterochromatin assembly 1-41
1.7.5 Mechanism of HP1-mediated silencing 1-42

1.8 Objectives of the research 1-43

Chapter 2 Materials and methods ***2-1***

2.1 The methods for molecular biology 2-1

2.1.1 5'RACE (5'-end of rapid amplification of cDNA ends) 2-1

2.1.2 Sequencing 2-3

2.1.3 Bacterialogical solutions 2-3

2.1.4 Preparation of competent cells 2-4

2.1.5 Transformation of competent cells 2-5

2.1.6 Plasmid DNA minipreps 2-5

2.1.6.1 Telt miniprep 2-5

2.1.6.2 Miniprep purification kits 2-6

2.1.7 Subcloning and expression constructs making 2-6

2.1.8 Recombinant protein expression 2-7

2.1.9 Purification of recombinant protein 2-8

2.1.9.1 Purification of glutathione S-transferase fusion protein 2-8

2.1.9.2 Purification of 6×histidine fusion protein 2-9

2.2 The methods for biochemical manipulation 2-9

2.2.1 Antibody production and purification 2-9

2.2.1.1 Immunising rabbit with fusion protein 2-9

2.2.1.2 Affinity purification of antibodies 2-10

2.2.2 Chemical Cross-linking of *x*HP1 proteins 2-11

2.2.3 Preparation of chicken chromatin and chicken chromatin DNA 2-11

2.2.4 Protein translation *in-vitro* using Rabbit Reticulocyte Lysate system 2-12

2.2.5 Labelling PE190 *Xenopus* satellite clone 2-13

2.2.6 GST pull-down assay 2-13

2.2.7 Histone H3-tail pull down 2-15

2.2.8 SDS –polyacrylaminde gel eletrophoresis 2-15

2.2.9 Western blotting 2-17

2.2.10 Far-western blotting 2-18

2.3 The methods for developmental studies 2-19

2.3.1 Isolation of DNA from red blood cells 2-19

2.3.2 Southern blotting 2-19

2.3.3 Obtaining *Xenopus* embryos 2-20

2.3.4 RNA isolation from *Xenopus* embryos 2-21

2.3.5 Preparation of RNA (*In vitro* transcription) 2-22

2.3.6 RT-PCR 2-23
2.3.7 The whole mount in situ hybridisation 2-24
2.3.8 Microinjection of *Xenopus* embryos 2-27

Chapter 3 Cloning and sequencing of a candidate HP1α and HP1γ cDNA in Xenopus laevis ***3-1***
3.1 Introduction 3-1
3.2 Results 3-2
3.2.1 Isolation of HP1 sequences 3-2
3.2.2 HP1 expression in *Xenopus* embryos 3-5
3.2.3 Spatial distribution of *x*HP1expression 3-7
3.3 Discussion 3-8

Chapter 4 Self-association and heterologous interaction of Xenopus HP1 proteins ***4-1***
4.1 Introduction 4-1
4.2 Results 4-1
4.2.1 Expression and Purification of *Xenopus* HP1 as recombinant proteins 4-1
4.2.2 Chemical cross-linking of *Xenopus* HP1 proteins 4-2
4.2.3 Self Association of *Xenopus* HP1 proteins 4-3
4.2.4 The chromo shadow domain is necessary for the self-association 4-4
4.3 Discussion 4-5

Chapter 5 Xenopus HP1α can interact with DNA and Chromatin ***5-1***
5.1 Introduction 5-1
5.2 Results 5-2
5.2.1 *x*HP1α has DNA binding activity, but not *x*HP1γ 5-2
5.2.2 *x*HP1α can bind chromatin, but not *x*HP1γ 5-3
5.2.3 Domain determination of *x*HP1α DNA and chromatin binding activity 5-4
5.2.4 Both *x*HP1& *x*HP1 bind histone H3 tails when methylated at lysine 9 5-5
5.2.5 *x*HP1α can bind to a specific population of chromatin and not histone H3-dependent 5-7

5.3 Discussion 5-8

Chapter 6 The Role of linker histones and histone tails in xHP1-chromatin interaction 6-1

6.1 Introduction 6-1

6.2 Results 6-3

6.2.1 Preparation of chromatin, depleted H1/H5 of chromatin and trypsinised chromatin from chicken erythrocyte 6-3

6.2.2 Fundamental analysis of *x*HP1 -chromatin interaction 6-4

6.2.2.1 xHP1 does not precipitate chromatin, depleted H1/H5 chromatin or chromatin DNA 6-4

6.2.2.2 xHP1 does not compete with xHP1 chromatin interaction 6-4

6.2.3 Characterisation of salt–dependent behaviour of *x*HP1α-chromatin interaction 6-5

6.3 Discussion 6-8

Chapter 7 HP1α and xHP1γ are required for post-MBT transcriptional gene regulation during Xenopus development 7-1

7.1 Introduction 7-1

7.2 Results 7-2

7.2.1 Controls for mRNA injection 7-2

7.2.2 Depletion of maternally derived *x*HP1α, *x*HP1γ 7-4

7.2.3 Overexpression of *x*HP1α induces dorsal defect in development and its function is conserved from *Xenopus* to Human 7-6

7.2.4 Expression of Dominant negative *x*HP1α 7-7

7.2.5 The role of *x*HP1 for the regulation of gene-expression in *Xenopus* embryo. 7-9

7.3 Discussion 7-10

Chapter 8 General Discussion 8-1

8.1 Summary of Results 8-1

8.2 The HP1 proteins in *Xenopus laevis* 8-3

8.3 Significance of the hinge region 8-6

8.4 HP1 and chromatin folding 8-9

8.5 Developmental role for Heterochromatin 8-11

8.6 HP1 and transcription regulation 8-15

8.7 Conclusion and subjects for future investigation..... 8-17

References.....R-1~25

Tables and Figures

Table 1-1 Relative Incidence of Human Ill Health due to Gene Mutationand to Chromosome Mutation..... 1-2
Table 1-2 Number and Type of Chromosomal abnormalities among spontaneous and Live Birth in 100,000 Pregnancies..... 1-3
Table 1-3 Distinction between euchromatic and heterochromatic regions of complex genomes 1-10
Table 1-4 Suppressors and enhancers of PEV 1-22
Table 1-5 members of the HP1 family..... 1-36

Table 2-1 Genotype of bacterial strain used in this work 2-5

Figure 1-1 Nucleosome core particle:..... 1-6
Figure 1-2 A Microscopists' View of Chromosome Organization 1-8
Figure 1-3 Polytene Chromosomes in the salivary glands of Drosophila melanogaster 1-16
Figure 1-4 An example of PEV on white (w)..... 1-18
Figure 1-5 Comparison of the structure of the MOD1-N chromo domain with that of the DNA binding domain of Sac7d (Edmondson, et al. 1995)..... 1-26
Figure 1-6 Sequences of the chromo domains..... 1-28
Figure 1-7 Schematic diagram showing locations of CDs and CSDs. 1-30
Figure 1-8 Molecular surface of residues 22–69 of the CD of mouseMOD1. 1-31

Figure 2-1 Overview of the 5' RACE procedure..... 2-2

Figure 3-1. Cloning full length HP1α and HP1γ by the 5' RACE system 3-10
Figure 3-2 Comparison of the DNA sequences of Xenopus HP1α cDNA with the published HP1α cDNA sequence..... 3-11
Figure 3-3 Comparison of the DNA sequences of Xenopus HP1γ cDNA

with the published HP1γ cDNA sequence. 3-12
Figure 3-4 Comparison of the derived protein sequences of Xenopus HP1α, γ with the published sequences. 3-13
Figure 3-5 Comparison of HP1 α amino acid sequences from Xenopus lavies, Mus musculus, Homo sapiens. 3-14
Figure 3-6 Comparison of HP1 γ amino acid sequences from Xenopus lavies, Mus musculus, Homo sapiens. 3-15
Figure 3-7 Comparison of Xenopus lavies HP1 α, γ amino acid sequences. 3-16
Figure 3-8 Autoradiographs of southern blots of Xenopus laevis DNA with HP1α, HP1γ and Polycomb2 probes. 3-17
Figure 3-9 Basic stages of Xenopus lavies development. 3-18
Figure 3-10 Formaldeyde-agarose gels of total RNA isolated from different Xenopus embryo stages and liver. 3-19
Figure 3-11. Calibration of reverse transcription (RT)-PCR amplifications. 3-20
Figure 3-12 RT-PCR Analysis of HP1α Expression in Different stages Xenopus embryos. 3-21
Figure 3-13. RT-PCR Analysis of xHP1γ Expression in Different stages of Xenopus embryos. 3-22
Figure 3-14. Localisation of xHP1 α transcripts during early Xenopus development by whole mount in situ hybridisation 3-23
Figure 3-15. Localisation of xHP1γ proteins in sections of Stage 32, tail bud embryos 3-24

Figure 4-1 Purification of Xenopus HP1 proteins as recombinant proteins. 4-7
Figure 4-2 Chemical Cross-linking of His-xHP1α and His-xHP1γ 4-8
Figure 4-3 xHP1α and xHP1γ self-associate and interact with each other. 4-9
Figure 4-4 Expression and purification of the different domains of GST fusion xHP1 protein constructs. 4-10
Figure 4-5 The shadow domain is responsible for the self-association and protein-protein interactions. 4-11
Figure 4-6 The structure of the shadow chromo domain dimer from MOD1. 4-12

Figure 5-1 Xenopus HP1α interacts with DNA 5-11
Figure 5-2 Xenopus HP1α DNA binding has no preference for Xenopus satellite DNA 5-12
Figure 5-3 Xenopus HP1 α interacts with chromatin. 5-14
Figure 5-4 Xenopus HP1α and HP1γ can heteromerize and then, bind to chromatin 5-15
Figure 5-5 Identification of DNA binding Domain of Xenopus HP1α.. 5-16
Figure 5-6 Identification of chromatin binding Domain of Xenopus HP1α 5-17
Figure 5-7 Hinge region of Xenopus HP1α is necessary for Chromatin and DNA binding..... 5-18
Figure 5-8 Xenopus HP1s are associate with core histones 5-19
Figure 5-9 Xenopus HP1α has specific interactions with histone H1 and H3..... 5-20
Figure 5-10 Xenopus HP1s bind to methylated histone H3 tails..... 5-21
Figure 5-11 The CD region of Xenopus HP1α shows a week chromatin binding activity 5-22
Figure 5-12 The Xenopus HP1α binds to a specific population of chromatin 5-23
Figure 5-13 The H3 tails do not interfere with interaction of GST-xHP1a with chromatin 5-24
Figure 5-14 Schematic diagram of Xenopus HP1 DNA and Chromatin binding 5-25

Figure 6-1 Background 6-11
Figure 6-2 Preparation of chromatin, depleted of H1/H5 chromatin and trpsinised chromatin from chicken erythrocyte 6-12
Figure 6-3 HP1a does not precipitate chromatin, depleted H1/H5 chromatin or DNA 6-13
Figure 6-4 xHP1g does not compete with xHP1a chromatin binding.... 6-14
Figure 6-5 The effect of a gradient of NaCl concentration on xHP1a binding of chromatin..... 6-15
Figure 6-6 The effect of a gradient of NaCl concentration on xHP1a binding of H1 & H5 depleted chromatin 6-16
Figure 6-7 The effect of a gradient of NaCl concentration on xHP1a binding of trypsinised chromatin 6-16
Figure 6-8 The effect of gradient of NaCl concentration on xHP1a binding

of DNA only 6-17
Figure 6-9 Without histone tails, HP1a chromatin binding has preference of the fraction with longer DNA fragment..... 6-18
Figure 6-10 The increased concentration of xHP1a elevates chromatin binding on a gradient of NaCl concentration..... 6-19
Figure 6-11 The increased concentration of xHP1a elevate the binding of H1 & H5 depleted chromatin on a gradient of NaCl concentration 6-20
Figure 6-12 The increased concentration of xHP1a elevate the binding of trypsinised chromatin on a gradient of NaCl concentration 6-21

Figure 7-1 β-galactosidase mRNA is translated in embryos and has a limited distribution after targeted microinjection 7-13
Figure 7-2 Depletion of xHP1 in Xenopus embryos pertubs development. 7-14
Figure 7-3 Over-expression of xHP1a and xHP1g shows different phenotypical defects in Xenopus embryos 7-16
Figure 7-4 Over-expression of human and xHP1a gives similar phenotypes in Xenopus embryos 7-18
Figure 7-5 Expression of dominant negative mutants of HP1a in the development of Xenopus embryos 7-20
Figure 7-6 Overexpression of xHP1 intrudes on gene–expression in Xenopus embryos..... 7-22

Figure 8-1 The result of non-human/mouse EST database searching in HP1β 8-5
Figure 8-2 An invariant sequences within the block is shaded and a region that conforms to a bipartite NLS is indicated by brackets..... 8-7
Figure 8-3 One proposed temporal pathway leading to the establishment of transcriptionally silent heterochromatic regions with regard to the covalent modifications in the histone H3 tail. 8-10
Figure 8-4 Localisation of xPolycomb transcripts during Xenopus early development by whole mount in situ hybridization..... 8-14
Figure 8-5 Brachyury expression during Xenopus gastrulation. 8-14
Figure 8-6 Role of HP1 complex in propagation of heterochromatin, gene silencing and transcription regulation..... 8-16

Abstract

It is usually the centromere that is required to ensure an equal distribution of replicated chromosomes to daughter nuclei. From simple yeast to humans the process of chromosome duplication and segregation is highly conserved and occurs by attachment of sister centromeres to the spindle and separation. Studies on gene silencing mechanisms links chromatin structure to centromeric function. If a gene is located near a centromere then its expression can be repressed. One model suggests that it is the spreading of centromeric chromatin that leads to gene silencing, however the degree of repression can be variable and affected by environmental and genetic factors. Mutations that alleviate gene silencing at heterochromatin also interfere with chromosome segregation. This implies there is a critical link between chromosome structure and centromere function. In the fruit fly, *Drosophlia melanogaster*, many genes have been identified that are required to maintain silencing at centromeres (position effect modifiers). Two of the genes involved, HP1 and Pc, contain sequence motifs called chromodomain. The chromodomains of HP1 are necessary for both its nuclear and heterochromatin localisation. Much of the work on the role of heterochromatin in centromere function has been done in genetically tractable organisms such as the fruit fly, *D. Melanogaster* and the yeast *S. pombe*. It would be useful if there were an animal biochemical system available for the molecular characterisation of heterochromatin formation.

In my study, I employed the South African clawed-toe frog, *Xenopus laevis*, as a vertebrate model system to address two questions. First, is HP1 protein necessary for *Xenopus* development? Second, What are the molecular partners for HP1? I

identified two full-length cDNA clones encoding HP1 homologues from *Xenopus*, *x*HP1α and *x*HP1γ. Both of these clones contain a chromodomain (CD) and chromoshadow domain (CSD). Functional analysis demonstrates that *x*HP1α and *x*HP1γ can homo- and heteromerdise *in vitro* and this is dependant on the CSD. A chromatin pull-down assay localised a novel chromatin-binding domain to the hinge region of *x*HP1α, which is not present in *x*HP1γ. Moreover, *x*HP1α shows a binding preference for histone H1 in a far-western assay. Additional analysis using salt-dependant folded chicken chromatin indicates that *x*HP1α favours binding to a highly compacted chromatin fibre containing linker histone. Taken together, it could be that this specific interaction is related to a particular type of chromatin, perhaps heterochromatin. It is also possible that this functional difference between *x*HP1α and *x*HP1γ is responsible for their differential sub-nuclear localisation.

RT-PCR analysis revealed that both *x*HP1α and *x*HP1γ are maternally abundant and their expression increases to a high level during neuralation stages. RNA *in situ* hybridisation demonstrates that *x*HP1α shares an overlapping pattern expression with *x*Polycomb 2. Expression was observed in the head and neural tube. To study the functional significance of HP1 in the development, we manipulated the expression of *x*HP1α and *x*HP1γ. Our data point towards an early development role for *x*HP1α and *x*HP1γ. Both the depletion and overexpression experiments clearly show that *x*HP1s are essential for early development after the mid-blastula transition (MBT). Moreover, when embryos overexpressed *x*HP1 α and *x*HP1γ, or both *x*HP1 α and *x*HP1γ together, these embryos also incorporated a significantly higher level of ^{32}S-UTP after MBT. These observations are consistent with the prediction that HP1 acts as an essential player in the dynamic organisation of nuclear architecture. It is possible that HP1 acts at a hub of silencing chromatin mechanisms, which are

required to maintain the higher order structure and the homogeneous appearance of chromatin before the onset of transcription at MBT. More importantly, after MBT, HP1 is key for transcription regulation. Deleting or overexpressing the core of this HP1 associated complex could result in corruption of the higher order chromatin structure and disrupt HP1-dependant gene silencing. The loss of function experiments indicate that both the CD and the CSD may be involved in gene expression regulation during neurulation of *Xenopus* embryos and these two domains could likely play different roles during development. To facilitate the interpretation of the phenotypes, it would be important to identify the genes that are regulated by *x*HP1s.

Acknowledgements

There are three key persons to help and push me completing my Ph D. The first one is my wife, Yi-Chen Lo. She initiated the idea of doing a PhD, which had never been in my career plan. Then my supervisor, Dr Richard Meehan who was brave enough to take me as his Ph D student and help me along these years. Finally and most importantly, my PhD study was supported by my parents who are a hard-working couple in Taiwan. Without their financial support, I would be impossible to do my study in Edinburgh.

Also I would like to thank Dr Sari Pennings and Dr Irina Stancheva for generously sharing their experiences and sources in *Xenopus* and chromatin studies. And Dr Jim Allan kindly provided chromatin sample for initiating chromatin pull-down assays. Thanks also to Shanmugasundaram Venkataraman, Carmel Reilly and Dr Donncha Dunican for helpful discussions in thesis preparation and English corrections. A special thank-you goes to Dr. Colin Davey for his critical reading and advice to this thesis.

Chapter 1 Introduction

1.1 Background

1.1.1 Aneuploidy

Chromosome mutation in general plays a prominent role in determining genetic ill health in human. In fact, the incidence of chromosome mutations ranks close to that of gene mutation in human live births (Table 1-1). This is particularly surprising when we realize that virtually all the chromosome mutations listed in the table arise anew with each generation. In contrast, gene mutations owe their level of incidence to a complex interplay of mutation rates and environmental selection that acts over many human generations. When the frequencies of various chromosome mutations in live births are compared with the corresponding frequencies found in spontaneous abortions (Table 1-2), it becomes clear that the chromosome mutations that we know about as clinical abnormalities are just the tip of an iceberg of chromosome mutations.

Eukaryotic cells have to ensure the correct partition of their genetic material at every cell division (mitotic and meiotic) in order to prevent chromosomal imbalances (aneuploidy) occurring in their daughter cells. As demonstrated in the table 1-1, 2, it is clear that aneuploidy represents the most common form of chromosome abnormality in humans contributing to a high incidence of spontaneous abortion, genetic disease

Table 1-1 Relative Incidence of Human Ill Health due to Gene Mutation and to Chromosome Mutation

Type of Mutation	Percentage of live births
Gene mutation	
Autosomal dominant	0.90
Autosomal recessive	0.25
X-linked	0.05
Total gene mutation	1.20
Chromosome mutation	
Autosomal trisomies (mainly Down syndrome)	0.14
Other unbalanced autosomal aberrations	0.06
Balanced autosomal aberrations	0.19
Sex chromosomes	
XYY, XXY and other	0.17
XO, XXX, and other	0.05
Total chromosome mutation	0.61

(Derived from Sankaranarayanan, 1979)

Table 1-2 Number and Type of Chromosomal abnormalities among spontaneous and Live Birth in 100,000 Pregnancies

	100,000 Pregnancies	
	15,000 spontaneous abortions	**85,000 live births**
	7,500chromosomally abnormal	**550 chromosomally abnormal**
Trisomy		
1	0	0
2	159	0
3	53	0
4	95	0
5	0	0
6-12	561	0
13	128	17
14	275	0
15	318	0
16	1229	0
17	10	0
18	223	13
19-20	52	0
21	350	113
22	424	0
Sex chromosome		
XYY	4	46
XXY	4	44
XO	1350	8
XXX	21	44
Translocation		
Balanced	14	164
Unbalance	225	52
Polyploid		
Triploid	1275	0
Teraploid	450	0
Other (mosaics, etc.)	280	49
Total	7500	550

(Derived from Sankaranarayanan, 1979)

and cancer progression. One example is Down's syndrome in which trisomy 21 is caused by nondisjuction of chromosome 21 in a parent that is chromosomally normal (Sankaranarayanan, 1979). Another example is somatic aneuploidy, which results in mosaicism with respect to chromosome content and is often observed in association with cancer (Watson et al., 1992). People suffering from chronic myeloid leukaemia (CML), a cancer of the white blood cells, frequently harbour cells containing the so-called Philadelphia chromosome. Chromosome disjunction usually introduces error in cell metabolism, and sometimes produces aneuploid gametes.

Many substructures are required for normal chromosome behaviour (e.g. centromeres, telomeres and replication origins); however, it is usually the centromere that is required to ensure the equal distribution of replicated chromosomes to daughter nuclei. From simple yeast to humans the process of chromosome segregation is highly conserved and occurs by attachment of sister centromeres to spindle and separation to opposite poles. The regions flanking the centromere often are rich in satellite DNA sequences and contain a considerable amount of constitutive heterochromatin. Recent cytogenetic and molecular studies complement many of genetic evidence that has revealed that heterochromatin is required for centromere function. Reduced chromosome transmission results from removal of flanking heterochromatin in *Drosophila melanogaster* (Wines and Henikoff 1992) and *Schizosaccharomyes pombe* (Steiner and Clarke 1994). In both organisms, modifiers that disrupt heterochromatic silencing impair chromosome transmission (Partridge et al., 2000; Wines and Henikoff 1992; Ekwall et al., 1997). One of the typical examples is 'Heterochromatin protein 1' (HP1). HP1 is associated with centromeric heterochromatin in *Drosophila*, mice and human (Chevillard et al., 1993; Wreggett et al., 1994; Kellum et al., 1995). Loss of function mutations in the gene

encoding HP1 in *Drosophila*, Su(var)2-5, decrease the mosaic repression observed for euchromatic genes that have been juxtaposed to centromeric heterochromatin (Eissenberg and Hartnett, 1993). These HP1 mutations also were associated with defects in chromosome morphology and segregation (Kellum and Alberts, 1995). Thus, flanking heterochromatin is a requirement for maintaining regional centromeres.

1.1.2 An Introduction to chromatin structure

A nucleosome is formed by the winding of a double stranded DNA twice around a protein called histone octamer. DNA in chromatin is organized in arrays of nucleosomes (Kornberg, 1977). Two copies of each histone protein, H2A, H2B, H3 and H4, are assembled into an octamer that has 145–147 base pairs (bp) of DNA wrapped around it to form a nucleosome core (of relative molecular mass 206K). This highly conserved nucleoprotein complex occurs essentially every 200 ± 40 bp throughout all eukaryotic genomes (McGhee and Felsenfeld, 1980). The repeating nucleosome cores further assemble into higher-order structures, which are stabilized by the linker histone H1 and these compact linear DNA. The nucleosome plays the role as the principal packaging element of DNA within the nucleus and it is the primary determinant of DNA accessibility. The physical properties of nucleosomes depend on solution conditions such as ionic strength, divalent-ion concentration, and on histone-modification state (Wallrath et al., 1994). The generally repressive nature of chromatin structure has long been related to transcription regulation (Wasylyk and Chambon, 1979). Chromatin organization can facilitate the activation of specific genes (Grunstein, 1990; Paranjape et al., 1994).

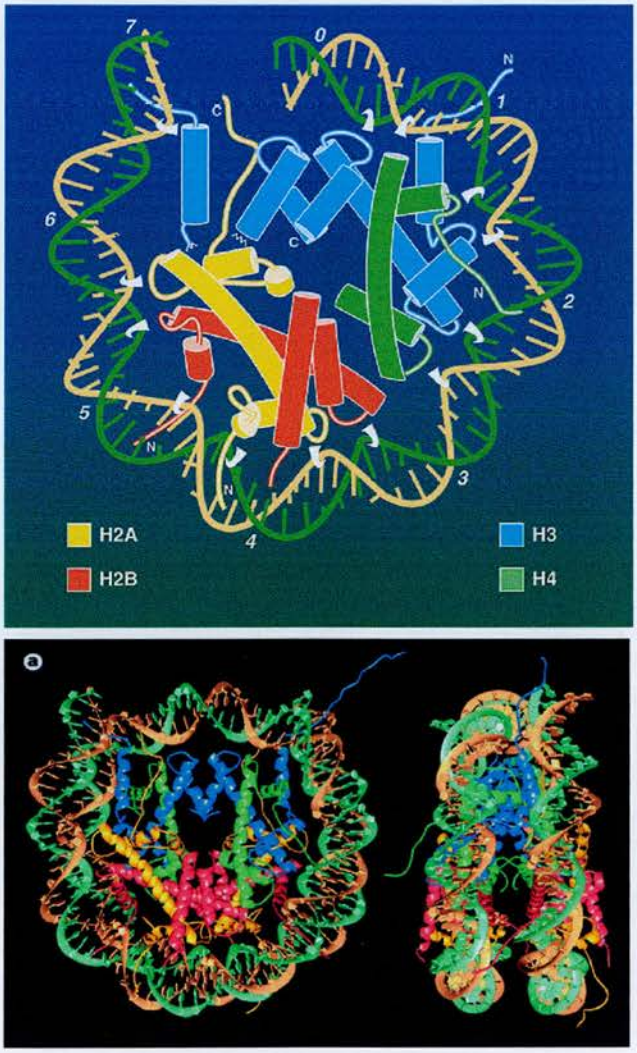

(Derived from Luger, et al. 1997)

Figure 1-1 Nucleosome core particle:

Ribbon traces for the 146-bp DNA phosphodiester backbones (brown and turquoise) and eight histone protein main chains (blue: H3; green: H4; yellow: H2A; red: H2B. The views are down the DNA superhelix axis for the left particle and perpendicular to it for the right particle. For both particles, the pseudo-twofold axis is aligned vertically with the DNA centre at the top.

Evidence supporting two themes is accumulating. First, histones collaborate with transcription factors to provide for their own removal or structural modification, resulting in gene derepression. This may occur by stepwise invasion of DNA-binding proteins entering at the terminal segments of the nucleosomal DNA (Polach and Widom, 1996). This mechanism is apparently insufficient in general, however, because several ATP-dependent chromatin-remodelling factors have been discovered that cause the core histones partially to lose or alter their grip on DNA (Felsenfeld, 1996). Second, the bending and supercoiling of DNA on a nucleosome can promote binding of transcription factors and supplement interactions between different factors (Schild et al., 1993, Truss et al., 1995).

It is now clear that histones are integral and dynamic components of the machinery responsible for regulating gene transcription. A wide-ranging literature documents a detailed collection of post-translational modifications including acetylation, phosphorylation, methylation and ubiquitination (van Holde, 1988) that take place on the `tail' domains of histones. These tails, which stick out from the surface of the chromatin polymer and are protease sensitive, comprise 25±30% of the mass of individual histones (van Holde, 1988; Wolffe and Hayes, 1999) thus providing an exposed surface for potential interactions with other proteins [for example, Sir3/4 and Tup1 proteins in yeast (Hecht et al., 1995; Edmondson et al., 1996)]. Because of the intrinsic disordered nature of histone tails, their precise location in higher-order fibres and the atomic details of their structure are not known (Luger et al., 1997; Luger and Richmond 1998) . Long-standing models have suggested that histone modifications may alter chromatin structure by influencing histone-DNA and histone-histone contacts (Wolffe and Hayes, 1999; Hansen et al., 1998).

1.2 Heterochromatin

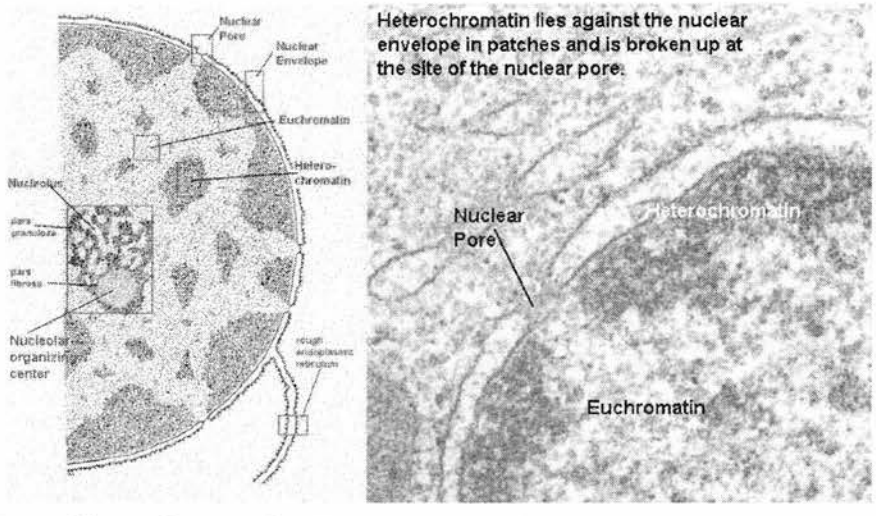

Derived from Alberts et al., 1994

Figure 1-2 A microscopist's View of Chromosome Organization

Chromatin can be divided into two types of material, which can be seen in the nuclear section of Figure 1-2. In most regions, the fibres are much less densely packed than in mitotic chromosome. This material is called **euchromatin**. It has a relatively dispersed appearance in the nuclear and occupied most of the nuclear region. Some regions of chromatin are very densely packed with fibres, displaying a condition comparable to that of the chromosome at mitosis. This material is called **heterochromatin**.

Heitz (1928) first identified heterochromatin as a differentially stained fraction of nuclear chromatin that is condensed throughout the cell cycle. Heterochromatin remains condensed in interphase, is transcriptionally repressed, replicates late in S phase, and sometimes is localized to the nuclear periphery. Heterochromatic regions are generally located at pericentric or telomeric locations. Heterochromatin is highly enriched in repetitive DNAs. The general picture is that heterochromatin is molecularly heterogeneous, with specific types of satellite and mild repetitive sequences preferentially clustered at certain chromosomal locations (Lohe *et al.*,

1993). The fact that heterochromatin is less accessible to transcription and recombination factors suggest that it consists of a condensed, inaccessible chromatin structure or high-order structure (Allshire and Karpen, 1997). An alternative form of histone H3, CENP-A is found preferably in the nucleosome of centromeric chromatin (Sullivan et al., 1994). The functional significant of this has yet to be established. Heterochromatic regions are responsible for essential biological functions, including centromere activity, telomere function, nuclear organization, the most highly expressed genes in the genome (ribosomal RNA genes), and the pairing of homologues in meiosis. The ribosomal genes are organized into tandem arrays in the heterochromatin in multicellular organisms (Wakimoto, 1998).

1.2.1 The heterochromatic state

Heterochromatin is a chromatin state. For instance, the inactive heterochromatic X chromosomes present in mammalian females are no different in sequence from their euchromatic counterparts (Migeon, 1994) . Although the DNA in the inactive X chromosome is also hypermethylated, methylation is not an obligate requirement for heterochromatin formation, which also occurs in organism that lack methylation, such as *Drosophila melanogaster* and *Schizosacchazomyces pombe*. The differences between heterochromatic and euchromatic state are indicated in Table 1-3. Heterochromatin consists of nucleosomes that have distinctly acetylated histone H3 and H4 tails (Braunstein et al., 1996); perhaps these acetylated tails interact with nucleosomes in proximity forming a higher order heterochromatic structure. Although it is less well known what such a putative structure looks like, it is thought that nucleosomes found in heterochromatin display more regular arrangement than those found in euchromatin (Wallrath and Elgin, 1995).

Table 1-3 Distinction between euchromatic and heterochromatic regions of complex genomes

Feature	Euchromatin	Heterochromatin
Interphase appearance	**Relatively uncondensed**	**Condensed**
Chromosomal location	**Distal**	**Preicentromeric**
Sequence composition	**Mostly non-repetitive**	**Repetitive**
Gene density	**High**	**Low or absent**
Replication timing	**Throughout S phase**	**Late S phase**
Meiotic recombination	**Normal**	**Low or absent**
Position-effect variegation	**Rare**	**Frequent**
Methylation state (in vertebrates)	**CpG islands hypomethylated**	**Fully methylated**
Histone acetylation	**Low to high**	**Low**
Nucleosome spacing	**Variable**	**Regular**
Nuclease accessibility	**Variable**	**Low**

Derived from Henikoff, 2000

We do not know precisely what constitutes a heterochromatic state but sensitive phenotypic assays for mosaic gene silencing, called position-effect variegation (PEV), allow us to detect its existence. Classical PEV in *Drosophila* and mouse occurs when a gene is juxtaposed to heterochromatin (Muller, 1932). PEV silencing can encompass genes that are hundreds of kilobases from the heterochromatin/euchromatin boundary. Related to classical PEV are examples in which transgenes are inserted into pericentric heterochromatic regions in flies (Wallrath and Elgin, 1995) and mammals (Festenstein et al., 1996; Milot et al., 1996). [There is a subsequent section (1.4) to discuss the phenomenon of PEV].

1.2.2 Heterochromatin formation

Blocks of repetitive DNA sequences have a common feature in that they can form heterochromatin. This phenomenon leads to the notion that sites buried within repeats could initiate the propagation of a heterochromatic state (Locke et al., 1988). However, at least some repetitive sequences have the intrinsic capacity to form heterochromatin: local duplications of a P transposon carrying a sensitive white gene reporter cause white gene PEV in flies (Dorer and Henikoff, 1994). As few as three copies of the transposon are sufficient, with increases in copy numbers leading to enhanced silencing. It was suggested that heterochromatin formation could account for the silencing of transgenes present in high copy number arrays in mammalian cells, and reduction of one such array led to activation of the reporter (Garrick et al., 1998). Thus, silencing of tandem transgene arrays has been assumed to result from insertion into an inactive site, rather than is due to local heterochromatin formation of the array itself (Dorer, 1997). Heterochromatic silencing of a near-by euchromatic gene by transgene arrays indicates that PEV does not require a specific initiation site

other than the repeat array itself. Taken together, these results suggest that repetitiveness alone is sufficient for formation of a heterochromatic state. What feature of local repetitiveness causes heterochromatin to form? In Henikoff's original *Drosophila* white gene study, reversing a transposon within an array led to strengthening of silencing (Dorer and Henikoff, 1994), and this was confirmed using a brown eye colour gene as reporter (Sabl and Henikoff, 1996). These findings suggested that inverted repeats, formed by neighbouring reversed transposons, were pairing up, and such pairing could trigger the heterochromatic state.

1.2.3 Long-range heterochromatic interactions

An assay of silencing demonstrated that distance from blocks of heterochromatin has affects on heterochromatic silencing as well. A *Drosophila* satellite-repeat block called brown Dominant (bw D) caused stronger trans-inactivation when it was closer to pericentric heterochromatin than when it was farther away (Talbert et al., 1994). Similar observations were made for the interaction of white-bearing transposon repeat arrays with blocks of heterochromatin (Dorer and Henikoff, 1997). The effect on bw D was found to correlate with its frequency of association with pericentric heterochromatin, as though the large block of heterochromatin enhances silencing. Perhaps transcription factors that are needed for expression of a reporter gene are less able to penetrate the hugely blocked heterochromatic 'compartment'.

Heterochromatic associations leading to silencing might represent a novel gene regulatory mechanism: inactive genes in human pre-B cells are found to associate with heterochromatic gamma satellite, whereas active B cell genes are not (Brown et al., 1997). In both Drosophila and human systems, associations between the reporter

gene and heterochromatin occur in a cell cycle-dependent manner (Csink and Henikoff, 1998). In *Drosophila*, associations are disrupted at S phase and only slowly reform during the G1 phase following mitosis. The cytological detection of interactions between genes and heterochromatin several megabases away can help rationalize many examples in which silencing and DNA methylation have been seen for distantly separated loci (Henikoff, 1997; Matzke and Matzke, 1998). Such findings challenge the assumption that genes are regulated solely by diffusible trans-acting factors. Rather, nuclear positioning may play a major role in gene regulation.

1.3 Heterochromatin and centromere

Heterochromatin, the major fractions of complex genomes, is found as blocks of repeats that may have no genes at all in the surrounding area. These consist primarily of tandemly repetitive satellite sequences and clusters of transposon-derived repeats, primarily around centromeres (Csink and Henikoff, 1998). Such heterochromatic regions are so large that the condensation is visible throughout the cell cycle. The consistent pericentric distribution of satellite sequences strongly suggests that the heterochromatic state plays an important role in centromere function. Thus, heterochromatin formation may have two distinct roles during the cell cycle: at interphase, heterochromatin may aid in gene regulation, and, at the onset of mitosis, heterochromatin may be needed for centromere function.

There is an implication from the occurrence of PEV and the inhibition of genetic recombination. Perhaps the very inertness of heterochromatin is key to centromere function (Csink and Henikoff, 1998). If heterochromatic compaction or

compartmentalization generally inhibits enzymatic processes during interphase, then the onset of replication origins might be similarly inhibited. As a result, replication forks that traverse heterochromatic blocks would initiate within flanking sequences. Because heterochromatic blocks are so large, replication tracks in heterochromatin would not finish until late in S phase. Centromeres are usually found within such late replicating regions of chromosomes.

It has been proposed that this putative requirement for late replication drives the evolution of pericentric regions (Csink and Henikoff, 1998). *Drosophila* chromosomes consist of blocks of satellite repeats on the order of a megabase in length separated by clusters of transposons (Lohe et al., 1993; Laurent et al., 1997). A similar organization might be found in human pericentric regions (Laurent et al., 1997), with the difference being that human centromeres are comprised of α-satellite blocks separated by clusters of L1 elements. Nevertheless, in flies several different satellites and transposons are found around centromeres. Multiple transposon insertions into satellite blocks might disrupt a centromere by allowing for replication origin initiating. The resulting premature replication would cause the chromosome to be lost forever unless a region nearby can assume centromere function by replicating sufficiently late. Over time, this process would lead to the accumulation of blocks of satellites separated by clusters of transposons that would encompass regions much larger than the centromere itself, as observed. By invoking a replication timing requirement for centromere function, the evolution model can rationalize the existence of human neocentric chromosomes that entirely lack satellite sequences but nevertheless segregate normally (du Sart et al., 1997; Tyler-Smith et al., 1999): what is necessary would not be satellite sequence per se, but rather replication behaviour that is characteristic of heterochromatin.

Several observations are consistent with this model. Satellite sequences are the major component of all animal and plant centromeres studied so far (Willard, 1998; Sun et al., 1997; Round et al., 1997; Kaszas and Birchler, 1998). Centromeres are consistently found within the latest replicating regions, with the exception of baker's yeast, which entirely lacks centromeric repeats and has centromeres that replicate very early (McCarroll and Fangman, 1988). It is likely that the heterochromatic state can inhibit replication origin initiating.

1.4 Heterochromatin and Position effect variegation

Background: Polytene Chromosomes

Polytene chromosomes are giant chromosomes common to many dipteran (two-winged) flies. They are really used for cytological studies because of their particular huge size. Since 1930's, scientists have discovered many cytological and phenotypical changes by observing polytene chromosomes. They begin as normal chromosomes, but through repeated rounds of DNA replication (~10) without any cell division (called endoreplication), they become large, banded chromosomes (see Figure 1.3). For unknown reasons, the centromeric regions of the chromosomes do not endoreplicate very well. As a result, the centromeres of all the chromosomes bundle together in a mass called the chromocenter.

Polytene chromosomes are usually found in some tissues of the larvae, like the salivary gland. Each cell now has many copies of each gene. Therefore it can transcribe at a much higher rate than with only two copies in diploid cells. The polytene chromosomes in Figure 1.3 are from the salivary glands of the fruit fly *Drosophila melanogaster*.

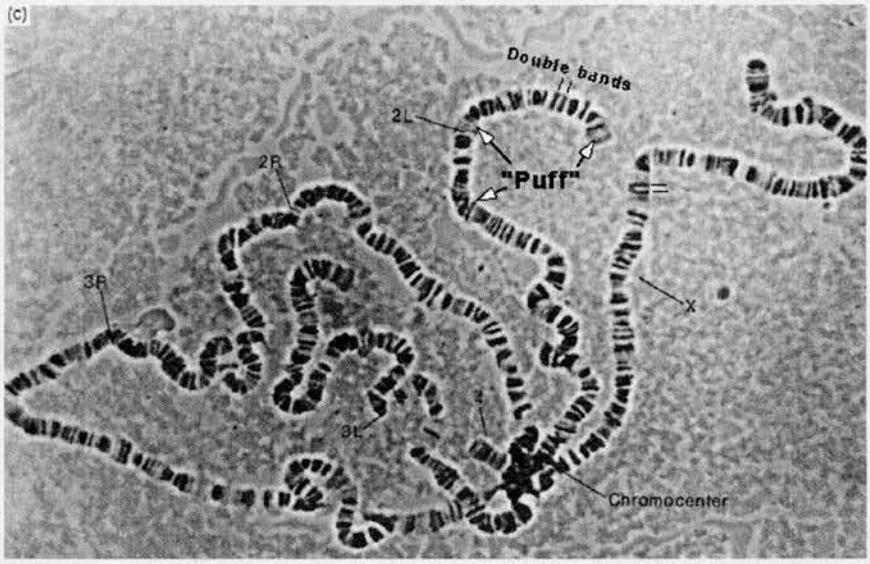

Derived from http://www.msg.ucsf.edu/sedat/harmon/

Figure 1-3 Polytene Chromosomes in the salivary glands of Drosophila melanogaster

1.4.1 Position effect and heterochromatin

Position effects (PEs) leading to a change in the expected level of gene expression, have been associated with integration or translocation of a gene with other regions of the genome. One particular type of PE, first observed in *Drosophila* (Muller, 1930), occurs through relocalisation of a gene into a heterochromatic environment. This relocalisation leads to a shutdown of expression of the gene in some of the cells. The cell-to-cell variegated expression could be created by a differential spreading of heterochromatin. This phenomenon, which is clonal and heritable in daughter cells, is known as position-effect variegation (PEV; Karpen, 1994) and has yet to be explained fully at the molecular level.

PEV was first characterized by Muller (1930) as the variable, but heritable, inhibition of euchromatic gene activity when artificially juxtaposed with heterochromatin by chromosome rearrangement. This is a position effect on gene

expression rather than a permanent alteration in an affected gene, since in several cases it has been possible to select for full expression by moving a position-affected gene away from heterochromatin (Henikoff, 1990). PEV can reveal the presence of heterochromatin even when heterochromatic blocks are below the limits of cytological detection. For example, telomeric heterochromatin is revealed by telomere position effects in both flies (Hazelrigg et al., 1984) and yeast (Gottschling et al., 1990), although these phenomena involve different protein components from those found for classical PEV in flies (Wallrath and Elgin, 1995; Talbert et al., 1994). In some cases, the relationship to classical PEV has been confirmed by demonstrating trans-acting suppression with reduction in the dosage of HP1 (Wallrath and Elgin, 1995; Dorer and Henikoff, 1997).

Mosaic expression is the most striking feature of PEV. For example, PEV of an eye pigment gene generally leads to a noticeable mixture of very small spots and large clones. The presence of clones indicates that a decision made early in development has been inherited during subsequent cell division (Kellum and Schedl 1991). Thus, PEV provides an attractive model system for investigating the determined state of a gene. This state appears to be an unstable one since exactly which cells and clones are mutant and which are wild types differs from eye to eye.

An intriguing aspect of PEV is the distance between the rearrangement breakpoint and the affected gene, in some cases over 50 polytene chromosome bands, or about a megabase. The term ‘heterochromatinisation’ has been used to describe this spreading into euchromatin (Henikoff, 1990), as polytene chromosome bands adjacent to rearrangement breakpoints seem to disappear into the chromocenter. It is recognized that position effects include a broad array of phenomena, such as

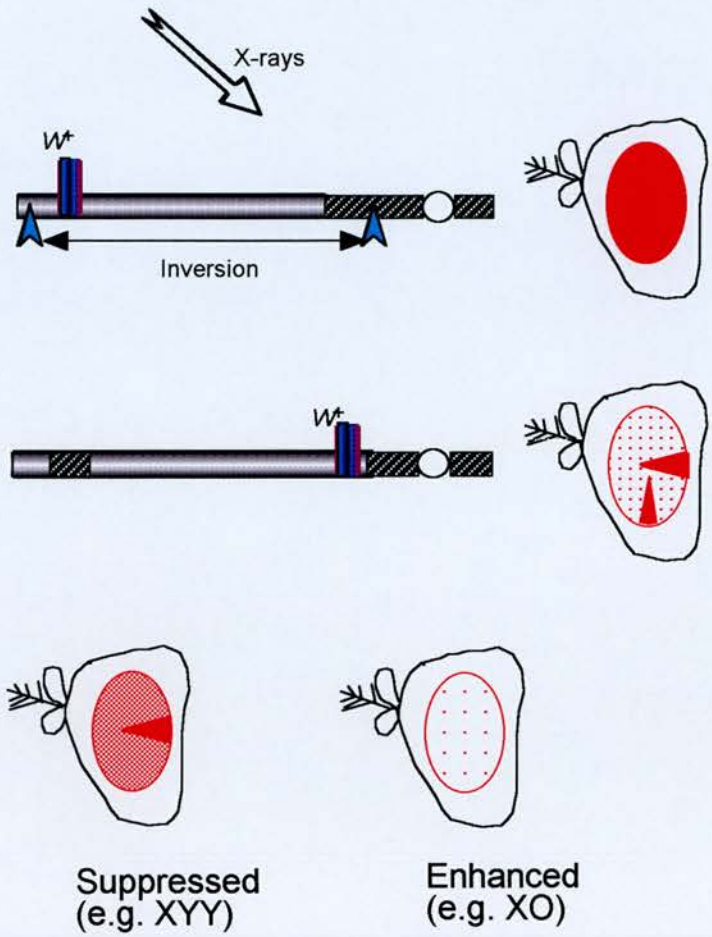

(Derived from Henikoff, 1990)

Figure 1-4 An example of PEV on white (w).

An X linked gene necessary for pigments in the eye. Ionizing radiation causes chromosomal breaks, leading to inversion and translocations. A white-mottled (w^m) allele can result when the gene is juxtaposed to heterochromatin (▨). Variegated expression is seen as numerous spots or clones of wild-type cells on a mutant background. An extra Y chromosome (for example in an XYY male) causes strong suppression of the phenotype, while lack of a Y chromosome in a male causes enhancement.

heterochromatin induced inhibition of transcription and reduction in DNA copy number, telomere-induced position effects, interaction between genes on separate chromosomes (trans-sensing effects), and inhibition of heterochromatic genes and chromosome and transmission function (Karpen, 1994).

1.4.2 Mechanisms of position effect variegation

PEV provides a model system to investigate the nature of an imprint that specifies the transcriptional state of a gene and the processes that influence its stability. Since heterochromatin can induce the inactivation of many euchromatic genes in *Drosophila,* studies of PEV more generally address the functional differences between heterochromatin and euchromatin. Two general models, cis-spreading and trans-interactions are proposed to explain the fundamental basis of PEV in *Drosophila.*

The cis-spreading model suggests that heterochromatin imposes an altered chromatin structure onto the euchromatic gene, preventing access of the transcriptional machinery and resulting in transcriptional repression. Variegation is accounted for by variation among cells. The hypothesis of the cis-spreading model arose from cytological observations on *Drosophila* polytene chromosomes (Spradling and Karpen, 1990). Euchromatin juxtaposed with heterochromatin via chromosome rearrangement can display diffuse banding and high compaction normally characteristic of the heterochromatic chromocenter. This visible 'heterochromatinisation' correlates with inhibition of gene function; those regions closest to the junction are most likely to appear compacted and to contain inactive genes. Grigliatti (1991) has devised elegant models that multimeric complexes of proteins normally present in heterochromatin are responsible for packing large

chromosomal domains in a repressed state. In these models, self-assembly of the complexes is responsible for euchromatic 'spreading' of repressed gene activity, clonal inheritance of inactivation, and sensitivity of PEV to the dosage of heterochromatin.

This cis-spreading model does not adequately explain some of the most impressive feature of PEV in *Drosophila.* For example, some rearrangement with heterochromatin-euchromatin breakpoints induce the variegation of genes located several megabases away from the breakpoint (Weiler and Wakimoto, 1995). Long-distance effects of such magnitude are difficult to explain by strict linear propagation of a chromatin state along the chromatin fibre. These features suggest that trans-interactions between different heterochromatic regions and the overall three-dimensional organization of chromosomes in the interphase nucleus are important for PEV. This type of position effect could act on genes located megabases away from the breakpoint.

Taken together, the current evidence supports the view that two epigenetic mechanisms contribute to the cell-to-cell phenotype variation: the cis-spreading effect of adjacent heterochromatin and the trans-effect due to chromosomal interactions mediated by heterochromatin. These two mechanisms are expected to influence each other. The type of heterochromatin at the breakpoint and the complexity of the rearrangement will determine their relative contributions to the final phenotypes.

1.4.3 Modifier of Position Effect Variegation

PEV can be altered by the products of a number of genes known as enhancers or suppressors of PEV, which are proteins that are thought to change chromatin

packing. A systematic genetic approach to identify trans-acting proteins that affect the severity of PEV has been conducted in the laboratory of Grigliatti (1991). Large-scale screens for mutations that act as dominant suppressors (Su(var)s) or enhancers (E(var)s) of the w^{m4} phenotype have been carried out, with the aim of recovering genes that encode proteins involved in the assembly or maintenance of chromatin. Hundreds of modifiers, representing at least 50 loci, have been identified (Grigliatti, 1991; Reuter and Spierer, 1992).

Interestingly, many of these mutations have no effect on gene silencing at telomeres (Wallrath and Elgin, 1995). Cloned modifiers and other mutations that modify PEV are shown in Table 1-4. Some modifier genes encode chromatin structural proteins; others encode proteins that could play indirect roles in regulating the formation of chromatin. Histone modification is one way of regulating chromatin formation. Active regions of the genome are associated with increased levels of acetylated core histones (Grunstein, 1997); therefore, a mutation causing increased histone acetylation is predicted to suppress PEV.

However De Rubertis and colleagues made the contradictory discovery that mutations within the histone deacetylase RPD3 enhance PEV in flies and yeast (De Rubertis *et al.,* 1996). The key to explain the phenomenon is the overall patterns of histone acetylation and the targets of the RPD3 deacetylase. Heterochromatin is generally hypoacetylated but, in *Saccharomyces cerevisiae and Drosophila*, H4 is exclusively acetylated at Lys12 (Grunstein, 1997). Acetylation at Lys5 and Lys12 of H4 is normally associated with newly synthesized DNA, followed by a rapid deacetylation. Yeast *rpd3* mutants show an increase in H4 acetylation at Lys5 and Lys12.

Table 1-4 Suppressors and enhancers of PEV

Suppressors and enhancers of PEV

Mutant	Effect on PEV	Protein; features	Reference
Su(var)2-5	Dominant Su(var)	HP1: chromo domain, chromo shadow domain, associate with heterochromatin	Eissenberg et al. 1990 James et al. 1989
Su(var)3-7	Dominant Su(var)	SU(VAR)3-7; seven widely spaced zinc fingers; associates with heterochromatin and HP1	Cleard, et al. 1997
Su(var)3-9	Dominant Su(var)	Chromo domain, SET domain, associate with HP1, H3 methytransferase	Tschiersch et al. 1994
Su(var)3-6	Dominant Su(var)	Protein phosphatase one; catalytic subunit	Baska e al., 1993
K43	Dominant Su(var)	ORC2; associate with HP1	Pak et al. 1997
Modulo	Dominant Su(var)	Basic amino and carboxyl domains; binds DNA and RNA	Garzino et al., 1992
Suppressor of zeste 5	Dominant Su(var)	S-adenosyl methionine synthetase; regulates spermine levels	Larsson et al., 1996
Lighten up	Dominant Su(var)	Dosage regulator of white, copia and blood	Csink et al., 1994
Weakerner of white	Dominant Su(var)	Dosage sensitive modifier of white, brown, scarlet and copia	Birchler et al., 1994
Modifier of white	Dominant Su(var)	Regulator of white	Bhadra and Birchler, 1996
Mutagen sensitive 209	Recessive Su(var)	PCNA; polymerase d processivity factor	Henderson et al., 1994
E(var)3-93D	Dominant E(var)	mod(mdg4); POZ domain; interacts with su(Hw); associates with euchromatin	Gerasimova et al., 1995
E(var)3-95E	Dominant E(var)	E2F transcriptional activator; cell cycle regulator	Seum et al., 1996
E(var)62/trithorax-like	Dominant E(var)	GAGA factor; POZ domain; associates with euchromatin	Granok et al., 1995
E(var)3-64BC	Dominant E(var)	RPD3; histone deacetylase	De Rubertis et al. 1996
E(var)3-64E	Dominant E(var)	Ubiquitin-specific protease	Henchoz et al., 1996
hel	Dominant E(var)	HEL; ATP-dependent RNA helicase; unusual DEAD box	Eberl et al., 1997
zeste	Recessive E(var)	DNA-binding protein; involved in transvection	Judd, 1995

Derived from Wallrath, 1998

Thus, the overall chromatin structure when *rpd3* is mutated may be of a more closed configuration, leading to enhancement of PEV expression.

Mutations within other protein-modifying enzymes and DNA-replication factors lead to either suppression or enhancement of PEV (Table 1-4). In *S. cerevisiae*, the multisubunit origin of replication complex (ORC) is required for both DNA replication and silencing at the mating type loci. Mutations in ORC subunits show that the processes are independent of each other (Fox et al., 1997; Dillin and Rine, 1997). ORC is hypothesized to recruit silencing factors, in particular SIR1, to the mating type loci. In *Drosophila*, a subunit of ORC, ORC 2, localizes to heterochromatin and defects in ORC 2 suppress PEV (Pak et al., 1997). The involvement of ORC in both yeast and *Drosophila* silencing suggests a conservation of silencing mechanisms. Supporting this, *Drosophila* ORC can complement the silencing, but not the replication defect, of a yeast *orc2* mutant (Ehrenhofer-Murray et al., 1995)

Defects in chromatin structural proteins also contribute to PEV. Heterochromatin protein 1 (HP1) and SU(VAR)3–7 are the structural building blocks of heterochromatin in *Drosophila*; a depletion of either protein leads to a suppression of PEV. Conversely, a decrease in the amount of a protein required to form or limit euchromatin should lead to an enhancement of PEV. An in-depth characterization of these chromatin structural proteins and their complexes will be an effective approach for understanding the formation of heterochromatin (Wallrath, 1998).

1.5 Chromo domain proteins and chromatin organisation

1.5.1 Identification of the chromo domain

The chromo domain (**chr**omatin **o**rganisation **mo**difier) was originally defined as a 37 amino acid residue region of homology shared by two *Drosophila* polypeptides, HP1 and Polycomb (Pc) (Paro and Hogness, 1991). This motif is 77% identical between the two proteins. The chromo domain motif has been gradually extended to around 50 amino acids as more HP1 and Pc-*like* chromo domain protein has been identified in different species. The HP1 chromo domain proteins are small molecules, generally less than 200 amino acids long with a molecular weight of approximately 25 kDa. All share a N-terminus of the chromo domain, which is separated by a 'hinge' region from another extensive C-terminal homology, called the chromo shadow domain (Aasland and Stewart, 1995). The PC-*like* proteins are larger than HP1, being over 300 amino acids in length. They possess neither the stretch of negatively charged amino acids adjacent to the chromo domain nor the chromo shadow domain, but they share a C-terminal homology called Pc-box, which is important for their function. In addition to the HP1 and Pc families, chromo domains have been found in a variety of other proteins and these are discussed later in this section.

1.5.2 The three-dimensional structure of the chromo domains

CDs are independent, globular domains (Kellum and Alberts, 1995) and all HP1-like proteins, including Swi6, carry a carboxy-terminal chromo shadow domain (CSD) (Kellum and Alberts, 1995; Ekwall et al., 1995). CSDs have only been found in proteins that also bear a CD, whereas CDs can exist in many forms. The roles of

these two motifs appear to be distinct. The three-dimensional structures of the CD from the mouse MOD1 (HP1•) and the CSD from the mouse MOD1 (HP1•) and the yeast SWI6 have elucidated by nuclear magnetic resonance (NMR) or X-ray crystallography. The NMR structure of the mouse MOD1 (HP1•) CD suggested that it might act to mediate interactions with other proteins through an unusual hydrophobic groove at the amino terminus (Ball et al., 1997). Comparison of different chromo domain sequences reveals that the most highly conserved residues are contained within the hydrophobic core. Solving the CD structure has led to a better understanding of mutations that are known to disrupt function in *Drosophila* HP1 (Platero et al., 1995) and Polycomb (Messmer et al., 1992). For example (Figure 1-5), the valine at the position 23 is part of the hydrophobic core but it is also exposed in the groove. Targeted mutation of V23M, which is equivalent to the *Drosophila* Su(var)2-5 allele (Akam, 1987; Platero et al., 1995), disrupts the structure of the CD. Likewise, the I26F mutation and the 64/65 deletion that are found in *Drosophila* Pc mutants (Messmer et al., 1992) appears to disrupt CD structure since both mutations affect the hydrophobic core. Many of the conserved residues found in the MOD1 (HP1β) CD are also conserved in the CSD and the CD of Pc.

A search of the available databases has shown that a structure similar to the MOD1 (HP1β) chromo domain had previously been found in the two-archaebacterial histones-like proteins, Sac7d and Sso7d (Edmondson et al., 1995). The CD-like region of Sac7 is known to bind non-specifically to the major groove of DNA, a property that is reflected in the net positive charge on the exterior of its β-sheets. By contrast, the overall surface charge of the MOD1 (HP1β) is negative, suggesting that the MOD1 (HP1β) chromo domain is more likely to be a protein interaction motif.

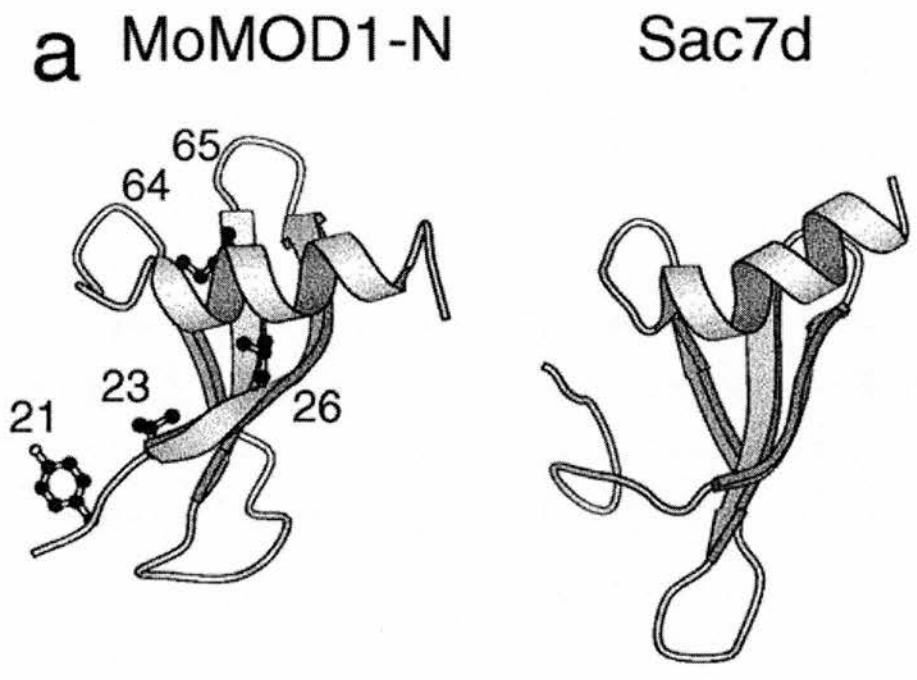

Figure 1-5 Comparison of the structure of the MOD1-N chromo domain with that of the DNA binding domain of Sac7d (Edmondson, et al. 1995).

(a) MOLSCRIPT (Kraulis, 1991) plots showing a comparison of the chromo domain from MOD1(left) with that of the DNA binding domain from Sac7d (right); the side chains of residues where mutation affects gene silencing and/or chromatin binding (Messmer et al., 1992; Platero et al., 1995) are shown.

Although analyses in *Drosophila* suggest that the Polycomb CD mediates interactions with other Polycomb-group (PcG) proteins (Horsley et al., 1996), no direct interactions with a CD have been reported. In contrast, a variety of factors are known to interact with HP1 proteins through their CSD (Le Douarin et al., 1996). Comparisons of the CSD-interacting domain of these proteins identified a common PxVxL motif. Mutation of this motif in TIF1β and CAF1 p150 prevents association with CSDs (Friedman et al., 1996; Margolin et al., 1994; Ryan et al., 1999). Moreover, CSDs themselves self-interact and interact with other CSDs (Friedman et al., 1996; Seeler et al., 1998).

To gain further insight into how CSDs might mediate protein–protein interactions, two groups have elucidated the structure of the Swi6 CSD after crystallisation and the mouse MOD1 (HP1•) CSD using NMR. (Cowieson et al., 2000; Brasher et al., 2000). The structure reveals that the CSD dimerises, with the dimer formed by contacts between helices from different molecules related by a non-crystallographic two fold axis. The most striking difference between the CD and the CSD structures is the helix H1. The CSD family has an insertion of 2-3 residues in this region, corresponding to an • helix H1 that is not seen in the mouse MOD1 (HP1•) CD structure. In addition, a proline [at position 157 of MOD1 (HP1β) or 311 of SWI6; Figure 1-6] that lies in the turn between helices H1 and H2 is absolutely conserved in the CSD family, but could be only sometimes found in the CD family. Interestingly, this proline and other conserved residues that are unique to the CSD family are all found at the dimer interface.

Comparison of the sequences and structures between the CD and CSD revealed that the CD displays more conservation in the three β strands than the CSD. When these regions of conservation were mapped onto the surface of the mouse MOD1

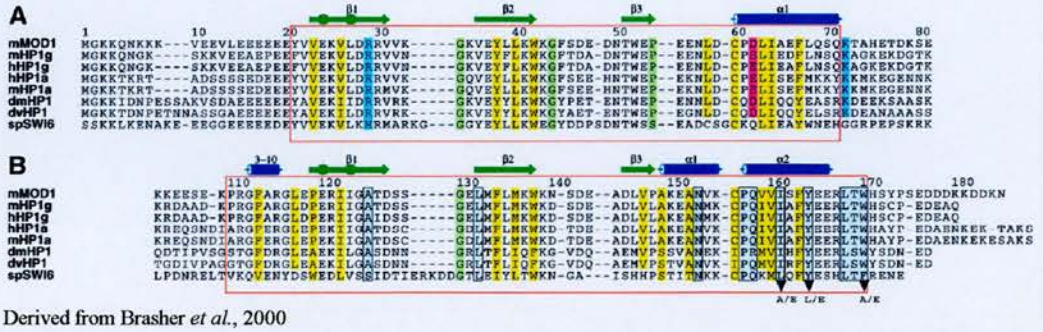

Derived from Brasher *et al.*, 2000

Figure 1-6 Sequences of the chromo domains.

(A) and the shadow chromo domain (B) form different HP1 proteins, numbered so that they are correspondent to MOD1. Secondary structure elements observed in MOD1 are shown above the alignments; cylinders represent 3_{10} (3-10) or α-helices (α1 and α2), arrows represents β-strands and circles indicate β-bulges. For each domain the residues that make up the hydrophobic core of a subunit are shaded in yellow and other residues considered important for the structure are shown in green (Gly and Pro). Charged residues in the chromo domain, which are replaced by hydrophobic residues in the shadow domain, are coloured blue (basic) and red (acidic). The red boxes enclose the structured parts of the proteins. The proteins are, from the top, mouse MOD1/human HP1β (residues 1-81 and 103- 185), mouse and human HP1γ (1-80 and 97-173), human and mouse HP1α (1-80 and 106-191). Drosophila melanogaster HP1 (1-84 and 132-206), Drosophila virilis HP1 (1-84 and 139-213) and Schizosaccharomyces pombe SWI6 (59-145 and 252-328)

(HP1β) CD, it was clear that they lined up across the face of the sheet to form a non-polar stripe with contributions from all three strands, which wind around the structure.

The CSD structure has shown that the CD and CSD have distinct structures and binding motifs based on a common structural core (Figure 1-7). Homologies between the two structures reside in their hydrophobic core, generated by three β strands and helix H2. Notably, the structural analysis suggests that the CSD provides at least two modes of protein interaction: first, the formation of stable dimers and, second, dimerisation generates an interaction pit that may allow docking of molecules with a hydrophobic pentapeptide sequence (Figure 1-8). It is possible that interactions with pentapeptide proteins provide functions such as targeting CSD-containing proteins to particular sites of chromatin. The possibility of heterodimerisation of CSD proteins may further contribute to the diversity of proteins that interact with the interaction pit.

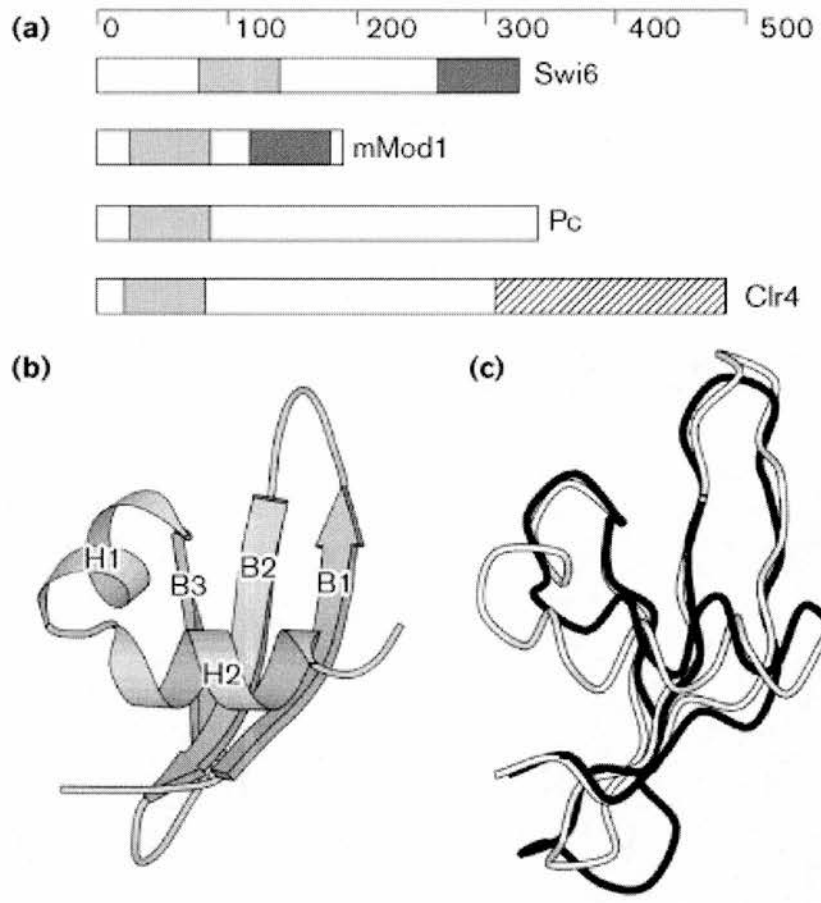

Derived from Cowieson *et al.*, 2000

Figure 1-7 Schematic diagram showing locations of CDs and CSDs.

(a) in proteins involved in gene silencing and maintenance of heterochromatin. Light gray, CDs; dark gray, CSDs; hatched box, SET domain. Amino-acid numbers are indicated by a scale bar. Swi6 is S. pombe Swi6; mMod1 is Mus musculus MoMOD1 (identical to HP1β and M31); Pc is Polycomb from D. melanogaster; Clr4 is S. pombe Su(var) 3-9 homologue. (b) Monomer fold for Swi6 CSD residues 266–324. The secondary structure elements are numbered in order from amino to carboxyl terminus; B1, B2 and B3 are β strands, and H1 and H2 are α helices. (c) Superposition of the structures of Swi6 CSD (white) and MoMOD1 CD (black).

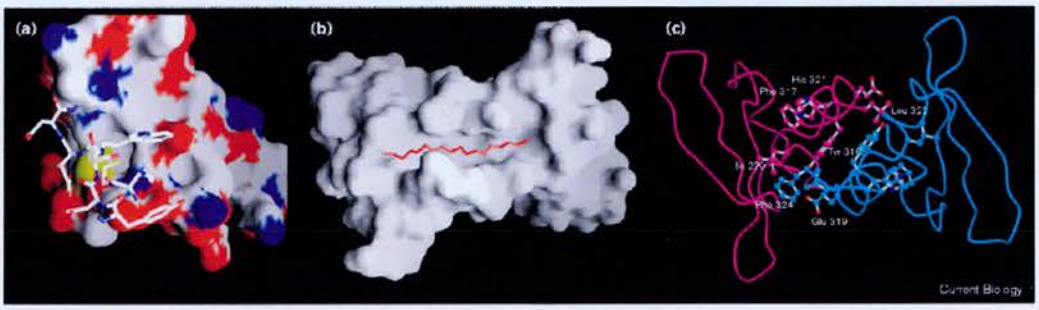

Derived from Cowieson *et al.*, 2001

Figure 1-8 The Ribbon models of CD from mMOD1and CSD from SWI6

Molecular surface of residues 22–69 of the CD of mouseMOD1. *(a) White, carbon; red, oxygen; blue, nitrogen; yellow, sulphur. The residues of Swi6 CSD have been superimposed by a least-squares algorithm. The view is centred on a deep hydrophobic groove noted by Ball, et al. (1997) in the CD structure, and proposed to be conserved in CSDs (Smothers and Henikoff, 2000). In the CSD of Swi6, amino-terminal residues can be seen to cover this groove. (b) A surface representation is shown of a dimer in the same orientation as in (c), looking down the dimer axis from the carboxyl terminus of the helices. A non-polar pit is delineated by a pentapeptide carbon backbone (red). The figure was generated by GRASP. (c) A backbone trace of the dimer in a similar orientation as that in (b). The side chains of residues that line the non-polar pit are shown. The trace was generated using MOLSCRIPT, followed by RASTER3D.*

1.5.3 Chromo domain proteins modulate chromatin organisation

The Polycomb family

The Polycomb-group (PcG) of protein are found to be non-randomly associated with over 100 chromosomal domains within polytene chromosomes (Zink and Paro, 1989; DeCamillis et al., 1992; Rastelli et al., 1993). Of particular interest are the homeotic genes that are regulated by PcG proteins. How PcG proteins are directed to particular regions such as the homeotic loci of the chromosome remains substantially unknown. Mutations in the gene encoding the PcG proteins generally lead to the activation of target genes. Changes in the expression of homeotic genes that control the segmental identity of the insect body following mutation of the PcG proteins have been studied in detail (Moehrle and Paro, 1994).

The Su(var)3-9 family

Su(var)3-9 is dominant over most PEV modifier mutations (Tschiersch et al., 1994) and mutants in the corresponding S. pombe clr4 gene (Ivanova et al., 1998), disrupt heterochromatin association of other modifying factors and result in chromosome segregation defects (Ekwall et al., 1996). Su(var)3-9 homologues are isolated from humans (SUV39H1) and mice (Suv39h1), and showed that they encode heterochromatic proteins that associate with mammalian HP1 (Aagaard et al., 1999). The SU(VAR)3-9 protein family combines two of the most evolutionarily conserved domains of the chromo (Aasland and Stewart, 1995; Koonin et al., 1995) and SET (Jenuwein et al., 1998) domains. The N-terminal chromo domain motif is smaller than the homology found when comparing HP1 and Pc. Mammalian SUV39 chromo domain encompass about 40 amino acid and share 20 % identity with the *Drosophila* proteins. The C-terminal 130 amino acid domain shares 36 % identity with the fly

protein. Whereas the 60-amino-acid chromo domain represents an ancient histone-like fold (Ball et al., 1997) that directs euchromatic or heterochromatic localizations (Platero *et al.,* 1995), the molecular role of the 130-amino-acid SET domain has remained unknown. The evolutionarily conserved SET domain was initially characterized as a common motif in the PEV modifier SU(VAR)3-9, the Polycomb-group protein E(Z) (Jones and Gelbart, 1993) and the trithorax-group protein TRX (Stassen et al., 1995). Recently it was reported that mammalian SUV39H1 or Suv39h proteins are SET-domain-dependent, H3-specific histone methyltransferases (HMTases) which selectively methylate lysine 9 (Lys 9) of the histone H3 N terminus-modification that appears intrinsically linked to the organization of higher-order chromatin.

The CHD family

The most divergent group of chromodomain proteins are those of the CHD family (Woodage et al., 1997). Members of the CHD family are around 200 kDa and are highly modular with several sequence motifs that show a consistent position along the length of the proteins. Examination of their organisation reveals that they fall into two sub-families. The first includes CHD1 and CHD2, which process two truncated N-terminal chromo domains that share up to 96 % identity with each other. A central SNF-2-helicase/ATPase domain is followed by a DNA-binding domain. The DNA-binding domain of the mouse CHD has shown to have a preference for A + T-rich DNA. It is this unique combination of **c**hromo domain, **h**elicase/ATPase and **D**NA-binding domain that gives this family of proteins their name. The second sub-family contains CHD3 and CHD4. These proteins have the same basic organisation although each of the **c h D** motifs is more divergent from those on

CHD1. Both CHD 3 and CHD4 also contain paired N-terminal PHD Zn-fingers that are not found in the other CHD sub-family members. A pilot study of CHD in *Drosophila* proposed that CHD protein might be involved in transcriptional activation through the remodelling of chromatin structure (Stokes et al., 1996). However, pivotal experiments in *S. cerevisiae* and *Xenopus laevis* discovered a new vision on this family of proteins. A null *ScCHD1* mutant was shown to relieve transcriptional repression (Woodage et al., 1997). The xCHD3 and 4 were shown to be a part of large 1-1.5 mDa complexes that included several notable components of the histone deacetylase RPD3 and RbAp48/p46 proteins (Wade et al., 1998). These finding suggested that remodelling of chromatin via the helicase/ATPase domains of CHD3/4 might be intimately involved in deacetylation of histones. Moreover, it has also been shown that KAP-1 interacts with CHD3 in two hybrid screens (Schultz et al., 1998), suggesting that the process of histone deacetylation and assembly of heterochromatin-like complex may be integrated during KRAB-mediated repression, with the key player, the transcriptional co-repressors KAP-1.

1.6 HP1 protein and the chromo domains

1.6.1 Identification of HP1

As mentioned before, the collection of genes identified as modifiers of PEV overlaps with genes that regulate homeotic gene expression (Fauvarque and Dura, 1993; Gindhart and Kaufman, 1995; Reuter and Spierer, 1992). This overlap strengthen the hypothesis that related molecular mechanism may underlie PEV homeotic gene regulation, an idea first suggested by the discovery that the HP1 and Pc share a 52 amino acid 'chromo domain' (Paro and Hogness, 1991). The chromo

domain is highly conserved through evolution and can be found in *S. pombe* swi6 gene. The SWI 6 protein is involved in the assembly of the chromosome domain containing the transcriptionally silent mating type cassettes. The chromo domain does seem to have a role in the subnuclear compartmentalization such as HP1 and polycomb (Pc) (Woffle, 1995).

The molecular analysis of the gene encoding the heterochromatin-binding protein HP1 (James and Elgin, 1986) and the discovery that it corresponds to the Su(var)2-5 (Eissenberg et al., 1990) was particularly important since the protein is localized predominantly to the chromocenter of salivary gland nuclei (James, *et al.*, 1989). The conservation of HP1 in evolutionarily distant species [mealybugs (Epstein et al., 1992), Drosophila virilis (Clark and Elgin, 1992), mice (Hamvas et al., 1992), Human (Saunders et al., 1993); Table 1-5) and the lethality of HP1 null alleles (Eissenberg and Hartnett, 1993), has suggested that HP1-like proteins are important for cell viability and development.

1.6.2 HP1 proteins and the chromo domains

The HP1 proteins share a characteristic stretch of negatively charged amino acids immediately adjacent to the N-terminus of the chromo domain. The chromo domain (CD) is separated by a 'hinge' region from another extensive C-terminal homology, called the chromo shadow domain (CSD) (Aasland and Stewart, 1995). This motif is a repeat of the chromo domain and suggests that the HP1 genes arose from a duplication of a smaller sequence encoding a polypeptide. Chromo domain mutations in HP1 and Pc abolish the genetic activity of these proteins. Solving the CD structure has led to a better understanding of those mutants (See 1.5.1).

Table 1-5 Members of the HP1 family

Members of the HP1 family					
Name	Organism	Size	Reported cytology	Silencing activity	References
Swi6p	*S. pombe*	328	Centromeres, telomeres, silent mating type cassettes	+	Lorentz et al., 1994
Hhp1p	*T. trmophilae*	184	Absent in micronuclei; enriched in condensed chromatin of macronuclei	—	Huang et al. 1999
pchet1	*P. citri*	173	Male specific nuclear protein; not heterochromatin specific	ND	Epstein et al. 1992
pchet2	*P. citri*	194	ND	ND	Epstein et al. 1992
HP1	*D. melanogaster*	206	Pericentric heterochromatin, telemeres, several non-pericentric sites	+	James and Elgin, 1986
DvHP1	*D. virilis*	213	ND	ND	Clark and Elgin, 1992
emb|CAB07241	*C. elegans*	175	ND	ND	Gene bank data base
gi|3702834	*C. elegans*	184	ND	ND	Gene bank data base
*x*HP1α	*X. laevis*	199	ND	ND	This work
*x*HP1	*X. laevis*	174	ND	ND	This work
CHCB1	*G. gallus*	185	ND	ND	Yamaguchi et al., 1998
CHCB2	*G. gallus*	174	ND	ND	Yamaguchi et al., 1998
mHP1α	*M. musculus*	191	ND	+	Le Douarin et al. 1996
M31; MOD1, HP1β	*M. musculus*	185	Pericentric heterochromatin	—	Singh et al. 1991
M32; MOD2, HP1γ	*M. musculus*	173	Euchromatin; excluded from heterochromatin	—	Saunders et al., 1993
hHP1α	*H. sapiens*	191	Pericentric heterochromatin	+	Singh et al. 1991
hHP1β	*H. sapiens*	185	Pericentric heterochromatin	—	Singh et al. 1991
hHP1γ	*H. sapiens*	173	Euchromatin; excluded from heterochromatin	+	Ye and Worman, 1996

Derived from Eissenberg and Elgin, 2000

Additionally, a CD swap experiment has shown indication to the function of the CD (Platero et al., 1995; Messmer et al., 1992). β-galactosidase fusion proteins with the CD of Pc, or either the CD or CSD of HP1, target β-galactosidase to euchromatic Pc binding sites or heterochromatic HP1 binding sites, respectively (Platero and Hartnett, 1995; Messmer et al., 1992; Powers and Eissenberg, 1993). As expected, a chimeric HP1–Pc fusion protein (in which the CD of HP1 is replaced with the CD of Pc) targets β-galactosidase to both HP1 and Pc binding sites. Interestingly, the chimeric protein also mislocalizes endogenous HP1 to euchromatic Pc sites and endogenous Pc to heterochromatin (Platero et al., 1995,1996). This latter behaviour implicates the chimera recruits the endogenous Pc via a CD of Pc and recruits the endogenous HP1 via CSD of HP1. Thus, it suggests that the CD of PC and CSD of HP1 in mediating protein–protein interactions in the nucleus.

1.7 HP1 function in chromatin organisation and gene expression

1.7.1 HP1 function in gene silencing

Self-association

HP1 family proteins undergo self-association, reported for *P.citri* HP1 proteins (Esptein et al., 1992), *h*HP1α and mHP1α (Le Douarin et al., 1996; Ye et al., 1997); heterologous interactions between *h*HP1α and *h*HP1γ have also been observed (Ye *et al.*, 1997). In the case of the human proteins, the associations depend on the CSD. Thus, there appears to be a complex and potentially dynamic collection of HP1-dependent interactions occurring in a variety of eukaryotic cells. Most of the interactions, which have been mapped, involve the CSD. The structure studies using crystallisation and NMR have brought up that dimerisation through the CSD of HP1-like proteins results in the formation of a hydrophobic pit, which provide an

environment for a putative protein-protein interaction.

Origin recognition complex and HP1

In *S. cerevisiae*, the multisubunit origin of replication complex (ORC) is required for both DNA replication and silencing at the mating type loci. Mutations in ORC subunits show that the processes are independent of each other (Aagaard et al., 1999; Le Douarin et al., 1996). ORC is hypothesized to recruit silencing factors, in particular SIR1, to the mating type loci. In *Drosophila*, a subunit of ORC, ORC 2, localizes to heterochromatin and defects in ORC 2 suppress PEV (Pak et al., 1997). During mitosis, all detectable ORC2 concentrates in the pericentric heterochromatin at a subset of HP1 binding sites. In polytene nuclei, ORC2 is distributed widely across all euchromatic chromosome arms but is largely excluded from the chromocenter. ORC1 interacts strongly with HP1 and both the CD and CSD of HP1 are required for this interaction (Pak et al., 1997). The functional significance of an ORC–HP1 interaction is unclear; while HP1 appears to be spatially restricted, ORC is thought to function at replication origins distributed throughout the genome. The involvement of ORC in both yeast and *Drosophila* silencing suggests a conservation of silencing mechanisms.

1.7.2 HP1 and Nuclear assembly

Lamin B receptor and HP1

The lamin B receptor (LBR) is an integral membrane protein of the nuclear envelope; it binds B-type lamins and double-stranded DNA, and may function as a chromatin-docking site at the nuclear envelope (Pyrpasopoulou et al., 1996). Interaction of human LBR with the human HP1 family proteins HP1α and HP1γ was

demonstrated by affinity chromatography and by co-immunoprecipitation (Ye and Worman, 1996) ; the interaction utilizes the CSD (Ye *et al.*, 1997). *In vitro* translated HP1 binds to a purified glutathione-*S* -transferase (GST)–LBR fusion protein, indicating direct interaction (Ye et al., 1997). Without genetic analysis, the functional significance of LBR –HP1 interaction is unclear but, in all eukaryotic cells, the inner nuclear membrane and nuclear lamina are closely associated with peripheral heterochromatin. It has been shown that nuclear membrane association can promote silencing in yeast (Andrulis et al., 1998). The possibility that HP1 could promote silencing through LBR-mediated association with the nuclear membrane is intriguing.

Inner centromere protein and HP1

Inner centromere protein (INCENP), a component of the mitotic chromosome scaffold, is associated with the centromere in early metaphase but moves progressively to the spindle fibres and the plasma membrane at the cleavage furrow. The centromere-targeting amino-terminal half of INCENP interacts with HP1α and HP1γ in a yeast two-hybrid screen of a HeLa cell cDNA library (Ainsztein et al., 1998). This interaction does not appear to be involved in targeting INCENP to the centromeric heterochromatin. The interaction of HP1 homologues with INCENP requires the ' hinge region ' of HP1 connecting the CD and CSD. The significance of the interaction remains unclear, however, as it does not seem to be required for INCENP function.

Chromatin assembly factor 1 and HP1

Chromatin assembly factor (CAF) is a three-polypeptide complex that mediates histone deposition on newly replicated DNA. A yeast two-hybrid protein screen of a mouse embryo cDNA library, using the mouse HP1 family protein MOD1 as bait, recovered cDNA clones encoding the large CAF-1 subunit p150 (Murzina et al., 1999). Comparing overlapping sequences of all cDNAs isolated in the screen, a MOD1 interacting region (MIR) was identified. MOD1 binds a GST –MIR fusion peptide *in vitro*; the CSD of MOD1 is both necessary and sufficient for this interaction. These results suggest that the HP1-binding and heterochromatin-targeting activities of the CAF-1 large subunit are dispensable for its role in nucleosome assembly during replication. MOD1 synthesized in early S phase, prior to the initiation of DNA replication, was localized to heterochromatin normally, indicating that replication-dependent chromatin assembly is not required for proper MOD1 targeting. The functional significance of CAF-1 binding in heterochromatin outside of S phase is unknown.

1.7.3 HP1 mediates transcription regulation

The transcription intermediary factors TIF1α and TIF1β/KAP-1 interact with nuclear hormone receptors and the Krüppel-associated box (KRAB) domains of several proteins; they may function as co-activators in ligand-dependent activation of transcription and co-repressors with KRAB-containing repressor proteins. Yeast two-hybrid protein screens of a mouse embryo cDNA library using TIF1α as bait recovered clones encoding the HP1 family proteins mHP1α and mMOD1 (Le Douarin et al., 1996). Mutations in TIF1α gene that blocked mHP1α and mMOD1 binding *in vitro* reduce TIF1α-mediated repression of a SV40 enhancer/promoter

reporter in NIH 3T3 fibroblasts (Ryan et al., 1999a). The physiological significance of the TIF1α –mHP1α association is unclear, as the HP1 binding domain proved dispensable for TIF1α -mediated repression in a transfection assay, and no significant subnuclear colocalization of mHP1α and TIF1α has been observed (Remboutsika et al., 1999). TIF1β/KAP-1 colocalises in heterochromatin with mouse M31, and in euchromatin with mouse M32 (Ryan et al., 1999b), consistent with an in *vivo* association between these proteins. A biochemical analysis has revealed that the CSD is responsible for the interaction (Lechner et al., 2000). The results suggest that TIF family could be a relevant target for HP1 in the nucleus and through these interactions HP1 might participate in transcription regulation.

1.7.4 Phosphorylation of HP1 and the regulation of heterochromatin assembly

In *Drosophila*, HP1 is multiply phosphorylated by serine/ threonine kinases, one of which is casein kinase II (CKII) (Zhao and Eissenberg, 1999); CKII phosphorylation of HP1 is required for efficient heterochromatin targeting (Zhao and Eissenberg, 1999). There is also indirect evidence for tyrosine phosphorylation of HP1 (Platero et al., 1995). Biochemical fractionation of HP1 suggests that differential HP1 phosphorylation may be associated with distinct complexes (Huang et al. 1998). Human and Tetrahymena HP1 proteins are also differentially phosphorylated; hyperphosphorylation of the *Tetrahymena* Hhp1p is induced by starvation and is correlated with decreased nuclear volume (Huang et al., 1999). In humans, hyperphosphorylation of HP1α and HP1γ is correlated with mitosis (Minc et al., 1999). The dynamic nature of HP1 phosphorylation suggests a regulatory function for this process.

1.7.5 Mechanism of HP1-mediated silencing

Although genetic and cytological evidence in *Drosophila* clearly implicates HP1 in heterochromatic position effect silencing, both the mechanism of silencing and the role of HP1 in the mechanism remain unknown. The structure of the HP1 protein, with two related heterochromatin-targeting domains, suggests that it acts as a bifunctional cross-linker, perhaps organizing higher order chromatin structure by linking or anchoring chromatin subunits. At the biochemical level, heterochromatin silencing is correlated with reduced accessibility of promoter sequences to nuclease attack (Wallrath and Elgin, 1995), while suppression of PEV by HP1 mutation is correlated with increased accessibility (Cryderman et al., 1998). The mechanism by which HP1 mediates this differential accessibility is unknown. In *Drosophila*, the heterochromatin does include a number of genes, some of which have been shown to require a heterochromatin context for their normal expression (Wakimoto and Hearn, 1990; Eberl et al., 1993). In rearrangements that separate the genes from their flanking heterochromatin such genes are misregulated. Mutations in several loci that cause suppression of classical PEV enhance the misregulation of rearranged heterochromatic genes (Hearn et al., 1991); these mutations include alleles of *Su(var)2-5*, the locus encoding HP1. In addition, certain pairwise combinations of PEV modifiers including *Su(var)2-5* result in misregulation of the heterochromatin gene light, when light remains in its normal chromosomal position (Clegg et al.,1998). Normally, HP1 may simply function as an organizer of higher order chromatin structure in the nucleus. This organizing property could serve to accommodate the transcription of genes that normally reside within heterochromatin. When the normal organization of heterochromatin is lost, through rearrangement to euchromatin or by depletion of structural subunits, misregulation of hetero-

chromatic genes would result. Conversely, rearrangements that place euchromatic genes next to a heterochromatic breakpoint could make genes near the breakpoint exposed to assembly into HP1-dependent heterochromatin, silencing those genes by template compaction.

1.8 Objectives of the research

The HP1 family of proteins represents the best-characterized heterochromatin-associated nonhistone chromosomal protein family in the eukaryotic kingdom. Its remarkable evolutionary conservation suggests a fundamental role for HP1 proteins in nuclear organization. The role of HP1 proteins in mediating position-effect silencing has proven especially useful in genetic strategies aimed at identifying candidate partners for HP1 in heterochromatin assembly. Future work on HP1 and its partners will be directed at defining its partial role as a subunit of heterochromatin, as a cofactor in gene regulation, and perhaps as an essential player in the dynamic organization of nuclear architecture.

Much of the work on underpinning the role of heterochromatin has been done in genetically tractable organisms such as the furitfly, *D. melanogaster* and the yeast, *S. pombe.* In humans immunological studies with antibodies have elucidated the structure of the centeromere/kinetochore through the cell cycle. It would be useful if there were a biochemical system available for the molecular characterisation of heterochromatin formation.

In my study, I employed the South African clawed-toe frog, *Xenopus laevis*, as a vertebrate model system to address two questions. First, is HP1 protein necessary for *Xenopus* development? Second, What are the molecular partners for HP1? *Xenopus*

laevis is a gentle fresh water animal that can be induced by simple hormone injection to lay eggs repeatedly. In addition, their large size of embryos, which allows mircomanipulation and microinjection, and rapid rate of development make *Xenopus* an excellent animal for analysing early vertebrate development. A typical example is the studies in Polycomb family, which has been addressed in developmental function using a *Xenopus* as a vertebrate model (Riijnen et al., 1995; Strouboulis et al., 1999).

Chapter 2 Materials and methods

2.1 The methods for molecular biology

2.1.1 5' RACE (5' -end of rapid amplification of cDNA ends)

5' -end of rapid amplification of cDNA ends is a procedure for amplification of nucleic acid sequences from a messenger RNA (mRNA) template (*x*HP1α, γ, in my cases) between a defined internal site and unknown sequences at 5' -end of the mRNA. The procedure is summarised in Figure 2-1. First strand cDNA is synthesised from total RNA using HP1α or γ specific primer (HSP1) and Reverse transcriptase. After first strand cDNA synthesis, the original mRNA template is removed by treatment with Rnase H, which is specific for RNA: DNA heteroduplex, and RNase T1. Unincorporated dNTPs, HSP1 and proteins are separated from cDNA using spin cartridges. A homopolymeric tail is then added to the 3' -end of the cDNA using dCTP and TdT *(terminal deoxynucleotidyl transferase)*. PCR amplification is accomplished using *Taq* polymerase, and a nested, HP1 α or γ specific primer (HSP2) that anneals to a site located within the cDNA molecule, and a deoxyinosine-containing anchor primer. Deoxyinosine has the capacity to base-pair with all four bases. The selective placement of deoxyinosine residues in the 3' region of the anchor primer maintains low stability on the primer's 3' end and creates a melting temperature (T_m) for the 16-base anchor region (66.6 ℃). This maximizes specific priming from oligo-dC tail, minimizes priming at internal C-rich regions of the cDNA.

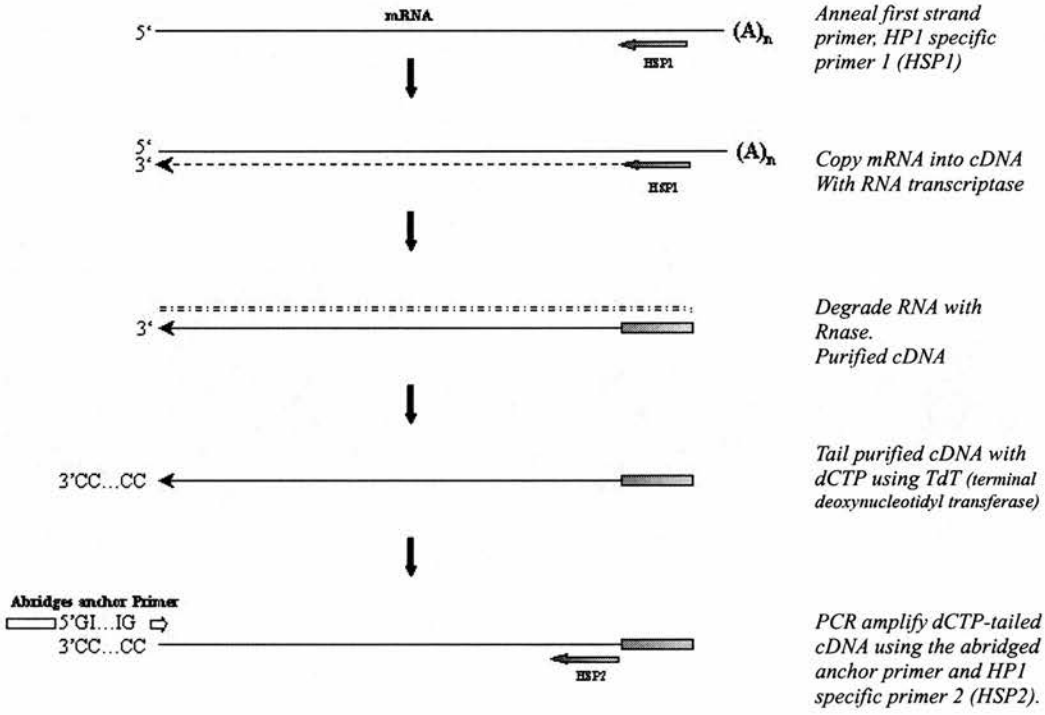

Figure 2-1 Overview of the 5' RACE procedure

The primers for 5'RACE

5'RACE abridged anchor primer

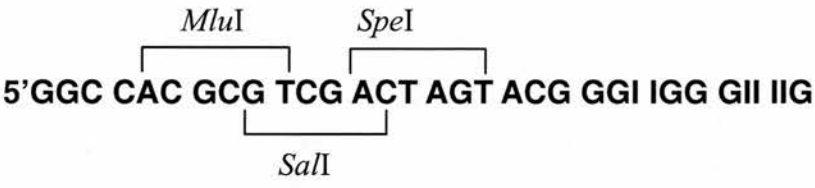

HSP1 α

5 '-CGA GGC AGG TAG GGA GAG TAG G

HSP2 α

5 '-GTG TGT GTC TGA ATG AAG AAG G

HSP1 γ

5 '-AAT CTT GAA GGT TCC TGA AGT G

HSP2 γ

5 '-TTT ATTGTG CTT CAT CCT CTG G

2.1.2 Sequencing

The services of DNA sequencing are provided by the Department of Veterinary Pathology in University of Edinburgh.

2.1.3 Bacteriological solutions

LB (Luria-Bertani) medium 1 litre

10 g Bacto®-tryptone
5g Bacto®-yeast extract
10 g NaCl

LB plates

Add 15 g of Bacto®-agar to one litre of LB medium. Autoclave. Allow to cool

to 50℃ before adding appropriate antibiotics.

TB (Terrific Broth)

12 g Bacto®-tryptone
24g Bacto®-yeast extract
4 ml glycerol

Dissolve the above components in approximately 900 ml water. Autoclave this solution and let the solution cool, add 100ml TB salt solution (0.017 M KH_2PO_4, 0.072M K_2HPO_4) and adjust the final volume to 1000 ml.

2.1.4 Preparation of competent cells

1. Inoculate 10 ml of LB medium (with a single colony). Incubate at 37℃ for 12-16 hours with vigorous shaking.
2. Using a 2litre flask, inoculate 500 ml of LB medium with 5 ml of cells from the overnight culture.
3. Shake the culture at 150-200 rpm at 37℃ until A_{600} reaches 0.45-0.55.
4. Chill the cells in ice for 10 minutes and then spin down at 5 Krpm, 4℃ for 5 minutes
5. Resuspend the cells in 10-20 ml of ice-cold trituration buffer (100 mM $CaCl_2$, 70mM $MgCl_2$) then dilute to 50 ml with the same buffer.
6. Incubate the cells on ice for one hour.
7. Centrifuge the cells at 1,800×g for 10 minutes and gently resuspend in 50 ml of ice-cold trituration buffer.
8. Pool the cells and add 80% glycerol dropwise with gentle swirling to afinal concentration of 15% (v/v). Aliquot the cells in 0.2-1.0 ml quantities, freese on dry ice and store at -80℃.

Table 2-1 Genotype of bacterial strain used in this work

XL-blue MRF	△(mcrA)183△(mcrCB0hsdSMR-mrr)173 endA1 upE44 thi-1 recA1 gyrA96 relA1 lac[F' pro AB $lacI^qZ$△M15Tn10(Tet^r)
BL21(DE3)pLys	F^-, *ompT, hsdS*$_B$ (r_B^-, m_B^-), dcm, gal, λ(DE3), pLys (Cam^r)
Bl21CodonPlus(DE3)-RIL	F^-, *ompT, hsdS*$_B$ (r_B^-, m_B^-), dcm, Tet',gal, λ(DE3), endA The[argU ileY leuW Cam^r]

2.1.5 Transformation of competent cells

1. Thaw a 200μl aliquot of competent cells on ice.
2. Add 1 ng of DNA (approximately 1μl of the ligation reaction) to the competent cells and mix gently. Incubate on ice for 30 minutes.
3. Heat the tube at 42℃ for 2 minutes. Place on ice to cool for 2 minutes.
4. Add 0.5 ml LB medium and incubate for 45 minutes at 37℃.
5. Plate 100-200 μl of the transformation mix onto selection plate (LB plate containing appropriate antibiotics, like ampicillin)

2.1.6 Plasmid DNA minipreps

2.1.6.1 Telt miniprep

1. Grow bacteria culture from a single colony in LB medium containing an appropriate antibiotic for 12-16 hours.
2. Spin down 2-3 ml in microcentrifuge tubes.
3. Resuspend in 600 μl TELT solution (50 mM Tris-HCl pH7.5, 62.5 mMEDTA, 2.5 M LiCl, 0.4% (v/v) Triton X100).
4. Add 40 μl 100mg lysozyme in TELT. Leave at room temperature for 2 minutes.
5. Heat the tubes at 100℃ for 2 minutes.
6. Spin the tubes at top speed at a bench top centrifuge for 15 minutes.
7. Remove supernatant to fresh tubes. Add o.6 volume of isopropanol and incubate

on ice for 2 minutes.

8. Spin the tubes at top speed at a bench top centrifuge for 20 minutes.

9. Wash the pellet in 70% (v/v) ethanol and air dry.

10. Resuspend the pellet in 100 µl TE buffer (10mM Tris-HCl, 1 mM EDTA, pH 8.0)

2.1.6.2 Miniprep purification kits

A commercial kit (Bio/Spin, Biogene) was also used in order to have higher quality of plasmid DNA preparation.

2.1.7 Subcloning and expression constructs making

5'RACE generated full-length *x*HP1α and *x*HP1γ DNA fragments were subcloned into a T vector, pXT [pGEM 7Zf based (Promega), modified by Harrison et al., 1994) and fully sequenced. PCR was used to generate full-length *x*HP1α and *x*HP1γ DNA fragments by designing sequence specific primers with *Nco*I restriction sites at the 5' end and *Bam*HI at 3' end. These products were subcloned in-frame into pXT vectors then the fragments were released from the vector by *Nco*I and *Bam*HI double digestion. Run the whole digested reaction into agarose gel and recover the released *x*HP1 DNA fragments from the gel using spin columns (Biogene). These products were then subcloned in-frame into the pET6H vectors [pET11D based (Novagen), modified by Cross et al. 1994) and the pGEX-2T vectors (Pharmacia Biotech).

PCR was also used to generate GST tagged constructs by designing sequence specific primers with *Eco*RI restriction sites at the 5' end and 3' end. These products were then subcloned into pXT vectors and relocated in-frame into the pGEX-2T vector (Pharmacia Biotech).

PCR primer for constructs making:

Nco-HP1α: 5'-GAC TGC CAT GGA CGC CAGTGACAC T

Bam- HP1α: 5'-AATATGGAT CCA ATG AAG AAG GGA AA

Nco-HP1γ: 5'-GCATGC CAT GGG GAA GAA ACA GAA T

Bam- HP1γ: 5 '-ATA TGG ATC CTC ATC CTC TGG ACA A

5'GST - HP1α: 5'-TTT CGG AGA ATT CAA ATG GAC GCC AGT GAC

3'GST- HP1α: 5'-GTT AAA AGA ATT CTT TAA CTT TTC ACC GCT

3'GST-HP1α-CD: 5'-TCTTGG AATTCG GCT CAG CCT CCT TCG CTT TCT

3'GST-HP1α-CD+H: 5 '-TGT CAG AAT TCT CTC TCC TCC TCT TTG CCT TAA

5' GST-HP1α-H+CSD: 5'-GAA GGG AAT TCA GCC AAA AGC CAA GAC GGA AAG

5' GST-HP1α- CSD: 5'-AAA GAG AAT TCG AGA GAG CAA TGA CAT CGC ACG

5'GST- HP1γ: 5'-TGA GAG TGA ATT CCC ATG GGG AAG AAA CAG

5' GST-HP1γ-H+CSD: GGC AGG ATT TCA AAA ACC AGA CAG CAA CAA AAG

3'GST- HP1γ: 5'-TGC AAG CGA ATT CAT TTA TTG TGC TTC ATC

2.1.8 Recombinant protein expression

1. Transformed the recombinant DNA plasmid into BL21(DE3)pLysS or BL21 codonplus® (Stratagene)
2. Pick recombinant colonies and grow them overnight at 37℃ in 50 ml of LB medium containing the appropriate antibiotic.
3. The next day remove 10-20 ml and inoculate into 500 ml of fresh LB medium containing the antibiotic. Allow the culture to grow at 37℃ to an A_{600} of 0.6.

4. Add 100mM IPTG to the bacterial culture to a final concentration of 0.5 mM
5. Incubate the culture for an additional 2-4 hours at 25 –30℃.
6. Harvest the cells by centrifugation at 8000×g for 10 minutes. Immediately proceed with the purification or freeze the cells at -20℃ for later use.
7. Resuspend the cells by stirring 25 ml of PBS (GST tagged) or start buffer (6×histidine tagged). **PBS**: 140 mM NaCl, 2.7 mM KCl, 10 mM Na_2HPO_4, 1.8 mM KH_2PO_4. **Start buffer**: 20 mM $Na_{2H}PO_4$, 0.5 M NaCl, pH 7.4.
8. Sonicate the suspension on the ice bath using 30-second pulse with 15-second rest between pulses for 4 minutes.
9. Centrifuge the crude lysate at 10,000×g for 15 minutes at 4 ℃ to remove cellular debris. Clarify the sample by filtering the supernatant through 0.45 μm filter before apply to a column.

2.1.9 Purification of recombinant protein

2.1.9.1 Purification of glutathione S-transferase fusion protein

1. Remove sufficient gel (1 ml for 500ml culture) of glutathione Sepharose 4B (Pharmacia Biotech) for use and transfer to an appropriate column.
2. Equilibrate the gel bed with 3 bed volume PBS (140 mM NaCl, 2.7 mM KCl, 10 mM Na_2HPO_4, 1.8 mM KH_2PO_4)
3. Apply the sample to the column and incubate with gentle agitation for 30 minutes. Discard the eluent. Wash the column three times with 10 bed volumes of PBS.
4. Elute the bound material three times with 5 bed volumes of elution buffer (10-100 mM Glutathione in PBS) and collect the fractions.
5. Analyse the eluted protein using SDS-PAGE and western blotting.

2.1.9.2 Purification of 6×histidine fusion protein

1. Remove enough volume of chelating sepharose (Pharmacia Biotech) and transfer to an appropriate column. Wash the gel three times with five-bed volume of water.
2. Charge the gel with 0.5 gel volume of 0.1 M NiSO4 solution for 15 minutes.
3. Wash the gel three times with five gel-bed volume of H_2O. The equilibrate the gel with start buffer (20 mM $Na_{2H}PO_4$, 0.5 M NaCl, pH 7.4)
4. Apply the sample to the column and incubate with gentle agitation for 30 minutes.
5. Wash the column three times with 10 bed volumes of start buffer.
6. Elute the bound material using 5 different elution-buffers with gradually increased L-histidine concentrations (10-100 mM) and collect the fractions.
6. Analyse the eluted protein using SDS-PAGE and western blotting.

2.2 The methods for biochemical manipulation

2.2.1 Antibody production and purification

2.2.1.1 Immunising rabbit with fusion protein

Approximately 100μg of purified His-*x*HP1α or His-*x*HP1γ were emulsified with an emulsified with an equal volume of adjuvant (TiterMax®, CytRx) by votexing. (Total volume of sample + adjuvant + 1 ml). The samples then were sent to Scottish Antibody Production Unit (SAPU) to immunise two rabbits (one for His-*x*HP1α and one His-*x*HP1γ). The immunization programme was design by SAPU. The bloods were taken form the two rabbit after 4-week immunisation to obtain serums. The serums were stored frozen at –80℃ for later use.

2.2.1.2 Affinity purification of antibodies

The sample containing antigen (in this case, a preparation of recombinant *x*HP1α or *x*HP1γ) was separated SDS-PAGE in a 10% gel (the sample was loaded

into all of the wells on the gel and transfer onto a nitrocellulose membrane. The membrane was stained in 0.2% Ponceau S in 0.5% acetic acid for 5 minutes then washed in water to remove the background staining. The band corresponding to the antigen (in this case the GST fusion *x*HP1α or *x*HP1γ appeared a broad band on the blot) was carefully excised from the blot using a scalpel. The Ponceau Swas removed from the affinity strip by washing in TBS (50 mM Tris-HCl, 150 mM NaCl, 0.5% Tween 20) several times (It is important to be able to determine which side of the strip has the antigen bound to it, especially once the Ponceau S is removed). The affinity strip was then incubated in blocking buffer (3% semi-skim milk in TBS) for 90 minutes in order to block any non-specific site on the membrane and then washed in TBS. The affinity strip was placed into a 15 ml Falcon tube full with immune serum and then was shaken gently at room temperature for 2 hours. The strip was remove from the serum and was washed three times for 5 minutes each in TBS to remove any unbound antibodies that may have been present. The antibodies specially bound to the antigen were removed from the strip by placing elution buffer (0.2 M glycine-HCL, pH 2.8) onto the strip (as much as could be held on the strip by surface tension) for 20 minutes. The elution buffer containing the eluted antibodies was removed from the affinity strip and neutralised immediately by adding an equal volume of 0.1 M Tris-HCl, pH 8.5. These affinity purified antibodies was store at 4 ℃ after addition of 0.1% sodium azide to them. If the affinity strip were to be reused , it was washed in TBS and stored at 4℃ in TBS , 0.1% sodium azide.

2.2.2 Chemical Cross-linking of *x*HP1 proteins

The cross-linker was glutaraldeyde, which has a dialdehyde. Its two aldehyde-groups can react with amino and other group in protein and can thus form cross-links

two molecules. The purified histidine-tagged *x*HP1α and *x*HP1γ proteins were dialysed into a phosphate buffered saline (PBS) and then incubated for 30 minutes at room temperature with a titrated amount (1-50 mM) of glutaraldeyde, and separated in SDS-PAGE. The same samples were also transferred onto nitrocellulose membranes and the recombinant proteins were visualized by western blotting with an anti-histidine tag antibody.

2.2.3 Preparation of chicken chromatin and chicken chromatin DNA

540 μl Chicken erythrocyte nuclei were digested with 60 unit/ml micrococcal nuclease for 20 minutes at 37 ℃ in nuclease digestion buffer (250 mM sucrose, 10 mM Tris-HCl pH 7.4, 10 mM NaCl, 3 mM $MgCl_2$, 0.1 mM PMSF). The nuclease was activated by adding 1 mM $CaCl_2$ at 37℃. Digestion was stopped in digestion buffer + 5 mM EDTA. The nuclei were gently centrifuged down at 2 Krpm for 2 minutes.

The nuclei then were lysed by resuspending in a resuspending buffer (10mM Tris-HCl pH 7.4, 10 mM NACl, 0.2mM EDTA), votexing and pelleting. The pellet was washed twice in 150 μl of the resuspending buffer. The prepared ' chicken chromatin' was in the two supernatants, which were then pooled together and adjusted to 500 μl.

67 μl of chicken chromatin was digested with proteinase K and followed phenol-chloroform extraction, ethanol precipitation. The pellet was redissolved in 67 μl TE buffer (10mM Tris-HCl pH 7.4, 10 mM NaCl, 0.2 mM EDTA) as chromatin DNA.

292 μl of the chicken chromatin was bound onto 0.275g hydroxylapatite (HAP) in a binding buffer (10 mM KP pH 6.8). Linker histone was depleted by extracting

the HAP-chromatin with an extraction buffer (600 mM NaCl, 10 mM KP). 'Depleted H1/H5 chromatin' was eluted from HAP in an elution buffer (150 mM KP pH6.8).

Half of depleted H1/H5 chromatin (62 µl was digested with 50 µg/ml of trypsin for 8 minutes at 37℃. Digestion was stopped with 200 µg/ml of TLCK on ice. The sample was the 'trypsinised chromatin.'

2.2.4 Protein translation *in-vitro* using Rabbit Reticulocyte Lysate system

Denature the template mRNA (transcripts of *in-vitro*-translated *x*HP1α or *x*HP1γ) at 65°C for 3 minutes and immediately cool in an ice-water bath. This increases the efficiency of translation, especially of GC-rich mRNA, by destroying local regions of secondary structure. Gently mix the rabbit reticulocyte lysate by stirring with a pipette tip upon addition of each component. Assemble the following reaction components to 0.5ml polypropylene microcentrifuge tubes.

Rabbit Reticulocyte Lysate (Promega)	35µl
Amino Acid Mixture, Minus Methionine, 1mM (Promega)	1µl
[^{35}S] methionine (1,200Ci/mmol)(Pharmacia Biotech)	2µl
Ribonuclease Inhibitor (40u/µl) (MBI)	1µl
RNA substrate in water (*x*HP1α or *x*HP1γ) (1µg/µl)	2µl
Nuclease-Free Water to a final volume of 50µl	

Immediately incubate the translation reactions at 30°C for 90 minutes. Analyze the results by separating the whole lysate using SDS-PAGE and of translation and detecting ^{35}S labeled proteins by autoradiography

2.2.5 Labelling PE190 *Xenopus* satellite clone

PE190 *Xenopus* satellite DNA clone was digested with *Hind* III to release the satellite insert from the vector. Both the satellite DNA and the vector were then labeled with ^{32}P-α CTP with the following protocol.

4 μg of digested DNA in 10-15μl of water

Add:

2 μl 10× reaction buffer (500mM Tris-HCl pH 8.0, 50 mM MgCl2, 10mM DTT)
20 μCi ^{32}P-α dCTP
2.5 μl 2 mM dNTP (without dCTP) (0.25 mM-final concentration)
1 unit Klenow fragment
Deionised water to 20 μl
Incubate the mixture at 30℃ for 15 minutes.
Stop the reaction by heating at 70℃ for 10 minutes.

2.2.6 GST pull-down assay

Targets for pull-down reactions

Chicken chromatin (In cooperation with **Dr. Sari Pennings**)

Chicken chromatin DNA (In cooperation with **Dr. Sari Pennings**)

Core histones (a gift of **Dr. James Allan**)

PE190 *Xenopus* satellite DNA clone

6× histidine tagged recombinant *x*HP1α or *x*HP1γ

In vitro translated ^{35}S-labelled *x*HP1α or *x*HP1γ

Materials

Glutathione Sepharose 4B

GST tagged proteins

GST-*x*HP1α, GST-*x*HP1α-CD, GST-*x*HP1α-CD+H, GST-*x*HP1α-H+CSD, GST-*x*HP1α-CSD

GST-*h*HP1α, GST-*h*HP1α-CD

GST-*x*HP1γ, GST-*x*HP1γ-H+CSD

Buffers

10×HEPES buffer: 100mM HEPES, 100mM KCl, 5mM EGTA

1× HEPES: 10mM HEPES, 10mM KCl, 0.5mM EGTA, 1mM DTT, 10% glycerol, Cocktail proteinases inhibitor

Protocol

1. Sepharose preparation (Glutathione Sepharose 4B, Phamacia Biotech)

   Use 25μl sepharose for each reaction. Wash a fresh aliquot of sepharose (in 20% ethanol) 3 times using 1× HEPES buffer and aliquot into 1.5 ml microcentrifuge tubes. Spin down the Sepharose at 8K rpm.

2. Immobilize GST fusion proteins on the Sepharose.

   Use 5 ~10 μg protein for each reaction. Mix GST fusion protein with the washed Sepharose and incubate at room temperature for 30 minutes with shaking, then wash the protein- Sepharose matrix 3 times using 1× HEPES buffer. Then aliquot the Sepharose into 1.5 ml microcentrifuge tubes.

3. Add 1× HEPES buffer to the microcentrifuge with the protein- Sepharose matrix to a total volume of 200 μl. For different incubation condition, a different incubating buffer should be used.

4. Add 5μg of chicken chromatin/targeted proteins to the above 200 μl of the protein-Sepharose matrix and incubate at room temperature for 1 hour with shaking; then spin down the sepharose. Remove the supernatants into fresh microcentrifuge tubes and retain it for the following step.

5. Wash the pellet fraction 3 times using 1× HEPES buffer and add 200 μl 1× HEPES buffer back to the bead.

6.1 For the chromatin pull-down: digest both the pellet and supernatant fractions

respectively using proteinase K; followed by phenol/chloroform extraction, ethanol precipitation. Analyse the chromatin DNA on a 1.5% agarose gel

6.2 For the protein pull-down: followed the final wash, mix the pellet with the protein sample buffer (see SDS-PAGE protocol) and analyse the targeted protein in SDS-PAGE.

2.2. 7 Histone H3-tail pull down

Targets for pull-down reactions

GST-*x*HP1α-CD
GST-*x*HP1α
GST-*h*HP1α
His-*x*HP1γ

Affinity matrices were generated and the pull-down reactions were performed by the same protocol with that in the GST pull-down assay but using tetrameric avidin resin preparation (TetraLink™, Promega) and biotinylated amino acids 1-21 of histones H3 either in the unmodified or dimethylated at lysine 9. A resin of 25 μl containing 0.1 mg of peptides was used for each pull-down reaction.

2.2.8 SDS –polyacrylaminde gel eletrophoresis

Standard SDS-PAGE gel preparation

1. Pour the separating gel

Set up the gel apparatus, prepare separating gel monomer. Add TEMED just prior to pouring gel. Allow to polymerize before adding stacking gel by overlaying gently with water.

Separating Gel, in 0.375 M Tris, pH8.8

	7%	10%	12%	15%
Distilled water	5.05 ml	4.05 ml	3.35 ml	2.35 ml
1.5M Tris-HCl, pH 8.8	2.5 ml	2.5 ml	2.5 ml	2.5 ml
10% SDS	0.1 ml	0.1 ml	0.1 ml	0.1 ml
Acylamide/Bis-acrylamide (30%/0.8% w/v)	2.3 ml	3.3 ml	4.0 ml	5.0 ml
Ammonium persulphate	0.05 ml	0.05 ml	0.05 ml	0.05 ml
TEMED	0.005 ml	0.005 ml	0.005 ml	0.005 ml
Total monomer	10 ml	10 ml	10 ml	10 ml

2. Pour the stacking gel

After the separating gel has polymerized, decant the overlay, prepare the stacking monomer, add the TEMED, and pour. Insert the comb and allow to polymerize completely before running.

Stacking Gel, 4 % gel in 0.125 M Tris, pH6.8

Distilled water	3.300 ml
1.5M Tris-HCl, pH 8.8	1.250 ml
10% SDS	0.05 ml
Acylamide/Bis-acrylamide (30%/0.8% w/v)	0.670 ml
Ammonium persulphate	0.015 ml
TEMED	0.025 ml
Total Stack monomer	5 ml

3. Sample buffer

Dilute samples at least 1:4 with sample buffer, heat at 95℃ for 5 minutes prior to loading

Sample buffer

Distilled water	4.0 ml
0.5 M Tris-HCl	1.0 ml
Glycerol	0.8 ml
10% SDS	1.6 ml
β-mercaptoethanol	0.4 ml
bromophenol blue	0.2g

4. Running the gel

Run the gel at constant voltage, 200V in 1× running buffer

5× Running Buffer, pH 8.3

Tris Base	15 g
Glycine	72 g
SDS	5 g
Distilled water to1 litre	

2.2.9 Western blotting

Run a normal SDS protein gel on a small BioRad protein gel system. Then soak the gel in 1× transfer buffer (0.025 M Tris-HCl, 0.192 M glycine) for ten minutes to leach out the SDS in the gel. At the same time presoak a nitrocellulose membrane and two sheets of 3MM papers in the same buffer.

Transfer protein from the gel to the nitrocellulose membrane using BioRad transfer apparatus in the same transfer buffer at 200 mA for one hour. For **core histones** transfer, use a different transfer buffer: 0.025 M Tris-HCl, 0.192 M glycine, 0.1 % SDS, 20% methanol and transfer at 230 mA for 2 hours.

After transfer wash the membrane with water and then block the membrane with a blocking buffer [2-5 % semi-skim milk (Marvel, Nestle) in TBS (50 mM Tris-HCl pH7.4, 150 mM NaCl)] for at least one hour in order to block any non-specific site on the membrane and then wash in TBS.

Incubate 1-4 hours (to overnight) with a proper dilution of primary antibody in the blocking buffer and then wash the membrane three times in TBS/0.5% Tween 20 (BDH), 15 minutes for each wash.

Followed a suitable secondary antibody incubation (conjugated with horse radish peroxidase, diluted in the blocking buffer) for one hour and then wash the membrane three times in TBS, 15 minutes for each wash.

Detect the desired signal using an ECL detection reagent (Pharmacia Biotech); follow the instruction provided by the manufacturer.

2.2.10 Far-western blotting

Run a 15 % normal protein gel of chromatin (including H1/H5) and core histones and transfer proteins on a nitrocellulose membrane. Block the membrane in an incubation buffer (50 mM Tris-HCl pH 7.5, 100 mM NaCl, 1 mg/ml BSA, 0.5% Tween 20) for one hour at room temperature. Incubate the blocked membrane with the incubation buffer plus 0.5 μg/ml of GST-*x*HP1α, the protein probe.

Wash the membrane three times with TBS/0.5% Tween 20, 15 minutes for each wash. Then incubate the membrane with a 1/5000 anti-GST antibody conjugated with peroxidase (Sigma) diluted in blocking solution.

After the incubation, wash the membrane three times with TBS/0.5% Tween 20, 15 minutes for each wash. Then develop the membrane with ECL system (Pharmacia Biotech).

2.3 The methods for developmental studies

2.3.1 Isolation of DNA from red blood cells

Collect the blood in a beaker containing 0.85×SSC from frogs and centrifuge

the blood at about 2000rpm to collect the red blood cells. Pour off the supernatant and partially resuspend the pellet in the residue supernatant and lyse the cells in reticulocyte standard buffer (RSB) (10 mM NaCl, 10 mM Tris-HCl pH 8, 5 mM $MgCl_2$) containing 0.05% Nonidet P-40 (NP-40). Start with a small volume (~5ml), resuspend cells and then increase volume to approximately 50ml. Hold the sample on ice for 1 minutes and collect the nuclei by centrifuging at about 2000rpm. Pour off the supernatant gently and resuspend the loose pellet by votexing. When the nuclei are thoroughly resuspended, adjust the volume to 50 ml with RSB containing 0.05% NP-40. Repeat the centrifugation and resuspending the nuclei few times until the nuclear pellet is white. Resuspend the pellet and add proteinase K to a final concentration of 200 μg/ml. Add one volume of 0.6 M NaCl, 20mM Tris-HCl (pH 7.4), 20 mM EDTA, and 1% SDS and mix thoroughly. Precipitate the DNA by adding 0.25 volume of 10 M ammonium acetate and mixing thoroughly.

Use a thin glass rod to spool the DNA out of the mixture and put the DNA into 70% ethanol and wash the DNA by gently inverting the tube until it is completely white. Draw off the ethanol and resuspend the DNA at an estimated concentration of 200 μg/ml.

2.3.2 Southern blotting

Alkaline Transfer

Electrophorese *Eco*RI, *Bam*HI and HindIII digested *Xenopus* genomic DNA in 1.5% agarose gels to separate the DNA. The gels then are rinsed in sterile water and subject to a transferring step. To perform the transfer, the gels are transferred to a buffer reservoirs containing supporting wicks (3MM Whatman paper) and alkaline transfer solution (0.4 M sodium hydrochloric acid). Dry transfer membranes

(Biodyne membrane, Pall) are placed directly on the gel. The transfers are allowed to proceed for overnight.

Hybridisation

After the transfer, remove the membrane from the gel surface. The membranes are fixed by exposure to 1000 μjoules of UV radiation. Then membranes can be hybridised with proper ^{32}P-lalled probes in hybridisation buffer (1mM EDTA, 0.5 M Na_2HPO_4 pH7.2, 7% SDS) at 65℃ with agitation for overnight.

Washes

1. Wash the membrane at 65℃, 2 times for 60 minutes each in the following
   1 mM EDTA, 40 mM Na_2HPO_4 pH7.2, 5% SDS
2. Wash the membrane at 65℃, 2 times for 60 minutes each in the following
   1 mM EDTA, 40 mM Na_2HPO_4 pH7.2, 1% SDS
3. After washing, the blotted membranes are ready for autoradiography.

2.3.3 Obtaining *Xenopus* embryos

Eggs were collected manually from female frogs one day after inducing ovulation by injection of human chorionic gonadotropin (hCG) into the dorsal lymph sac. Eggs are maintained in 1x MBS (88 mM NaCl, 1mM KCl, 0.7 mM $CaCl_2$, 1mM $MgSO_4$, 5 mM HEPES pH 7.8 and 2.5 mM $NaHCO_3$). Using freshly prepared testis does the in vitro fertilisation. The first sign of fertilisation (within a few minutes) is a contraction of the pigmented animal hemisphere to less than one half of the egg. Approximately 20 minutes after fertilisation the eggs rotate within the vitelline membrane so that the animal hemisphere faces upward.

Alternatively embryos can be obtained using natural mating. Induce females' ovulation by injecting with 500-800 units of hCG and stimulate male sexual activity by injection of 50 units of hCG a few days before mating. Males and females can be allowed to mate naturally in containers. Natural mating is convenient way to obtain many different stages of embryos at once.

After the first cleavage, dejelly the embryos by swirling gently in 1× modified Marc's Ringer (MMR) with 2% (w/v) cysteine at pH 8.0 [MMR: 0.1M NaCl, 2.0 mM KCl, 1 mM $MgSO_4$, 2 mM $CaCl_2$, 5mM HEPES (pH 7.8), 0.1mM EDTA.]. Gently swirl the embryos for 2-4 minutes until the jelly membranes are visible in the solution and eggs have started to pack.

2.3.4 RNA isolation from *Xenopus* embryos

Allow the embryos to settle and resuspend in 4 volumes of premixed proteinase K mix [20 mM Tris (pH 7.6), 100mM NaCl, 30 mM EDTA, 1% SDS and 0.5 mg/ml proteinase K]. Homogenise the embryos and incubate the proteinase reaction for 1.5 hours at 37℃. Then add the same volume of a 1:1 mix of phenol: chloroform to the sample. Vortex and centrifuge the sample at 12,000g for 5 minutes. Transfer the aqueous phase to a fresh tube. Extract the sample by another 1:1 of phenol: chloroform again and repeat the extraction two more times. Transfer the aqueous layer to a fresh tube and added 2.5 volumes of ethanol and collect the precipitated nucleic acid by centrifuging at 12,000 for 20 minutes. Carefully decant the ethanol and resuspend in TE and add 1/10 volume of 10x NEB4 (New England Biolabs). Add RNase-free DNase I to the concentration of 1unit/200 μl and incubate for 20 minutes at room temperature. Stop the DNase reaction by extracting with 2 volume of a 1:1 mix of phenol: chloroform and then 2 volume of chloroform. Transfer the

aqueous phase to a clean tube and add 135 µl per 400 µl sample of 10 M LiCl (autoclaved). Store at 4℃ for several hours, or overnight. LiCl will highly preferentially precipitate RNA.

Centrifuge the sample for 20 minutes at 12,000g. Carefully discard the supernatant and resuspend the pellet in distilled water. Add 2.5 volumes of ethanol and 0.1 volume of sodium acetate (3M, pH4.8). Collect the precipitate RNA by centrifugation and redissolve the RNA in distilled water. Determine the concentration and quality of the solution by measuring the $OD_{260/280}$. Store the RNA as an aqueous solution at -80℃. Embryos contain approximately 5 µg of total RNA. This protocol routinely produces yields of 90%.

2.3.5 Preparation of RNA (*In vitro* transcription)

RNAs produced by *in vitro* transcription were introduced into embryos by microinjection and used to test the effects of overexpression, expression of dominant-negative constructs and antisense interference of gene expression. For a 20 µl reaction volume, assemble the following ingredients in a prewarmed tube.

Linear template DNA (0.5-1 mg/ml)	2 µl
2× mRNA nucleotide triphosphate mix (6 mM ATP, CTP, UTP; 3mM GTP and 9 mMm7(5')Gppp(5')G cap analog (New England Biolabs)	10 µl
DTT (200mM)	2 µl
BSA (1mg/ml)	2 µl
10× mRNA transcription buffer (120 mM $MgCl_2$, 800mM HEPES pH7.5, 20mM spermidine-HCl	2 µl
RNase inhibitor (20 units/ml)	0.5 µl
T7/SP6 polymerase (20 units/ml)	1.5 µl

Mix gently and incubate the reaction for 2 hours at 37℃. Then add 2 units of RNA-free DNase I and incubate for a further 10 minutes at 37 minutes. Precipitate the RNA with ethanol and resuspend in DEPC-treated water twice.

2.3.6 RT-PCR

First strand cDNA synthesis

A 20-μl reaction volume is used for 1-5 μg of total RNA. Add the following components to a nuclease-free microcentrifuge tube:

1 μl oligo (dT) 12-18 (500μg/ml)

1-5 μg of total RNA

Sterile, distilled water to 12 μl

Heat mixture to 70℃ for 10 minutes and quick chill on ice. Collect the components of te tube by brief centrifugation and add

4 μl 5×First strand buffer [250mM Tris-HCl (pH8.3), 375 mM KCl, 15 mM $MgCl_2$]

2μl 0.1 M DTT

1μl 10 mM NTP Mix (10 mM each dATP, dGTP, dCTP and dTTP at pH7.0)

Mix contents of the tube gently and incubate at 42℃ for 2 minutes. Add 1μl (200 unites) reverse transcriptase (GIBCOBRL, life Technology). Mix by pipetting up and down. Incubate 50 minute at 42℃. Inactivate the reaction by heating at 70℃ for 15 minutes. The cDNA can be used as a template for amplification in PCR.

PCR reaction

Use 1μl of 1:10 dilution of cDNA for *x*HP1α and 1μl of cDNA for *x*HP1γ amplification. Add the following to a PCR reaction tube for a final reaction volume of 100 μl:

10 µl	10× PCR buffer (200 mM Tris-HCl pH8.4, 500mM KCl)
3 µl	50mM $MgCl_2$
2 µl	10 mM dNTP Mix
1 µl	5'HP1α/γ primer (10 µM)
1 µl	3'HP1α/γ primer (10 µM)
1 µl	*Taq* DNA polymerase
1 µl	1:10 dilution of cDNA for *x*HP1α or 1:1 cDNA for *x*HP1γ
80 µl	autoclaved, distilled water

The PCR programme are listed below:

95℃ for 3 minutes for denature

Denature:	95℃ for 3 minutes
Annealing:	51℃ for 1 minutes
Extention:	72℃ for 1 minutes

Perform 36 cycles the above reaction cycle.

2.3.7 The whole mount in situ hybridisation

Reagent for *in situ* hybrydisation

1. Nucleotide Stocks

   2.5 mM nucleotide mix with digoxigenin-11 UTP (Boehringer Mannhein)

10 mM CTP	10 µl
10 mM GTP	10 µl
10 mM ATP	10 µl
10 mM UTP	6.5 µl
10 mM dig-11 UTP	3.5 µl

2. MEMFA

   0.1 M MOPS (pH 7.4)

   2 mM EGTA

   1 mM $MgSO_4$

   3.7% formaldehyde

3. PTw

   1×PBS with 0.1% Tween-20

4. Triethanolamine, 0.1M (pH7.0-8.0, Sigma)

   Make up 0.1M Triethanolamine in DEPC treated water.

5. hybridisation buffer

50% formamide	5× SSC

1 mg/ml Torula RNA
100μ/ml heparin
1× Dehart's solution
0.1% Tween 20
0.1% CHAPS
10 mM EDTA

6. 20×SSC, 1 litre, pH 7.0
   175.3g NaCl
   88.2 g sodium citrate
7. Maleic Acid buffer (MAB)
   100 mM maleic acid
   150 NaCl (pH 7.5)
8. Alkaline phosphatase buffer
   100 mM Tris (pH 9.5)
   50 mM $MgCl_2$
   100 mM NaCL
   0.1% Tween
   2 mM levamisol

Probe synthesis

The same protocol with the preparation of RNA for *in vitro* transcription, except that using 2.5 mM dig-NTP stock instead of the 2× mRNA nucleotide triphosphate mix. After precipitating the RNA, remove the supernatant and resuspend the probe in hybridisation buffer.

Preparation of embryos

Albino embryos are prepared for in situ hybrydisation by fixation with MEMFA and dehydration/storage with ethanol.

Hybridisation

1. Rehydrate fixed embryos by washing the embryos in each of the following solution for 5 minutes.

   75% ethanol, 25% water

   50% ethanol, 50% water

   25% ethanol, 75% PTw

100% PTw

2. Permeabilise the embryos by incubating them for approximately 15 minutes at room temperature in 10μg/ml of proteinase K.
3. Wash the embryos twice for 5 minutes in 0.1 M triethanolamine (pH7.0-8.0; Sigma).
4. Add 12.5 μl of acetic anhydride (Sigma) and incubate for 5 minutes and repeat one more time.
5. Refix embryos for 20 minutes in PTw containing 4% paraformaldehyde and wash the embryos twice for 3 minutes in PTw.
6. Replace half volume of PTw with hybridisation buffer. (without mixing)
7. Once the embryos have settled down through the dense layer of buffer, remove the entire buffer and replace with fresh hybrydisation. Incubate for 10 minutes at 60℃ in a shaking water bath.
8. Replace hybridization buffer and replace with fresh hybridization buffer containing 0.5μg/ml probe. Hybridise overnight at 60℃.
9. Remove solution containing probe. Rinse the embryos for 10 minutes at 60℃ in fresh hybridization buffer and then wash three times in 2×SSC for 20 minutes at 60 ℃.

Antibody incubation

1. Replace 2×SSC with MAB and wash for one more time for a total 10 minutes.
2. Replace MAB with MAB containing 2% BMB locking reagent (Boeringer Mannheim) and incubate for 1 hour at room temperature with agitating.
3. Replace solution with fresh MAB containing 2% BMB blocking reagent and a 1/2000 dilution of the affinity-purified antidigoxigenin antibody coupled to

alkaline phophatase (Boeringer Mannheim). Rock vertically overnight at 4℃.

4. Remove excess antiboby by washing eight times 20-minute washes in MAB at room temperature.
5. For the chromogenic reaction, first wash embryos twice for 5 minutes at room temperature in alkaline phosphatase buffer and replace the last wash with BM purple or with alkaline phosphatase buffer containing 4.5 μl NBT and 3.5μl BCIP. Incubate at room temperature until staining becomes apparent.
6. When staining becomes apparent, replace the solution with fresh MEMFA and incubate at room temperature overnight.
7. Remove background with several washes of buffered 70% ethanol (prepare the ethanol with PTw as the aqueous component).
8. Dehydrate the embryos by incubating in two changes of methanol (5 minutes each).
9. Clear the embryos by removing most of the methanol and replacing it with 2:1 BB/BA. After the embryos settle through the BB/BA, replace with fresh BB/BA.

2.3.8 Microinjection of *Xenopus* embryos

Injection checklist

2% cysteine (w/v) in 1/3 × MMR or water, pH 8.0. Prepare fresh on day of injection.

70% ethanol (For sterilisation of instrument)

4% Ficoll in 1/3× MMR

Hairloop or blunt eyebrow knife (for pushing embryos around)

Microinjector

1/3 × MMR

1 × MMR

mRNA (for injection). Prepare fresh dilution on day of injection

Injection needles (drawn-out micropipettes)

Injection dishes

Watchmakers forceps, sharp and blunt (for removing the vitelline membrane)

All of the reagents and equipment for injection and manipulation are assembled before beginning any microinjection procedure. After fertilisation, the dorsal side of the embryo can be distinguished reasonably accurately by the lighter pigmentation characteristic of the animal hemisphere. This allows specific targeting of injection.

Chapter 3 Cloning and sequencing of a candidate HP1α and HP1γ cDNA in *Xenopus laevis*

3.1 Introduction

The molecular events, which lead to aneuploidy, will be only understood by investigating the biochemical basis of normal centromeric structures. Much of the work on underpinning the role of heterochromatin in centromere function has been done in genetically tractable organisms such as the fruit fly, *D. melanogaster* and the yeast, *S. pombe.* It would be useful if there were a biochemical system available for the molecular characterisation of heterochromatin formation. Nuclear and chromatin assembly has been reconstituted *in vitro* by using cell-free extracts from the eggs of the South African clawed toad *Xenopus laevis,* which contain large stockpiles of disassembled nuclear components intended for use during early development. Each unfertilised *Xenopus* egg contains sufficient stores for precursors to assemble up to 12,000 nuclei in the absence of *de novo* transcription. In addition the regulation of early development in *Xenopus* can be studied via the microinjection. *Xenopus* is now commonly used for development studies. A great advantage of using *Xenopus* is that its oocytes, eggs and embryos are easily obtained. In order to analyse the function of HP1 isoforms in *Xenopus*, four cDNA libraries: testis, Stage 3 oocyte, Stage 6 oocyte,

and Stage 28 embryo were screened for isolating the cDNA sequences encoding the HP1 sequences.

3.2 Results

3.2.1 Isolation of HP1 sequences

As a first step towards analysing heterochromatin proteins in *Xenopus*, the cDNAs for HP1 were isolated by standard methods. Preliminary experiments using antibodies to *Drosophila* HP1 and mammalian HP1 suggest there is HP1 in *Xenopus* oocyte extracts (R. Meehan unpublished data). Pak *et al.*, (1997) identified two subtypes of *Xenopus* HP1 homologues, HP1α, and HP1γ by a two-hybrid screen for proteins that were bound to the *Xenopus* homologue of Orc1p (Xorc1) fused to the Lex A DNA binding domain. The two clones they isolated are not full length as both lacked truncated parts of amino acid sequences in the N terminal region. The amino acid sequences of *x*HP1α and *x*HP1γ were compared to various chromo-domain containing proteins: *Drosophila* HP1, mouse HP1α, mouse HP1γ, human HP1α and human HP1γ homologues. This reveals that *Xenopus* HP1 protein is a member of the HP1 protein family and is highly conserved in evolution (Figure 5).

Following this study, a series of experiments was designed to clone the full length of *Xenopus* HP1 proteins by the Polymerase Chain Reaction (PCR) technique. Four different cDNA libraries: testis, Stage 3 oocyte, Stage 6 oocyte, Stage 28 embryo (cloned in the ZAP EXPRESS^{TM} EcoRI/XhoI vector cloning kit, [Stratagene]) were screened. Using human HP1α and HP1γ DNA sequences as hybridisation

probes, *x*HP1α gene expressions were detected in testis, Stage6 oocyte, and Stage 28 embryo cDNA libraries (Data not shown). The result implies that there is abundant HP1 protein in *Xenopus* Stage 6 oocytes.

The strategy used was PCR amplification with a 3' downstream specific primer and a 5' universal primer located in the vector. This method was shown to amplify DNA methyltransferase I in the *Xenopus* St.28 cDNA library in this laboratory. However, no amplification of *x*HP1 genes in all libraries could be obtained.

Two nested-pairs of primers for *x*HP1α and *x*HP1γ were then designed to amplify truncated *x*HP1 cDNAs from oocyte cDNA library. The results demonstrated the existence of *x*HP1α and *x*HP1γ genes in this library. Consequently, the truncated *x*HP1 cDNAs were incorporated in the pET expression vector and the recombinant proteins were used to raise antibodies in rabbits against *x*HP1α and *x*HP1γ.

A subsequent strategy was to amplify the full length genes in oocyte cDNA libraries. To achieve this end, the 5' RACE system (LIFE TECHNOLOGY) was used. Four positive PCR products were obtained from the PCR amplification of Stage 3 and Stage 6 oocyte library, two for *x*HP1α and two for *x*HP1γ (Figure 1). All the PCR products are over 750 base pairs. Following amplification, 5' RACE products were cloned and sequenced. Both HP1α cDNAs contain an open reading frame (ORF) of 600 base pairs and the two HP1γ cDNAs contain an open reading frame of 525 base pairs. All of the ORFs start at ATG initiation cordons and in frame stop cordons, TAA. Potentially, these products include the full length of HP1 cDNAs.

To inspect the new *x*HP1 sequences, comparison of the newly obtained HP1 cDNAs and the published cDNA sequences (Figure 2, 3 and 4) were performed. The result shows that the new *x*HP1α cDNA sequence is 174 base pairs or 58 amino acids longer than the published sequences(Pak et al., 1997). However, the new

*x*HP1γ cDNA sequence is only 10 base pairs or 4 amino acids longer than the previously published one. HP1 protein homologous alignments were performed with the protein sequences derived from *Xenopus lavies, Mus musculus* and *Homo sapiens* using GeneJockeyII software. However, for a technical reason, the GeneJockeyII software could not make an *x*HP1α sequences comparison. Thereafter, STRUCTURAL GENETIC matrix was used to compare the *x*HP1α homologues. The derived new *x*HP1α protein sequence shows 74% identity with that of *Mus musculus* and *Homo Sapiens* HP1α and the sequence contains the full sequences of the conserved chromo domain and chromo shadow domain (Figure 5). Both domains are 100% identical with that of *Mus musculus* and *Homo sapiens* HP1α. The comparison of HP1γ protein sequences shows a 90% identity between frog and mammalian HP1γ and 100% identity in chromo and chromo shadow domains (Figure 6). In addition, the alignment between *x*HP1α and *x*HP1γ shows 63% identity and the two protein sequences share the high conserved chromo and chromo shadow domains. To sum up, the two new *x*HP1 cDNAs are the full-length clones of HP1 homologues in *Xenopus laevis* and they contain the two functional chromo domains.

To examine the copy number of *x*HP1 DNA sequences in the frog genome, *Xenopus* genomic DNA was probed with *x*HP1α, *x*HPγ and *x*Polycomb2, which is also a member of the chromo protein family. As a result, both the *x*HP1α and *x*HPγ blots show simple patterns, compared to *x*Polycomb2. There is probably only a low copy-number of both *x*HP1α and *x*HPγ genes encoded in the *Xenopus* genome (Figure 8).

Nevertheless, there is a third isoforms of HP1 both in mammals and birds, called HP1β. In order to identify HP1β in frogs, the PCR screens were done in the *Xenopus* Stage 6 oocyte cDNA libraries. The degenerated primers were designed

from the highly conserved region of human HP1β. A number of different primers were tested in an attempt to generate specific fragments. Different strategies were tried to increase the stringency of hybridisation for example, by increasing the annealing temperatures during the PCR reaction to favour exactly matched DNA hybrids. However, in all the cases the results were difficult to analyse due to the presence of multiple PCR products.

3.2.2 HP1 expression in *Xenopus* embryos

The requirement for HP1 proteins during frog development were analysed initially by studying the expression levels of HP1 mRNA during development. To represent an entire frog's development process, oocytes and embryos from different representative stages were collected. Those samples were including the two different stages of oocyte, 7 different stages of embryos, which were: egg, blastula, mid-blastula, gastrula, neurula, tail bud, and stage40 embryos. In addition, a liver sample from a mature male frog was also collected. The life cycle of *Xenopus laevis* development is shown in figure 9. The total RNAs in several different stages of *Xenopus* embryos were isolated by standard methods (see Chapter 2). The yields of total RNAs were determined spectrophotometrically at 260 nm. To determining the integrity of the RNAs, the RNAs were taken using equal amounts (10 μg) and run into a formaldehyde-agarose gel (Figure 10). All the RNAs exhibited the clear 28S and 18S ribosomal RNA in ethidium bromide staining with a near 2:1 ratio, indicating that no significant degradation of RNA had occurred.

To detect the expression levels of HP1 mRNAs during development, all the total RNAs were used to synthesise the first strand of cDNAs by reverse transcription

(RT). The cDNAs were amplified using *x*HP1α or *x*HP1γ primers. To determine the linear range of PCR amplification, *x*HP1α cDNAs were amplified using different volumes in descending order (1-7 μl) of 1:10 diluted Stage 6 oocyte first strand cDNA. A blank PCR was run for calibration purpose and to confirm the exclusion of DNA contamination from outside sources. The equivalent amount of PCR products were analysed on a 1% agarose gel followed by phosphor-imager quantification. A calibration of the quantification was performed by regression analysis using EXCEL software. The calibration showed a 0.9577 correlation coefficient and a linear range of between 0-7 μl of 1:10 dilution of first strand oocyte cDNA (Figure 11).

As a consequence of the calibration result, all the different development stages of first strand cDNA were diluted in the ratio 1:10. The *x*HP1α cDNA amplification was performed using 1μl of the diluted first strand cDNAs. On the other hand, histone H4 expression levels were used to normalise the HP1 expression levels since histone H4 is a housekeeping gene that is fairly constant during the developmental stages. The highest-expression levels for both mRNAs were found in two stages of oocyte maturation. These mRNAs are of maternal origin (Figure 12A, B). Each unfertilised *Xenopus* egg contains sufficient stores of precursors to assemble up to 12,000 nuclei and transcription in the embryo, and is activated only after the mid-blastula transition (MBT). The presence of HP1α transcripts prepared during oogenesis indicates that *x*HP1α is one of many essential components present during early frog-embryo development. To characterise the transcription level of *x*HP1α during developmental stages, the intensities of HP1α PCR products were normalised to that of histone H4 and calibrated (Figure 12C). After normalisation, the zygotic transcription of *x*HP1α increases right after mid-blastulation and continues to increase to its highest level during neurulation. From then on the *x*HP1α expression

decreases to a similar level observed during blastula stages. Noticeable was the fact that *x*HP1α transcripts are almost undetectable in male frog liver. This implies that *x*HP1α may be essential to the early development in frogs and is closely correlated to neural development.

The same approach with *x*HP1α was used to analyse the *x*HP1γ expression level in several different developmental stages. In the initial experiments, PCR amplifications were unable to detect the *x*HP1γ expression, probably due to their lower abundance. However, using non-diluted first strand cDNA of *x*HP1γ, the resultant PCR products appear at a reasonable level (Figure 13A). The highest expression is found at Stage 6 oocyte. This also implies that *x*HP1γ may be essential in the early development of frogs. The intensities of *x*HP1γ PCR products are also normalised to that of histone H4. The graphic representation of *x*HP1γ expression (Figure 13B) shows that the highest expression level occurs during neurulation but only 1/2 the level of *x*HP1α transcription at the same stage. In summary, the results suggest that in frogs both *x*HP1α and *x*HP1γ are present during early development and may be significant for neurulation.

3.2.3 Spatial distribution of *x*HP1expression.

The whole mount RNA *in situ* hybridisation technique was used to investigate the expression patterns of *x*HP1α in *Xenopus* embryos. The experiments reveal that *x*HP1α is predominantly expressed in the ectoderm of blastula embryos (Figure 14). Transcripts of XHP1α were expressed throughout the entire ectoderm. By Stage 20, (neurula stage) and Stage 25 (organeogesis), *x*HP1α is expressed in the dorsal cell layers but the expression almost disappears from the ventral epidermis

(Figure 14D, E). The gene is expressed along the entire anterior-posterior axis. In the tail bud stage transcripts of *x*HP1α are localised in the head region, along the entire spinal chord, and in somites.

However, using whole mount *in situ* hybridisation was unable to detect the expression patterns of *x*HP1γ transcripts. This may be due to the low abundance of the transcripts. Alternatively, a purified anti-*x*HP1γ antibody (purification protocol see Chapter 2) was used to determine the *x*HP1γ protein localisation in *Xenopus* embryos in collaboration with my wife, Yi-Chen Lo. However, since the early-stage embryos are still filled with abundant yolky materials, *Xenopus* embryos are extremely fragile and the sections are not easily prepared. Therefore, only tail bud stage embryos were used for the antibody staining. The immunostaining of *x*HP1γ protein (Figure 15) is localised in nuclei. The distribution of XHP1γ protein is found in the region of the head, along the entire spinal chord and in somites. The ventral epidermis showed less staining.

3.3 Discussion

*x*HP1α and *x*HP1γ full length cDNA sequences were isolated and sequenced. The results demonstrate that there is probably only a low copy number of both *x*HP1α and *x*HPγ genes encoded in the *Xenopus* genome. The alignments of cDNA and derived protein sequences show high identities both with mouse and human homologues. The results also confirm that both the chromo domain and chromo shadow domain are highly conserved from frogs to humans during evolution. Maternal transcripts of both genes are present, but the *x*HP1α gene in frogs is expressed at a higher level than *x*HP1γ at different developmental stages. Although

the *x*HP1γ transcripts pattern is undetectable using *in situ* hybridisation, its protein localisation reveals a similar pattern with *x*HP1α transcripts.

Figure 3-1. Cloning full length HP1α and HP1γ by the 5' RACE system

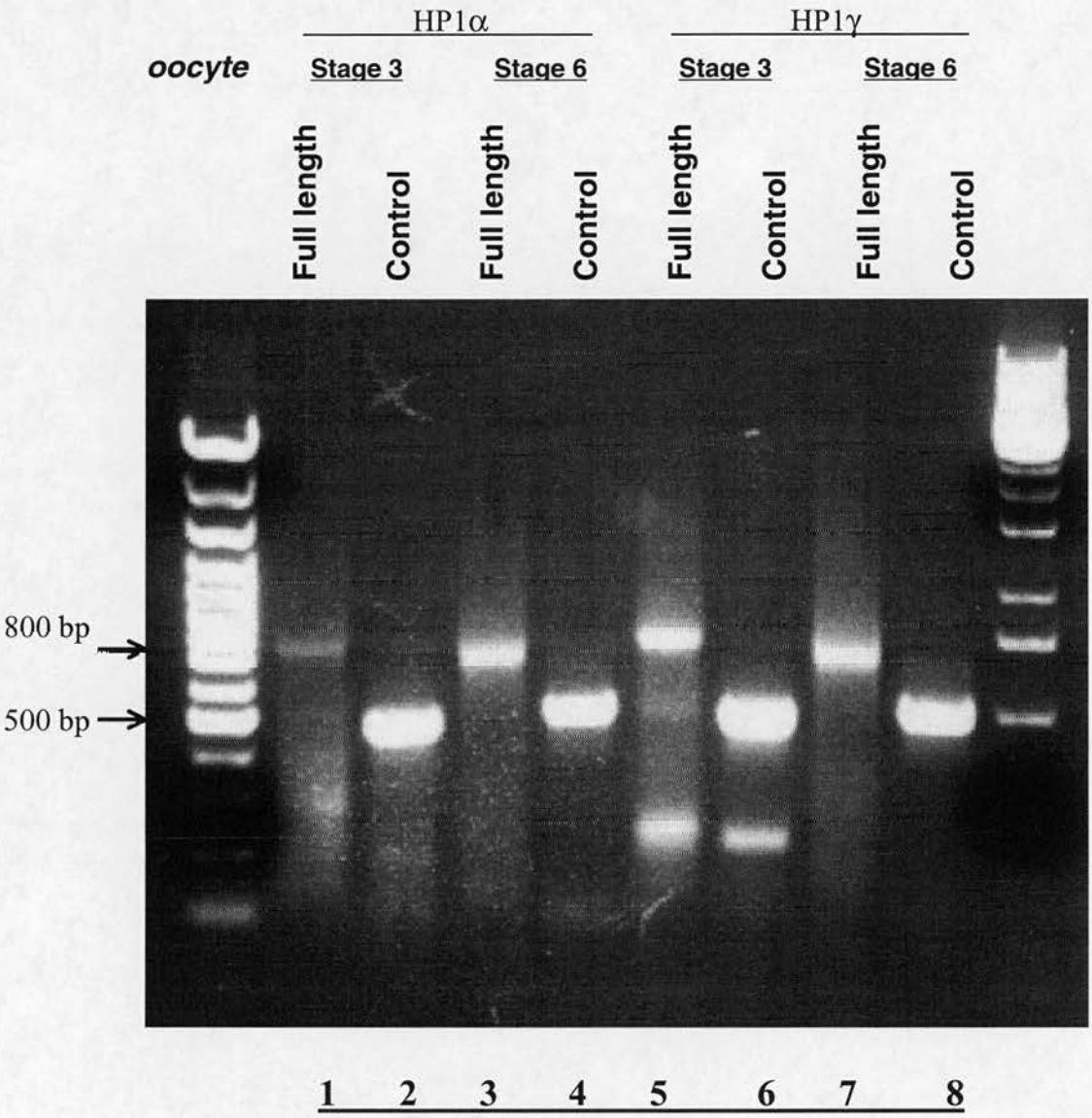

Figure 3-1. cDNA templates were generated from Stage 3 oocyte and Stage 6 oocyte by reverse transcription and amplified by PCR (Stage 3 oocyte; lanes 1,2,5 & 6), (Stage6 oocyte; 3, 4, 7, 8 lanes) Full length PCR amplifications (1, 3, 5, 7 lane) were amplified using Taq DNA polymerase, a nested, gene-specific primer for HP1α and HP1γ respectively, and an abridged anchor primer provided with the 5' RACE system (LIFE TECHNOLOGIES). Control PCR amplifications (2, 4, 6, 8 lane) were amplified using a pairs of nested primers for HP1 α & γ, which were used to produce two short clones of HP1 α & γ for making recombinant protein to raise HP1 antibodies.

Figure 3-2 Comparison of the DNA sequences of Xenopus HP1α cDNA by 5' with the published HP1α cDNA sequence.

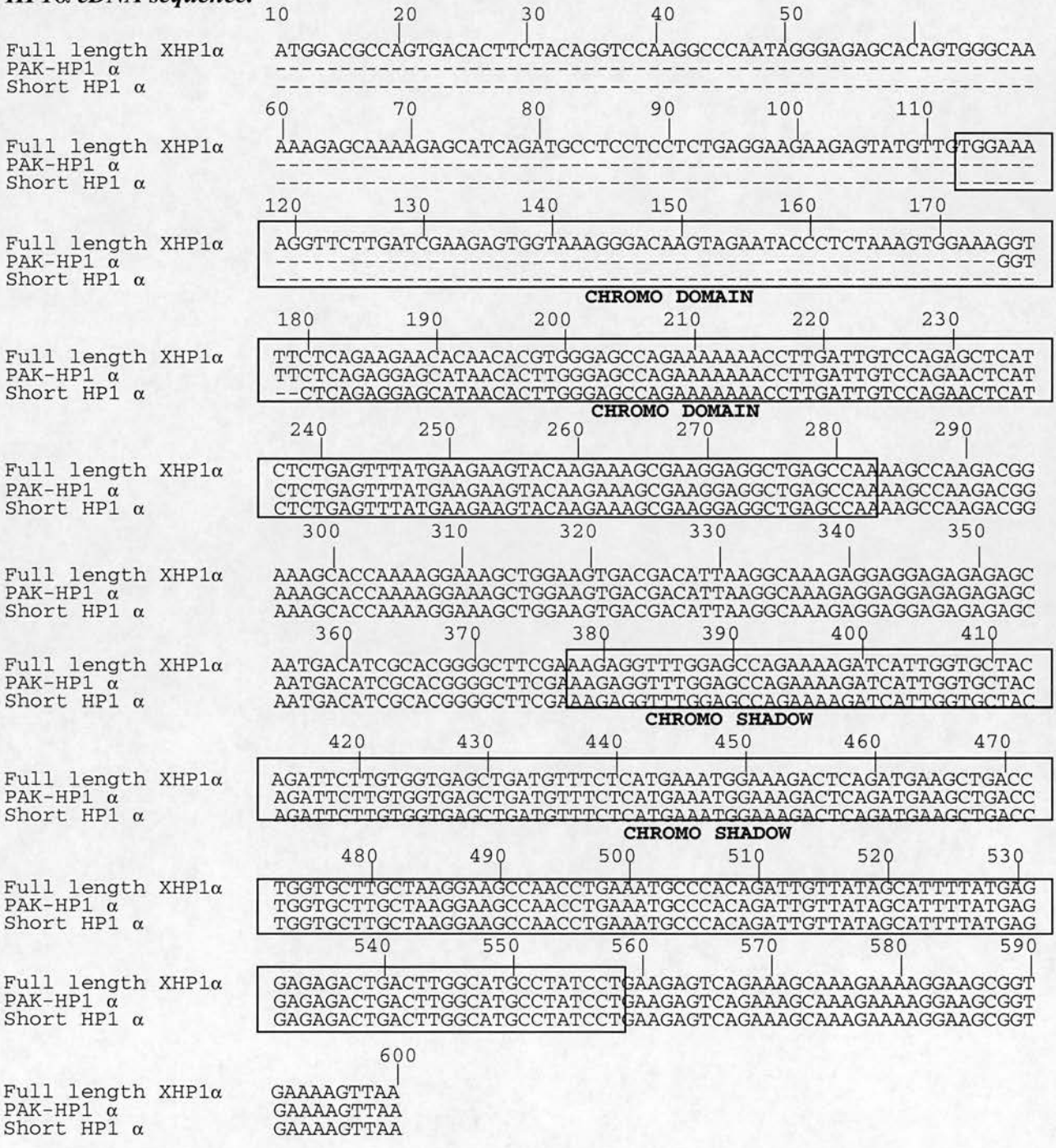

Figure 3-2. The published sequence is abbreviated to PAK-HP1α which was published in Pak's paper (Pak *et al.* 1997). The short HP1α was amplified with primer pairs, which were based on the published sequence. It was expressed as a recombinant protein used to raise an antibody in rabbits. Closed boxes correspond to the conserved chromo domain and chromo shadow domain.

Figure 3-3 Comparison of the DNA sequences of Xenopus HP1γ cDNA with the published HP1γ cDNA sequence.

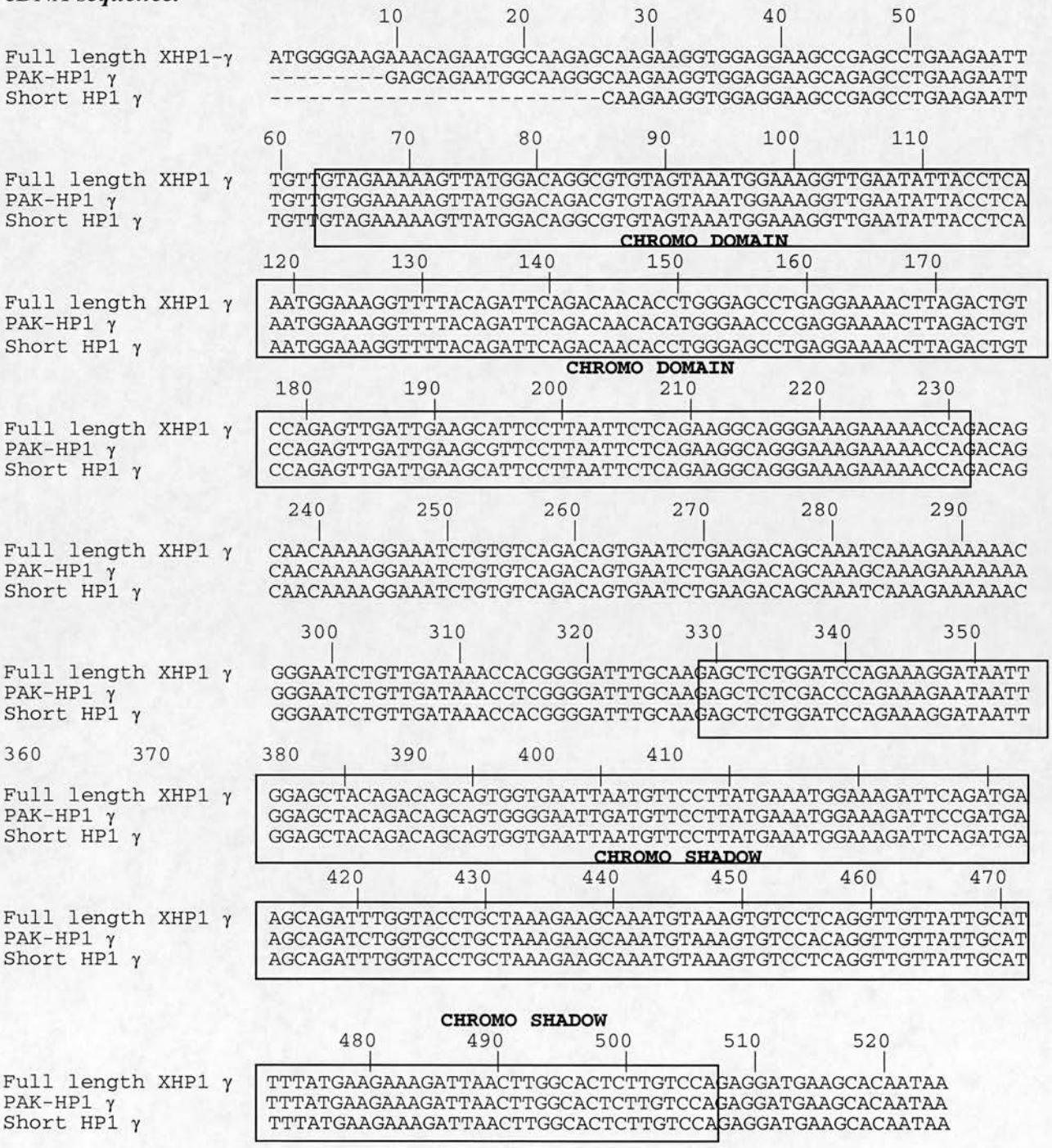

Figure 3-3.The published sequence is abbreviated to PAK-HP1 γ which was published in Pak's paper (Pak *et al.* 1997). The short HP1 γ was amplified with primer pairs, which was based on the published sequence. It was expressed as a recombinant protein used to raise an antibody in rabbits. Closed boxes correspond to the conserved chromo domain and chromo shadow domain.

Figure 3-4 Comparison of the derived protein sequences of Xenopus HP1α, γ with the published sequences. Closed boxes indicate the conserved chromo domain and chromo shadow domain.

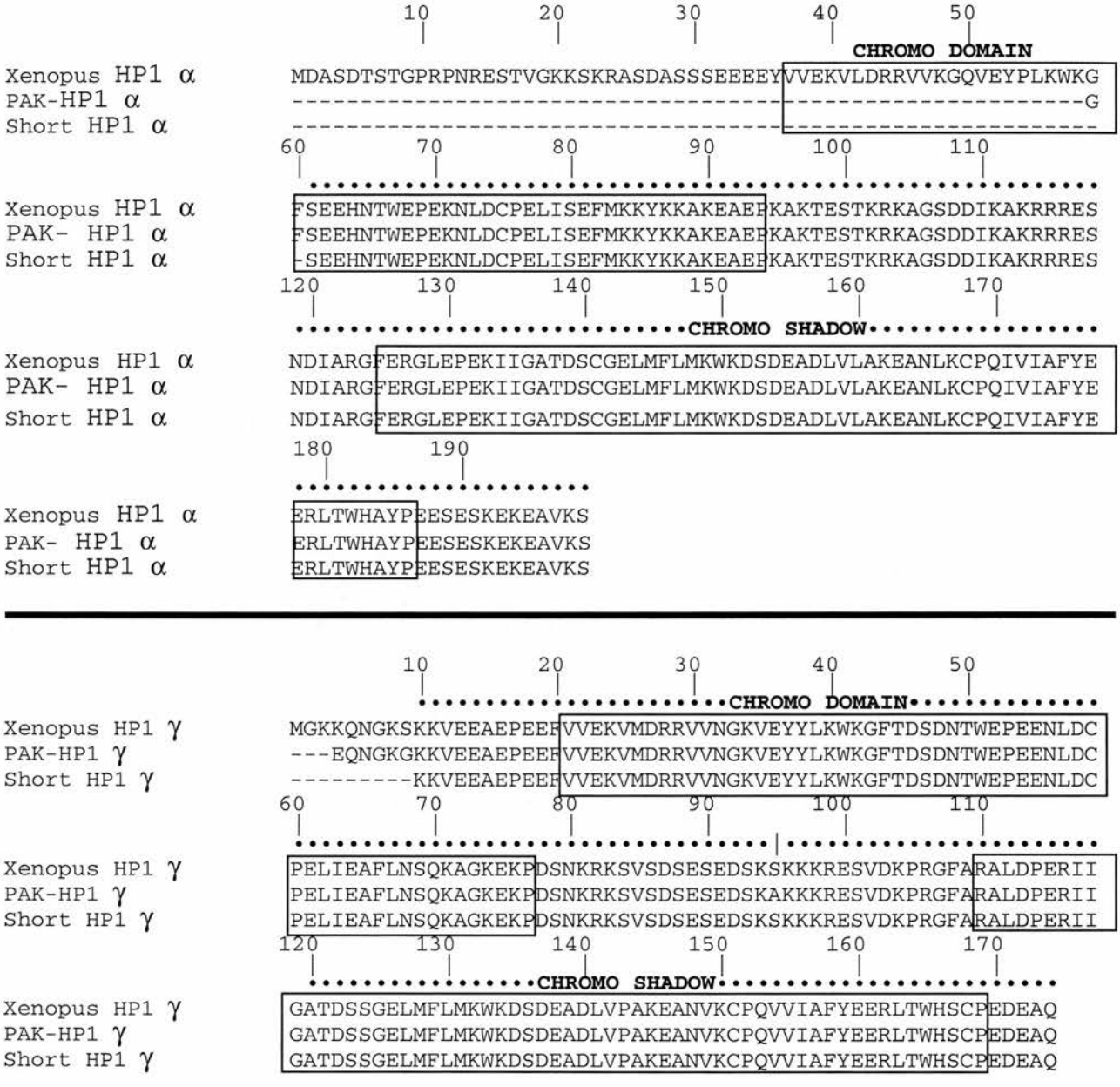

Figure 3-5 Comparison of HP1 α amino acid sequences from Homo sapiens, Mus musculus, Xenopus laevis.

```
          10        20        30        40        50        60
           |        |         |         |         |         |
hHP1ax1    ----------------MGKKTKRTADSSSSEDEEEYVVEKVLDRRVVKGQVEYLLKWKG
mHP1ax2    ----------------MGKKTKRTADSSSSEDEEEYVVEKVLDRRMVKGQVEYLLKWKG
xHP1ax0    MDASDTSTGPRPNRESTVGKKSKRASDASSSE-EEEYVVEKVLDRRVVKGQVEYLLKWKG
                            :***:**::*:**** ************:************
Prim.cons. MDASDTSTGPRPNRESTMGKKTKRTADSSSSEDEEEYVVEKVLDRRVVKGQVEYLLKWKG

                   70        80        90       100       110       120
                    |         |         |         |         |         |
hHP1ax1    FSEEHNTWEPEKNLDCPELISEFMKKYKKMKEGENNKPREKSESNKRKSNFSNSADDIKS
mHP1ax2    FSEEHNTWEPEKNLDCPELISEFMKKYKKMKEGENNKPREKSEGNKRKSSFSNSADDIKS
xHP1ax0    FSEEHNTWEPEKNLDCPELISEFMKKYKKAKEAE---PKAKTESTKRKA----GSDDIKA
           ******************************** **.*   *: *:*..***:    .:****:
Prim.cons. FSEEHNTWEPEKNLDCPELISEFMKKYKKMKEGENNKPREKSESNKRKS2FSNSADDIKS

                  130       140       150       160       170       180
                    |         |         |         |         |         |
hHP1ax1    KKKREQSNDIARGFERGLEPEKIIGATDSCGDLMFLMKWKDTDEADLVLAKEANVKCPQI
mHP1ax2    KKKREQSNDIARGFERGLEPEKIIGATDSCGDLMFLMKWKDTDEADLVLAKEANVKCPQI
xHP1ax0    KRRRE-SNDIARGFERGLEPEKIIGATDSCGELMFLMKWKDSDEADLVLAKEANLKCPQI
           *::** ************************:**********:************:*****
Prim.cons. KKKREQSNDIARGFERGLEPEKIIGATDSCGDLMFLMKWKDTDEADLVLAKEANVKCPQI

                  190       200
                    |         |
hHP1ax1    VIAFYEERLTWHAYPEDAENKEKETAKS
mHP1ax2    VIAFYEERLTWHAYPEDAENKEKESAKS
xHP1ax0    VIAFYEERLTWHAYPEESESKEKEAVKS
      ****************::*.****:.**
Prim.cons. VIAFYEERLTWHAYPEDAENKEKE3AKS
```

Figure 3-5 The CLUSTAL programme was used to align HP1α from human, mouse and *Xenopus*. The N-terminal Chromo domain and C-terminal chromo shadow domain are underlined.

Figure 3-6 Comparison of HP1 γ amino acid sequences from, Homo sapiens, Mus musculus, Xenopus laevis.

```
           10        20        30        40        50        60
            |         |         |         |         |         |
mHP1gx1     MGKKQNGKSKKVEEAEPEEFVVEKVLDRRVVNGKVEYFLKWKGFTDADNTWEPEENLDCP
hHP1gx2     MGKKQNGKSKKVEEAEPEEFVVEKVLDRRVVNGKVEYFLKWKGFTDADNTWEPEENLDCP
xHP1gx0     MGKKQNGKSKKVEEAEPEEFVVEKVMDRRVVNGKVEYYLKWKGFTDSDNTWEPEENLDCP
            ****************************:***********:********:**********
Prim.cons.  MGKKQNGKSKKVEEAEPEEFVVEKVLDRRVVNGKVEYFLKWKGFTDADNTWEPEENLDCP
                   70        80        90       100       110       120
                    |         |         |         |         |         |
mHP1gx1     ELIEDFLNSQKAGKEK-DGTKRKSLSDSESDDSKSKKKRDAADKPRGFARGLDPERIIGA
hHP1gx2     ELIEAFLNSQKAGKEK-DGTKRKSLSDSESDDSKSKKKRDAADKPRGFARGLDPERIIGA
xHP1gx0     ELIEAFLNSQKAGKEKPDSNKRKSVSDSESEDSKSKKKRESVDKPRGFARALDPERIIGA
            **** ********** *..****:*****:********::.********.*********
Prim.cons.  ELIEAFLNSQKAGKEKPDGTKRKSLSDSESDDSKSKKKRDAADKPRGFARGLDPERIIGA
                  130       140       150       160       170
                    |         |         |         |         |
mHP1gx1     TDSSGELMFLMKWKDSDEADLVLAKEANMKCPQIVIAFYEERLTWHSCPEDEAQ
hHP1gx2     IDSSGELMFLMKWKDSDEADLVLAKEANMKCPQIVIAFYEERLTWHSCPEDEAQ
xHP1gx0     TDSSGELMFLMKWKDSDEADLVPAKEANVKCPQVVIAFYEERLTWHSCPEDEAQ
             ********************* *****:****:********************
Prim.cons.  TDSSGELMFLMKWKDSDEADLVLAKEANMKCPQIVIAFYEERLTWHSCPEDEAQ
```

Figure 3-6 The CLUSTAL programme was used to align HP1γ from human, mouse and *Xenopus*. The N-terminal Chromo domain and C-terminal chromo shadow domain are underlined.

Figure 3-7 Comparison of Xenopus laevis HP1 α, γ amino acid sequences. Closed boxes correspond to the conserved chromo domain and chromo shadow domain. The sequences alignment shows *Xenopus* HP1 α and γ have a **63% identity**.

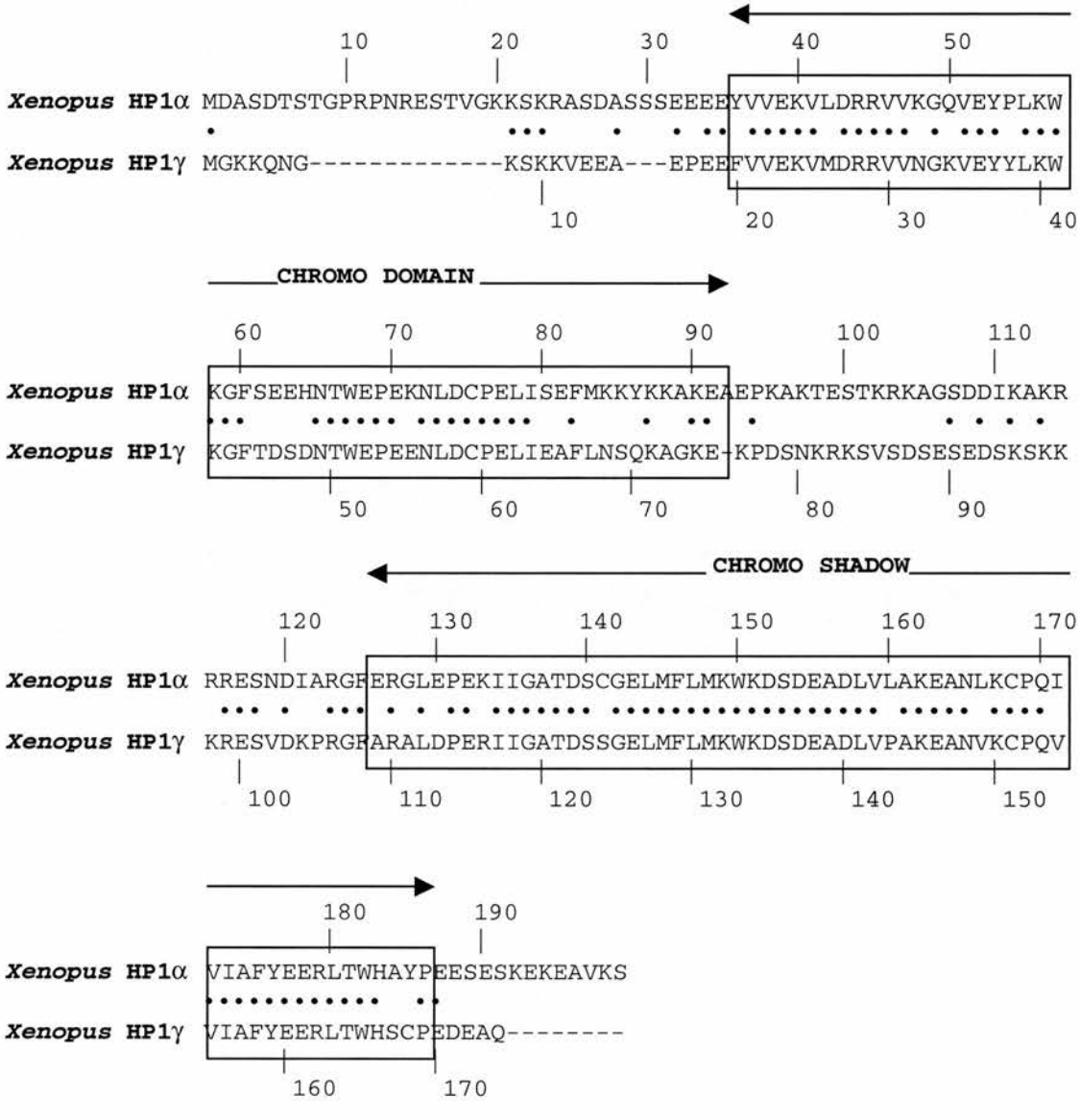

Figure 3-8 Autoradiographs of southern blots of* Xenopus laevis *DNA with HP1α, HP1γ and Polycomb2 probes.

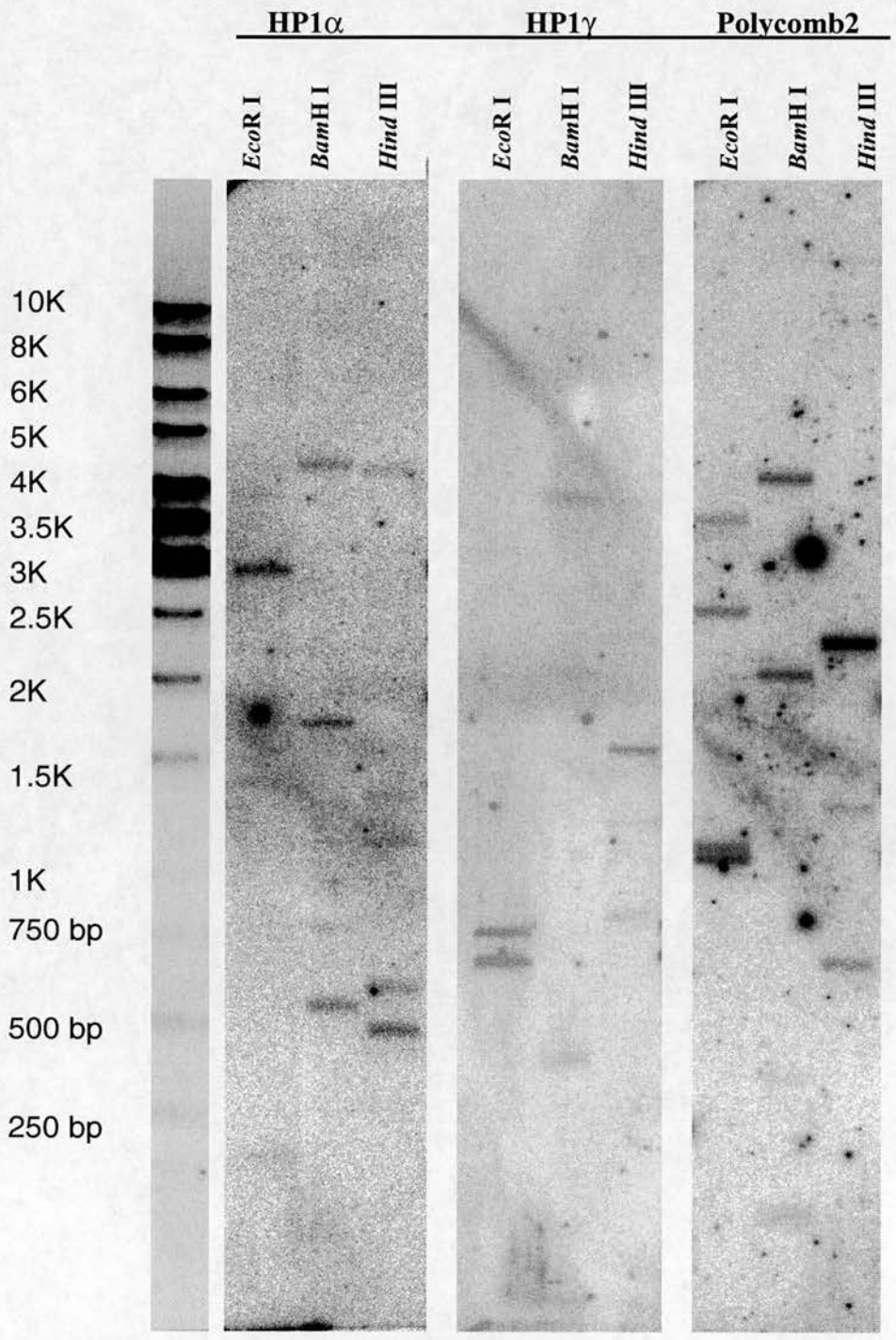

Figure 3-8. Genomic DNA isolated from female *Xenopus* blood nuclei was digested using three different restriction enzymes, *Eco*R I, *Bam*H I and *Hind* III. The DNA fragments were transferred onto nitrocellulose membranes. Membranes were hybridised with HP1α, HP1γ and polycomb2 cDNA probes.

Figure 3-9 *Basic stages of* Xenopus lavies *development.*

This diagram is derived from PRINCIPLES OF DEVELOPMENT (Wolpert, 1998)

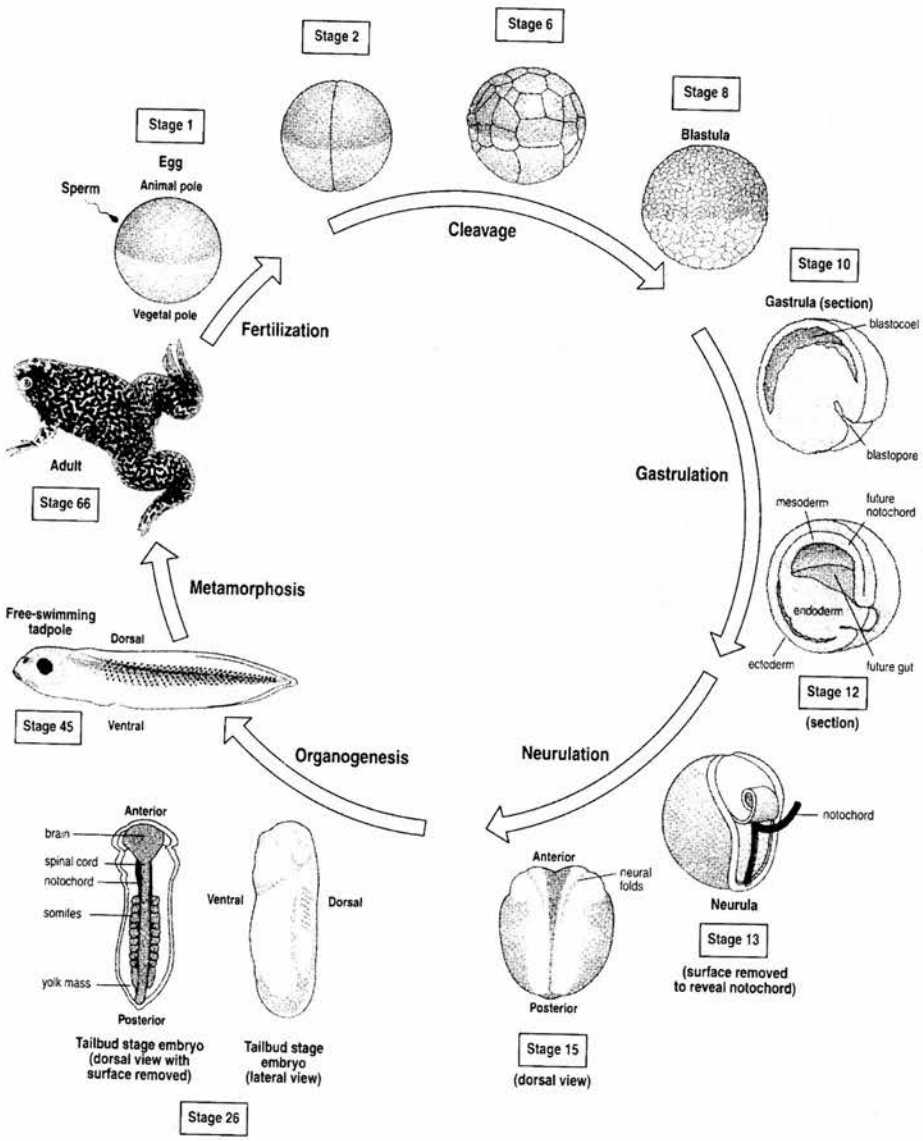

Figure 3-10 *Formaldeyde-agarose gels of total RNA isolated from different* Xenopus *embryo stages and liver.* ***Total RNA from liver was isolated from mature male frog liver. Approximately 10*** μg ***of total RNA were loaded per lane.***

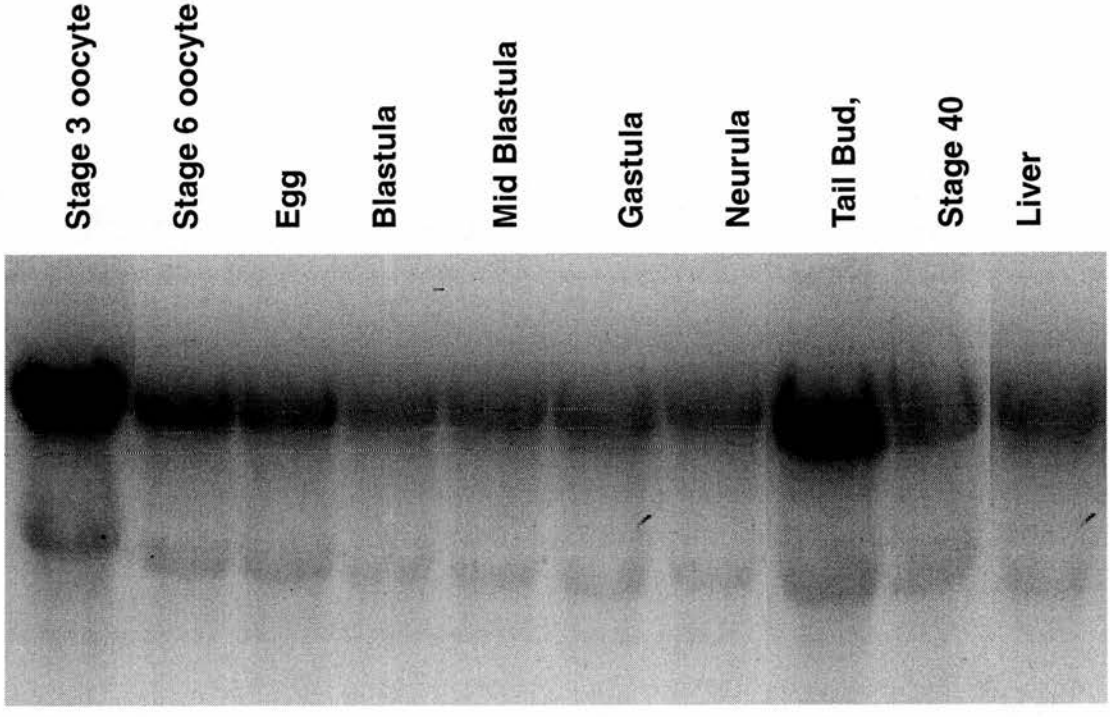

Figure 3-11. Calibration of reverse transcription (RT)-PCR amplifications.

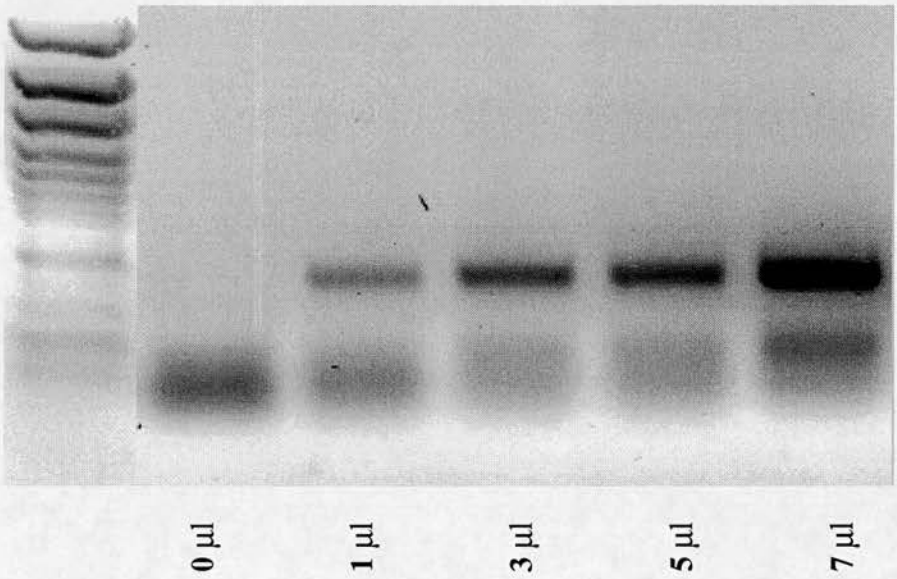

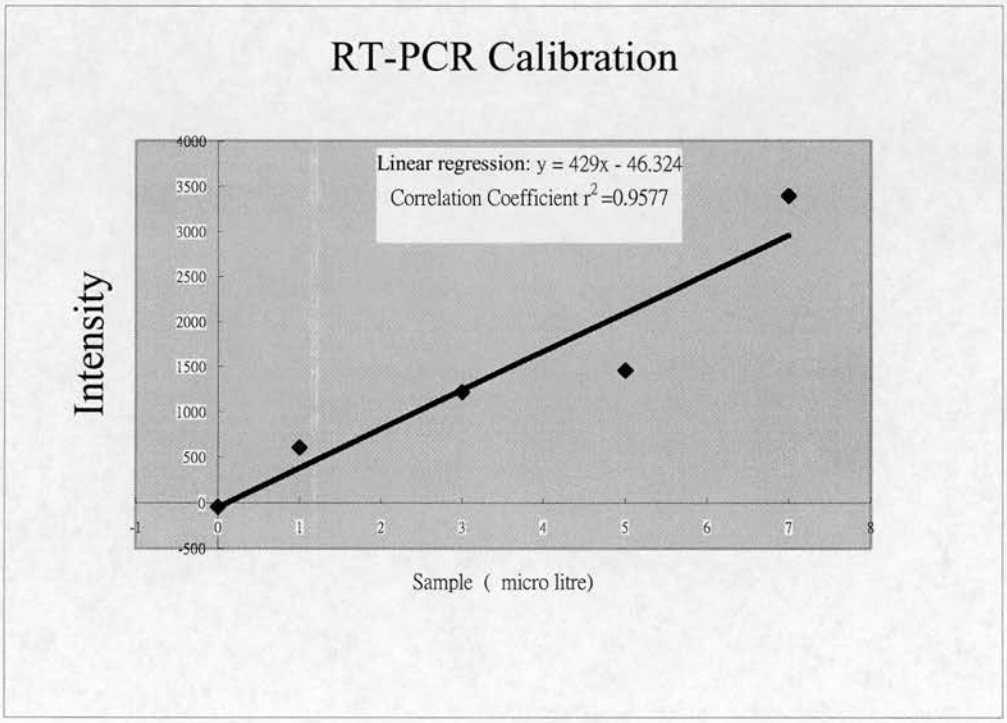

Figure 3-11. *Xenopus* oocyte total RNA (4 µg) was used to make 20µl cDNA by reverse transcription. A 1:10 dilution of cDNA was made. Different volumes (1, 3, 5, 7 µl) of the diluted cDNA were amplified by PCR amplification using a pair of *Xenopus* HP1 α primers. Equivalent amounts of PCR products were loaded per lane. The intensities of each lane were quantified using a phosphorimager (FLA-200, FUJI) and calibrated by EXCEL software.

Figure 3-12 RT-PCR Analysis of HP1α Expression in Different stages Xenopus embryos.

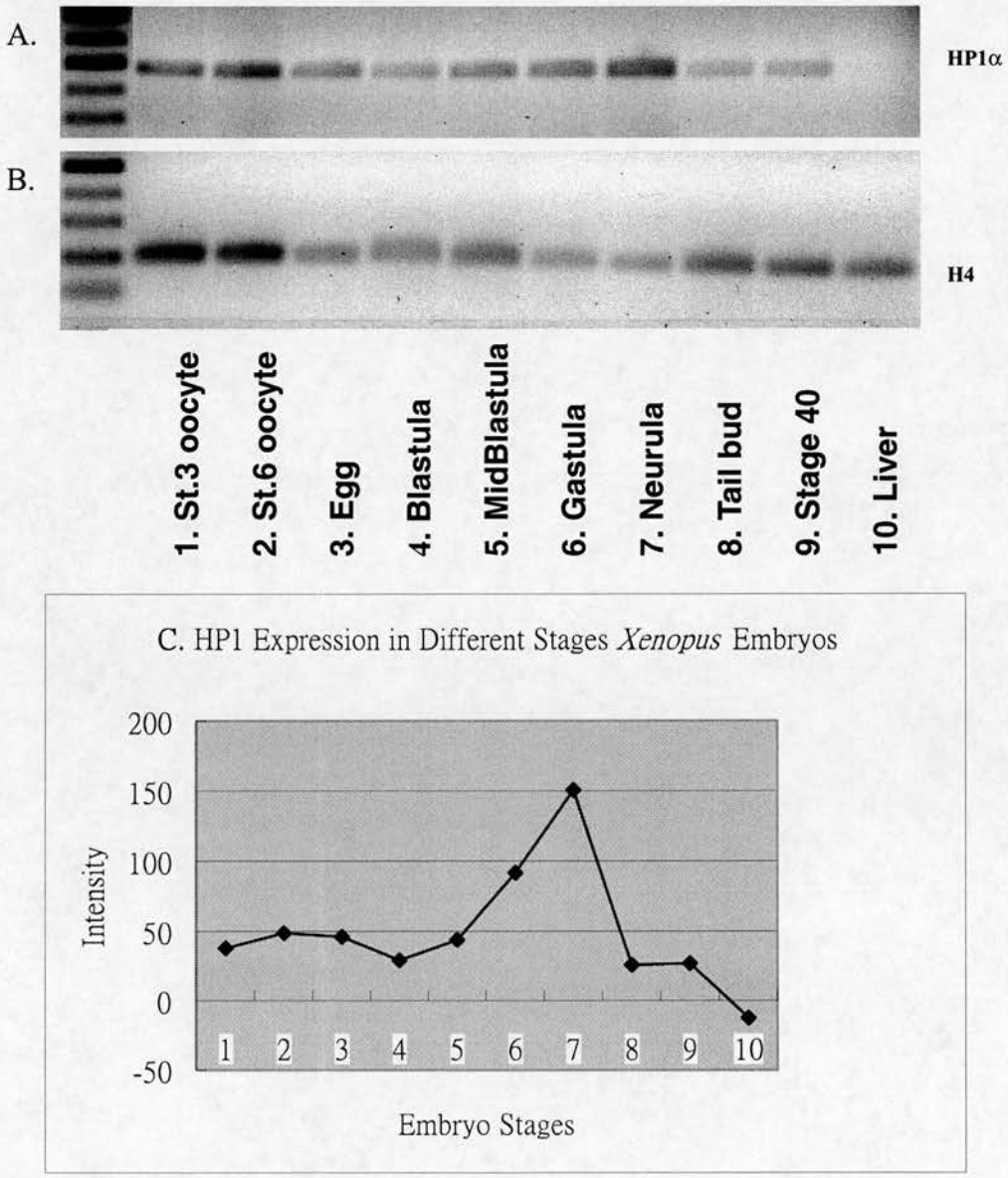

Figure 3-12. Total RNA isolated from different stages of *Xenopus* embryos was used to PCR amplification by a pair of HP1α primers. H4 primers were designed and were used to PCR amplification as a control. **A**. Expression of HP1α varied in different stages of *Xenopus* embryos. **B**. Expresssion of H4 in different stages of *Xenopus* embryos. **C**. A graphical representation of HP1α expression normalised to H4 expression over different stages of *Xenopus* embryos. The intensities of each lane were quantified by phosphoimager (FLA-200, FUJI) and calibrated by EXCEL software.

Figure 3-13. RT-PCR Analysis of xHP1γ Expression in Different stages of Xenopus embryos.

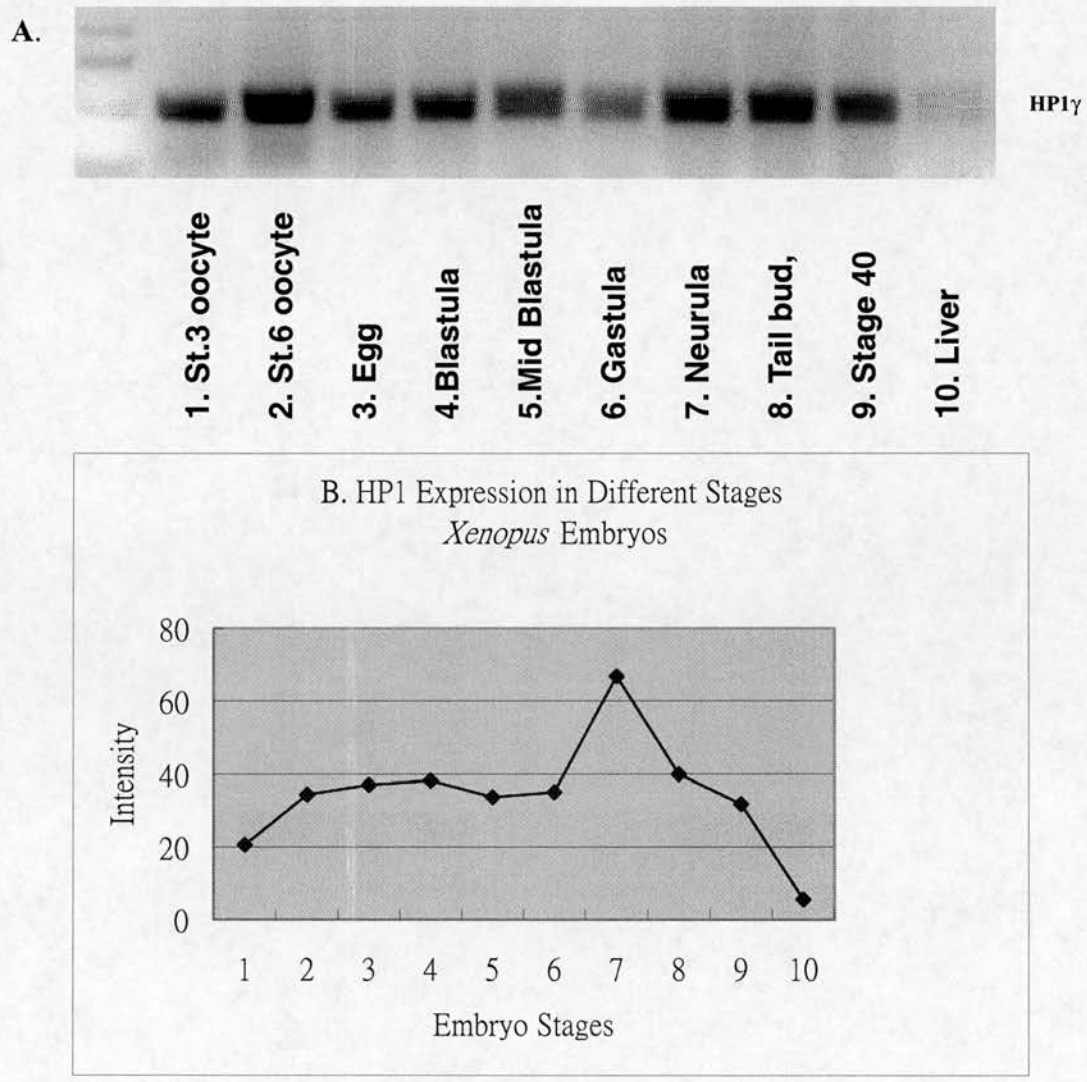

Figure 3-13. The equivalent cDNAs used in Figure 12 without dilution were used in the analysis of HP1γ expression. Each cDNA (1 μl) of was used to amplify HP1γ cDNA. **A**. Expression of HP1γ varied in different stages of *Xenopus* embryos. **B.** A graphical representation of HP1γ expression normalised to H4 expression over different stages *Xenopus* embryo. The same quantification procedures with HP1 α expressions were also applied to HP1γ expressions but adjusted for the dilution factor.

Figure 3-14. Localisation of xHP1 α transcripts during early Xenopus development by whole mount in situ hybridisation

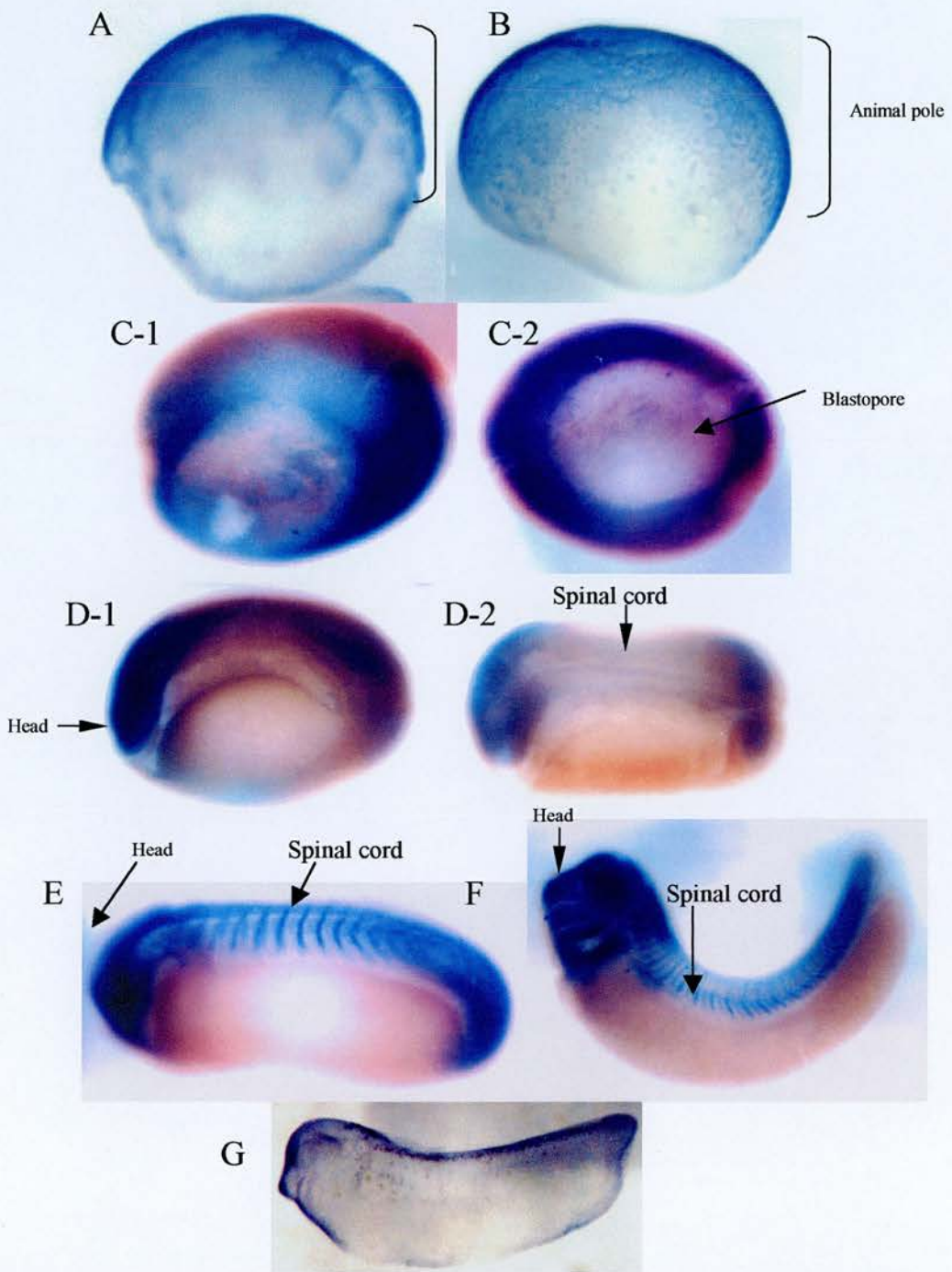

Figure 3-14. Developing embryos at Stage 6 (A), Stage 8 (B), Stage 10 gastrula(C-1, C-2), Stage 20 neurula (D-1, D-2), Stage 25 organogenesis (E), Stage32, tailbud (F) were hybridised with antisense *x*HP1α probe. (G) A Stage-32 embryo was hybridised with sense *x*HP1α probe hybridisation as a negative control.

Figure 3-15. Localisation of xHP1γ proteins in sections of Stage 32, tail bud embryos.

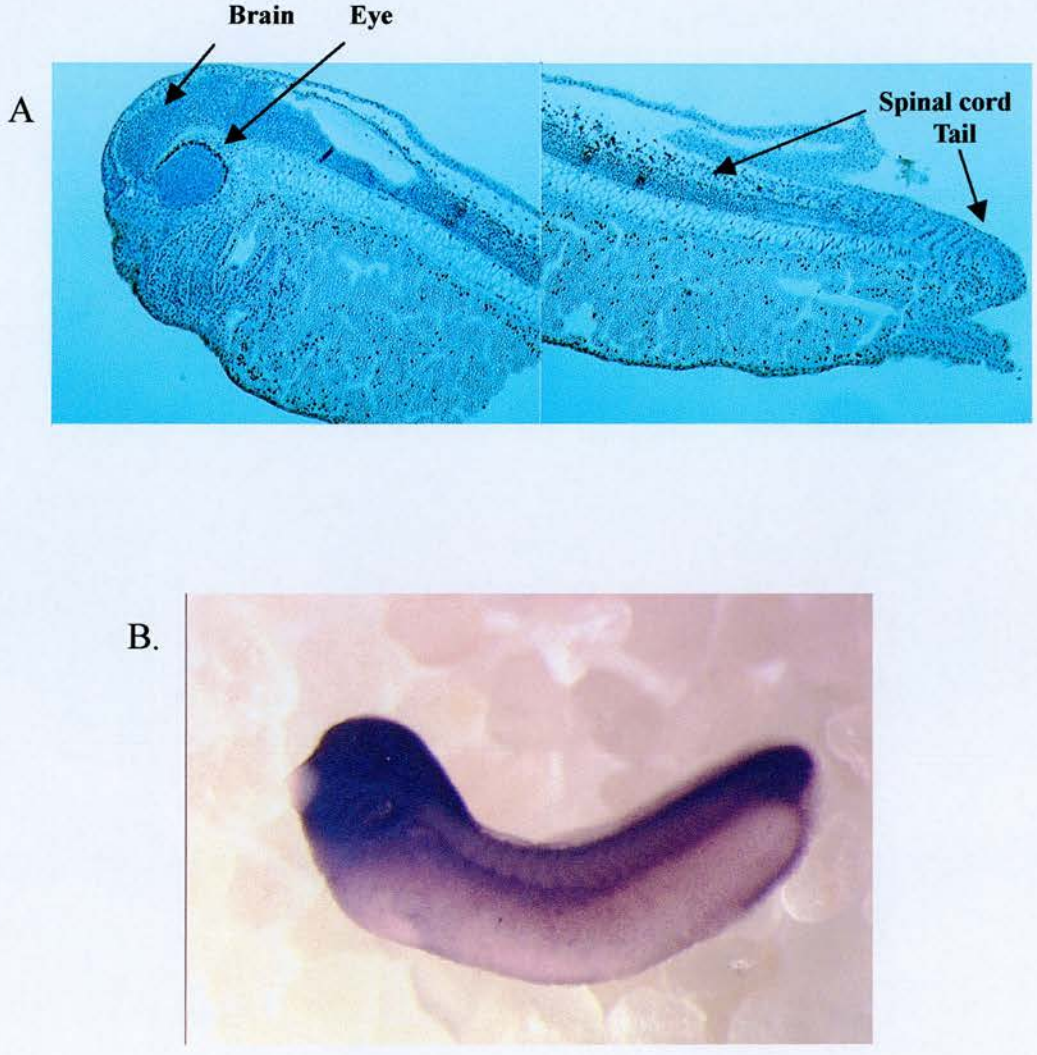

Figure 3-15. A. *x*HP1γ proteins are detected in the head region, brain, and along the spinal chord, and tail region. B. The whole mount *in situ* hybridisation of *x*HP1 γ in developing embryos Stage32, tailbud. The picture is derived form Gawantka et al., 1998.

Chapter 4 Self-association and heterologous interaction of *Xenopus* HP1 proteins

4.1 Introduction

Previous studies have shown that HP1 family proteins undergo self-association. This self-association implies that HP1 might form multimeric complexes to organise higher order heterochromatin structure (Ryan et al., 1999; Eissenberg and Elgin, 2000; Wang et al., 2000). This self-association has been reported for *P. citri* (Citrus red mite) HP1 proteins (Epstein et al., 1992), $HP1^{hs\alpha}$ and mHP1α (Ye et al., 1997). Heterologous interactions between $HP1^{hs\alpha}$ and $HP1^{hs\gamma}$ have also been observed (Ye et al., 1997). In the case of human proteins, the associations depend on the chromo shadow domain (CSD).

To understand the evolution of the HP1 family protein, it is essential to identify whether the *Xenopus* HP1 proteins have the same biochemical features with their homologues in mammals. In order to characterize the biochemical function of *Xenopus* HP1 proteins, *x*HP1α and *x*HP1γ were synthesized bacterially and purified by chromatography. Chemical cross-linking and GST pull-down experiments were performed to determine the propensity of the two *x*HP1 proteins to self-associate.

4.2 Results

4.2.1 Expression and Purification of *Xenopus* HP1 as recombinant proteins

When conducting the self-association experiments, it is useful to express *x*HP1α

and *x*HP1γ bacterially with different N-terminal tags. To this end, the two full-length cDNAs of *x*HP1α and *x*HP1γ were introduced into *E.Coli* expression vectors with two different tags: the 6×histidine tag (Cross et al., 1994) and the GST (glutathione S-transferase) tag (Amersham Pharmacia). Using standard methods (See Chapter 2) the recombinant vectors were transformed a suitable strain of *E. coli* and induced to express the recombinant proteins. For the histidine-tag proteins, both *x*HP1α and *x*HP1γ were not expressed to a high degree. One affinity chromatograph did not produce a high yield of protein . Therefore, additional ion exchange chromatography (anion and cation exchange) was used in order to increase the purity of the end-products (Figure 4.1, A and B; see Chapter2). The ion exchange resulted in adequate purity of the recombinant proteins.

Both GST-fusion *x*HP1α and *x*HP1γ were expressed at the high levels in the soluble *E. coli* fractions using standard methods. In particular, GST-*x*HP1γ was expressed at a very high degree (Figure 4.1, D). Purification of the GST-*x*HP1α and *x*HP1γ was obtained by single-step affinity purification. The end-products were pure enough to perform the assays.

4.2.2 Chemical cross-linking of *Xenopus* HP1 proteins

As the first attempt to determine if *Xenopus* HP1 protein can interact with itself, chemical cross-linking reactions are tested to reveal the association. The purified histidine-tagged *x*HP1α and *x*HP1γ proteins were incubated for 30 minutes with a titrated amount of cross-linking reagent, glutaraldeyde, and separated in SDS-PAGE (Figure 4.2, A and C). The same samples were also transferred onto nitrocellulose membranes and the recombinant proteins were visualized by western blotting with an anti-histidine tag antibody (Figure 4.2, B and D).

For *x*HP1α, the non cross-linked starting material had a molecular weight round 28 KD in the control (lane 1, H_2O added instead of glutaraldehyde). *x*HP1α started to produce a band with a dimer size (56 KD) at 5 mM glutaradehyde and the monomer was much reduced with 20 mM glutaraldehyde (Figure 4.2, A and B).

Similar but distinct cross-linking patterns were obtained with *x*HP1γ. The dimerising process of *x*HP1γ was not as efficient as that with *x*HP1α. The non cross-linked starting material of *x*HP1γ displayed a band of around 21 KD at all concentrations from 0 mM to 50 mM glutaraldehyde (Figure 4.2, C). A similar result was seen with immunoblotting. *x*HP1γ displayed a dimer band with a size of 42 KD at 10 mM glutaraldehyde and the dimer band became stronger when the higher concentrations of glutaraldehyde were added, in this case as high as 50 mM glutaraldehyde. However, in the immunoblotting experiment, as the monomer bands faded at 30 mM and 40 mM, the dimer bands also decreased in strength. A possible interpretation for this occurrence is that a tighter aggregation might occur in *x*HP1γ dimerisation, so masking the histidine-tag from the antibody. This could imply that *x*HP1γ has a different conformation of its dimerised structure when compared with *x*HP1α, and also as anti-his antibody was able to detect the *x*HP1α dimer at the high glutaraldehyde concentration.

4.2.3 Self Association of *Xenopus* HP1 proteins

Mouse HP1-type proteins self-associate in a yeast two-hybrid assay (Le Douarin et al., 1996). Human $HP1^{hs\alpha}$ and $HP1^{hs\gamma}$ also self-associate and interact with each other in a pull-down assay (Ye et al., 1997). In order to examine the self-association of *Xenopus* HP1 proteins, two different types of *in vitro* pull-down assays are used. The first assay took the advantage of two different tagged recombinant HP1 proteins.

GST- *x*HP1α and GST-*x*HP1γ fusion protein were used to pull down histidine tagged *x*HP1α (His-*x*HP1α), which was shown using immonoblotting with the anti-histidine monoclonal antibody. This pull-down reaction was stable in high salt concentrations up to 1.0 M NaCl. Furthermore, there was no protein in the pull-down reaction using GST (Figure 4.3, A). Similarly, histidine-HP1γ (His-HP1γ) was also pulled-down by the GST-*x*HP1γ fusion protein and shown using coomassie blue staining and immunoblotting. This pull-down reaction was also resistant to 1.0 M salt incubation and was not found in the GST pull-down fraction. (Figure 4.3, B). These results show that *x*HP1α and *x*HP1γ can both self-associate and associate with each other *in vitro*. Moreover, this interaction is stable in 1.0 M NaCl.

4.2.4 The chromo shadow domain is necessary for the self-association

To identify the domain of *Xenopus* HP1 proteins responsible for the self-associations and the heterologous interactions, various portions of *Xenopus* HP1 proteins were designed to fuse with GST. All the constructs are summarised in a schematic diagram in Figure 4.4-A. The various constructs of GST-fusion *Xenopus* HP1 proteins were expressed and purified as soluble proteins using the same method applied to the full-length fusion proteins. The SDS-PAGE illustrated in Figure 4.4-B shows the GST fusion protein constructs which include five different truncated *x*HP1α and one truncated *x*HP1γ. The truncated *x*HP1 proteins are: *x*HP1α chromo domain (GST-HP1α-CD); *x*HP1α hinge region and chromo shadow domain (GST-HP1α-H+CSD); *x*HP1α chromo domain and hinge region (GST-HP1α-CD+H); *x*HP1α chromo shadow domain (GST-HP1α-CSD); *x*HP1α hinge region (GST-HP1α-H) and *x*HP1γ hinge region and chromo shadow domain (GST-HP1γ-H+CSD). The gel also shows GST only and full-length *x*HP1α and

*x*HP1γ GST fusion proteins (GST-HP1α, GST-HP1γ).

To confirm the associations of *x*HP1 proteins and to discover the interaction region, pull-down assays were tested using S^{35}-labled *x*HP1α and S^{35}-labled *x*HP1γ made by *in vitro* translation instead of histidine-tagged *x*HP1 proteins (Figure 4.5). S^{35}-labled *x*HP1α was pulled down by the GST-HP1α, GST-HP1α-H+CSD, GST-HP1γ and GST-HP1γ-H+CSD from reticulocyte lysates (Figure 4.5-A, lane 3, lane 5, lane 6 and lane 7), but not GST alone and GST-HP1α-CD (Figure 4.5-A lanes 2 and 4). Furthermore, GST-HP1γ, GST-HP1γ-H+CSD and GST-HP1α pulled down S^{35}-labled XHP1γ (Figure 4.5-B, lanes 3, 4 and 5). Hence, these results verify that *x*HP1α both self-associates and *x*HP1α associates with *x*HP1γ. Additionally, the chromo domain is not necessary for these associations. These results are consistent with those in 4.2.3. The self-association of *x*HP1α and *x*HP1γ, and heterologous interaction between *x*HP1α and *x*HP1γ are steady and stable *in vitro*.

4.3 Discussion

Two previous studies have demonstrated that chromo domain and chromo shadow domain were chemically cross-linked independently (Cowell and Austin, 1997; Yamada et al., 1999). In contrast, the other two studies reported that only the CSD is necessary and sufficient for self-association and heterologous interaction between HP1α and HP1γ in a two-yeast hybrid assay with human proteins (Le Douarin et al., 1996) and *in vitro* binding assay with mouse proteins (Ye et al., 1997). The results I obtained via cross-linking assays and *in vitro* assays reported here are consistent with the idea that the CSD is responsible for the associations. The CD and CSD have their greatest sequence divergence in their carboxyl-terminal regions

(Aasland and Stewart, 1995; Koonin et al., 1995). One possibility to explain the associations is related to this divergence. The highly conserved aromatic amino acid (F167, Y168 in HP1α of mouse; F175, Y176 in *x*HP1α) might play important roles in protein-protein interactions (Ye et al., 1997). In fact, the chromo domain and chromo shadow domain NMR structure (Ball et al., 1997; Brasher et al., 2000) have been resolved and concluded that the HP1β of mouse (MOD 1) forms a dimer in solution. Furthermore, the structure studies show that the dimerisation occurs via the CSD, even though the two domains share a similar compact folding pattern. The interface of the dimer principally involves the c-terminal α-helices of each monomer. The main contact residues, which formed the dimer interface, are I161, Y164, L168 (I173, Y176, L182 in *x*HP1α). The highlighted residues referred to in are conserved in *x*HP1α and *x*HP1γ. The same principles should be able to apply onto *Xenopus* HP1 proteins. The sequence alignments show that *x*HP1 sequences are conserved throughout the evolution. The results recorded in this chapter suggest that the biochemical functions of mammalian HP1 are also conserved in *Xenopus*.

Figure 4-1 Purification of Xenopus HP1 proteins as recombinant proteins.

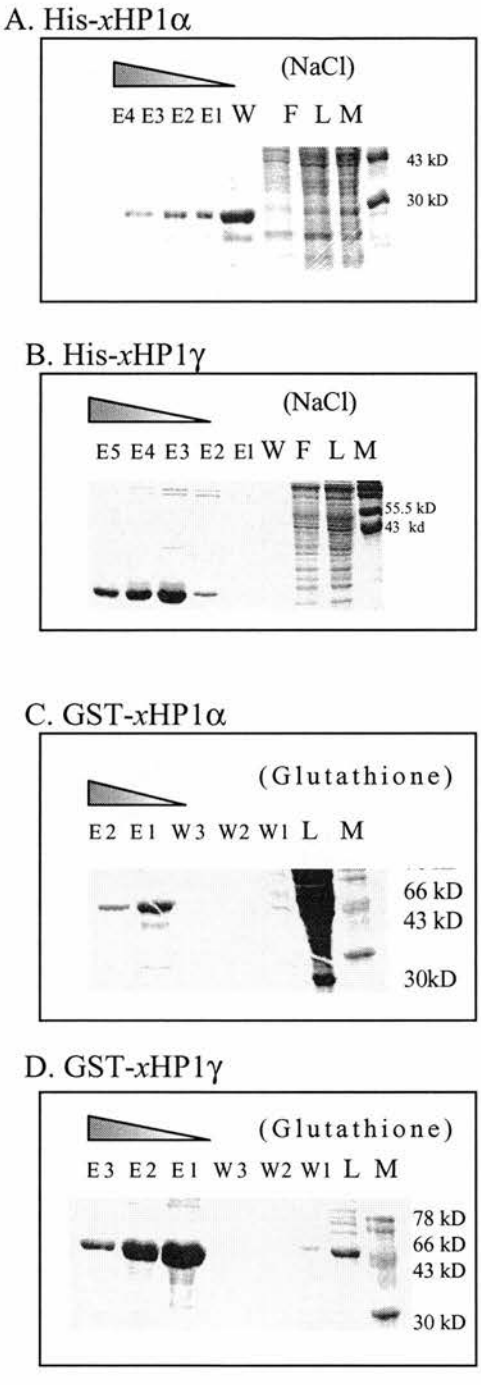

Figure 4-1. (A and B) *x*HP1 α and *x*HP1γ were expressed in *E. coli* with 6 histidine fused onto the N-terminal and purified chromatographically as soluble proteins. (C and D) N-terminal GST (glutathione S-transferase) fusion of *x*HP1 α and *x*HP1γ were expressed in *E. coli* and GST affinity purified as soluble proteins. A full description of the purification procedure is given in Chapter 2. Abbreviations: M, marker; L, crude lysate; F, flow through; W, wash; E, elution.

Figure 4-2 *Chemical Cross-linking of His-xHP1α and His-xHP1γ•*

A. His-*x*HP1α Cross-linking

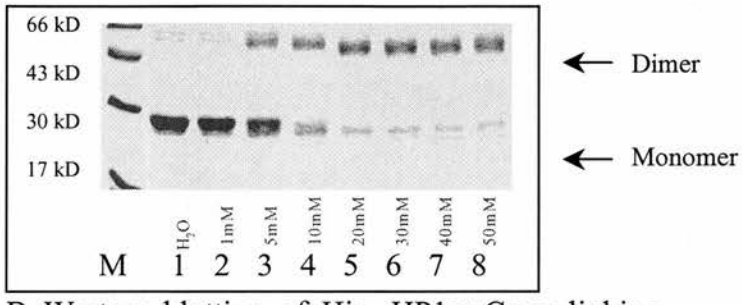

B. Western blotting of His-*x*HP1α Cross-linking by anti-his MAb.

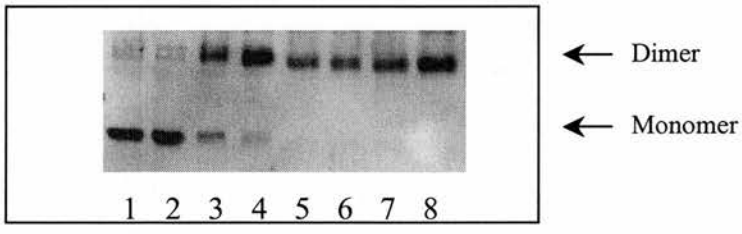

C. His-*x*HP1γ Cross-linking

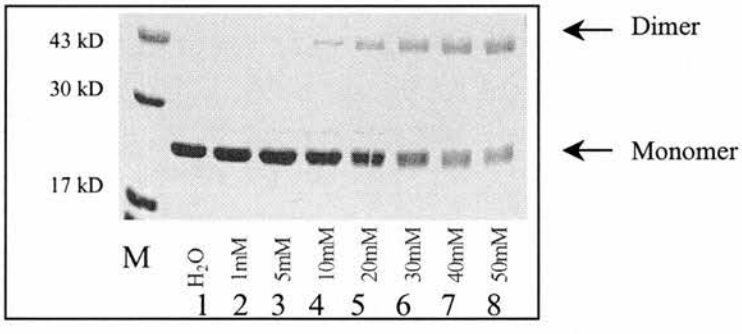

D. Western blotting of His-*x*HP1γ Cross-linking by anti-his MAb.

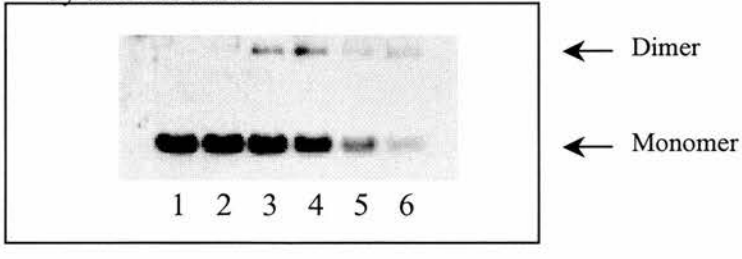

Figure 4-2. (A and B) the purified His-*x*HP1αand His-*x*HP1γ was cross-linked with a titrated concentration of glutaraldehyde and separated in 10 % SDS-PAGE. The concentration of glutaraldehyde was from 0 mM to 50 mM. (C and D) The same cross-linked products of A and B were transferred onto nitrocellulose membranes and detected by anti-histidine tag antibody. Abbreviation: M, size marker.

Figure 4-3 *xHP1α and xHP1γ• self-associate and interact with each other.*

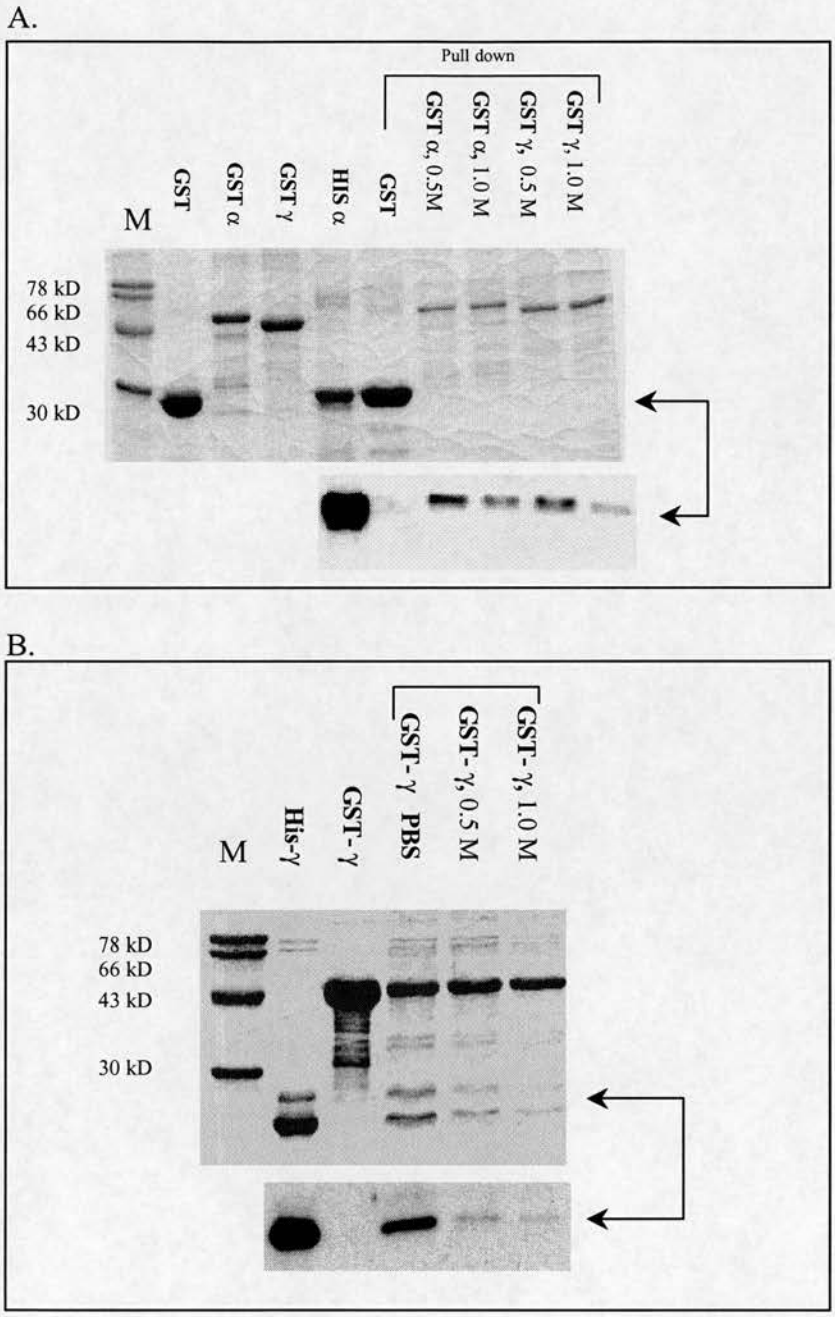

Figure 4.3 (A) Purified His-*x*HP1α• was incubated with GST, GST fusion *x*HP1α(GST-α) and *x*HP1γ(GST-γ) coupled to glutathione-Sepharose in PBS with the addition of 0.5 M and 1.0 M NaCl. The Sepharose was then spun down and washed. The bound proteins were separated by SDS-PAGE and examined by western blotting using anti-histidine tag antibody. (B) Purified His-HP1γ• was incubated with GST-γ coupled to glutathione-Sepharose in PBS with the addition of 0.5 M and 1.0 M NaCl and analysed as the same method with (A). Abbreviation: M, size marker.

Figure 4-4 *Expression and purification of the different domains of GST fusion xHP1 protein constructs.*

A. Schematic diagram of GST fusion constructs.

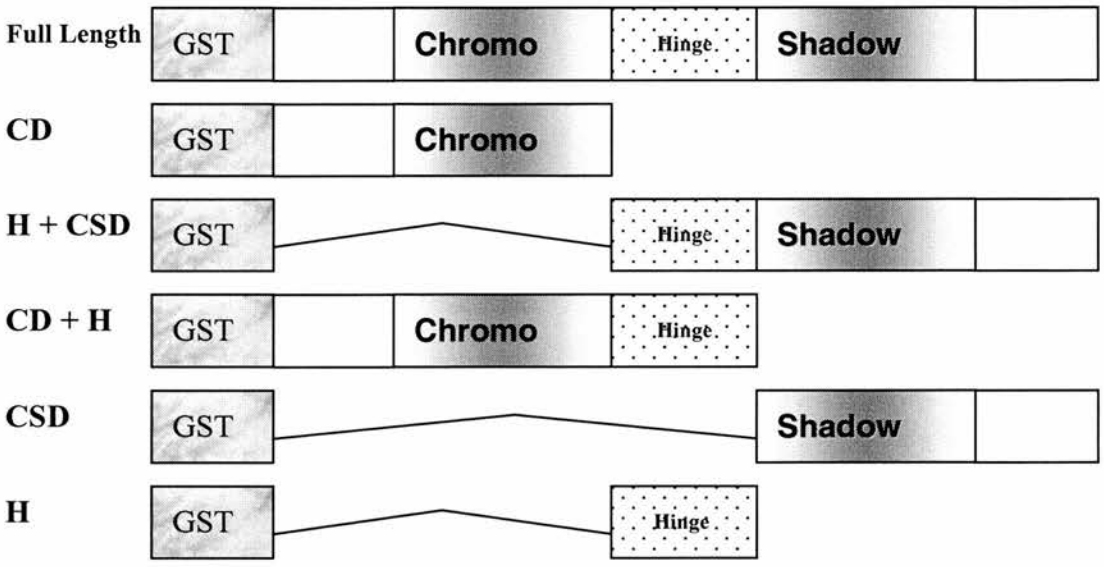

B. The GST fusion HP1 constructs affinity purified as a soluble protein

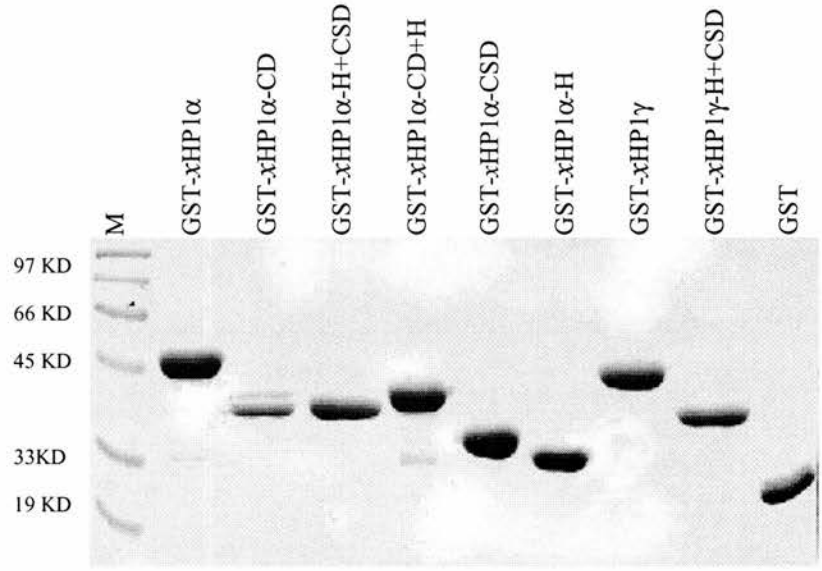

Figure 4-4. (A) Schematic diagram of the GST-*x*HP1 constructs used in this study. (B) The indicated GST-fusion proteins were expressed in *E. coli* and affinity purified as soluble proteins and using in the binding assays. Abbreviation: M, size marker. GST is not drawn to scale.

Figure 4-5 *The shadow domain is responsible for the self-association and protein-protein interactions.*

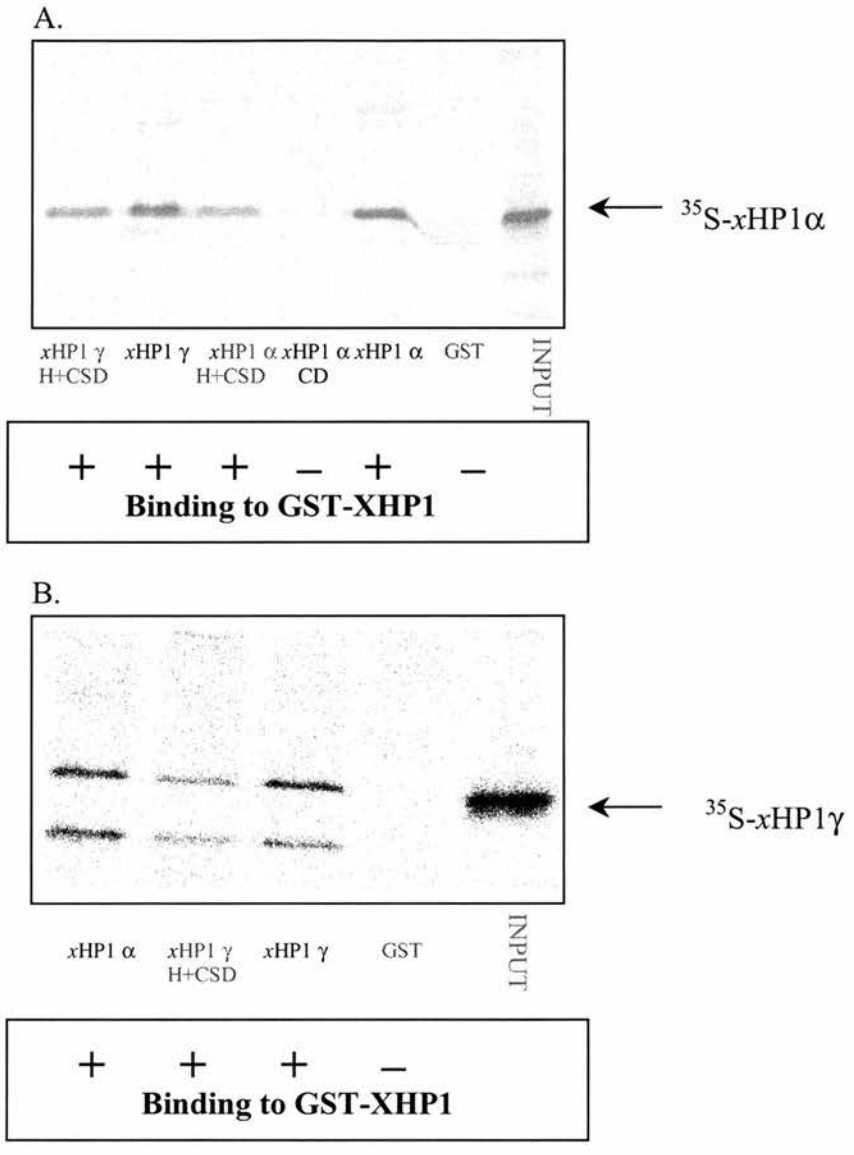

Figure 4.5 (A and B) ^{35}S-*x*HP1α• and ^{35}S-*x*HP1γ were prepared by in-vitro transcription-translation of full-length cDNAs, and the [^{35}S]methionine-labeled protein (arrow) was used in binding reactions with the indicated GST fusion proteins. All the GST-*x*HP1 constructs bound to [^{35}S] methionine-labeled protein were indicated by the plus signs. The input lanes represent the half amount of the total ^{35}S-*x*HP1 in each reaction mixture. No binding was observed in reactions containing GST alone and chromo domain (CD) construct. Only 50% of inputs are shown in the gels.

Figure 4-6 The structure of the shadow chromo domain dimer from MOD1.

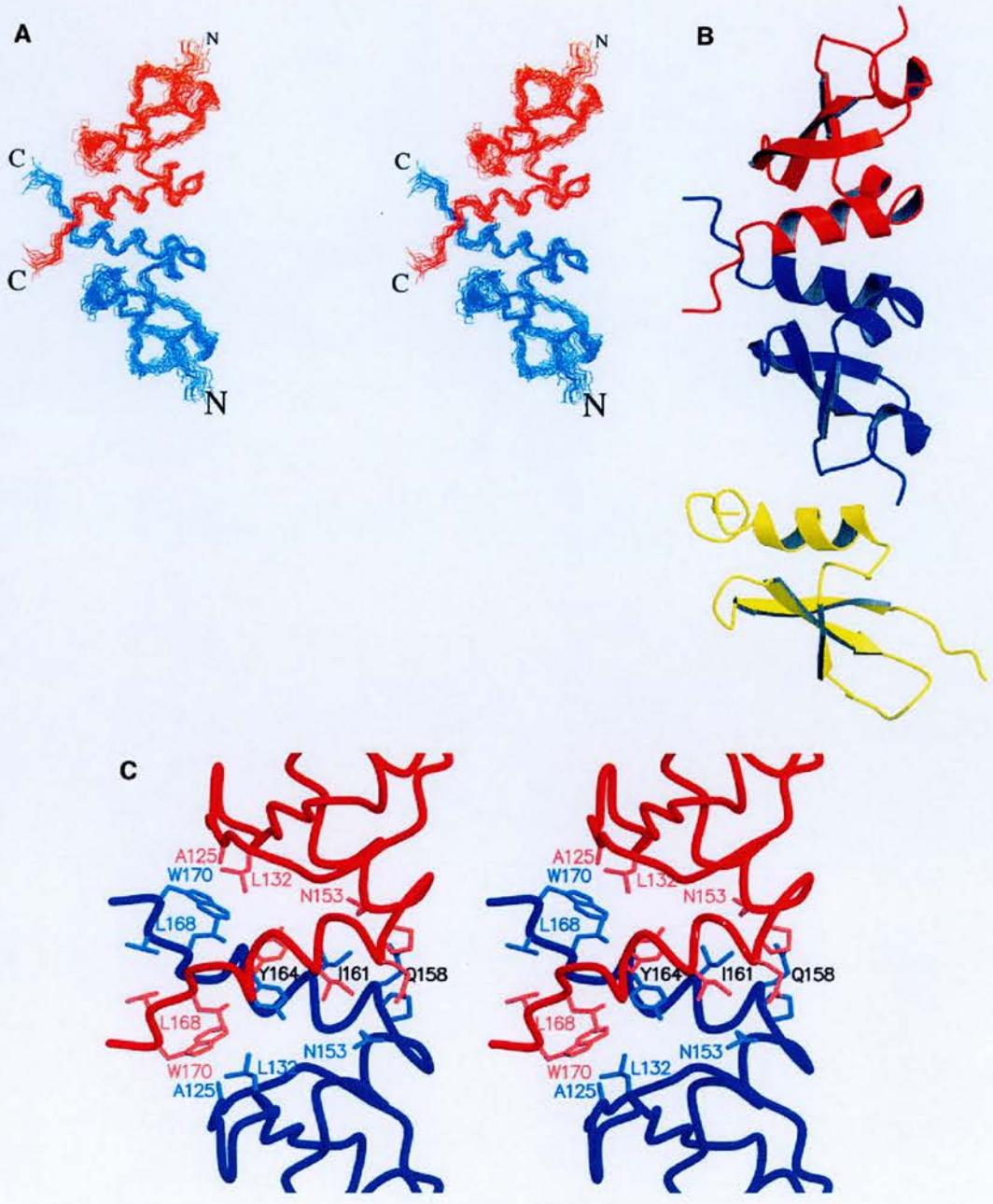

Figure 4.6 A model of CSD dimer structure published by Brasher et.al, 2000. (**A**) A stereo plot of the backbone traces of the ensemble of 16 calculated structures; the two monomers are depicted in red and blue. (**B**) A cartoon representation of the shadow chromo domain dimer (again red and blue) with the chromo domain from MOD1 (yellow) for comparison. (**C**) A close up stereo view of the inter-monomer interface with the side chains of interfacial residues shown; key residues are labelled.

Chapter 5 Xenopus HP1α can interact with DNA and Chromatin

5.1 Introduction

Three isoforms of heterochromatin protein 1, (HP1), α,β and γ have been identified in mammals, which localise to different sub-nuclear locations. In mouse cells, heterochromatin enriched in HP1α and HP1β is separate from less well-characterised nuclear regions enriched in HP1γ, which may correspond to euchromatin (Horseley et al, 1996). More diverse spatial patterns are evident in human cells, where each HP1 homologue targets distinct heterochromatin domains (Minc et at., 1999; Nielsen et al., 1999). HP1α was detected predominantly in heterochromatic region. The large blocks of condensed heterochromatin also contain endogenous HP1β and HP1γ. However, HP1β and HP1γ were detected in many additional sites dispersed with the nucleus in regions consistent with euchromatin.

HP1 is tentatively estimated to have a three-domain structure from several studies (Aasland and Stewart, 1995; Powers and Eissenberg, 1993; Platero et al., 1995) All three mammalian HP1 homologues share this tripartite structure. Two highly conserved regions have been identified at the both ends by comparing the *Drosophila* HP1 with the homologues of mealybug, mouse and human (Clark and Elgin, 1992 ; Epstein et al., 1992; Singh et al,. 1991;Saunders et al., 1993). Near the N-terminus is located a "chromo domain" (CD), which is similar to the *Drosophila* Polycomb and *Schizosaccharomyces* Swi6 proteins (Lorentz et al. 1994), both of

which are also involved in mediating gene repression. Another evolutionarily conserved region, called "chromo shadow domain" (CSD), existed at the C-terminus (Aasland and Stewart, 1995). Cytological analysis of HP1-β-gal fusions of *Drosophila* showed that the CSD corresponds to the nuclear localisation domain (Powers and Eissenberg, 1993). In addition, a central less conserved region (Hinge) is important for the "heterochromatin binding" of the β-gal fusion in the cell nucleus in conjunction with the CSD (Powers and Eissenberg, 1993). It is thought that this binding event occurs via direct binding of HP1 with chromatin, as *Drosophila* HP1 binds to nucleosomes and DNA in vitro (Zhao et al., 2000). In this chapter, I aim to reveal biochemical differences between the different HP1 isoforms that may underlie their different chromatin locations. The two HP1isoforms (α and γ) from *Xenopus laevis* were characterised in terms of DNA and chromatin binding.

5.2 Results

5.2.1 *x*HP1α has DNA binding activity, but not *x*HP1γ

In a previous study, Sugimoto and colleagues used gel mobility shift assays and South-Western-type blotting to demonstrate the DNA binding activity of the recombinant human HP1α. The minimum DNA–binding region was limited to the internal 64 amino acid stretch that is less-conserved between human and fruit fly but retains one half portion of the chromo domain. To determine if *Xenopus* HP1α and γ had similar properties, GST-*x*HP1 fusion proteins were immobilised on glutathione S-sepharose beads and challenged with *Ecor*I or *Hpa*II digested plasmid DNA (Bluescript), or MNase digested chicken chromatin DNA (Figure 5.1). In these three cases, only GST-*x*HP1α retained the DNA on the matrix, whereas GST-*x*HP1γ or GST alone did not. GST-*x*HP1α retained different lengths of DNA equally well

(Figure 5.1, B). As a result, this experiment showed that only *Xenopus* HP1α, but not HP1γ has DNA binding ability *in vitro*. Also, this binding activity has no length preference.

To test whether *x*HP1α had any sequence preference, a 741 bp *Satellite*1 repeat sequence was tested in a pull-down assay. The *Satellite1* repeat sequence is present at around $2\text{-}4\times10^4$ copies in the *Xenopus* genome and localises to pericentromeric DNA in half of its chromosomes (Lam and Carroll, 1983). It is possible that the *Satellite1* sequence is the endogenous binding site for *x*HP1α, since it also shows a pericentromeric localisation. In this case, a satellite clone (PE190 requested from Lam and Carroll) was used in the pull-down assay. The PE190 clone was digested to release the *Satellite1* insert from the parental vector and both the insert and the vector were end-labelled with ^{32}P-α-ATP. In addition a number of pull-down reactions were carried out in the presence of increasing amounts of *E.coli* competitor DNA. As shown in Figure 5.2, *x*HP1α did not appear to have any sequence preference for the *Satellite1* repeat sequence compared to the vector sequence despite the presence of a large molar excess of competitor DNA. As a conclusion, *Xenopus* HP1α but not HP1γ has a non-specific DNA binding activity.

5.2.2 *x*HP1α can bind chromatin, but not *x*HP1γ

It has been recently shown that *Drosophila* and mammalian HP1 are associated with nucleosomal core particles in vivo (Nielsen et al. 2001). To test whether *Xenopus* HP1 proteins can bind to chromatin directly, the pull-down assay was repeated with purified chicken chromatin instead of chromatin DNA. Any resulting interaction was identified by determining whether there was chicken DNA present in the supernatant (S) or the pellet (P). Under a 20 mM salt condition with an increasing

GST-*x*HP1α concentration, more chromatin was retained in the matrix (Figure5.3). Nevertheless up to 20 μg of GST-*x*HP1γ and GST alone did not bound chromatin. Although HP1α and HP1γ are localised to different sub-nuclear locations, there is still a possibility that HP1 isoforms can form a complex, which interacts with chromatin. To test this hypothesis, 6×histidine *x*HP1α was added to GST-*x*HP1γ, which had been coupled to a glutathione bead and used in a pull-down assay. Under these conditions, shown in figure 5.4, the chromatin could be retained on the matrix. Therefore, at least *in vitro, Xenopus* HP1α and HP1γ can combine together and interact with chromatin. This result implied that there might be an undetectable amount of HP1α spreading over large areas of chromatin, which complexes with many other proteins, including HP1γ. Thus, although HP1γ does not show DNA and chromatin binding activities, with the assistance of HP1α and other proteins, HP1γ then is able to associate with chromatin.

These results clearly show that only *x*HP1α, but not *x*HP1γ interacts with chromatin directly, nevertheless the two isoforms of *Xenopus* HP1 can form a complex and bind to chromatin.

5.2.3 Domain determination of *x*HP1α DNA and chromatin binding activity

To investigate whether *Xenopus* HP1 proteins bound chromatin by one of their domains, additional experiments were performed to localise the DNA and chromatin binding activity of *x*HP1α using various truncated GST fusions (Figure 4.4). Figure 5.5 demonstrates that part of the DNA binding activity resides in the hinge (H) region, as the CSD, by itself, cannot bind DNA. However, a fusion comprising of the H and CSD domains can bind DNA. This implies that the H region has intrinsic

DNA binding activity; despite this, it is also apparent that the CD of *x*HP1α has a DNA binding activity that is enhanced in the presence of the H region. In fact, the H region by itself binds DNA avidly, as shown in figure 5.7. This result actually agrees with the previous report published by Himeno's group (Sugimoto et al., 1996) As controls the CD and full length of human HP1α were also tested in the pull-down assays. These two proteins also bound DNA in the same assay condition. Succinctly, *Xenopus* HP1α, like human HP1α, has a non-specific DNA binding activity that is localised to the H and CD region.

HP1 is defined as a non-histone chromosal protein primarily associated with heterochromatin region in Drosophila (James et al. 1989). The chromatin consists of arrays of nucleosomes with approximately 145 bp of DNA wound around an octamer of core histones. Although the above results indicate the DNA binding activity resides in the hinge and CD region, it is important to know that whether they also bind chromatin. Further experiments (Figure 5.6) were carried out to localise the chromatin-binding domain by using the same series of truncated GST fusions that were used to identify the DNA biding domain. In this case the chromatin-binding domain was localised to the H region (Figure 5.6 and 5.7), which is a 23 amino acid motif. This result differs from the previous report from Eissenberg and colleagues. They suggested that *Drosophila* HP1 can bind directly to nucleosomes but intact native HP1 is required for such interactions (Zhao et al. 2000).

5.2.4 Both *x*HP1α & *x*HP1γ bind histone H3 tails when methylated at lysine 9

The above results clearly show that *x*HP1α can interact with nucleosome DNA and chromatin. The protein core of this nucleoprotein complex is an octamer

containing two of each of the histones H3, H4, H2A and H2B. Thus, another question occurs to us: would *Xenopus* HP1 proteins directly interact with H2A, H2B, H3 or H4, the components of the core particle. To answer this question, the GST-*x*HP1 fusion proteins coupled to beads were challenged with purified chicken core histones. As shown in Figure 5.8, the interactions between both *x*HP1α and *x*HP1γ and all core histones were observed. In addition, the interactions between *x*HP1α and core histones were assayed by far western blot analysis, using GST-*x*HP1α as a probe and detecting the interaction using anti-GST anti-body. The result was that the GST- *x*HP1α bound to the histones H3 and linker histone H1 specifically (Figure 5.9).

Two reports (Bannister et al. 2001; Lachner et al., 2001) demonstrate that mammalian HP1 can bind to histone H3 tails when methylated at lysine 9 and the chromo domain of HP1 is responsible for the binding activity. One possibility may explain why we were unable to detect pull down chromatin with *x*HP1γ and the CD of *x*HP1α. The chicken chromatin that we are using may not contain any methylated histone H3. To check this possibility, we also surveyed the chicken chromatin using an antibody which specifically detects dimethylated H3-tails and found that (Figure 5.9) at least, a proportion of histone H3 in the chicken chromatin is methylated. It has been known that the globular domains of each individual histone are responsible for most of the histone-histone and histone-DNA interactions, which hold this complex macromolecular assembly together. In addition the N-terminal regions (tails) of the histones are flexible and highly mobile (Cary et al. 1978). Therefore, we considered a role for histone H3 tail binding in the HP1-nucleosome interaction. We tested this possibility by challenging recombinant HP1 proteins with affinity matrices that containing amino acids 1-21 of histones H3 either in the unmodified or dimethylated

at lysine 9 (Figure 5.10). Using the same conditions as Jenuwein and colleagues (Lachner et al. 2001) , we found that, as expected, human HP1α preferentially binds to the methylated H3 peptide (Me-H3-tail) but not its unmodified counterpart (H3-tail). The same preference for Me-H3-tail is exhibited by *x*HP1γ and *x*HP1α, however, the affinity for *x*HP1α appears to be lower than its human counterpart and *x*HP1γ. When we tested the CD domain of *x*HP1α in isolation, it had the same preference for the Me-H3-tail as *x*HP1γ. It is possible that this is due to sequence differences in the N-terminal tail and hinge region of *x*HP1α, which affects its overall conformation and will be the subject of future investigations.

In a conclusion, the methylated histone H3 tails interacts with the CD of *Xenopus* HP1s; however, this interaction seems not to be responsible for the binding activity of *x*HP1α and chromatin under our assay conditions.

5.2.5 *x*HP1α can bind to a specific population of chromatin and not histone H3-dependent

Our assays routinely employ 5-10 μg of chromatin in our pull-down assays, which differs from the protocol used by Bannister and colleagues (Bannister et al. 2001), who used 200 μg in their assays with mouse HP1β (m HP1β). In their case, approximately 1%, or less, of the input chromatin was found to be associated with the GST-mHP1β. In my assays, 20 mM salt condition, neither the CSD nor the CD domain can bind chromatin, although the CD domain could bind DNA very well (Figure 5.7). The same assay showed that the full length human HP1α could bind chromatin but no chromatin binding activity for the isolated CD could be detected although it too could bind DNA well. We repeated the pull-down experiment using 300 μg, instead of 3 μg of chromatin and found that the CD could not fish out a

significant portion of chromatin from the input chromatin. Full-length *x*HP1α was very efficient in interacting with this substrate whereas as an equal amount of *x*HP1γ was very inefficient in binding chromatin (Figure 5.11). We reasoned that the ability of the CD of *x*HP1α to interact with chromatin is maybe masked by the presence of the H region.

Interestingly, the nucleosomal pattern of the chromatin was altered relatively to the input chromatin pulled down by *x*HP1α (Figure 5.11 and 5.12). In this case I am gratefully got the help of Sari Pennings, she analysed the two populations of chromatins using the phosphor-imager. As representing in figure 5.12, *x*HP1 actually pulled a specific population of chromatin, which had a shorter interval DNA 200 ± 3 base pairs compared to 210 ± 1 base pairs of the input chromatin, and had a longer DNA sticking out at the end of the nucleosomal arrays, 59 ± 13 base pairs compared to 0±7 base pairs of the input chromatin. This may represent chromatin of a specific sequence context or alternatively has an altered confirmation with respect to bulk chromatin. Therefore, it is possibility that this chromatin represents the chromatin with methylated histone H3, which may interact with *x*HP1α specifically. To test this possibility, we repeated the pull-down assay using 300 μg chromatin in the presence of unmodified histone H3 tails and dimethylated histone H3 tails. However, we found that neither unmodified nor dimethylated histone H3 tails altered the efficiency of *x*HP1α chromatin binding. It is possible the small hinge region has a universal chromatin-binding activity whereas the CD is only able to interact with a specific population of chromatin, which might consist a type of classical satellite DNA and will be the subject to future investigations.

5.3 Discussion

The DNA binding assays in this chapter provide a clear evidence for the interaction between DNA and *x*HP1α, but not *x*HP1γ. Neither length nor sequence preference was observed for this DNA binding activity. These results are consistent with a recent study based on *Drosophila* HP1 (Zhao et al. 2000). While it makes sense that HP1 could interact with DNA, a general and sequence-nonspecific affinity for DNA cannot explain the relatively restricted chromosomal distribution *in vivo*. Also, the evidence that only one of *x*HP1 isoforms has DNA binding activity cannot explain their differential sub-nuclear localisations. Similar but different from DNA binding, the chromatin-binding assays give evidence that only *x*HP1α can bind chromatin and the binding domain is even shorter. Only the hinge region is sufficient for the chromatin binding. The hinge region consists of 23 amino acids and shows only 50% consensus to mammalian counterparts (Figure 5.14). This observation actually differs from the two recent reports, which claim that the chromo domain of mammalian and Swi6 can specifically bind to lysine 9 methylated-H3 *in vivo* (Lachner et al. 2001; Bannister et al. 2001). This chromo domain H3-binding activity has been related to the propagation of heterochromatic subdomains in native chromatin. Thus, this binding is required for the heterochromatin localisation and also for propagation of heterochromatin. However, our results cannot see such strong binding of CD domain to chromatin. In contrast, we observed a very weak chromatin-binding activity in CD domain and a fairly strong binding activity in the hinge region. Eissenberg and colleagues demonstrate that *Drosophila* HP1 can bind directly to nucleosomes but intact native HP1 is required for such interactions (Zhao, *et al.* 2000). The important point is that the same constructs, *x*HP1γ and the CD of *x*HP1α that can bind an exposed methylated H3 tails are unable to interact with

native chicken chromatin. The far western analysis of native core histones confirmed the specificity of the interaction between *x*HP1α and histone H3. These data further support the notion that it is the hinge region of *x*HP1α that has intrinsic chromatin binding activity. In the far western assay, *x*HP1α was able to interact with linker histone H1. Linker histones are believed to absolutely required for the *in vitro* formation of highly folded 30 nm chromatin fibres. Nucleosomal arrays interact with linker histones to form a highly folded transcriptionally repressive '30 nm diameter' chromatin fibre (van Holde, 1988; Wolffe, 1995; Fletcher and Hansen, 1996), and with different chromatin-associated protein to form other types of specific functional chromosomal domains (Wolffe, 1995; Hansen, 1997). In our results, *x*HP1 shows a preference for histone H1, but not H5. Intriguingly, Nielsen and colleagues also demonstrate that mouse HP1α can interact with linker histone H1 and the interaction domain is localised to the hinge region (Nielsen et al. 2001). Taken together, it could be this specific interaction is related to a particular formation of chromatin, which composes the heterochromatin. That is an interesting point to be investigated in the future.

Our assay also demonstrates that the *x*HP1α can pick up a specific population of chromatin out of the bulk chromatin; however, we do not know if this particular population of chromatin has any specific properties, with respect to sequence or chromatin organisation. Presumably, there are other HP1 interacting factors that confer additional specificity on HP1 binding in heterochromatin. Although we did not see that methylated H3 tails interrupts *x*HP1α chromatin-binding activity, one still cannot preclude that the tails may play a role in the targeting of HP1 proteins to specific chromosomal sites. Relevant to this is the recent demonstration that *in vivo* abrogation of the histone H3 methyltansferase activity of Suv39h1 prevents that

heterochromatin association of HP1 proteins. This result indicate that methylation of H3 tails may be critical in directing the localisation of HP1s to heterochromatin (Rea et al., 2000). Whether or not other post-translational modifications, such as acetylation and/or phosphorylation, may also be involved remains to be determined.

Figure 5-1 Xenopus HP1α interacts with DNA

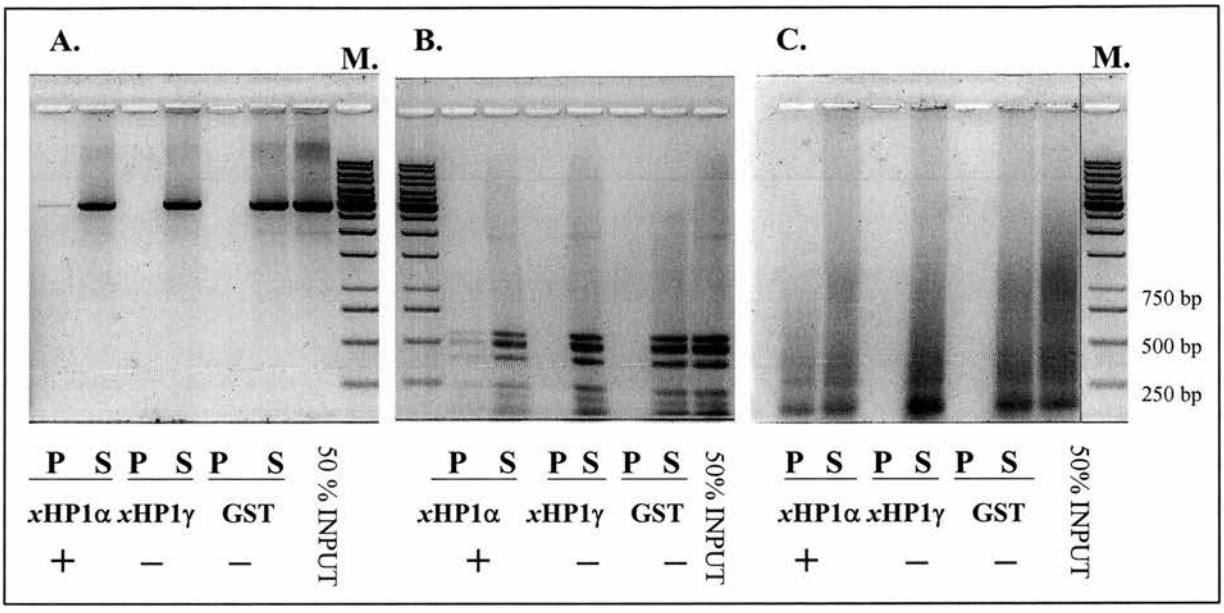

Figure 5.1 (A) *Eco*RI digested pBS plasmid, (B) *Hpa*II digested pBS plasmid and (C) digested chicken chromatin DNA were incubated with GST fusion *x*HP1α10μg, GST fusion *x*HP1γ10 μg and GST 10 μg coupled to Glutathione-Sepharose in the incubation buffer of 10 mM HEPES, 10 mM KCl, 0.5 mM EGTA, 0.1% NP-40, 10% glycerol and proteinase inhibitors. Glutathione-Sepharose was then spun down and washed. The DNA in the pellet and the supernatant fractions were separated by 1.5% agarose gel and visualised by ethidium bromide staining. The GST- *x*HP1α, which bound to DNA, is indicated by the plus (+) signs. Abbreviation: M, DNA size maker; P, pellet; S, supernatant.

Figure 5-2 Xenopus HP1α DNA binding has no preference for Xenopus satellite DNA

A.

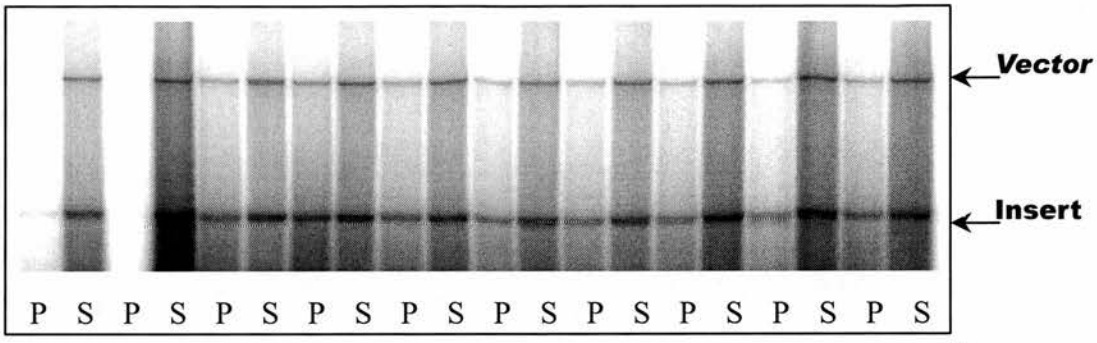

B.

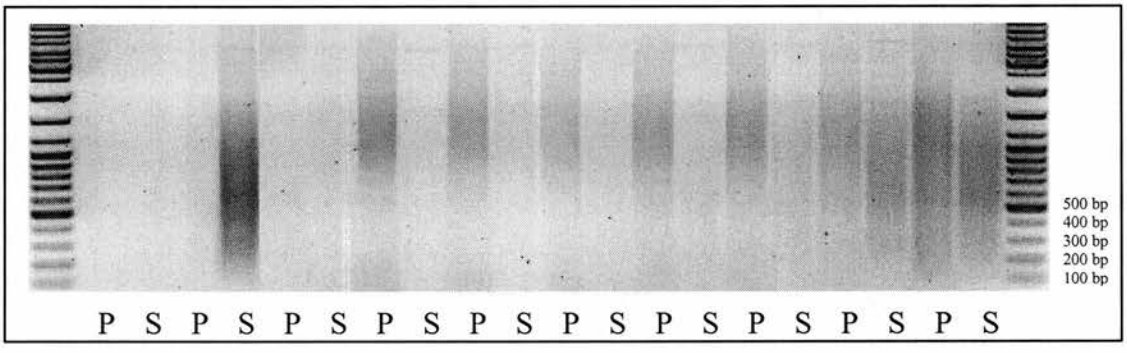

C.

P	S	P	S	P	S	P	S	P	S	P	S	P	S	P	S	P	S	P	S
0 ng		1000ng		0 ng		10 ng		20 ng		50 ng		100 ng		200 ng		500 ng		1000 ng	
GST				GST-*x*HP1α															

D.

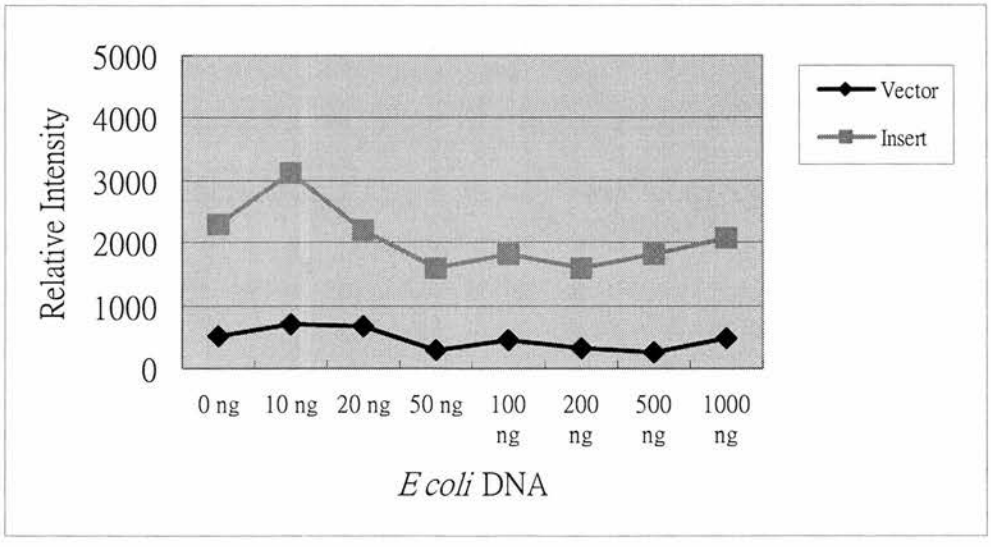

Figure 5.2 (A) pE190 *Xenopus* satellite DNA clone was digested with *Hind* III to release the satellite insert from the vector. Both the satellite DNA insert and the vector were radio-ladled with ^{32} P-α CTP with Klenow fragment. The labelled satellite insert and vector were incubated with GST fusion *x*HP1α 1 0 μg) and GST (10 μg) coupled to Glutathione-Sepharose in the incubation buffer as in Figure 5.1. In addition, different amount of *EcoR*I digested *E. coli* genomic DNA was included as competitor, as indicated in (C). Glutathione-Sepharose was then spun down and washed. The DNA in the pellet and the supernatant fractions were separated on a 1.5% agarose gel. The gel then was dried and detected by autoradiography. (C) Prior to the gel drying, the *E. coli* genomic DNA was detected by ethidium bromide staining. (D) The satellite insert and the vector indicated here are as in (A). The diagram shows that in the pellet fractions, there are no dramatic changes in the interaction between the satellite DNA and the vector DNA with GST-HP1α in different amount of *E. coli* genomic DNA are included. Abbreviation: M, DNA size maker; P, pellet; S, supernatant.

Figure 5-3 Xenopus HP1 α interacts with chromatin.

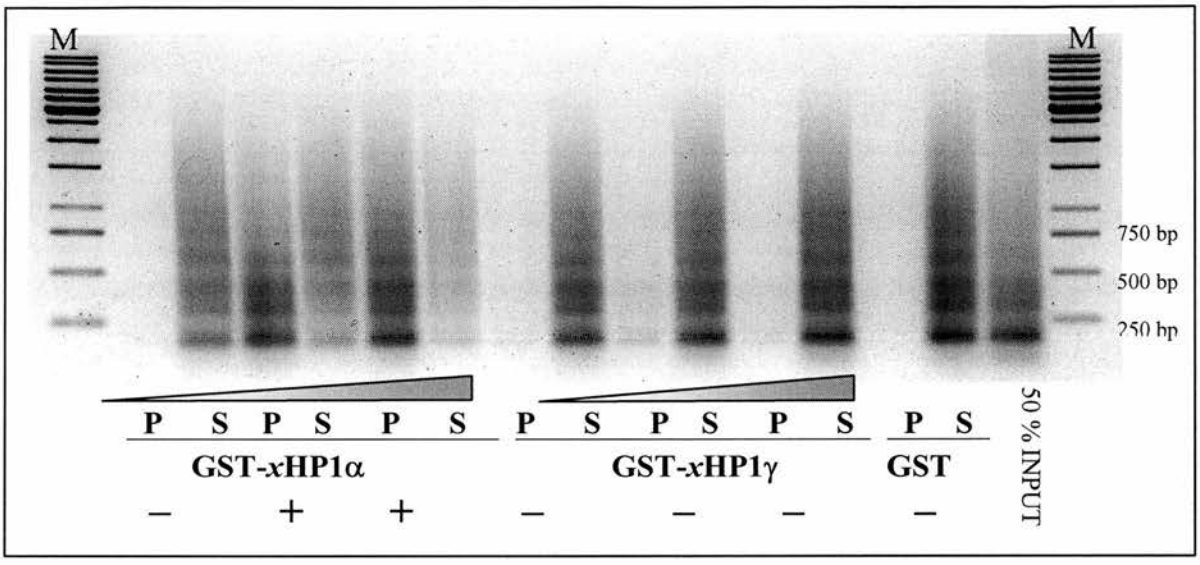

Figure 5.3 MNase digested chicken chromatin (3 μg) were incubated with increased amounts of GST fusion *x*HP1α (GST-*x*HP1α: 5, 10 or 20 μg) and GST fusion *x*HP1γ (GST-*x*HP1γ: 5, 10 or 20 μg), and GST (10 μg) coupled to Glutathione-Sepharose in the incubation buffer as in **Figure 5.1**. Glutathione-Sepharose was then spun down and washed. The chromatin in the pellet and the supernatant fractions were phenol/chloroform extracted and separated on a 1.5% agarose gel and visualised by ethidium bromide staining. Abbreviation: M, DNA size maker; P, pellet; S, supernatant.

Figure 5-4 Xenopus HP1α and HP1γ can heteromerize and then, bind to chromatin

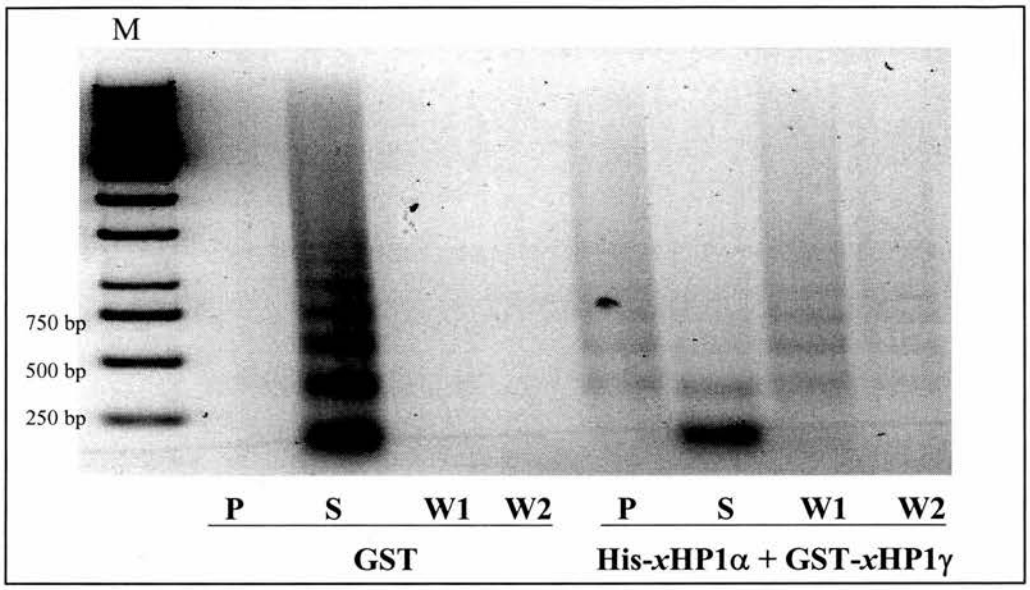

Figure 5.4 MNase digested chicken chromatin (3 μg) were incubated with Histidine tag *x*HP1α (His-*x*HP1α 10 μg) in the incubation buffer as in **Figure 5.1** for 10 minutes and followed by adding GST fusion *x*HP1γ (GST-*x*HP1γ 10 μg) coupled to Glutathione-Sepharose. GST (10μg) coupled to Glutathione-Sepharose played a control reaction. Glutathione-Sepharose matrices was then spun down and washed. The chromatin in the pellet, the supernatant and the washing fractions were phenol/chloroform extracted and separated on a 1.5% agarose gel and visualised by ethidium bromide staining. Abbreviation: M, DNA size maker; P, pellet; S, supernatant; W1: wash 1; W2: wash 2.

Figure 5-5 Identification of DNA binding Domain of Xenopus HP1α

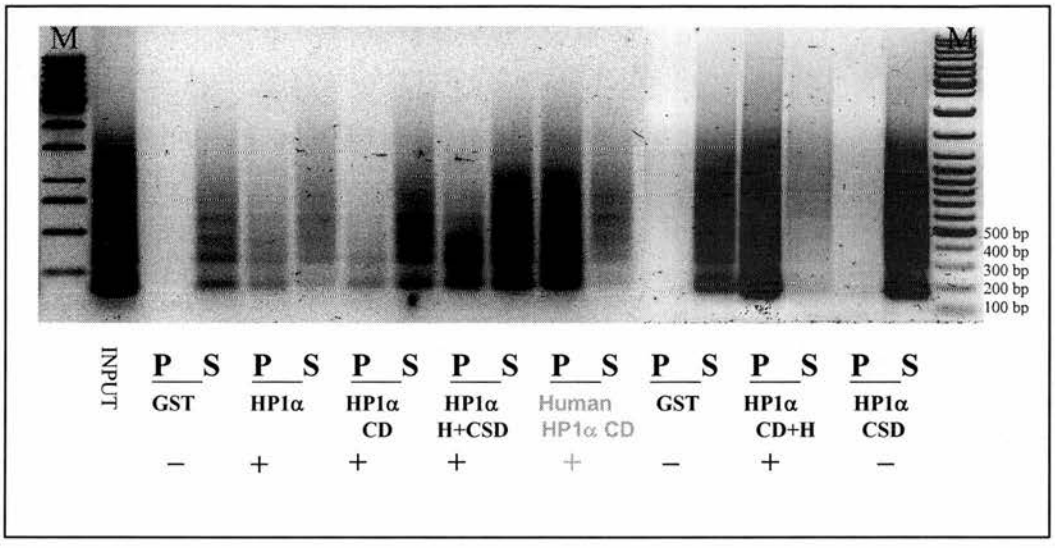

Figure 5.5 MNase digested chicken chromatin DNA (3 μg) was incubated with GST fusion *x*HP1α constructs (10μg) and GST (10μg) coupled to Glutathione- Sepharose in the incubation buffer as in **Figure 5.1**. Glutathione-Sepharose matrices was then spun down and washed. The chromatin DNA in the pellet and the supernatant fractions were separated on a 1.5% agarose gel and visualised by ethidium bromide staining. The GST-*x*HP1 constructs, which bound to DNA were indicated by the plus (+) signs. Abbreviation: M, DNA size marker; P, pellet; S, supernatant; CD, chromo domain; H, hinge region; CSD, shadow domain.

Figure 5-6 Identification of chromatin binding Domain of Xenopus HP1α

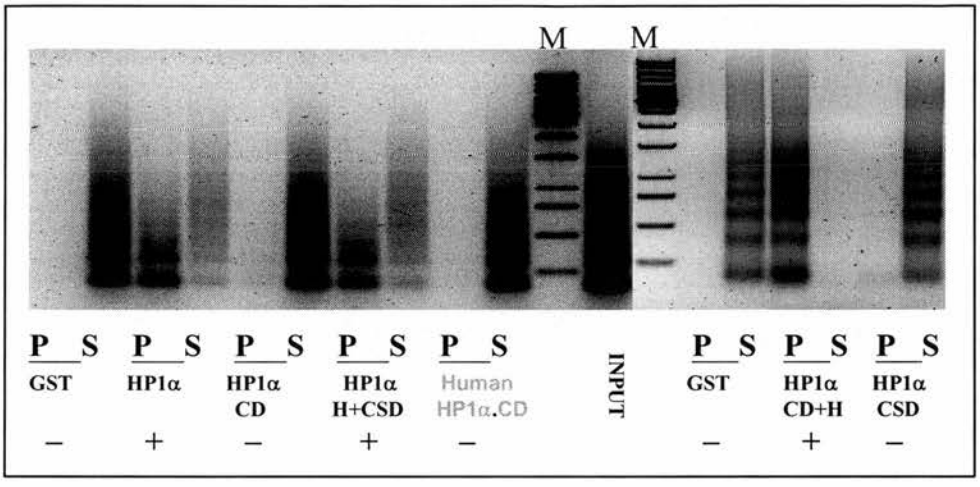

Figure 5.6 MNase digested chicken chromatin (3 μg) was incubated with GST fusion *x*HP1α 10 μg) constructs and GST (10 μg) coupled to Glutathione-Sepharose in the incubation buffer as in **Figure 5.1**. Glutathione-Sepharose matrices was then spun down and washed. The chromatin DNA in the pellet and the supernatant fractions were phenol/chloroform extracted and separated on a 1.5% agarose gel and visualised by ethidium bromide staining. The GST-*x*HP1 constructs, which bound to chromatin were indicated by the plus (+) signs. Abbreviation: M, DNA size marker; P, pellet; S, supernatant; CD, chromo domain; H, hinge region; CSD, shadow domain.

Figure 5-7 Hinge region of* Xenopus *HP1α is necessary for Chromatin and DNA binding

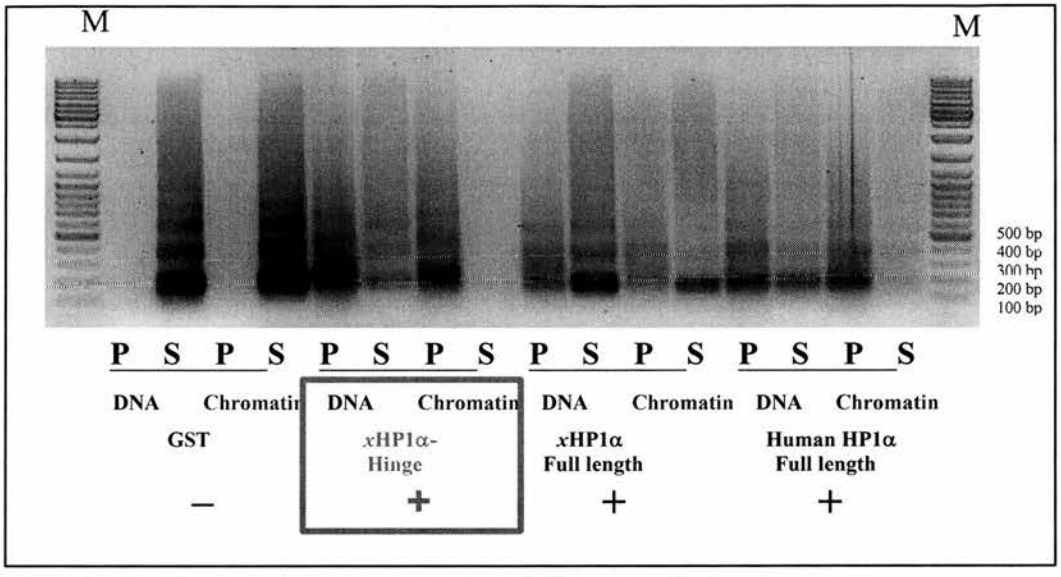

Figure 5.7 MNase digested chicken chromatin (3 μg) was incubated with GST fusion *x*HP1α full length (10 μg), hinge region (10 μg), GST fusion human HP1α full length (10 μg) and GST (10 μg) coupled to Glutathione-Sepharose in the incubation buffer as in **Figure 5.1**. Glutathione-Sepharose matrices was then spun down and washed. The chromatin DNA in the pellet and the supernatant fractions were phenol/chloroform extracted and separated on a 1.5% agrose gel and visualised by ethidium bromide. The GST-*x*HP1 constructs, which bound to chromatin were indicated by the plus (+) signs. Abbreviation: M, DNA size marker; P, pellet; S, supernatant; CD, chromo domain; H, hinge region.

Figure 5-8 Xenopus HP1s are associate with core histones

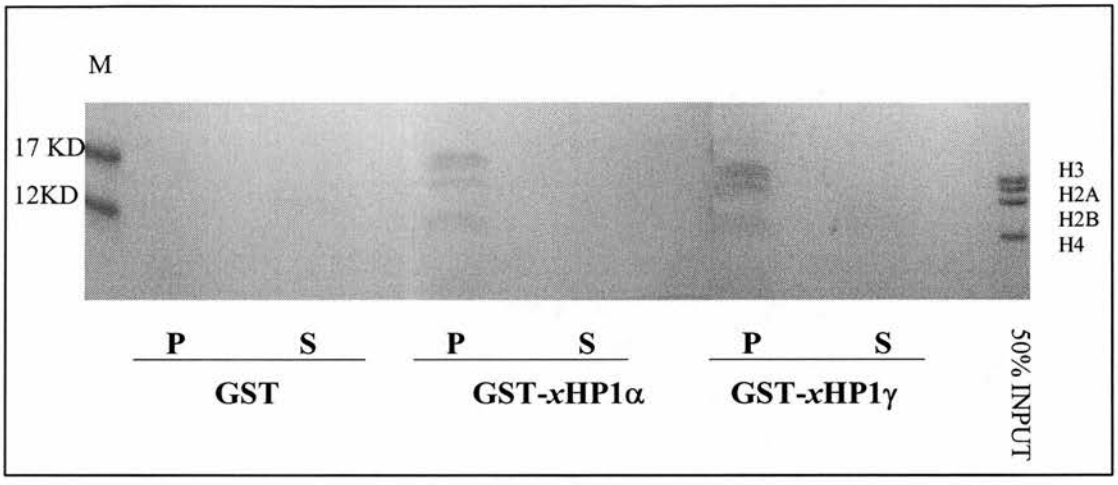

Figure 5.8 Chicken core histones (H2A, H2B, H3 and H4; 5 μg) were incubated with GST fusion *x*HP1α (GST-*x*HP1α, 10 μg) and GST fusion *x*HP1γ (GST-*x*HP1γ, 10 μg), and GST (10 μg) coupled to Glutathione-Sepharose in the incubation buffer as in **Figure 5.1,** in addition of 0.5 % albumin. Glutathione-Sepharose matrices was then spun down and washed. The core histones in the pellet and the supernatant fractions were separated by 1.5% SDS-PAGE and visualised by coomassie blue staining. Abbreviation: M, protein size marker; P, pellet; S, supernatant.

Figure 5-9 Xenopus HP1α has specific interactions with histone H1 and H3

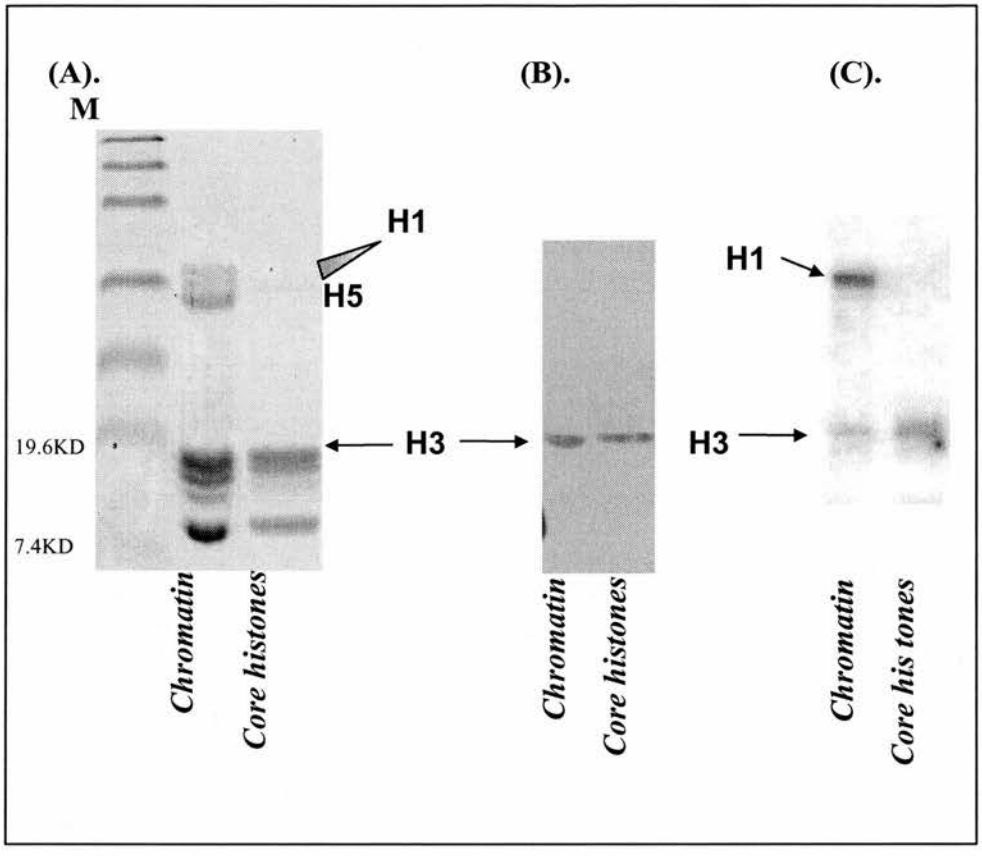

Figure 5.9 (A) Chicken chromatin preparation that includes histone H/ H5 (10 μg) and chicken core-histones stripped of H1/H5 (5 μg) were analysed by SDS-PAGE and visualised by coomassie blue staining. (B) The same samples shown in (A) were electro-blotted onto nitrocellulose membrane and western-blotted with anti-methyl-H3. (C) Far Western with GST-*x*HP1α. The same membranes in (B) was probed with GST-*x*HP1α (0.5 μg/ml) and western-blotted with anti-GST.

Figure 5-10 Xenopus HP1s bind to methylated histone H3 tails

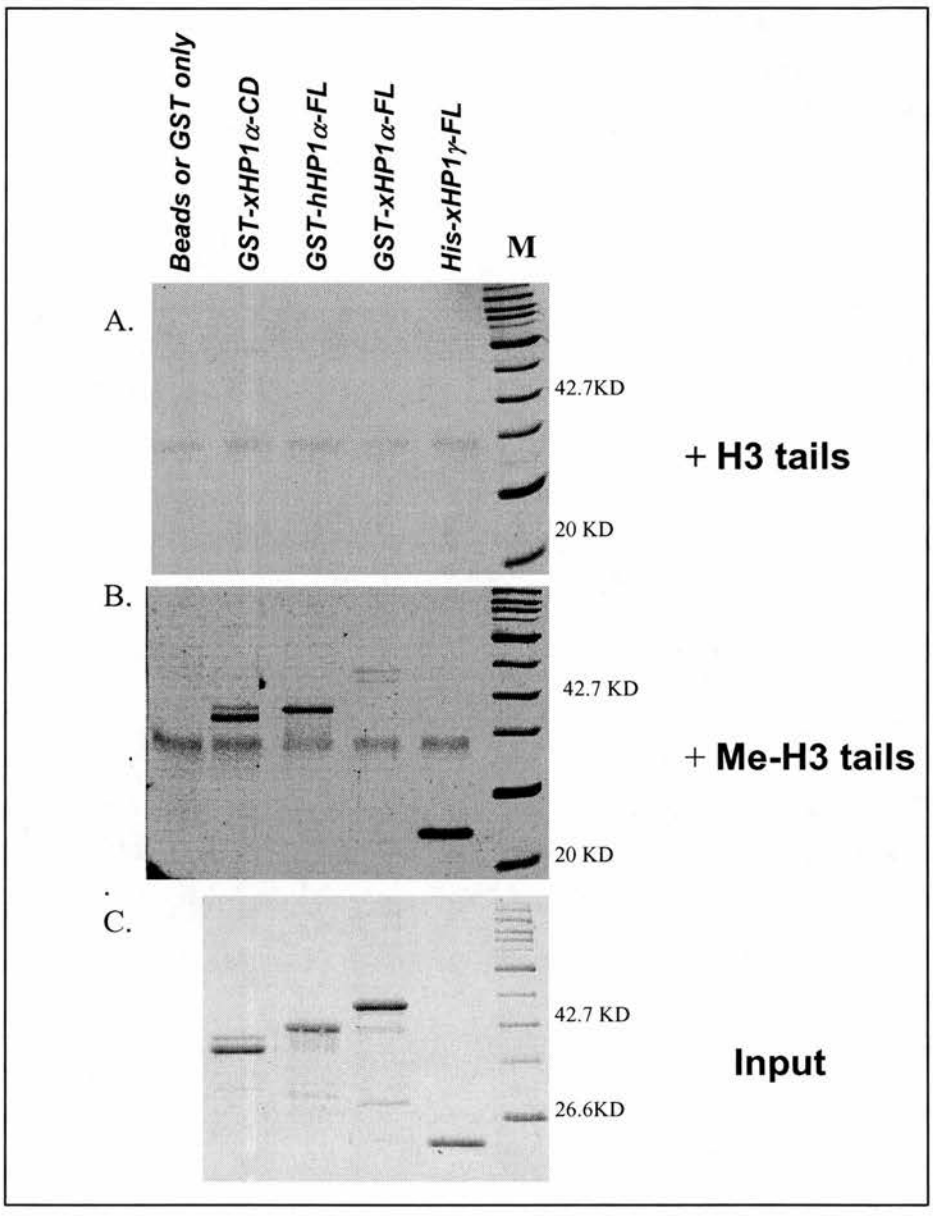

Figure 5.10 *in vitro* pull-down assays were performed with affinity matrices that present either (A) Unmodified (H3-tail) or (B) Lys-9 dimethylated (Me-H3-tail) N-terminal sequences of histone H3. The matrices were incubated with beads/GST only, GST-*x*HP1α-CD, GST-hHP1α-FL, GST-*x*HP1α-FL or His-*x*HP1γ-FL in the PBS buffer. The matrices was then spun down and washed. The proteins in the pellet were separated by 10% SDS-PAGE and visualised by coomassie blue staining. (C). The input proteins. Abbreviation: M: size marker, CD: chromo domain, FL: full length, PBS: phosphate buffer saline.

Figure 5-11 The CD region of Xenopus HP1α shows a weak chromatin binding activity

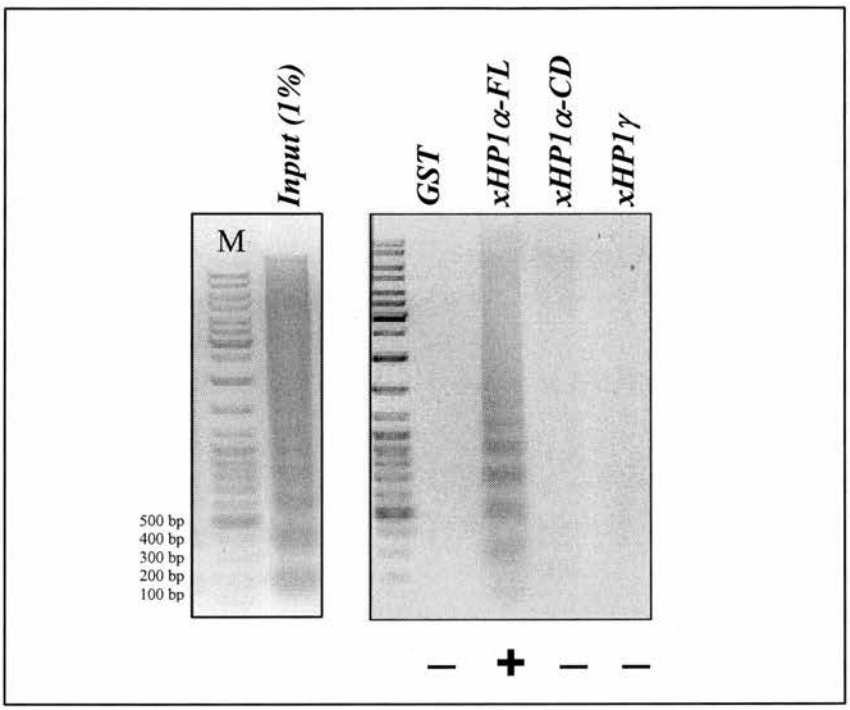

Figure 5.11 MNase digested chicken chromatin (300 μg) was incubated with GST fusion *x*HP1α full length (GST-*x*HP1α-FL)(10 μg), CD region (GST-*x*HP1α-CD) (10 μg), GST fusion *x*HP1γ full length (GST-*x*HP1γ-FL) (10 μg) and GST (10 μg) coupled to Glutathione-Sepharose in the incubation buffer as in **Figure 5.1**. Glutathione-Sepharose matrices were then spun down and washed. The chromatin DNA in the pellet and the supernatant fractions were phenol/chloroform extracted and separated on a 1.5% agarose gel and visualised by ethidium bromide. The 1/100 input of chromatin was loaded on to the gel as indicated. The GST-*x*HP1 constructs that bound to chromatin were indicated by the plus (+) signs. Abbreviation: M, DNA size marker; CD, chromo domain; FL: full length.

Figure 5-12 The Xenopus HP1α binds to a specific population of chromatin

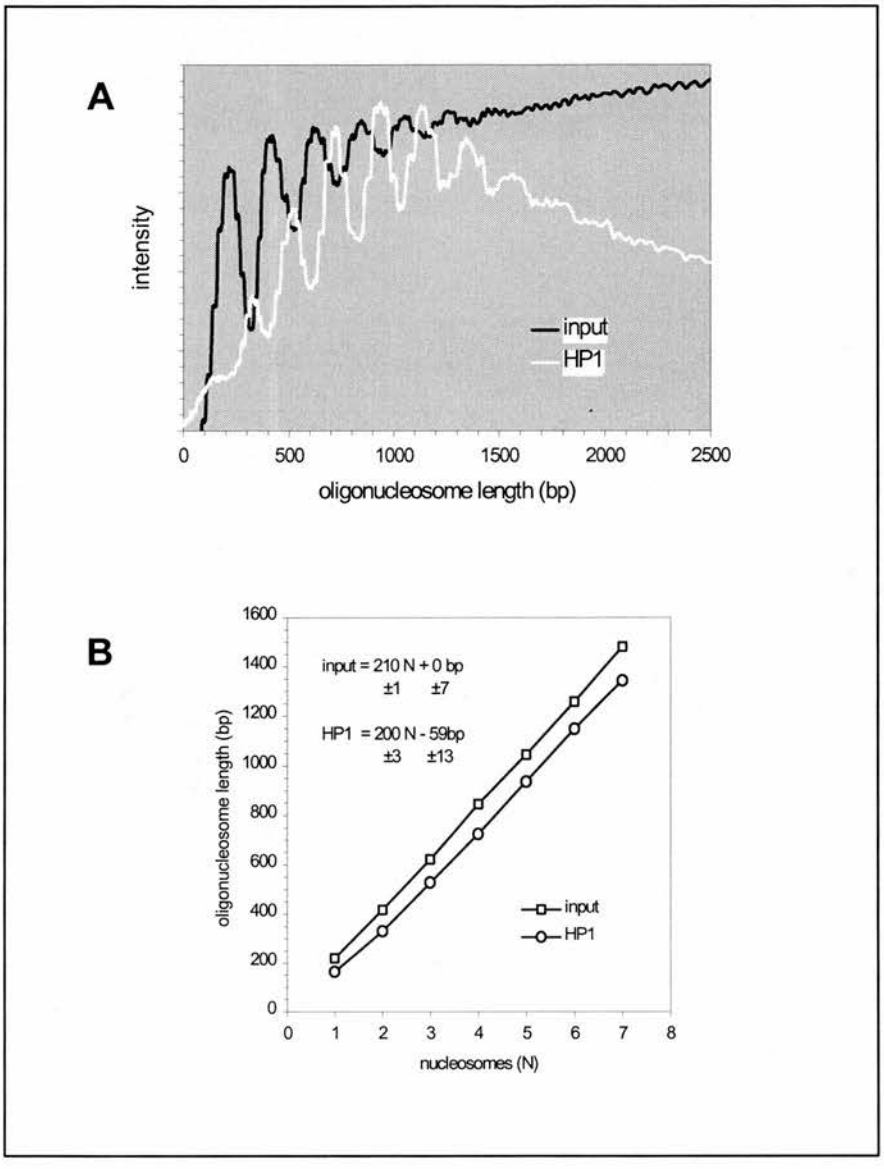

Figure 5.12 The schematic analysis of the chromatin bound to *x*HP1α compared to the input chromatin. The input and *x*HP1α-FL lanes in **Figure 5.11** were analysed using phosphoimager (A) and plotted (B) by oligonucleosome length versus nucleosomes.

Figure 5-13 The H3 tails do not interfere with interaction of GST-xHP1a with chromatin

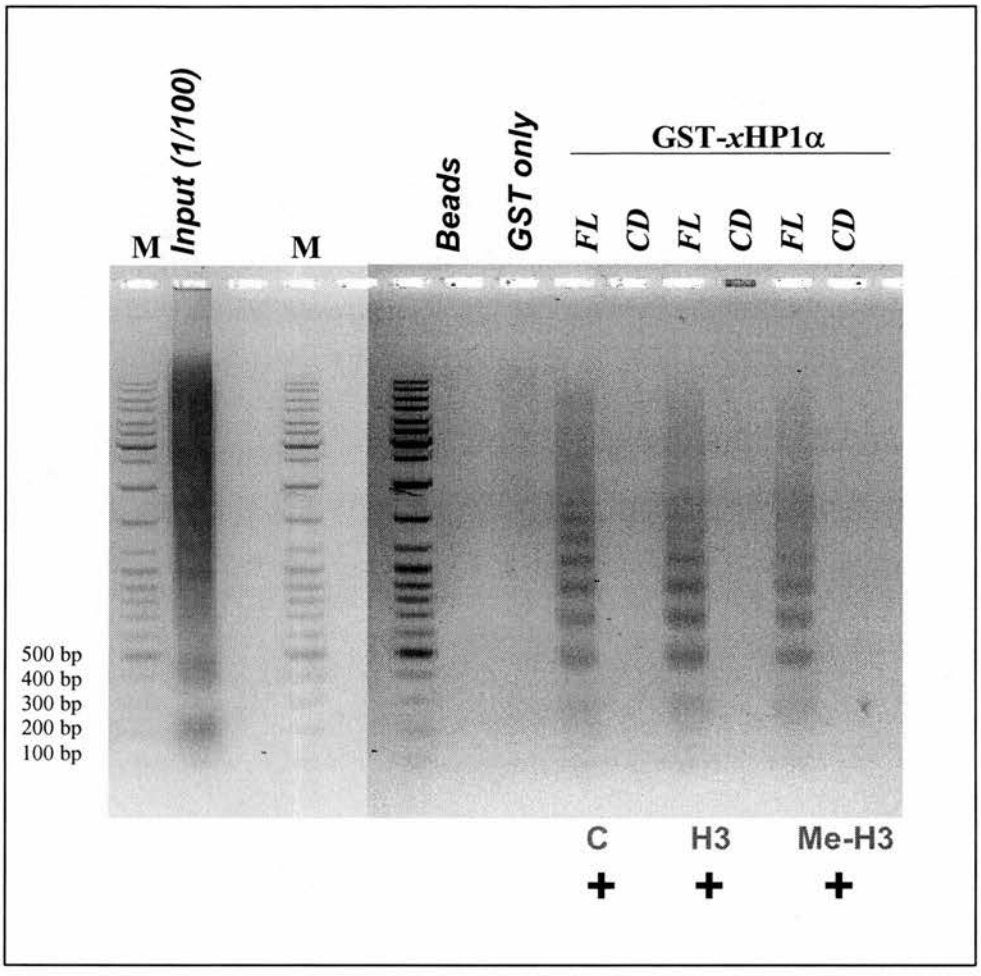

Figure 5.13 MNase digested chicken chromatin (300 μg) was incubated with GST fusion *x*HP1α full length (10 μg), GST (10 μg) coupled to Glutathione-Sepharose and the Sepharose (beads) in the incubation buffer as in **Figure 5.1** in the presence of H3-tails or Me-H3 tails as indicated. Glutathione-Sepharose matrices were then spun down and washed. The chromatin DNA in the pellet and the supernatant fractions were phenol/chloroform extracted and separated on a 1.5% agarose gel and visualised by ethidium bromide. The 1/100 input of chromatin was loaded on to the gel as indicated. The samples that bound to chromatin were indicated by the plus (+) signs. Abbreviation: M, DNA size marker. C: control. H3: histone H3.Me-H3: methylated histone H3. CD: chromo domain. FL: full length

Figure 5-14 Schematic diagram of Xenopus HP1 DNA and Chromatin binding

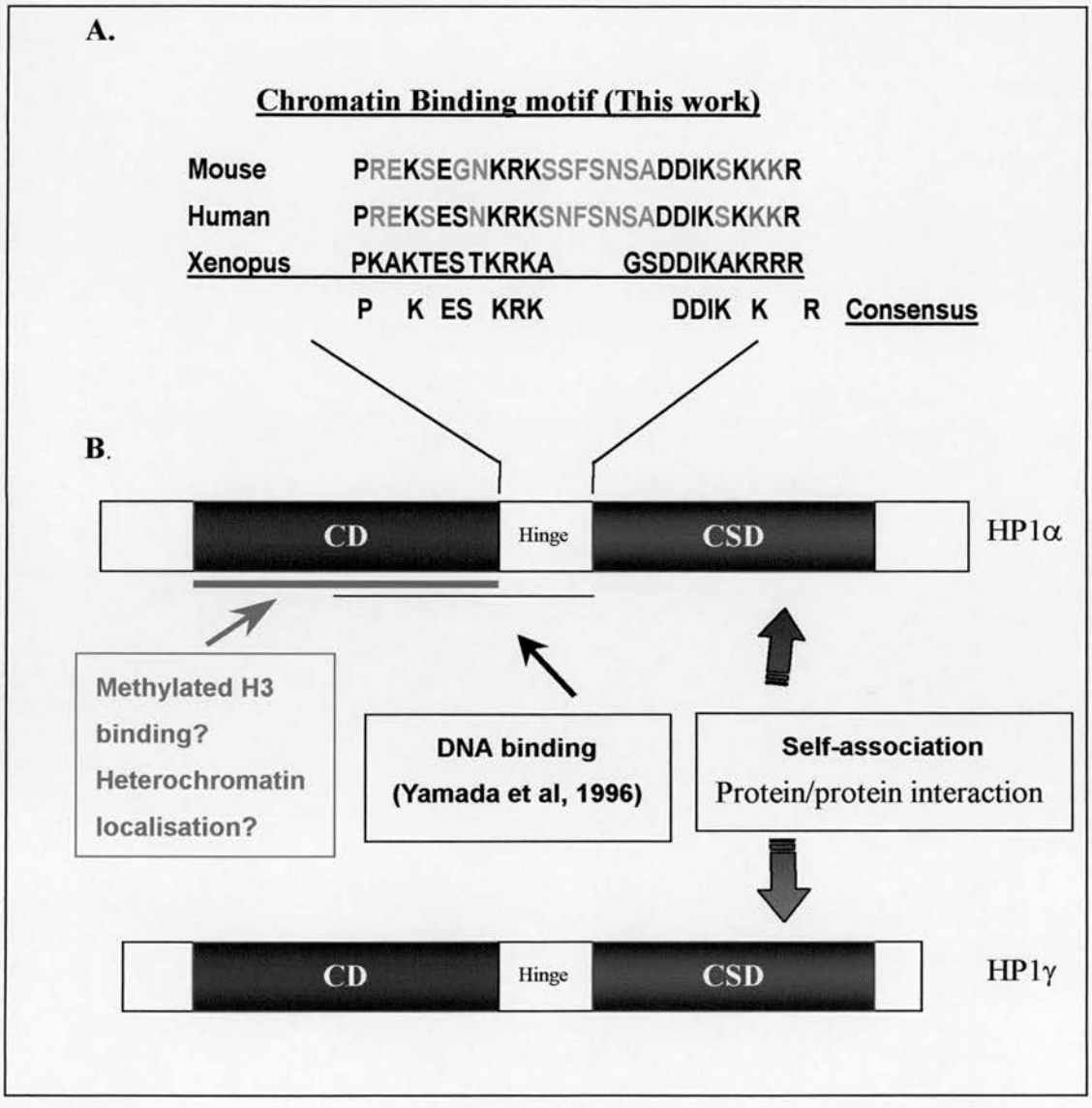

Figure 5.14 Schematic representation of the generic HP1. (A) Amino acid alignment of hinge region of *Xenopus*, mouse and human HP1α. This motif is responsible for HP1α chromatin binding. In *Xenopus,* this motif is only 23 amino acids long. A single amino terminal chromo domain motif (CD) and a single carboxy-terminal chromo shadow domain (CSD) motif are separated by a variable length linker (hinge) region. The DNA and protein-protein interaction regions are indicated.

Chapter 6 The Role of linker histones and histone tails in *x*HP1-chromatin interaction

6.1 Introduction

The nucleosome core particle consists of approximately 146 base pairs of DNA wrapped around a histone core in one and three-quarter left-handed super-helical turns. The protein core of this nucleoprotein complex is an octamer containing two of each of the histones H3, H4, H2A and H2B, organised in a tripartite structure consisting of two histone H2A-H2B dimers associated with a histone H3-H4 tetramer which serves as a scaffold (Arents et al. 1991).

Characterisation of defined model systems reconstituted from core histone octamers and tandemly repeated 5S rDNA has demonstrated that nucleosomal arrays possess the intrinsic ability to form both moderately folded and extensively folded conformational states in the presences of cations (Hansen et al. 1989; Garcia-Ramirez et al., 1992; Schwarz and Hansen 1994 ; Fletcher and Hansen 1995; Tse and Hansen 1997). Experiments with proteolytic fragments of histone H1 and nucleosomes containing mixtures of all the DNA sequences in the genome suggest that the structured domain of histone H1 binds where DNA enters and exits the nucleosome and across the few central turns of DNA in the structure (Allan, et al. 1980, 1981, 1986). This interaction at the periphery of the particle has been proposed

to seal two turns of DNA around the histone octamer, leading to further stabilisation of the interaction of DNA with the octamer (Simpson, 1978). In histone-depleted chromatin, the fibres are more extended, which is consistent with the entry and exit point of DNA wrapping around the octamer being further apart (Thoma, 1979). Linker histones are believed to be required for the *in vitro* formation of highly folded 30 nm chromatin fibres (Allan et al., 1981, 1986; Thoma and Koller, 1977; Thoma et al. 1979) . Folding experiments performed in NaCl and $MgCl_2$ have shown that H5 binding markedly stabilises both the intermediate and extensively folded states of nucleosomal arrays without fundamentally altering the intrinsic nucleosomal array folding pathway (Carruthers et al., 1998, see also Figure 6.1.1-6.1.3). Furthermore, it is now well established that high-order folding of nucleosomal arrays is strictly dependent on the core histone N termini acting through multiple molecular mechanisms (Allan et al. 1982; Garcia-Ramirez et al., 1992; Fletcher and Hansen, 19995; Tse and Hanssen, 1997; Tse et al., 1998; Moore and Ausio, 1997). The electron micrograph in Figure 6.1.4, shows that the salt-dependent folding of oligonucleosomes in the absence of linker histones involves the bending of the linker DNA region connecting adjacent nucleosomes (Garcia-Ramirez et al., 1992). In figure 6.1.5, it is also shown that removal by trypsin of the N-terminal tails of the core histones prevents the oligonucleosomes from folding. The cartoon in figure 6.1.6 shows a representation summarising the conformational transition of the nucleosome core particles.

HP1 is known as a functional subunit of heterochromatin and performs a chromatin binding activity (Chapter 5). However, it is still unknown how HP1 participates in the chromatin folding and interacts with the linker histones and the core histones N termini. In this chapter, I have examined the role of the

salt-dependent folded state of native chromatin in the interactions between *x*HP1α and three different species of chromatin (chromatin, chromatin depleted of H1/H5 and trypsinised chromatin). I also have investigated the function of linker histones and histones N-terminal tails in the association of *x*HP1α and chromatin. For this purpose, the chicken erythrocyte chromatin was prepared and one portion of the chromatin was carefully stripped of linker histones. Trypsin treatment resulting histone N-terminal removal chromatin was also performed. All the different species of chromatin were used to perform a series of pull-down assays in the presence of a gradient of NaCl concentrations. The possible functional relevance of these results is discussed.

6.2 Results

6.2.1 Preparation of chromatin, depleted H1/H5 of chromatin and trypsinised chromatin from chicken erythrocyte

In order to obtain the material for the following experiment, we collaborated with Sari Pennings who processed the preparation of chicken erythrocyte chromatin using a standard methods described in Chapter 2. Following the preparation, the chromatin was stripped off linker histones using a centrifugal filtration step in the presence of 600mM NaCl, which resulted in a 64% depletion of linker histones from chromatin. The 64% depleted chromatin was used for the experiment in figure 6.3-6.9. The previous studies (van Hole, 1988) have shown that linkers are necessary for the chromatin salt-dependent folding and to achieve this, it requires 1-2 linkers histones per nucleosome. Therefore, 64 % depletion of linker histones should have disrupted the higher level of chromatin folding. The chromatin was subsequently treated by trypsin for digesting off the N-terminal histone tails (Figure 6.2, A). For

the experiment in figure 6.10-6.12, the depletion of linker histones was completed by applying chromatin onto a hydroxylapatite column, which resulted in completely depleting linker histones from chromatin. The chromatin consequently was treated with trypsin for digesting off the N-terminal histone tails (Figure 6.2, B)

6.2.2 Fundamental analysis of *x*HP1α-chromatin interaction

6.2.2.1 xHP1α does not precipitate chromatin, depleted H1/H5 chromatin or chromatin DNA

As mentioned in the introduction, nucleosomal arrays possess the intrinsic ability to form both moderately folded and extensively folded conformational states in the presences of cations. In order to investigate the mechanistic roles of *x*HP1 in chromatin salt-dependent folding, the first step was to understand if *x*HP1 took part in chromatin folding. This was achieved by observing whether *x*HP1 could oligomerise chromatin, chromatin depleted of H1/H5 or nucleosomal DNA at physiological NaCl concentrations. A recombinant 6×histidine *x*HP1α was used to test the potential possibility of precipitating chromatin, depleted H1/H5 chromatin or chromatin DNA at three different NaCl concentrations (0mM, 40mM and 80 mM). Samples subsequently were spun to verify if the precipitation occurred. The pellets and supernatants fractions were analysed in agarose gels. As shown in figure 6.3, in all three cases, two different amount of *x*HP1α (10 or 20 μg) did not precipitate chromatin, depleted H1/H5 chromatin or nucleosomal DNA at 0, 40, and 80 mM NaCl. The results demonstrated that *x*HP1 does not induce oligomerisation of chromatin *in vitro* in the case of either with or without linker histones.

6.2.2.2 xHP1γ does not compete with xHP1α-chromatin interaction

The α and γ forms of mammalian HP1 have been defined to localise to

heterochromatic and euchromatic regions respectively (Nielsen *et al.* 2001). However, the biochemical results show that *x*HP1α and *x*HP1γ interact *in vitro*, and only *x*HP1α shows DNA and chromatin binding activities (Chapter 4 and 5). It would be important to know whether *x*HP1γ played a role in or interfered with DNA- and chromatin-binding activities by *x*HP1α. To answer this question, the same pull-down protocol as described in chapter 4, has used with a recombinant GST-*x*HP1α to perform pull-down assays of chromatin, chromatin depleted of H1/H5 or nucleosomal DNA in the presence of 6×histidine *x*HP1γ. As shown in figure 6.4, A and B, the increased concentration of *x*HP1γ (10-20 μg) did not interfere with *x*HP1α chromatin binding activity in the samples with or without linker histones. Interestingly, in the case of chromatin DNA, the increased concentrations of *x*HP1γ interfered with the *x*HP1α DNA binding (Figure 6.4, C). These results further demonstrate that *x*HP1α processes different binding activities with DNA and chromatin *in vitro*, which are possibly because the distinct protein-protein interaction domains (CD and CSD) are separated from the chromatin-binding domain (Hinge region). There is also an implication that *x*HP1γ may require an euchromatin binding adaptor to attach onto chromatin, involving *x*HP1α and the aid of other proteins, which generate a *x*HP1γ-specific binding site.

6.2.3 Characterisation of salt–dependent behaviour of *x*HP1α-chromatin interaction

HP1α is heterochromatin localised, chromatin-binding protein. Little is known about the role of HP1α on chromatin folding and organisation. As a first step in a long-term investigation of the mechanistic roles of HP1 in chromatin organization, we have combined a standard protocol of salt-dependent chromatin folding with a

pull-down assay. Based on these assays, we could obtain knowledge of whether HP1 chromatin-binding activity preferred different types of chromatin folding, and whether there was a structural and functional interplay between the linker histones and the core histone N-termini tails. As an initial approach, 10 μg *x*HP1 was used to perform pull-down assays, which were carried out in three different species of chromatins, (chromatin, chromatin depleted of H1/H5, trypsinised chromatin) and nucleosomal DNA in a gradient of NaCl (0-100mM) incubating buffer (Figure 6.5-6.8). As a result, we exploited the fact that *x*HP1α prefers binding with a more compact folding of chromatin. Furthermore, in the case of chromatin lacking linker histones and core histone tails, *x*HP1α may interact with linker DNA (Figure 6.9). These data yields some key observations. First, *x*HP1α bound better to the longer chromatin (> dimer) at 20 mM to 100 mM NaCl and mono-nucleosomes stayed behind in the supernatant fractions (Figure 6.5). Second, a similar phenomenon also appeared in the pull-down assays using chromatin depleted of H1/H5 and trypsinised chromatin, however there were few important differences in those two species of chromatin. In the assay of chromatin depleted of H1/H5, the trend of preferring the long chromatin lost at around 80mM NaCl and was most unapparent totally at 100 mM NaCl (Figure 6.6). The possible interpretation is that the chromatin depleted of H1/H5 forms irregular clumps at higher NaCl, on which *x*HP1α has no longer any binding activity. Third, at 0-40 mM NaCl, *x*HP1α could not bind to trypsinised chromatin well but the trend of preferring the long chromatin began at the 0 mM NaCl and became more apparent as the NaCl concentration increased (Figure 6.7). At 80 and 100 mM NaCl, the fractions of long trypsinised chromatin began to be lost in the washing steps. In addition to low-resolution agarose analysis, the samples from the assays of depleted H1/H5 chromatin and trypsinised chromatin were run

into acrylamide gels to get higher resolution of the size of the DNA fragments (Figure 6.9). It clearly shows that in the absence of the histones tails, the *x*HP1α bound to the fractions of chromatin with longer linker DNA. Finally, In the case of chromatin DNA, there were lower activities of *x*HP1α DNA binding at 0 and 10 mM NaCl, but at 20-100 mM the *x*HP1α bound to DNA equally well and there were no longer any length preference for these binding activities.

To understand more about the stoichiometry of *x*HP1α chromatin binding, 20 μg of *x*HP1α was used instead of 10 μg in a repeat of the pull-down assays with a gradient of NaCl concentration (Figure 6.10-12). It appeared that *x*HP1α pulled down the three different species of chromatin equally well at moderate NaCl concentration (20-60mM). The main differences were shown at the two ends of the gradient NaCl treatments. At the end of high NaCl concentration, the assays of chromatin and chromatin depleted of H1/H5 shared the same trend (Figure 6.10,11). The binding affinity of all length of chromatin started to drop at 60 mM NaCl, although there was large portion of mono-nucleosome left in supernatant at 80 and 100 mM NaCl. In contrast, *x*HP1α could pull down most of the trypsinised chromatin at 40-100 mM NaCl. Nonetheless, at low NaCl end the results were different. At 0 mM-40mM NaCl, most of the chromatin was shifted to the pellet fraction. However, *x*HP1α preferred to bind the short fraction (< trimer) of depleted H1/H5 and trypsinised chromatin at 0,10 mM NaCl.

In a conclusion, doubling the *x*HP1α concentration to 20 μg narrowed the difference in the pull-down assays with these three species of chromatin. Nonetheless, it appeared that *x*HP1 preferred a more compact folding of the chromatin and the depleted H1/H5 chromatin at the high concentration of NaCl. In addition, in the case of lacking of the linker histones and the core histone tails,

*x*HP1α preferred to interact with the short fraction of depleted and trypsinised chromatin at very low NaCl concentration. The chromatin depleted of H1/H5 has a characteristic that was intermediate between chromatin and trypsinised chromatin.

6.3 Discussion

In the absence of other chromatin-associated proteins, nucleosomal arrays are capable of forming extensively folded structures through a mechanism that is dependent on cations (Schwarz and Hassen, 1994) and multiple distinct functions of the core histone N-termini (Garcia-Ramirez et al., 1992; Fletcher and Hansen, 1995; Tse and Hansen, 1997; Tse et al. 1997). In this work, the results demonstrates that *x*HP1α does not impair or participate in intrinsic chromatin folding, although HP1 is an essential component of heterochromatin, which is required in a precise stoichiometry to properly set up and/or maintain the inactivated state of genes (Nielsen et al., 2001). The results in figure 6.4 show that *x*HP1γ does not compete with *x*HP1α chromatin binding activity. It indicates that while *x*HP1α and *x*HP1γ are associated with each other, this association does not interfere with the chromatin and DNA binding by *x*HP1α. A recent report provides evidence that mouse HP1α, β, γ homo- and heteromerise in living cells, however, these proteins exhibit different patterns of sub-nuclear localisation (Minc et al. 1999, 2000; Nielsen et al. 1999), which in the case of HP1γ, are highly dynamic during the cell cycle (Minc et al. 1999). Furthermore, the immunodetection all three isoform of mouse HP1 in interphase nuclei revealed a substantial proportion that fluoresce strongly with AT-rich satellite DNA found in constitutive heterochromatin. Thus, the result in figure 6.4 supports the hypothesis that HP1 isoforms can become a complex, which interacts with chromatin and the α form of the protein plays a role as a chromatin

adaptor of the HP1 associated protein complex (Also, see Figure 5.4). Therefore, the AT-rich heterochromatin area may represent regions in which HP1α anchors. However, how HP1α recognises this specific region is still unknown.

It has been observed by electron microscopy (EM) that in low ionic strengths (2mM < I < 20mM) chromatin strands depleted of linker histones appear as an extended "beads-on-string" structure (Thoma et al., 1979), whereas H1-containing chromatin adopts a zigzag-like conformation (Thoma et al., 1979; Worcel et al., 1981). At > 60 mM NaCl, H1-containing chromatin compacts into 30-nm fibre, while strands of H-1depleted chromatin tend to form poorly defined clumps on the EM grid (Figure 6.1.4). In this work, the possible participation of *x*HP1α in chromatin folding has been suggested by my results in this chapter. Taken these observations together, the results indicate that *x*HP1α favours binding to a linker histone-containing highly compacted chromatin fibre. Using the Far Western blotting study, it has been shown in chapter 5 that *x*HP1α can interact specifically with histone H3 and linker histones but not with the other core histones. This interaction supports the idea that chromatin binding by *x*HP1α involves an interaction with linker histones-containing chromatin. It is still not clear what the *x*HP1α interaction with histone H3 could actually mean as histone tails are important in chromatin folding and important in the regulation of transcription and functions in gene silencing (Hartzog and Wintson, 1997; Strahl and Allis, 2000). In fact, HP1s also has essential roles in these two activities.

It is clear from the results in figure 6.1.5 that upon removal of the histones tails, the oligonucleosome fibres remain in essentially unfolded conformation and are unable to achieve higher levels of compaction. It also has been shown that the trypsinised chromatin displays a sharper and narrower transition in salt-dependent

sedimentation tests (Garcia-Ramirez et al., 1992) than that observed for the non-trypsinised chromatin. The transit midpoint is centred at 10-12 mM NaCl compared to the midpoint of 25 mM NaCl observed for its non-trypsinised counterpart. The result in Figure 6.7 also demonstrated a pattern transition of chromatin binding by *x*HP1α, which is in agreement with the above observation. In fact, without histone tails *x*HP1α has a preference of binding to linker DNA but it has no preference in chromatin depleted of H1/H5. Therefore, it may imply that without the assistance of histone tails, *x*HP1α and chromatin will not form a proper association. It also implicates that through the histone tails modification (acetylation, methylation and phosphorylation) and the dynamic of linker histones, *x*HP1α may slide around in nucleosome arrays via this activity to regulate cis- and trans-acting regulatory factors, which control transcription and chromatin folding.

Figure 6.1.1

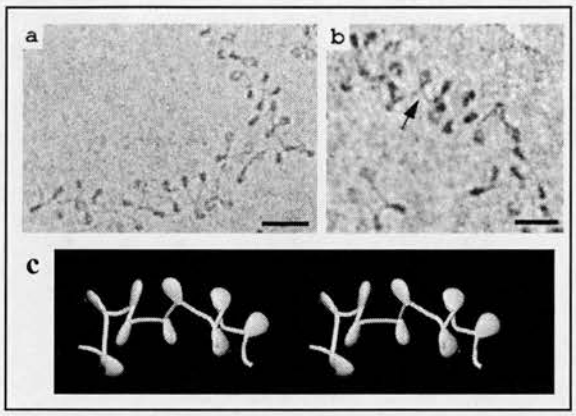

(Bednar *et al.*, 1998)

Figure 6.1.1 (a and b) soluble chromatin from chichen erythrocyte nuclei vitrified in ≈5mM NaCl and imaged unfixed and unstained in the frozen hydrated state.Arrows denotes nucleosomes with the linker histone-dependent "stem" conformation. (c) Stereo pair of a 3D model of a 9-nucleosome segment of a chicken erythrocyte chromatin fiber imaged in ≈5mM NaCl . Nucleosomes and their associated "stems" are representd by pear-shaped solids, all of which point toward the fibre interior. (Bar = 30nm) (Taken from Bednar *et al.*, 1998)

Figure 6.1.2

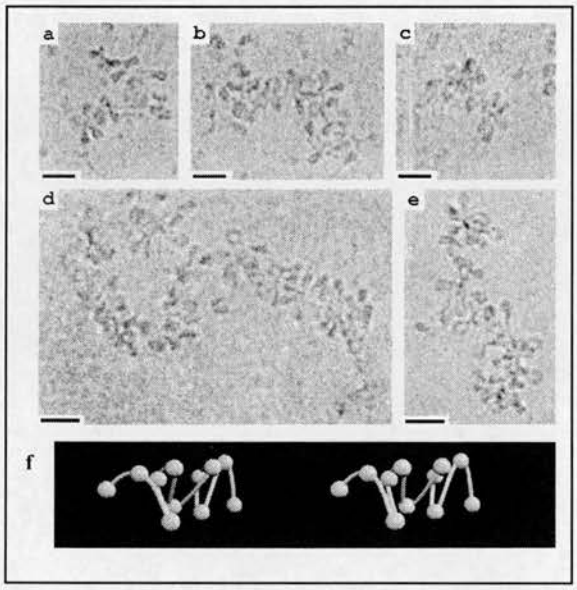

(Bednar *et al.*, 1998)

Figure 6.1.2 Electron cryomicroscopy from COS-7 cells (a-c) vitrified in ≈40mM NaCl and chicken erythrocyte nuclei (d and e) imaged in ≈15mM NaCl. The fibre structure is consistent with an accordion-like compaction of the loose zigzags. (f) Stereo pair of a 3D model of a chicken erythrocyte oligonucleosome vitrified in ≈80 mM NaCl and reconstructed from a tomographic tilt series. The quality of the the reconstruction allowed nucleosome locations and linker path to be identified, but details of nucleosome orientation and linker entry-exit sites were not resolved. (Bar = 30nm) (Taken from Bednar *et al.*, 1998)

Figure 6.1.3

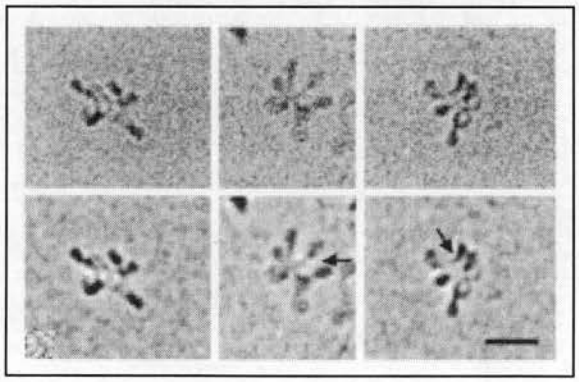

(Carruthers *et al.*, 1998)

Figure 6.1.3 Electron cryomicroscopy of native chicken erythrocyte chromatin (N = 5-7) vitrified in 5mM NaCl, can see clearly individual nucleosome and linker DNA. The zigzag architecture produces a starlike conformation and the linker DNA stem motif is common (arrows)
(Bar = 30nm) (Taken from Carruthers *et al.*, 1998)

Figure 6.1 .4 Oligonucleosome complex depleted linker histones at different ionic sterngth

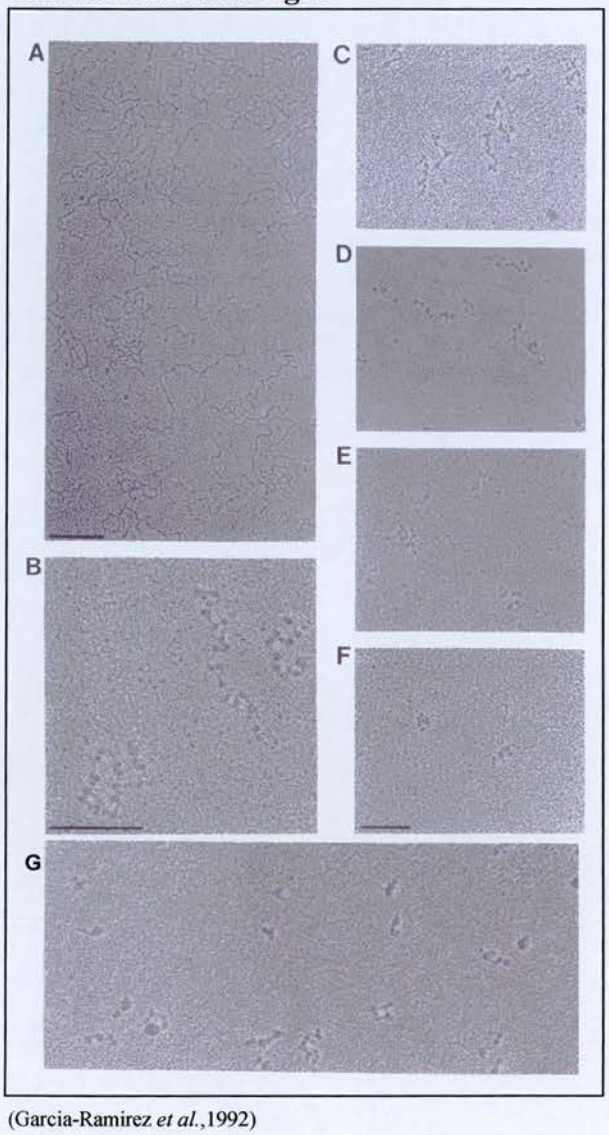

(Garcia-Ramirez *et al.*,1992)

Figure 6.1.5 Trypsinised oligonucleosome complex at different ionic sterngth

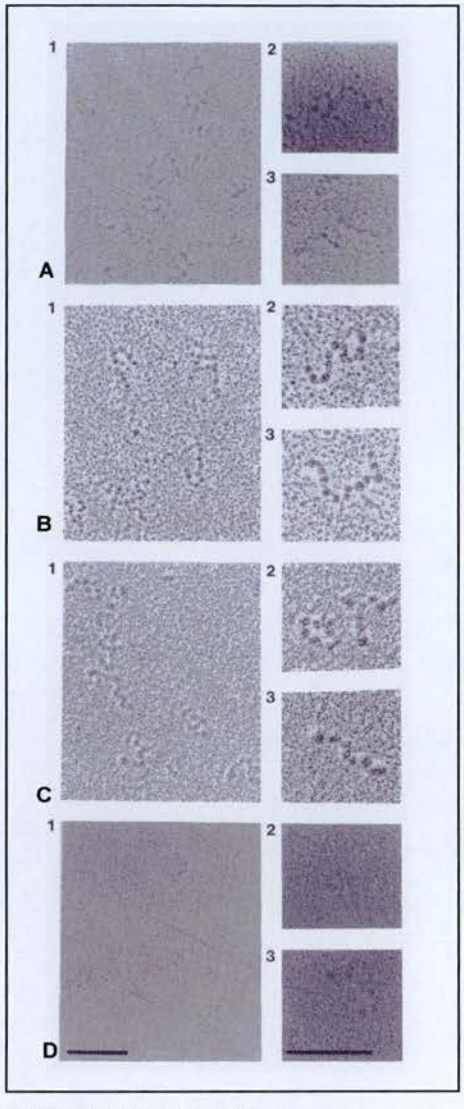

(Garcia-Ramirez *et al.*,1992)

Figure 6.1.4 Electron micrographs. (Taken from Garcia-Ramirez *et al.*,1992) (A), DNA template in 5 mM TEA, pH 7.0, 0.2mM EDTA. (B),.oligonucleosome complex depleted **linker histones** in under the same ionic conditions as in (A). (C-G), oligonucleosome complexes in 0, 20, 40, 80 and 100 mM NaCl in 5 mM TEA, pH 7.0, 0.2 mM EDTA buffer. The bar is 0.2 μm.

Figure 6.1.5 Electron microscopy analysis of the oligonucleosome complex obtained by reconstruction with **trypsinised core histones** at different ionic strength. (Taken from Garcia-Ramirez *et al.*,1992) (A), 0 mM NaCl; (B), 20 mM NaCl; (C),40 mM NaCl; and (D), 100mM NaCl in 5mM TEA, pH 7.0, 0.2mM EDTA buffer. The bar is 0.2 μm.

Figure 6.1.6 Schematic representation of the salt dependent conformational transition of native nucleosome core particles and typsinied nucleosome core particles.

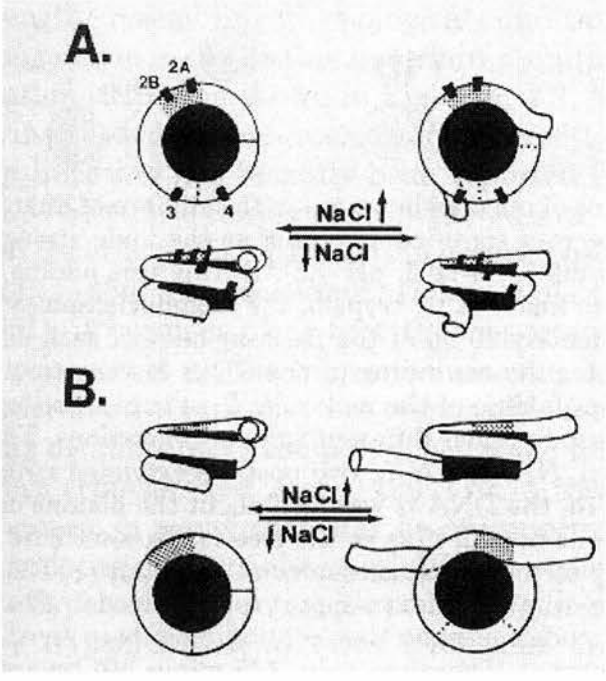

(*Garcia-Ramirez et al.*,1992)

Figure 6.1.6 A, Native nucleosome core particles and B, trypsinised nucleosome core particles. The black circle indicates the histone ocatomer and the open ribbon the DNA. The shared region ≈10bp located 20 bp away from the DNA end represents the site of interaction of the histone H2A-H2B tails (Ausio *et al.*, 1989). There are two such regions symmetrically positioned in each nucleosome. For clarity, only one of them is shown.

Figure 6.2 Preparation of chromatin, depleted of H1/H5 chromatin and trypsinised chromatin from chicken erythrocyte

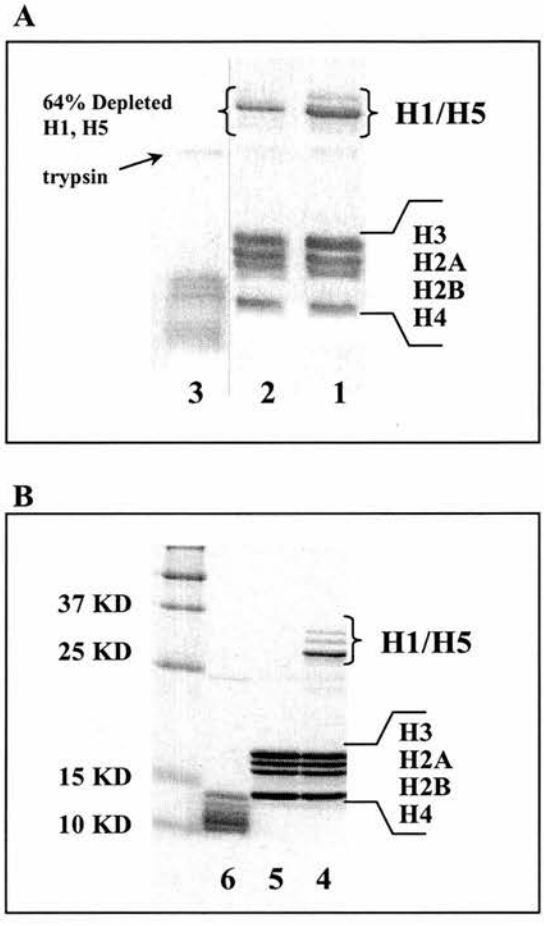

Figure 6.2 The chromatin used in the pull down experiments were prepared from chicken erythrocyte nuclei as in chapter 5. The protein content in the chromatins were separated using 15% SDS-PAGE and visualized by coomassie blue staining. (A) The chromatins used for the experiments in figure 6.3-6.9. Lane 1: chromatin with H1 & H5. Lane2 : H1& H5 were depleted by 64% using centrifugal filtration step. Lane3: The H1& H5 depleted chromatin was treated with trypsin. (B) The chromatins used for the experiments in figure 6.10-6.12. Lane 4: chromatin with H1 & H5. Lane 5 : H1& H5 were depleted 64% using hydroxylaptite binding. Lane 6: The H1& H5 depleted chromatin was treated with trypsin.

Figure 6.3 HP1α does not precipitate chromatin, depleted H1/H5 chromatin or DNA

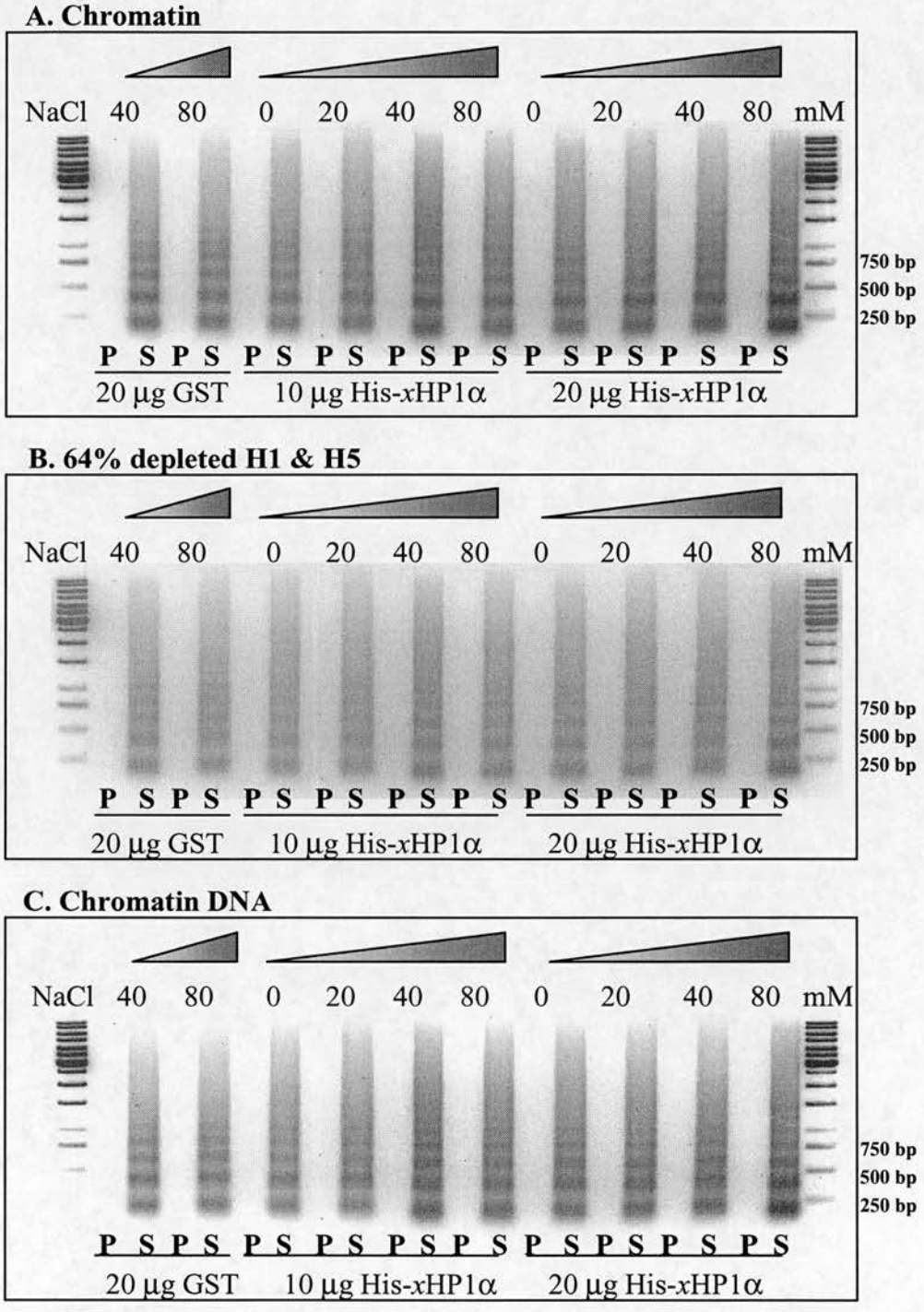

Figure 6.3 (A) chromatin, (B) 64% depleted H1 & H5 chromatin (C) digested chicken chromatin DNA were incubated with 20 μg GST, 10 μg His-*x*HP1α and 20 μg His-*x*HP1α, **which were dissolved in the incubation buffers**, with different NaCl concentrations (0~80 mM). After 30 minutes incubation, all the samples were spun at 13,000 rpm. The pellets and the supernatant fractions were separated by 1.5% agarose gel and visualized by ethidium bromide staining. Abbreviation: P: pellet; S: supernatant.

Figure 6.4 *x*HP1γ does not compete with *x*HP1α chromatin binding

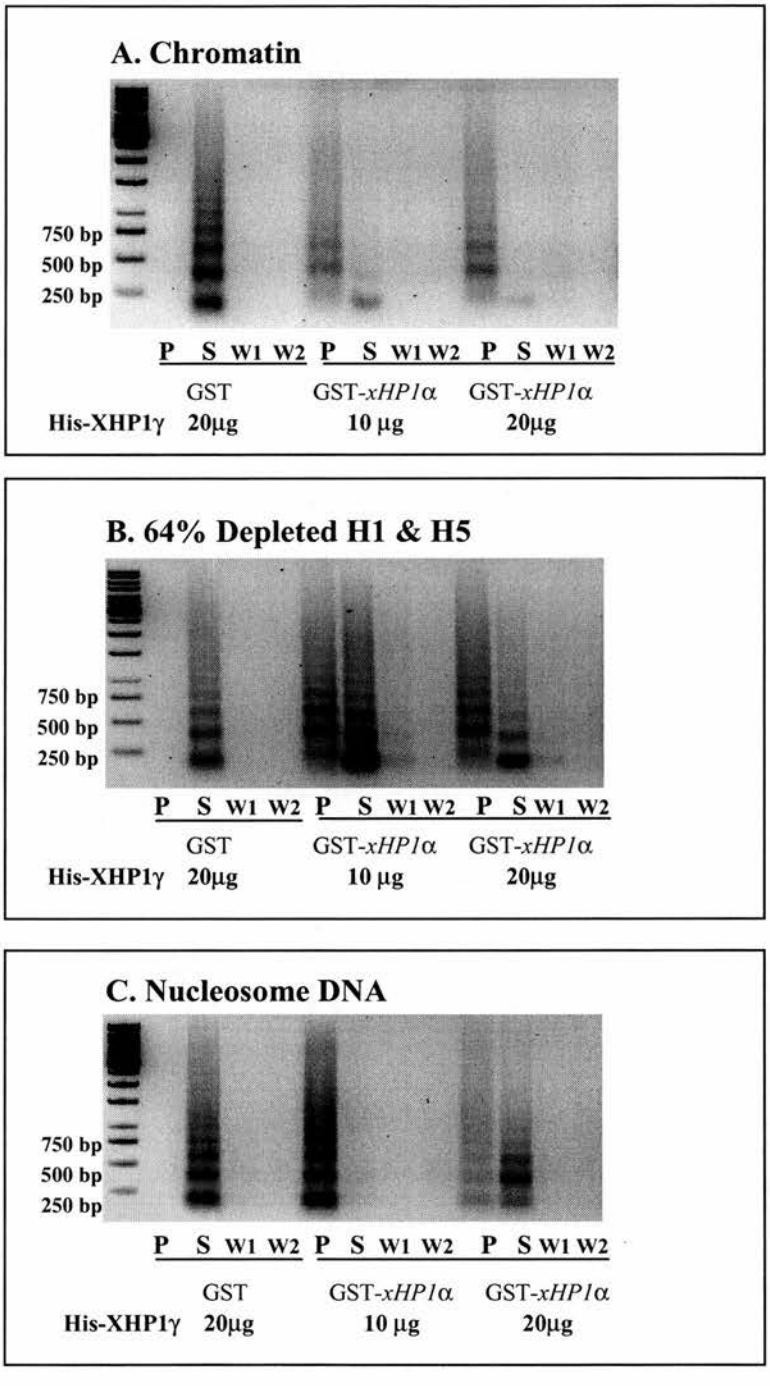

Figure 6.4 (A) chromatin, (B) 64% H1 & H5 depleted chromatin (C) digested chicken Nucleosome DNA were incubated with 10 μg GST or 10 μg GST-*x*HP1α **coupled to Glutathione-Sepharose** with 20 mM NaCl for 30 minutes and added 10 μg or 20 μg His-*x*HP1γ into the incubation buffers for another 30 minutes incubation. All the samples were spun at 13,000 rpm and were washed two time with the same buffer. The pellets, the supernatant and the washing fractions were separated by 1.5% agarose gel and visualized by ethidium bromide staining. Abbreviation: P: pellet; S: supernatant. W1,W2: 1st and 2nd washing elute.

Figure 6.5 The effect of a gradient of NaCl concentration on *x*HP1α binding of chromatin

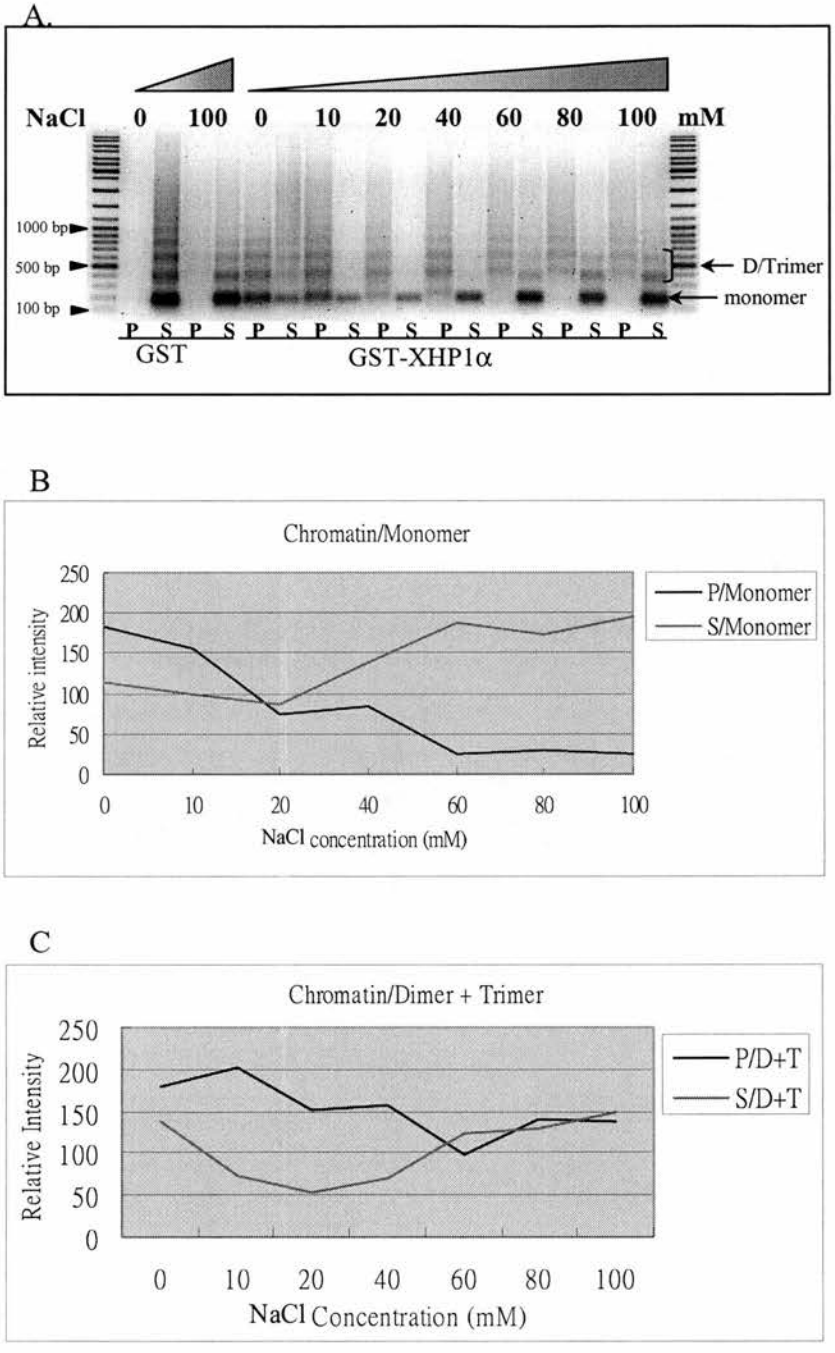

Figure 6.5 (A) chromatin was incubated with 10 μg GST or 10 μg GST-*x*HP1α **coupled to Glutathione-Sepharose** with a different concentration of NaCl (0-100 mM) for 30 minutes. All the samples were spun at 13,000 rpm. The pellets and the supernatant were separated by 1.5% agarose gel and visualized by ethidium bromide staining. (B&C) The monomer and the dimer + trimer revealed in the gel were quantified using phosphor imager and plotted by relative intensity versus NaCl concentration. Abbreviation: P: pellet; S: supernatant; D+T: the dimer + trimer.

Figure 6.6 The effect of a gradient of NaCl concentration on *x*HP1α binding of H1 & H5 depleted chromatin

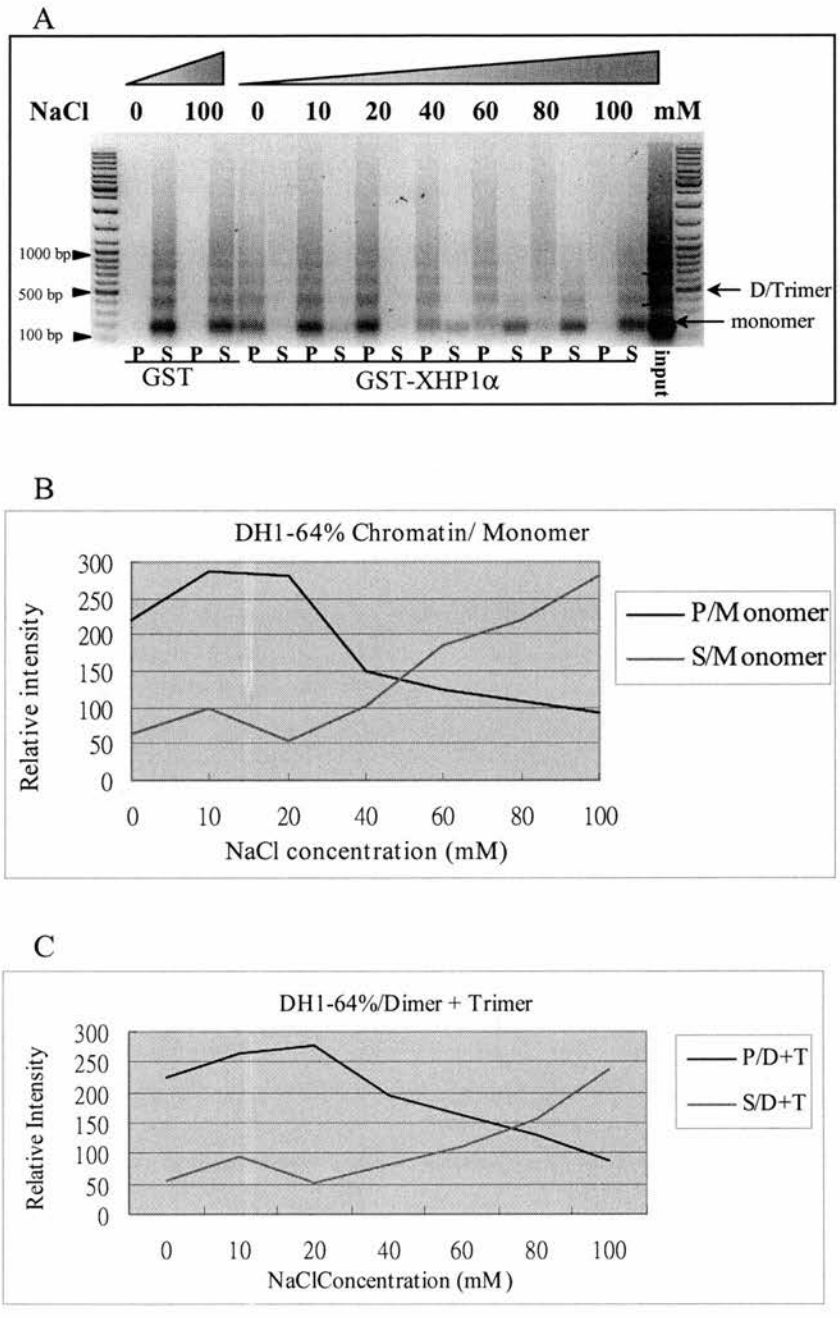

Figure 6.6 (A) 64% H1 & H5 depleted chromatin was incubated with 10 μg GST or 10 μg GST-*x*HP1α **coupled to Glutathione-Sepharose** with a different concentration of NaCl (0-100 mM) for 30 minutes. All the samples were spun at 13,000 rpm. The pellets and the supernatant were separated by 1.5% agarose gel and visualized by ethidium bromide staining. (B&C) The monomer and the dimer + trimer revealed in the gel were quantified using phosphor imager and plotted by relative intensity versus NaCl concentration. Abbreviation: P: pellet; S: supernatant; D+T: the dimer + trimer.

Figure 6.7 The effect of a gradient of NaCl concentration on *x*HP1α binding of trypsinised chromatin

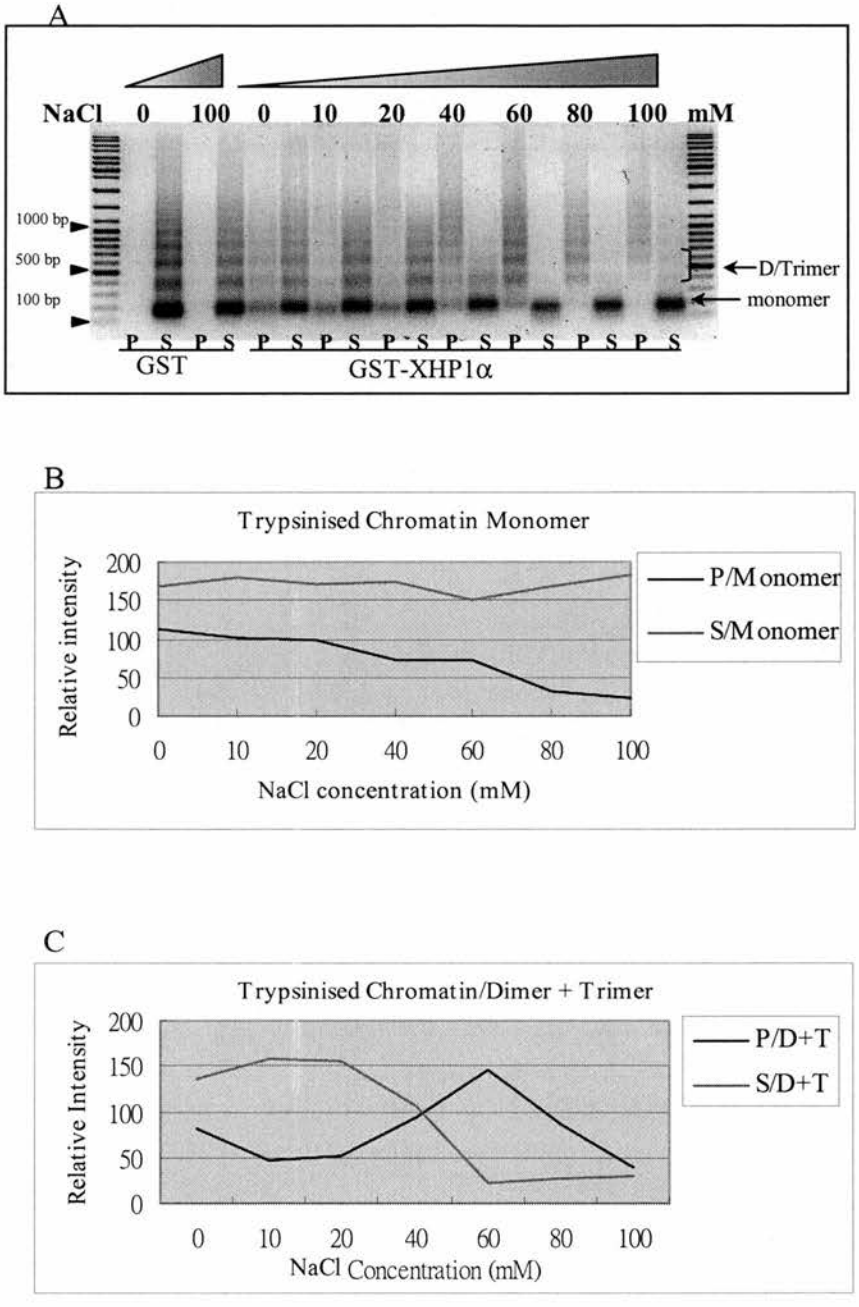

Figure 6.7 (A) Trypsinised chromatin was incubated with 10 μg GST or 10 μg GST-XHP1α **coupled to Glutathione-Sepharose** with a different concentration of NaCl (0-100 mM) for 30 minutes. All the samples were spun at 13,000 rpm. The pellets and the supernatant were separated by 1.5% agarose gel and visualized by ethidium bromide staining. (B&C) The monomer and the dimer + trimer revealed in the gel were quantified using phosphor imager and plotted by relative intensity versus NaCl concentration. Abbreviation: P: pellet; S: supernatant; D+T: the dimer + trimer.

Figure 6.8 The effect of gradient of NaCl concentration on *x*HP1α binding of DNA only

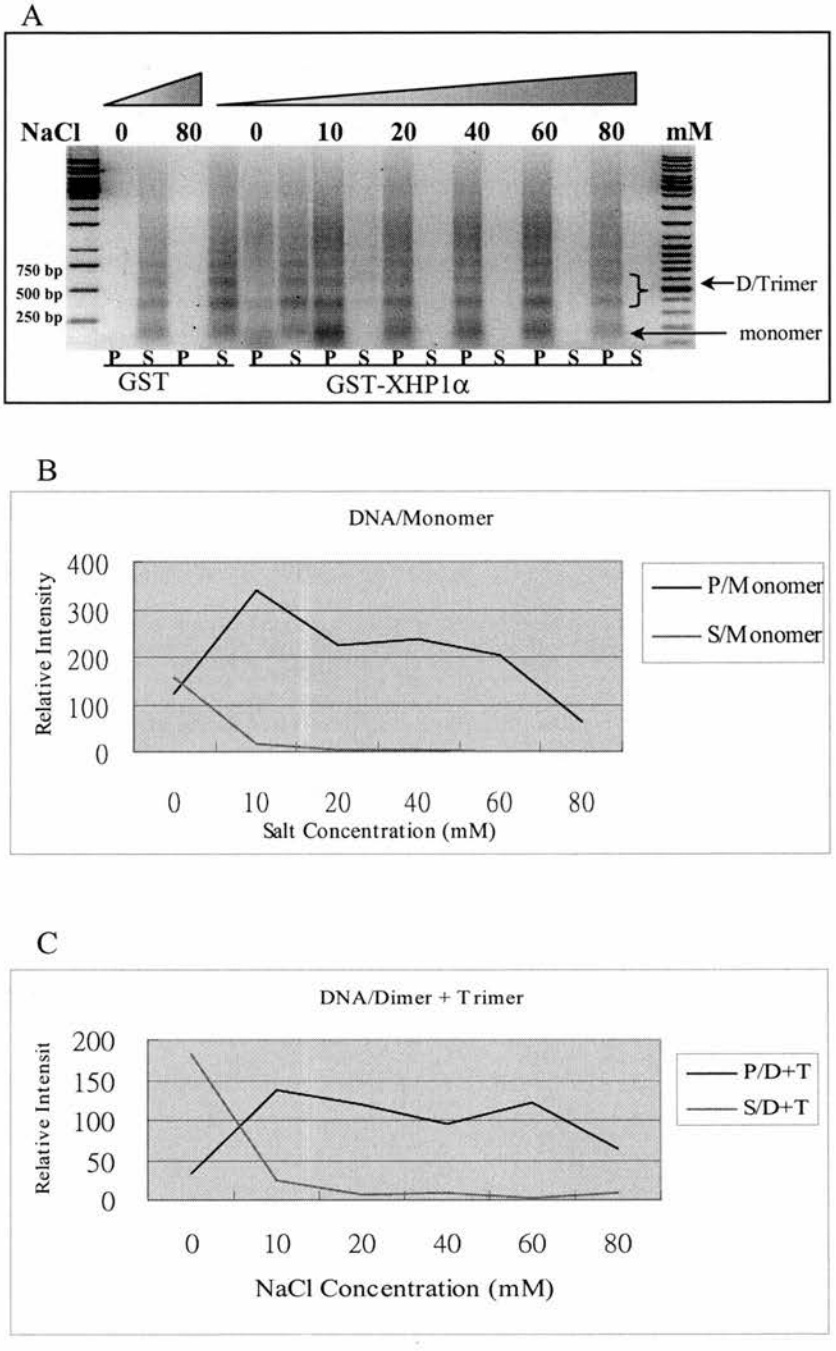

Figure 6.8 (A) Chromatin DNA was incubated with 10 μg GST or 10 μg GST-*x*HP1α **coupled to Glutathione-Sepharose** with a different concentration of NaCl (0-80 mM) for 30 minutes. All the samples were spun at 13,000 rpm. The pellets and the supernatant were separated by 1.5% agarose gel and visualized by ethidium bromide staining. (B&C) The monomer and the dimer + trimer revealed in the gel were quantified using phosphor imager and plotted by relative intensity versus NaCl concentration. Abbreviation: P: pellet; S: supernatant; D+T: the dimer + trimer.

Figure 6.9 Without histone tails, HP1α chromatin binding has preference of the fraction with longer DNA fragment

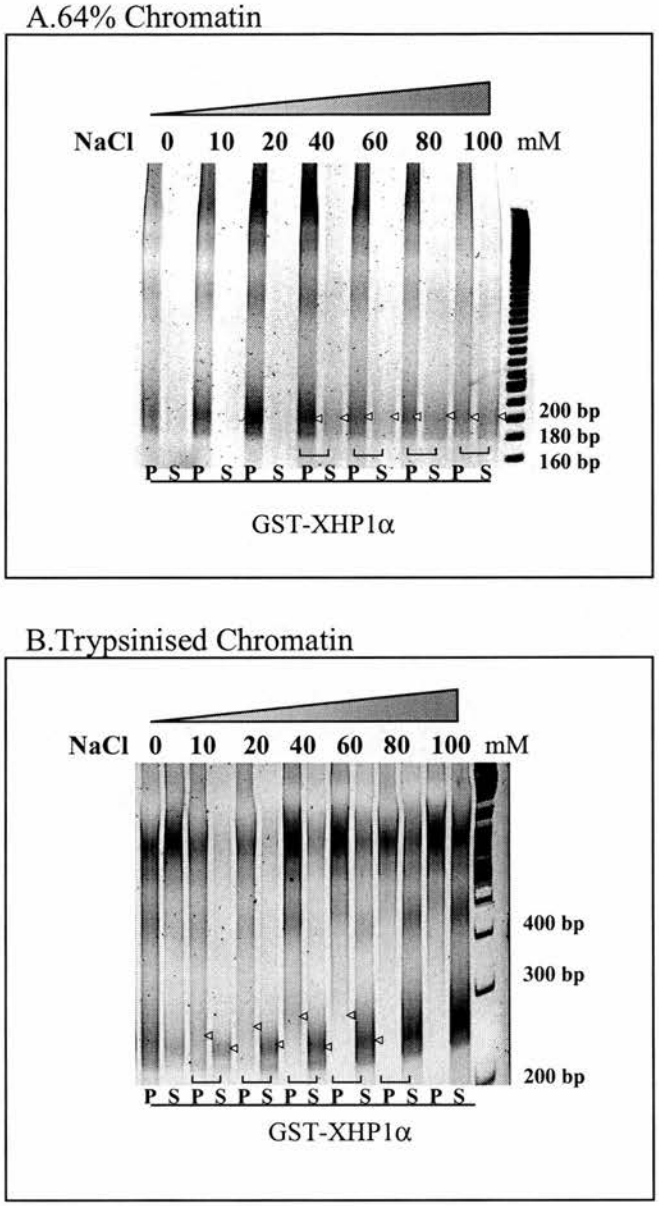

Figure 6.9 The same samples with figure 6.3 (A) and 6.4 (B) were separated using 6% PAGE. The monomers in the pellet and supernatant fractions are indicated by arrow heads (◃).

Figure 6.10 The increased concentration of *x*HP1α elevates chromatin binding on a gradient of NaCl concentration

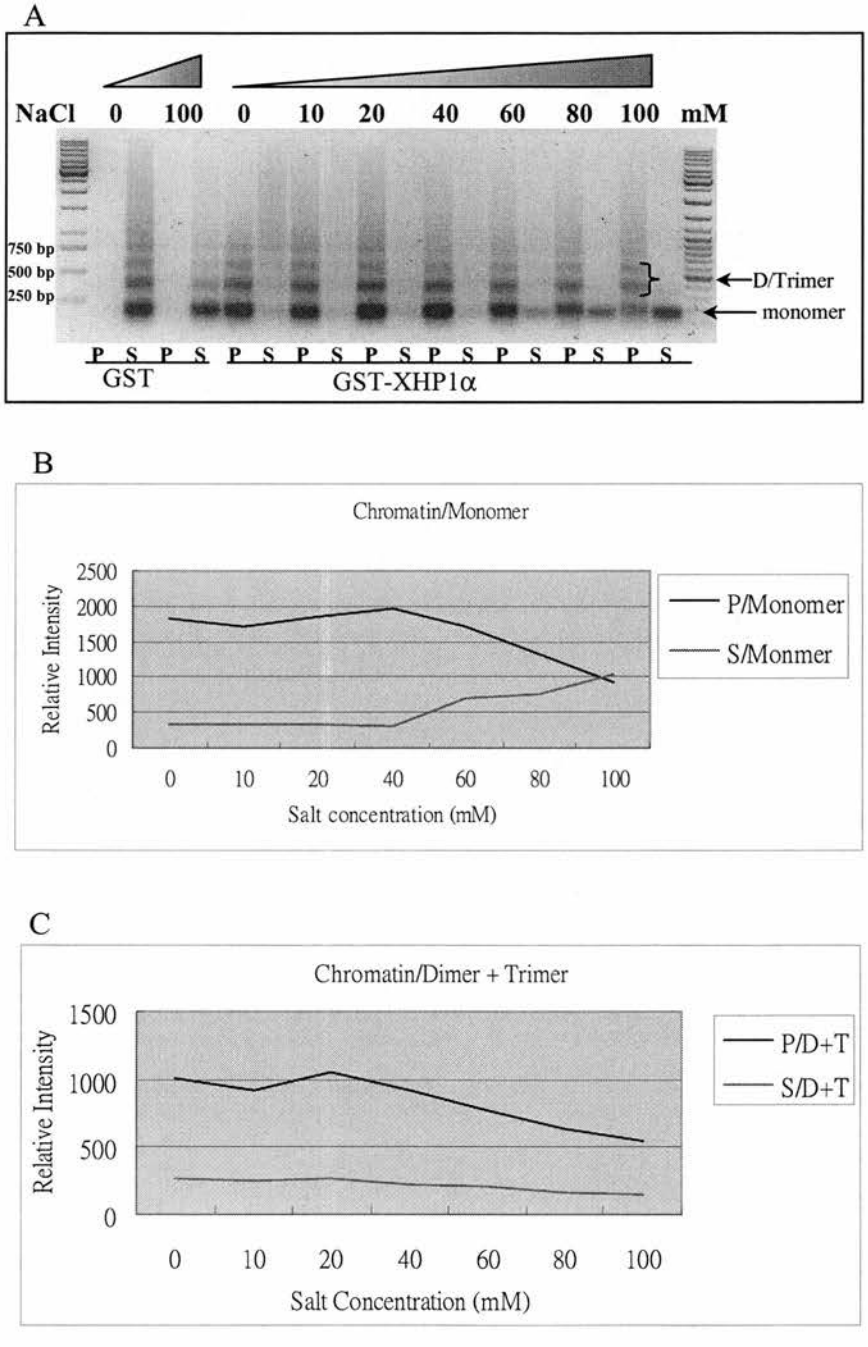

Figure 6. 10 (A) chromatin was incubated with 20 μg GST or 20 μg GST-*x*HP1α **coupled to Glutathione-Sepharose** with a different concentration of NaCl (0-100 mM) for 30 minutes. All the samples were spun at 13,000 rpm. The pellets and the supernatant were separated by 1.5% agarose gel and visualized by ethidium bromide staining. (B&C) The monomer and the dimer + trimer revealed in the gel were quantified using phosphor imager and plotted by relative intensity versus NaCl concentration. Abbreviation: P: pellet; S: supernatant; D+T: the dimer + trimer.

Figure 6.11 The increased concentration of *x*HP1α elevates the binding of H1 & H5 depleted chromatin on a gradient of NaCl concentration

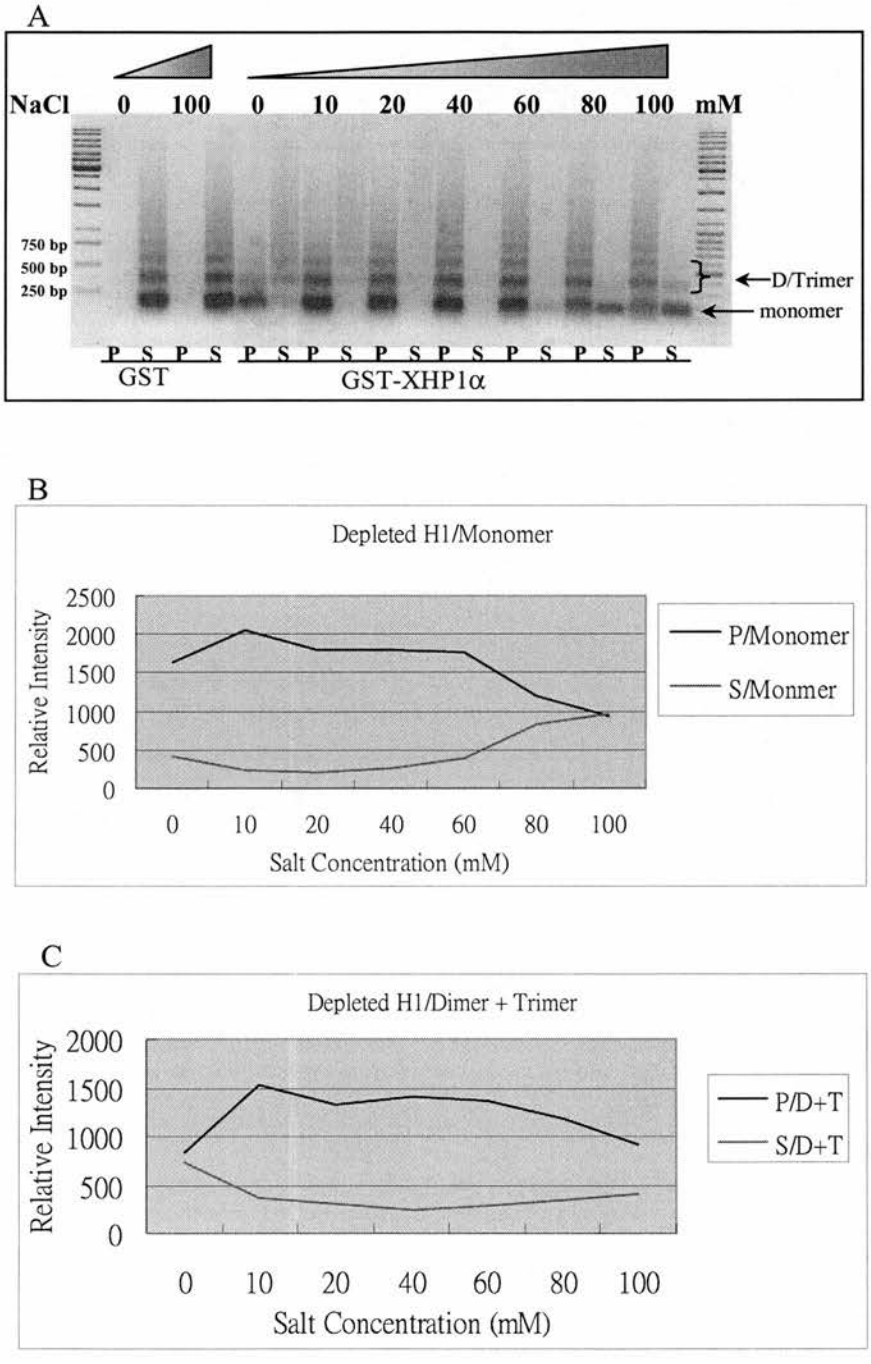

Figure 6.11 (A) H1 & H5 depleted chromatin was incubated with 20 μg GST or 20 μg GST-*x*HP1α **coupled to Glutathione-Sepharose** with a different concentration of NaCl (0-100 mM) for 30 minutes. All the samples were spun at 13,000 rpm. The pellets and the supernatant were separated by 1.5% agarose gel and visualized by ethidium bromide staining. (B&C) The monomer and the dimer + trimer revealed in the gel were quantified using phosphor imager and plotted by relative intensity versus NaCl concentration. Abbreviation: P: pellet; S: supernatant; D+T: the dimer + trimer.

Figure 6.12 The increased concentration of *x*HP1α elevate the binding of trypsinised chromatin on a gradient of NaCl concentration

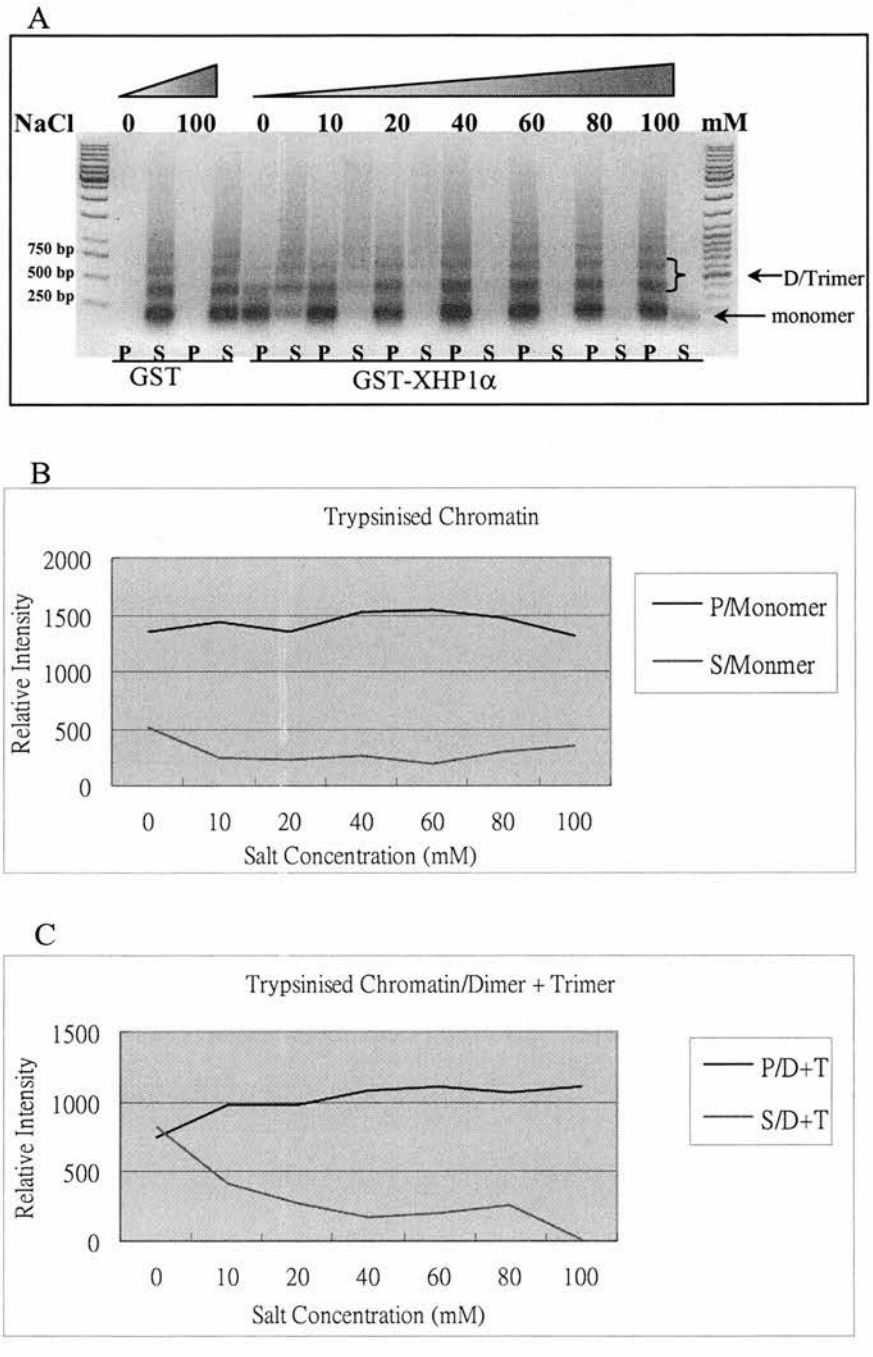

Figure 6.12 (A) Trypsinised chromatin was incubated with 20 μg GST or 20 μg GST-*x*HP1α **coupled to Glutathione-Sepharose** with a different concentration of NaCl (0-100 mM) for 30 minutes. All the samples were spun at 13,000 rpm. The pellets and the supernatant were separated by 1.5% agarose gel and visualized by ethidium bromide staining. (B&C) The monomer and the dimer + trimer revealed in the gel were quantified using phosphor imager and plotted by relative intensity versus NaCl concentration. Abbreviation: P: pellet; S: supernatant; D+T: the dimer + trimer.

Chapter 7 *x*HP1α and *x*HP1γ are required for post-MBT transcriptional gene regulation during *Xenopus* development

7.1 Introduction

In *Drosopihla melanogaster*, the genetic dissection of heterochromatin is aided by the availability of numerous rearrangements, which lead to variegated expression of euchromatic genes that have come to be relocated near the heterochromatic breakpoint. A number of loci have been identified which, when mutated, act as dominant modifiers of such variegating position effects (Reuter et al., 1982; Sinclair et al., 1989; Reuter and Wolffe, 1981; Reuter et al., 1982; Locke et al., 1988; Wustmann et al, 1989). Many of these loci are believed to encode chromatin proteins or factors that modify chromatin structure. One of these loci, *Su(var)2-5* that encodes heterorchromatin protein 1 (HP1), has been identified and characterised in *Drosophila melanogaster*. Loss of function mutations in the gene of *Su(var) 2-5* encoding HP1 in *Drosophlia* decrease the mosaic repression observed for euchromatic genes that have been juxtaposed to centromeric heterochromatin (Kellum and Alberts 1995). Mutations in *Su(var)2-5* gene also cause recessive embryonic lethality, which is found to be associated with defects in chromosome morphology and segregation. While some of these defects are seen throughout

embryonic development, both the frequency and severity of the defects are greatest between cycles 10 and 14 when zygotic transcription apparently begins (Edgar and Schubiger, 1986).

Xenopus laevis is a vertebrate model organism widely used in the field of development biology. To investigate the function of newly cloned genes, over-expression or ectopic expression by microinjection of DNA or mRNA has been performed in *Xenopus* embryos. Methods for loss of function analysis used in the Xenopus system are injections of antisense RNAs (Streinbeisser et al. 1995), DNA expression constructs generating antisense RNA (Lantinkic and Smith, 1999), or mRNA encoding dominant negative constructs, which have been applied for studies of ligands, receptors, intracellular signaling components, or transcription factors. I employed *Xenopus laevis* in this study as a vertebrate model to address the embryonic roles of *x*HP1α and *x*HP1γ. I demonstrate that both the deletion and the overexpression of *x*HP1s RNA result in abnormality in gastrulation that is reflective of the functional requirement of these proteins in gastrulation and subsequent neural development.

7.2 Results

7.2.1 Controls for mRNA injection

Injection of cleavage-stage embryos with mRNA has been the most popular way to overexpress genes in *Xenopus*. This straightforward procedure allows up to 5 ng of RNA to be introduced into the embryos (Krieg and Melton, 1987) and the injected mRNAs are generally translated immediately. Although the usefulness of mRNA injection is clear, the interpretation of results requires appropriate controls. A successful control mRNA must meet several requirements: (1) it must be non-toxic

and non-reactive so that it does not change the development fate of the labelled cell; (2) it must be small enough to diffuse quickly through the injected cell, before the cell divides, so that all of the descendants are evenly and completely labelled, but large enough not to pass through the numerous junctions between adjacent blastomeres (Guthrie et al, 1988); (3) it must remain detectable throughout development and not be diluted by cell mitosis or intracellular degradation; and (4) it should be easily detectable by simple histological procedures.

In my injection experiments, β-galactosidase (β-gal) mRNA was chosen as a control injection in paralleled with the *x*HP1 mRNAs injections. β-gal is derived from a non-vertebrate (bacteria) and can be easily distinguished from endogenous vertebrate proteins. It has no known deleterious effects on developing vertebrate cells, is very stable and can be detected in the descendant cells as late as up to the tadpole stages 45-48 by simple histological procedures. The β-gal mRNA injected embryos are normally fixed with formaldehydes and the enzyme activity of β-gal can be detected by applying a substrate that undergoes a colorimetric reaction, producing an insoluble, blue coloured precipitate. The location of the precipitate indicates the cellular location of the β-gal, which was encoded by the injected mRNA. An advantage of this technique is that the preparations are essentially permanent and can be used as reference material for years. (Sive et al., 1998).

As a control injection experiment, the albino embryos were injected into one blastomere of two-cell stages embryos with 340 pg of β-gal mRNA, or mixed mRNAs of β-gal (340 pg) and anti-sense RNA of *x*HP1α (720 pg) or *x*HP1γ (530 pg). After fixing and performing colour reactions, the embryos showed a one-sided, even blue colour pattern on the surfaces (Figure 7.1 A, D, E). I also performed an injection of 340 pg of β-gal mRNA into 44 wild-type embryos and left them to grow until tail

buds. As a result, 31 embryos out of 44 (70.5 %) grew normally until the tailbud stage 35 and 10 out of 44 (22.7%) survived with a non-specific defective phenotype. 3 injected embryos (6.8%) died before tailbud (Figure 7.1 B, C). In parallel, a collection of 60 non-injected wild type embryos developed normally until the tailbud stage 35 with only 5% (n=3) defective embryos.

In conclusion, first of all, the microinjection technique performed in the injection experiment was able to deliver mRNAs into the embryo blastomere without damaging the cells. Most of the injected embryos survived until the tailbud stage 35. Second, the injected mRNAs could be translated into protein that can be histologically detected in the embryos. Finally, the *in vitro* translated mRNA was not toxic to the embryos, as most of the β-gal mRNA-injected embryos grew normally.

7.2.2 Depletion of maternally derived *x*HP1α, *x*HP1γ

To determine whether the maternal *x*HP1α and *x*HP1γ are essential for the early *Xenopus* embryo development, I used antisense RNA microinjection to deplete maternally derived *x*HP1α and *x*HP1γ mRNAs. Early embryos were injected with antisense RNA derived from full length of *x*HP1α or *x*HP1γ cDNA. Control and injected embryos were cultured until the equivalent of the tadpole stage 35 and monitored and recorded for their phenotypic appearance at blastula, gastrula and neurula respectively. Figure 7.2-A and Figure 7.2-B summarise the results of the experiments with the microinjection of antisense RNA. As mentioned previously, the injection of 340 pg of β-gal of sense RNA into the one blastomere of two-cell stages embryos had no noticeable effect on embryos survival or appearance. In contrast, significant development abnormalities appeared when antisense *x*HP1α or *x*HP1γ RNA was injected. Embryos injected with720 pg of antisense *x*HP1α RNA exhibited

a considerable delay in development during the blastula and gastrula stages when compared to the control embryos of the same stages. When the injected embryos were allowed to develop further, nearly 30% of them died during neurulation while 40 % of the embryos exhibited a defect in dorsal development and stopped growth at this stage (Figure 7.2 C). Only few embryos (less than 3 %) survived during the neurulation and grew up to tailbud showing severe axis truncation.

A much more dramatic phenotype was caused by injection of antisense *x*HP1γ RNA. A considerable number of embryos injected with 530 pg antisense *x*HP1γ RNA died during blastula and more than 50% of the embryos died during gastrulation. Virtually, the development of most of the embryos (more than 90%) was arrested during early gastrula stage, not showing any sign of narrowing (convergence) and elongation (extension) of dorsal ectoderm, which will form all of the components of the central nervous system (Egaleson and Harris, 1990). Furthermore, the dead phenotype presented an abnormal pigmentation on the animal pole and membrane-bound bodies (apoptotic bodies). These features are similar to characters of ionising-radiation-induced apoptosis in early Xenopus embryos (Anderson et al, 1997). The possibility of apoptosis induced by depletion of *x*HP1γ in early development is subject to future investigation.

In conclusion, both maternally *x*HP1α and *x*HP1γ are crucial for early development in *Xenopus*. The depletions of maternally stock of *x*HP1α or *x*HP1γ, although having different phenotypic effects, impair the normal embryo development in *Xenopus*.

7.2.3 Overexpression of *x*HP1α induces dorsal defect in development and its function is conserved from *Xenopus* to Human

In order to test whether interference with the expression levels of *x*HP1α and *x*HP1γ proteins might influence early embryonic development, as a pilot experiment, *x*HP1α or *x*HP1γ RNA derived from full length of *x*HP1α or *x*HP1γ cDNA (200 pg of each RNA) was injected of into one blastomere of two-cell embryos (Figure 7.3). Blastopore formation during gastrulation occurred normally in both *x*HP1α and *x*HP1γ RNA injected embryos. However, the formation of the neural plate proceeded aberrantly in *x*HP1α RNA-injected embryos that had apparently normally head structure but almost completely missing the dorsal trunk tissues and had a very short axis (Figure 7.3 D). This phenotype was observed in approximately 40% (n = 49) of the embryos (Figure 7.3 C). In the case of *x*HP1γ RNA injection, the embryos developed a normal formation of the neural plate and displayed a clear anteroposterior axis in neurula. However, an elongated anteroposterior axis became apparent at tailbud stage and caused the embryos bent to one side (Figure 7.3 E). Approximately 30 % (n = 38) of the embryos displayed the dorsalisation phenotype (Figure 7.3 C). This suggest that *x*HP1α and *x*HP1γ essential for the formation of embryo dorsal tissues.

The above results clearly show that embryo development at the stage of neuralation is altered by overexpressed *x*HP1α and *x*HP1γ during early stages. Nevertheless, *x*HP1α overexpression displayed a more dominant defect in the formation of the anteroposterior axis. To understand more about the influence of *x*HP1α overexpression in early development, I decided to repeat the overexpression experiment of *x*HP1α using a higher dose of RNA for the microinjection. In addition, I performed the injection of the human HP1α (*h*HP1α,) RNA into the early stage of

Xenopus embryo to address whether the function of HP1α is conserved in early development of different organisms. *x*HP1α RNA (940 pg) (Figure 7.4-A) was injected into both blastomeres of two-cell embryos. Approximately 53 % of injected embryos develop normally as evidenced by blastopore formation during gastrulation. The rest of the embryos became arrested during gastrulation (47%) (Figure 7.4-B). The dorsal defect of the embryos became apparent at late neurula and tailbud stages (Figure 7.4-C). A significant number of the embryos (45.2%) exhibited a severe bending from ventral to dorsal and truncated axis during neurulation, implying that a perturbation of axis formation during neural development occurred (Figure 7.4-C). In addition to the *x*HP1α overexpression, the expression of *h*HP1α also displayed a severe bending from ventral to dorsal during neurulation with an almost identical phenotype to its *Xenopus* counterpart. Although only 26% of the embryos exhibited the phenotype, much less than the proportion exhibited by the embryos with *x*HP1α overexpression, it is possible that this is due to experimental variations during the two injections, or that it represents functional differences between the protein sequences. A previous study has shown that the CD of M31 can functionally replace the CD of swi6p, demonstrating that the classical CD function is conserved from yeast to humans (Wang et al. 2000). Given the similarity of the phenotypes and the conservation in the amino acid sequences, these experiments imply that *x*HP1α function could be substituted by cross-specious HP1α during *Xenopus* embryo development.

7.2.4 Expression of Dominant negative *x*HP1α

HP1 contains two protein-interaction modules that correspond to the amino chromo domain (CD) and carboxyl chromo shadow domain (CSD). A variety of

studies implicate these domains in HP1 function, including nuclear organisation, chromosome segregation, and gene silencing (Henikoff, 2000). However, it has never been addressed what role these two chromo domains may play during early embryo development. To address this question, I decided to carry out the loss of function analysis by injection of *h*HP1α mRNAs that contain mutation in the CD and CSD domain.

According to the results in the previous section, the *x*HP1α function is conserved from *Xenopus* to human; it would be convenient to do a test using the mutant form of human HP1α generated from previous studies. To this end, we obtained mutant forms of *h*HP1α, which has previously characterised in detail (Lechner et al. 2000), from the laboratory of Frank Rauscher III's. One of the mutants has a point mutation in amino acid sequence 129 (A129R), which is located in CSD. This mutation essentially abolishes the interaction between *h*HP1α and many partner proteins, such as KAP-1, SP100, LBR and CAF-1p150. The other amino acid substitution is places in CD, amino acid sequence 21 (V21M), which correspondent to the lethal mutation in *Drosophlia* HP1 encoded by Suvar 2-5. I performed an injection experiment using sense RNAs derived from the two mutant form of *h*HP1α cDNAs, accompanying an injection of wild type *h*HP1α RNA (WT) (Figure 7.5 A). A considerable number of embryos grew normally in WT, A129R and V21M injected embryos until gastrula (Figure 7.5). However, intriguing phenotypes became obvious during neurulation. WT and A129 displayed a similar phenotype, which was the dorsal bending of the embryos. In contrast, V21M injected embryos exhibited a normal neural development and axis formation. However, most of the embryos that survived to neurula were arrested at this stage and displayed an increased growth of the two sides of embryos, where were probably derived from

lateral plate in mesoderm (Figure 7.5 E). The results interestingly indicate that both CD and CSD may be involved in the regulation of genes during neurulation of *Xenopus* embryos and these two domains are likely to play different roles during development.

7.2.5 The role of *x*HP1 for the regulation of gene-expression in *Xenopus* embryo.

In order to test whether in *Xenopus* embryos *x*HP1 operates as a transcription regulator, we decided to investigate on the level of transcription when *x*HP1α or *x*HP1γ were overexpressed during *Xenopus* embryo development. This was done by measuring the incorporation of ^{35}S-UTP into total RNA after injection of *x*HP1α or *x*HP1γ sense RNA (Figure 7.6 A). In collaboration with Dr. Irina Stancheva, embryos were injected with 500 pg of *x*HP1α or *x*HP1γ RNA or a mixed RNA of 250pg *x*HP1α and 250pg *x*HP1γ into both blastomeres of 2-cell *Xenopus* embryos. Surprisingly, we found that the embryos overexpressing *x*HP1α or *x*HP1γ incorporated nearly double amount of ^{35}S-UTP during gastrulation, in comparison to the control, non-injected embryos. In the case of the embryos injected both *x*HP1α and *x*HP1γ RNA together, the incorporation level was four times higher than that of the control embryos or two times higher than the embryos overexpressing *x*HP1α or *x*HP1γ only (Figure 7.6 B). In neurula, the incorporation of ^{35}S-UTP in the embryos overexpressing *x*HP1α or *x*HP1γ remained two times higher than the control embryos. The embryos injected with both *x*HP1α and *x*HP1γ RNA incorporated approximately 30% more ^{35}S-UTP than the control embryos but less than *x*HP1α or *x*HP1γ RNA overexpressing siblings.

The increased incorporation of ^{35}S-UTP indicated that transcription regulation

in *Xenopus* embryos was altered by the overexpressions of *x*HP1 proteins. This suggests that *x*HP1s plays a key role in maintaining normal level of transcription.

7.3 Discussion

It is generally believed that HP1 may simply function as an organiser of higher order chromatin in the nucleus. This organising property may serve to accommodate the transcription of genes that reside within heterochromatin. Conversely, rearrangements that place euchromatin genes next to a heterochromatin breakpoint could make genes assembly into HP1 dependent heterochromatin and silence those genes by template occlusion (Eissenberg and Elgin, 2000).

In *Drosophila*, loss of function mutations in the gene encode HP1 suppress the position-effect variegation, and also causes embryonic lethality. The lethality was found to be associated with defects occurring between cycles 10 and cycles 14 of early embryo cell divisions when gene transcription is activated (Kellum and Alberts 1995). This study concluded that HP1 is required for normal nuclear morphology and mitosis. The early embryonic development in *Drosophila* (Edger et al, 1986) and amphibians (Gurdon and Woodland, 1968; Newport and Kirschner, 1982) is characterised by a period of rapid cell/nuclear cycles, little or no transcription, and a homogeneous appearance of chromatin. Both types of embryos undergo an analogous transition period that involves a slowing of the cell cycle, the onset of transcription of most genes, and an increased heterogeneity in chromatin appearance. This transition takes place during nuclear cycles 10 to 14 in *Drosophila* (Edger and Schubiger, 1986). In *Xenopus*, transcription in early development remains fully repressed until the 13th cell cycle post-fertilisation. At this stage, the mid-blastula transition (MBT) occurs relatively abruptly with a generalised reactivation of gene

expression. The distinct properties of heterochromatin are thought to be due to a specialised nucleoprotein organisation during this transition.

To study the functional significance of HP1 in the development, I manipulated the expression of the *Xenopus* homologues of these proteins, *x*HP1α and *x*HP1γ. My data point towards an early development role for *x*HP1α and *x*HP1γ. Both the depletion and overexpression experiments clearly show that *x*HP1 proteins are essential for early development after the MBT. This observation is consistent with the prediction that HP1 may act as an essential player in the dynamic organisation of nuclear architecture.

My observation in the S^{35}-incorporation experiment suggests that *x*HP1 may act as a core component in the higher order chromatin structure, in which many other factors are involved. The functional heterogeneity of heterochromatin is reflected by the fact that regions of heterochromatin contain actively transcribed gene. The ribosomal genes are organised into tandem arrays in the heterochromatin in multicellular organisms. *Drosophila* has on the order of 20-protein-encoding, heterochromatic genes. Importantly, at least seven of these genes have been shown to require proximity to heterochromatin for their normal expression. Thus, the results of the S^{35}-incorporation experiment have to be interpreted by at least two different directions. First, depleting or overexpressing the core of this HP1-associated complex would result in corruption of the higher order chromatin structure and disrupt HP1-dependent gene silencing and then result in the increased transcription level of affected genes. Second, the activation of heterochromatic genes, for instances, the ribosomal genes could be affected by this structure disruption. Alternatively, the hundreds copies of the genes previous may be in the control of heterochromatic mediating, then burst into high level of transcription. Thus, the

increased S^{35}-incorporation level may only be sourced from heterochromatic genes.

More importantly, HP1 may still be key for transcriptional regulation. The RT-PCR analysis in Chapter 3 has shown that the expression level of *x*HP1α increases to its highest level during neurulation. The whole mount *in situ* hybridisation of *x*HP1α and immunostaining of *x*HP1γ also show that *x*HP1s have a strong expression in the head and in the neural tube. There is a strong implication that *x*HP1α may be functionally significant for neural development. The results in Figure 7.5 interestingly indicate that both CD and CSD may be involved in regulation of gene expression during neurulation of *Xenopus* embryos and these two domains are likely to play different roles during development. To facilitate the interpretation of the phenotypes, it would be important to identify the affected genes, which are regulated by HP1α. This will be the subject of future investigations to reveal whether there is a pattern of HP1-related gene expression.

Figure 7.1 β-galactosidase mRNA is translated in embryos and has a limited distribution after targeted microinjection

A.

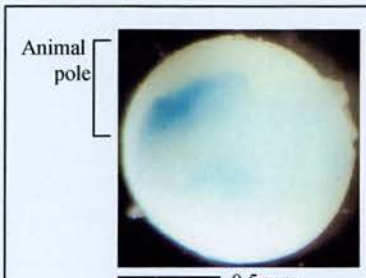

Albino embryo injected β-gal RNA in one cell

B.

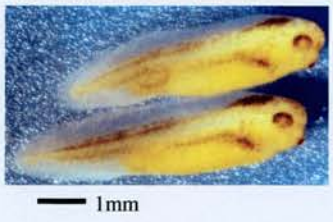

Wild type embryo injected β-gal RNA in both cells

C.

Inhibitory Reagents	Dosage of injection samples	Number of injected embryos	Normal	Defective phenotype	Dead
Wild type	0	60	57 (95%)	0	3 (5%)
β-gal	340 pg	44	31 (70.5%)	10 (22.7%)	3 (6.8%)

D.

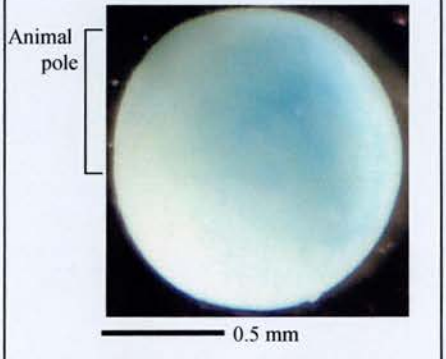

β-gal +Anti- xHP1α RNA injected in one cell

E.

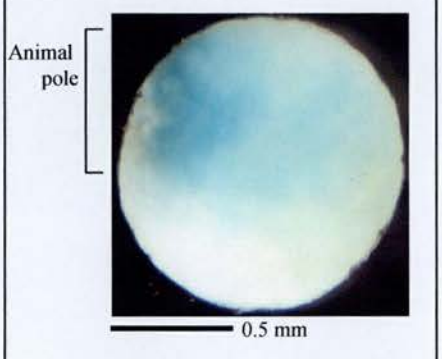

β-gal +Anti- xHP1γ RNA injected in one cell

Figure 7.1 (A) Albino embryos at the 2-cell stage were injected with 340 pg of β-galactosidase (β-gal) sense RNA into one of the cells. The injected embryos were collected at stage 9 (late blastula) and fixed. The β-gal expression was detected using a colorimetric reaction. (B) Wide type embryos at 2-cell stage were injected with 340 pg of β-gal sense RNA into both cells and 70 % of the injected embryos grew normally to tadpole stage 35. (C) Table showing dosages of β-galactosidase RNA injected into both cells of 2-cell stage embryos and number of embryos that were injected, in parallel with wild type embryos. (D & E) Albino embryos at the 2-cell stage were injected with 340 pg of (β-gal) sense RNA and anti-*x*HP1α (720 pg)/anti-*x*HP1γ RNA (530pg) into one of the cells. The injected embryos were collected at stage 9 (late blastula) and fixed. The β-gal expression was visualized using the method in (A).

Figure 7.2 Depletion of *x*HP1 in *Xenopus* embryos pertubs development.

A.

Injected RNAs	Dosage of injection samples	Number of injected embryos
β-gal	340 pg	44
Anti-sense *x*HP1α	720 pg	94
Anti-sense *x*HP1γ	530 pg	102

B.

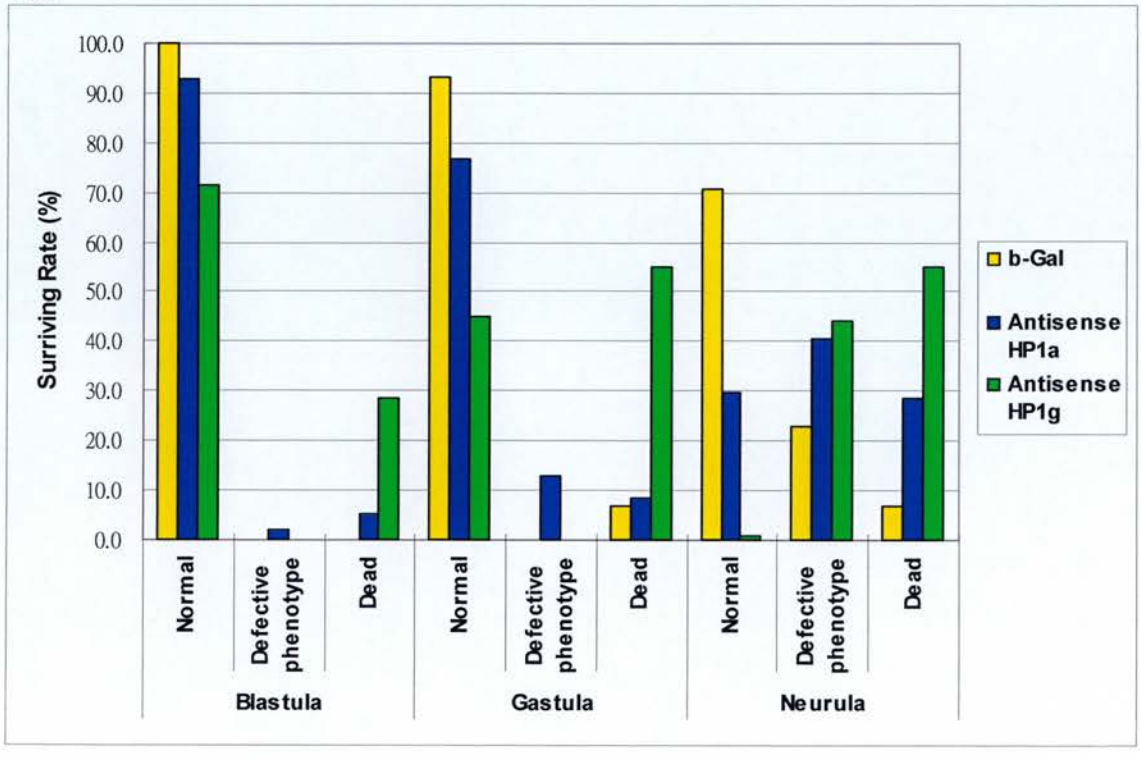

C.

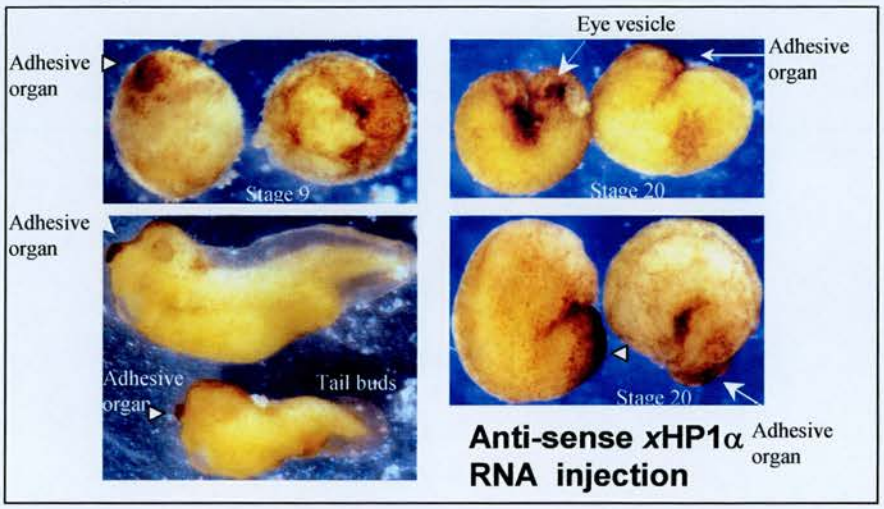

D.

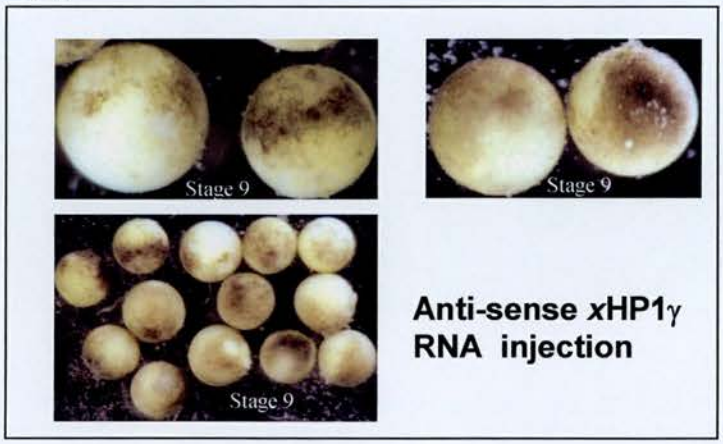

Figure7.2 (A) Table showing dosages of β-galactosidase, *x*HP1α anti-sense or *x*HP1γ anti-sense RNA injected into both cells of wild type 2-cell stage embryos and number of embryos that were injected. (B) The schematic diagram of phenotypes of the injected embryos. (C) The phenotypes of the *x*HP1α anti-sense RNA injected embryos at stage 9, 20 and tadpole stage 32-35. (D) All the *x*HP1γ anti-sense RNA injected embryos died at stage 9. The phenotype was similar to that of X-ray induced apoptosis.

Figure 7.3 Over-expression of *x*HP1α and *x*HP1γ shows different phenotypical defects in *Xenopus* embryos

A.

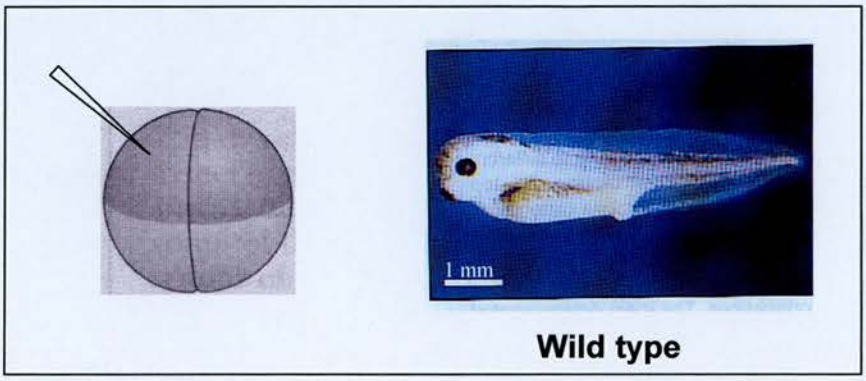

B.

Injected RNAs	Dosage of injection samples	Number of injected embryos
Sense *x*HP1α	200 pg	49
Sense *x*HP1γ	200 pg	38

C.

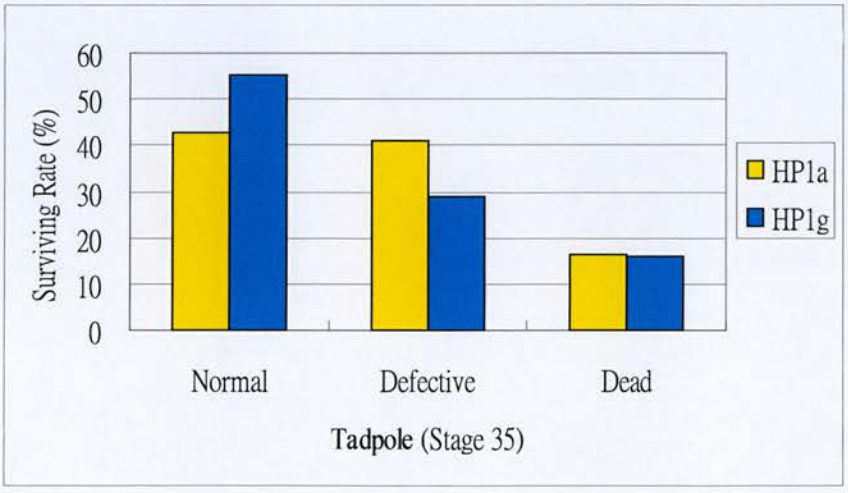

D.

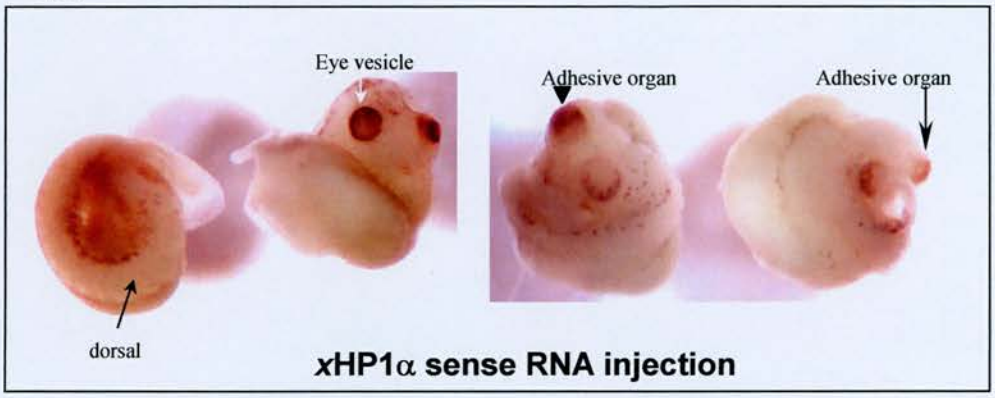

E.

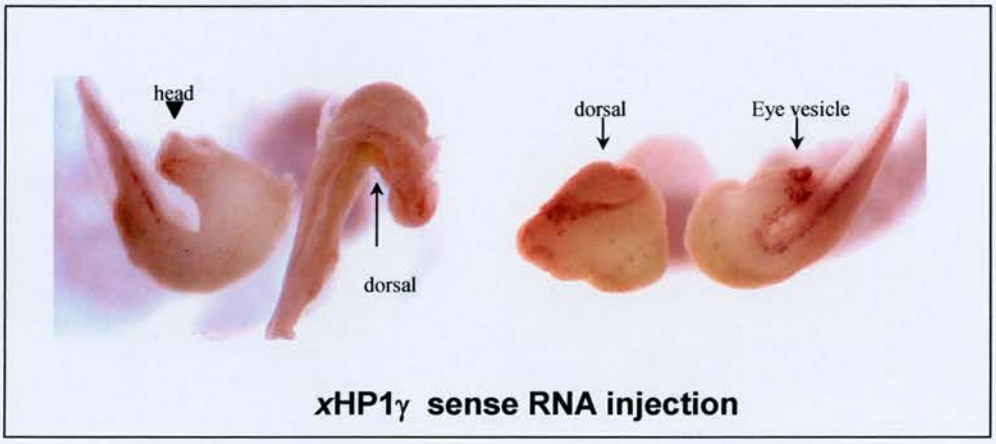

Figure 7.3 (A) Sense RNAs of *x*HP1α and *x*HP1 γ were injected into 1 cell of 2-cell stage pigmented embryo and the injected embryos were grown to the equivalent of tadpole stage 35 (Wild type embryos is shown.)(B) The table showing dosages of *x*HP1α sense or *x*HP1γ sense RNA were injected into one cell of wide type 2-cell stage embryos and the number of embryos were injected. (C) A schematic diagram of phenotypes of the injected embryos at stage 35. (D) The phenotypes of the *x*HP1α sense RNA injected embryos at tadpole stage35. (E) The phenotypes of the *x*HP1γ sense RNA injected embryos at tail bud stage 35.

Figure 7.4 Over-expression of human and *x*HP1α gives similar phenotypes in *Xenopus* embryos

A.

Injected RNAs	Dosage of injection samples	Number of injected embryos
Sense XHP1α RNA	940 pg	93
Sense Human HP1αRNA	960 pg	96

B.

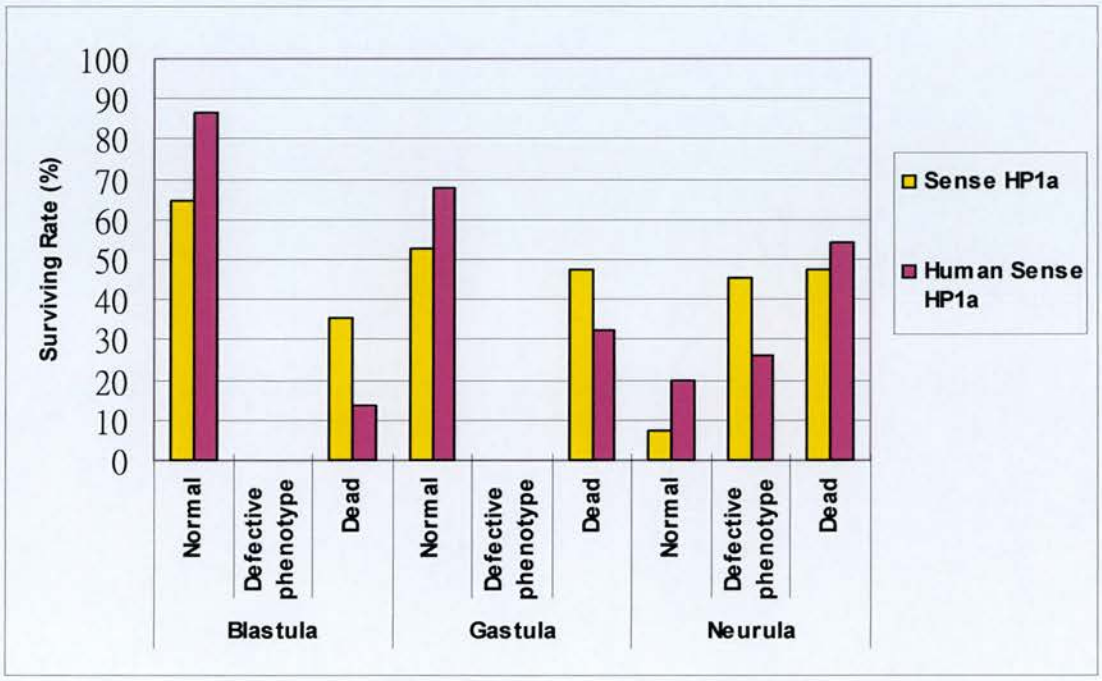

C.

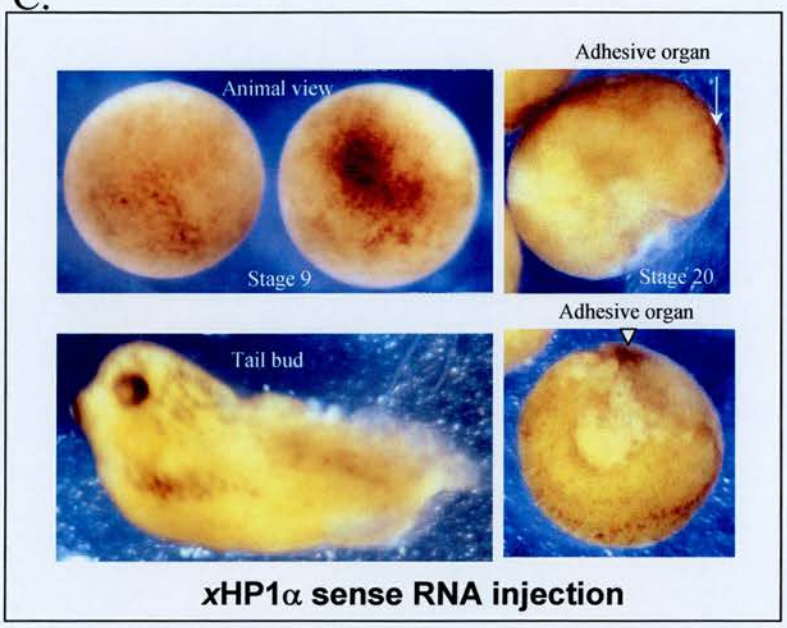

D.

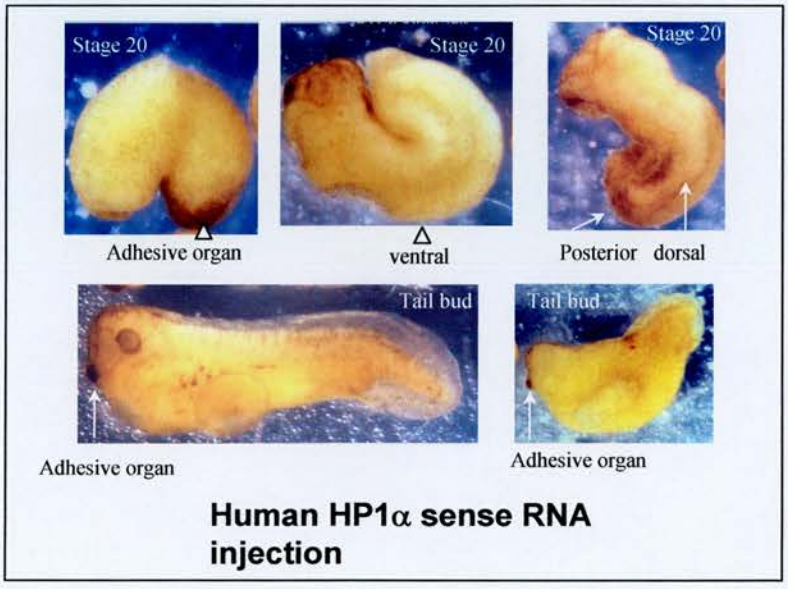

Figure7.4 (A) The table showing dosages of *x*HP1α sense or human HP1α sense RNA were injected into both cells of wide type 2-cell stage embryos and number of embryos were injected. (B) The schematic diagram of phenotypes of the injected embryos. (C) The phenotypes of the *x*HP1α sense RNA injected embryos at stage 9, 20 and tadpole stage 35. (D) The phenotypes of the human HP1α RNA injected embryos at stage 20 and tadpole stage 35.

Figure 7.5 Expression of dominant negative mutants of HP1α in the development of *Xenopus* embryos

A.

Human HP1α	Dosage of Injection samples	Number of injected embryos	T× repression	KAP-1/ TIF1-β	SP100	LBR
WT	960 pg	41	++	++	++	++
A129R (CSD)	960 pg	70	–	–	–	–
V21M (CD)	960 pg	59	Corresponding to lethal mutation in *Drosophlia*			

(Lechner et al, 2000, MCB)

B.

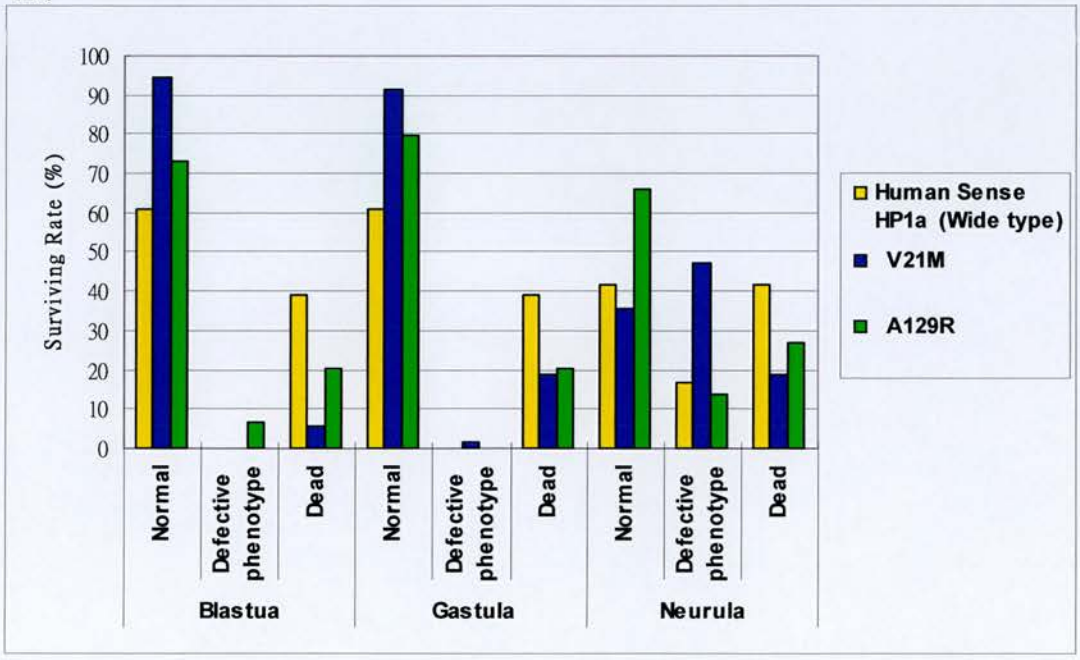

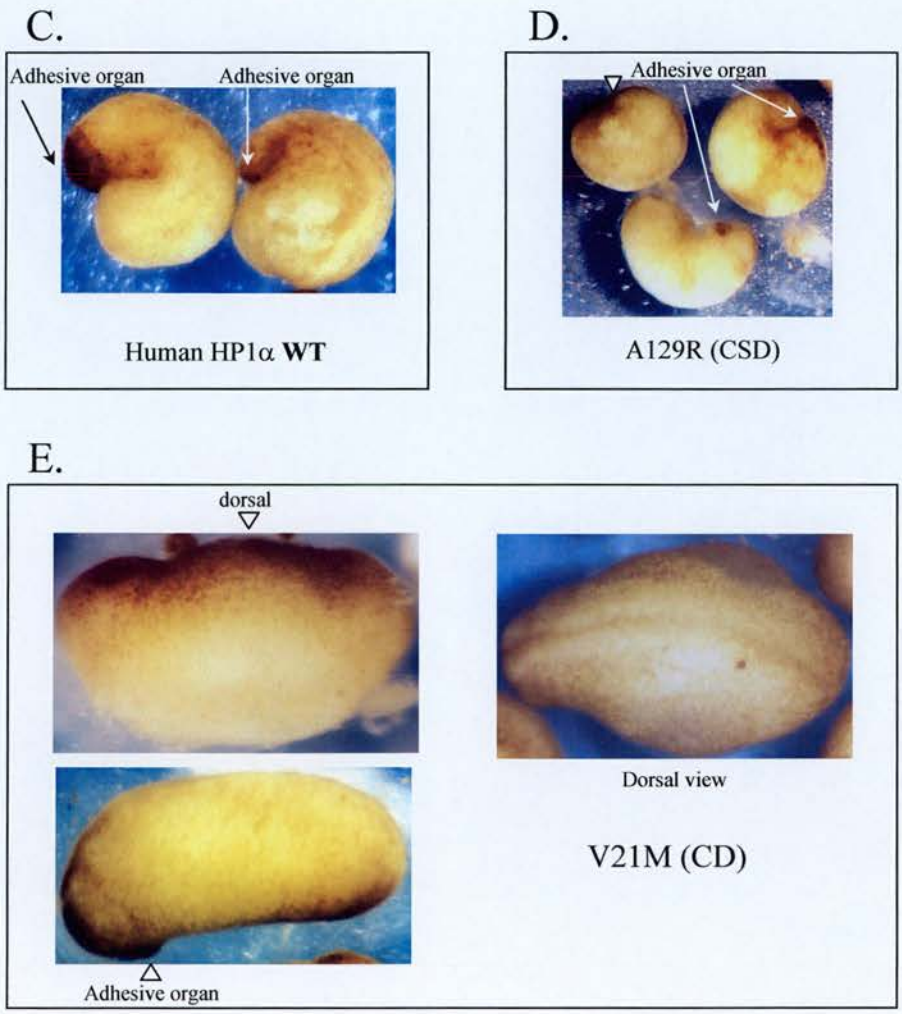

Figure7.5 (A) Table showing dosages of wild type (WT) and mutant form (A129R and V21M) human HP1α sense RNA, which were injected into both cells of wide type 2-cell stage embryos and the number of injected embryos. (B) The schematic diagram of phenotypes of the injected embryos. (C, D & E) The phenotypes of the WT, A129R and V21M human HP1α sense RNA injected embryos at stage 20 (early tailbud).

Figure 7.6 Overexpression of *x*HP1 intrudes on gene–expression in *Xenopus* embryos.

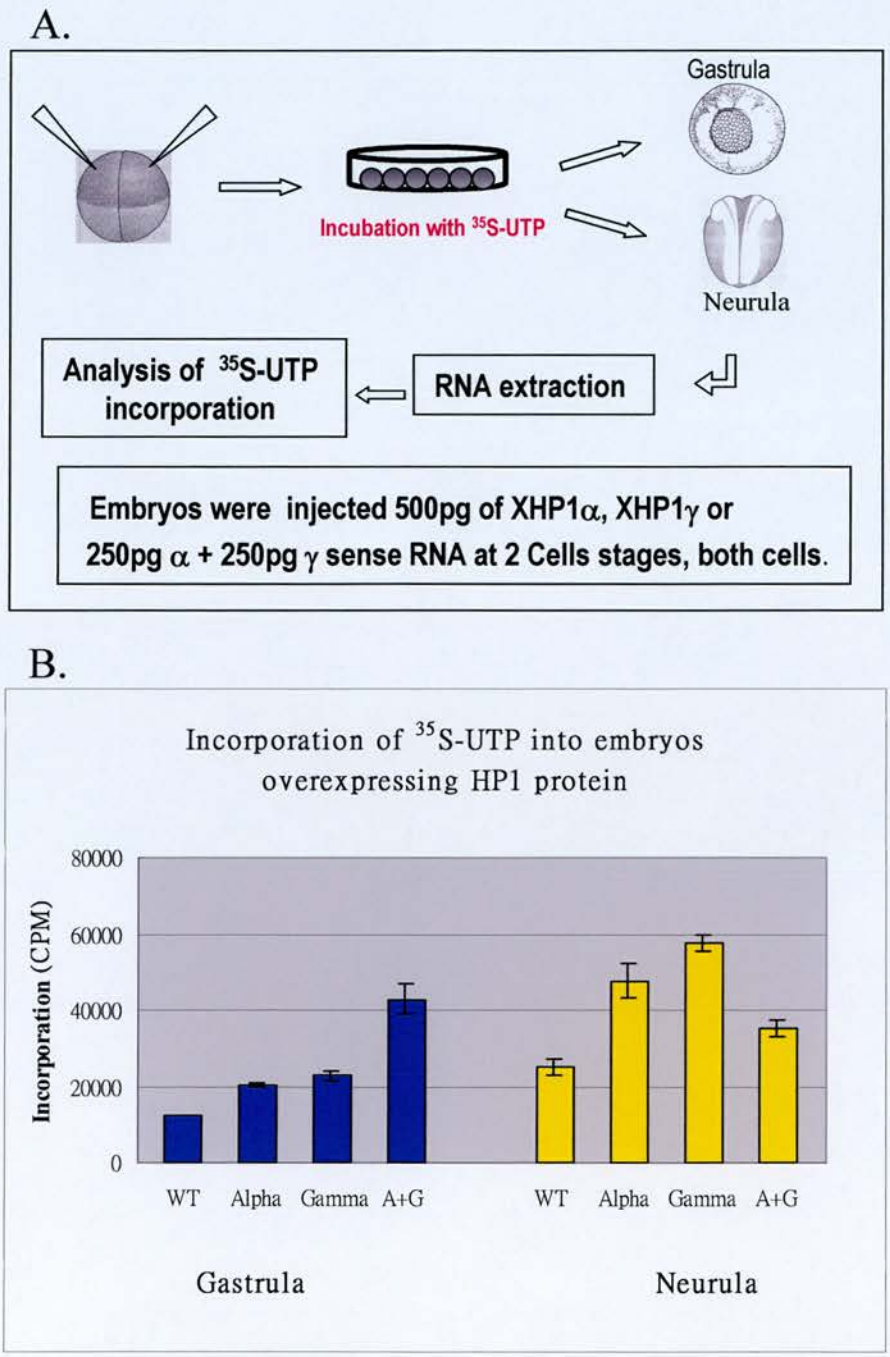

Figure 7.6 The effect of over-expression of *x*HP1 on embryo development as measured by the level of the incorporation of ^{35}S-UTP after the injection of *x*HP1α and *x*HP1γ sense RNA. (A) The schematic diagram showing the procedure of the incorporation experiments. (B) The schematic diagram showing the levels of ^{35}S-UTP incorporated in the wide type (WT) and the injected embryos.

Chapter 8 General Discussion

8.1 Summary of Results

The work presented in this thesis describes the characterisation of two homologues of HP1 (heterochromatin protein 1) in *Xenopus laevis*. Two full-length cDNA clones of HP1 homologues, *x*HP1α and *x*HP1γ are identified from *Xenopus*. Both of these clones contain a chromo domain (CD) and chromo shadow domain (CSD). RT-PCR analysis revealed that both *x*HP1α and *x*HP1γ are maternally abundant and their expression increases to a high level during neurulation stages, but *x*HP1α gene is expressed in higher level than *x*HP1γ at different developmental stages in frogs. RNA *in situ* hybridisation demonstrates that *x*HP1α shares an overlapping pattern expression with *x*Polycomb2. Expression was observed in the head and neural tube. Although the *x*HP1γ transcripts pattern is undetectable using RNA *in situ* hybridisation, its protein localisation reveals a similar pattern with *x*HP1α transcripts.

The results of the self-association assays demonstrate that *x*HP1α and *x*HP1γ can homo- and heteromerdise *in vitro* and the associations are dependent on the CSD. The result is consistent with the other two studies reported that only the CSD is necessary and sufficient for self-association and heterologous interaction between HP1α and HP1γ in a two-yeast hybrid assay with human proteins (Le Douarin et al., 1996) and *in vitro* binding assay with mouse proteins (Ye et al., 1997).

The DNA binding assays provide a clear evidence for the interaction between DNA and *x*HP1α, but not *x*HP1γ. Neither length nor sequence preference was observed

for this DNA binding activity. The chromatin pull-down assay localised a novel chromatin-binding domain to the hinge region of *x*HP1α, which is not present in *x*HP1γ. The hinge region consists of 23 amino acids and shows only 50% consensus to mammalian counterparts. This result differs from the previous report from Eissenberg and colleagues. They suggested that *Drosophila* HP1 can bind directly to nucleosomes but intact native HP1 is required for such interactions (Zhao et al. 2000).

Additional analysis using salt-dependent folded chicken chromatin indicates that *x*HP1α favours binding to a highly compacted chromatin fibre containing linker histone. The results demonstrate that *x*HP1α does not impair or participate in intrinsic chromatin folding, although HP1 is an essential component of heterochromatin, which is required in a precise stoichiometry to properly set up and/or maintain the inactivated state of genes (Nielsen et al., 2001). In the case of the interaction between xHP1α and the chromatin without histone tails, *x*HP1α has a preference of binding to linker DNA but it has no preference in chromatin depleted of H1/H5. Therefore, it may imply that without the assistance of histone tails, *x*HP1α and chromatin will not form a proper association. Using the Far Western blotting study, it shows that *x*HP1α can interact specifically with histone H3 and linker histones but not with the other core histones. This interaction supports the idea that chromatin binding by *x*HP1α involves an interaction with linker histones-containing chromatin. Taken together, it could be that this specific interaction between *x*HP1α and chromatin is related to configuration of a particular type of chromatin, perhaps heterochromatin. It is also possible that this functional difference between *x*HP1α and *x*HP1γ is responsible for their differential sub-nuclear localisation.

To study the functional significance of HP1 in the development, I manipulated the expression of *x*HP1α and *x*HP1γ. My data point towards an early development role for *x*HP1α and *x*HP1γ. Both the depletion and overexpression experiments clearly show

that *x*HP1s are essential for early development after the mid-blastula transition (MBT). The results interestingly indicate that both CD and CSD may be involved in the regulation of genes during neurulation of *Xenopus* embryos and these two domains are likely to play different roles during development. Moreover, when embryos overexpressed *x*HP1 α and *x*HP1γ, or both *x*HP1 α and *x*HP1γ together, these embryos also incorporated a significantly higher level of ^{32}S-UTP after MBT. These observations are consistent with the prediction that HP1 acts as an essential player in the dynamic organisation of nuclear architecture. It is possible that HP1 acts at a hub of silencing chromatin mechanisms, which are required to maintain the higher order structure and the homogeneous appearance of chromatin before the onset of transcription at MBT. More importantly, after MBT, HP1 is key for transcription regulation. Deleting or overexpressing the core of this HP1 associated complex could result in corruption of the higher order chromatin structure and disrupt HP1-dependent gene silencing. The loss of function experiments indicate that both the CD and the CSD may be involved in gene expression regulation during neurulation of *Xenopus* embryos and these two domains could likely play different roles during development.

8.2 The HP1 proteins in Xenopus laevis

In this study, I identified two full-length cDNA clones encoding HP1 homologues from *Xenopus*, *x*HP1α and *x*HP1γ. The alignments of cDNA and derived protein sequences show high identities with mouse and human homologues. Both of these clones contain a chromo domain (CD) and chromo shadow domain (CSD). The results confirm that the chromo domain and chromo shadow domain are highly conserved from frogs to humans throughout evolution. Nevertheless, there is a third isoform of HP1 in mammals and avia, called HP1β. A recent report describes two newly discovered

Drosophila HP1-like proteins (HP1b and HP1c), and characterises the subnuclear localization patterns of comparing them with that of the originally described fly HP1 protein (here designated HP1a) (Smother and Henikoff, 2001). The data reveal a similar localisation pattern, comparing them with HP1 homologues in mammals and avian.

In order to identify HP1β in frogs, the PCR screens have been done in the *Xenopus* cDNA libraries. However, in all the cases the results were difficult to analyse due to the presence of multiple PCR products. To prevent the technical difficulties, the coding sequences of mammalian HP1β were used to search non-human/mouse expressed sequence tag (EST) database (PSI-BLAST protein database). The searching generated three *Xenopus* cDNA clones as candidates of HP1β homologue (as indicated by arrows in Figure 8-1), however most of the high-score alignments were located at both chromo domains, but not at the hinge region, which is the most discriminated sequences among HP1 homologues. None of the sequences were likely to be *Xenopus* HP1β. Also there is no trace of zebra fish's HP1β in the up-to-date database. However, recently another two homologues of HP1 are identified from *Drosophila* EST database. It could be that the database of frog and fish contain limited information or this isoform of HP1 does not exist in *Xenopus laevis*.

Figure 8-1 The result of non-human/mouse EST database searching in HP1β

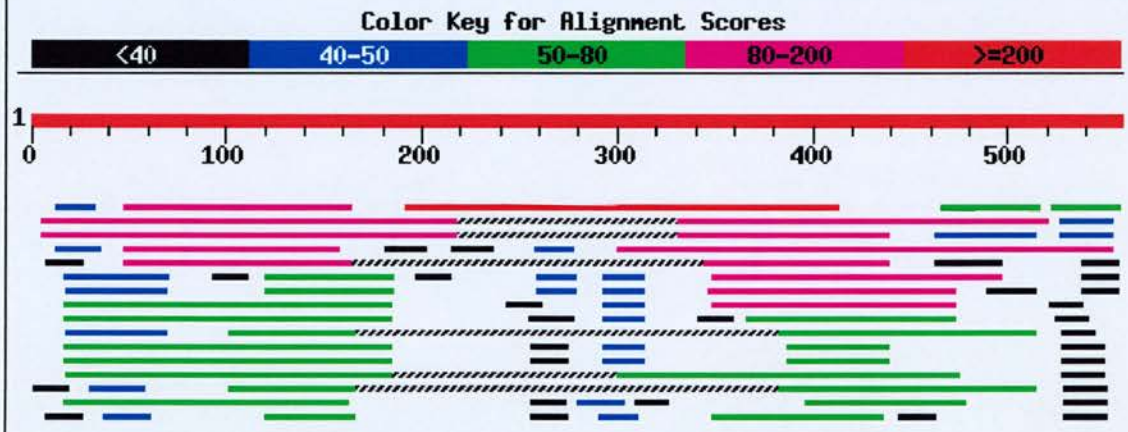

Sequences producing significant alignments: (bits) Value

gi|11670815|gb|BF561085.1|BF561085	UI-R-E1-fe-b-03-0-UI.r1 .. .	212	7e-53	Rattus norvegicus cDNA
gi|15373779|gb|BI533212.1|BI533212	fr79a05.x1 zebrafish adu. .	147	4e-33	
gi|15374059|gb|BI533492.1|BI533492	fr79a05.y1 zebrafish adu. .	135	1e-29	
gi|7282591|gb|AW595333.1|AW595333	fk30f06.y1 zebrafish fin ..	123	5e-26	
gi|11783467|gb|BF612636.1|BF612636	df09a05.y1 Wellcome CRC	98	3e-18	
gi|6195698|gb|AW147802.1|AW147802	da04h10.y1 Xenopus laevis	98	3e-18	
gi|8281513|gb|BE017065.1|BE017065	fk75d02.y1 Zebrafish Rese..	96	1e-17	
gi|13565844|gb|BG554064.1|BG554064	dab78e05.y1 NICHD XGC Em	86	1e-14	
gi|6342134|gb|AW164958.1|AW164958	da20b04.y3 normalized Xen...	86	1e-14	

8.3 Significance of the hinge region

A large number of detailed studies focus on the role of chromo domains. In contrast, there is only a minimal characterisation of the HP1 hinge, which is thought to be merely a linker that connects the two chromo-domains of HP1. A few studies indicate that the hinge may function as more than just a linker and might contribute more directly to HP1 function. First, the *in vitro* binding capacity of the HP1 chromo shadow domain for lamin B receptor is increased by addition of the hinge sequence, suggesting that the hinge may cooperate with chromo domain modules or contribute to their stability (Ye et al., 1997). Second, yeast two-hybrid experiments map HP1's interaction with inner centromere protein (INCEP) to the hinge, indicating that the segment may selectively interact with other proteins *in vivo* (Ainsztein et al., 1998). Third, artificially truncated forms of HP1 that localize to heterochromatin and contain chromo shadow domain also include a substantial portion of the hinge (Platero et al., 1995; Powers and Eissenberg, 1993), suggesting that the hinge might contribute to targeting. Fourth, recent studies in *S. pombe* describe a nuclear localization signal (NLS) within the hinge that effectively targets the HP1 homologue Swi6 to the nucleus (Wang, et al. 2000).

Finally, Comparison of HP1 homologues also reveal a conserved block of 25 amino acids contained within the hinge [Smothers and Henikoff, 2001 (Figure 8-2)]. They find that not only the NLS is conserved but also an invariant KRK sequence is also present. The hinge sequence is largely hydrophilic, lacking hydrophobic core residues that could contribute to a globular tertiary structure. The NLS consists of two basic amino acids (K or R), followed by a 10-residue spacer region and another three basic amino acids within the next five positions. Furthermore, the spacer residues found within bipartite NLS sequences are largely acidic.

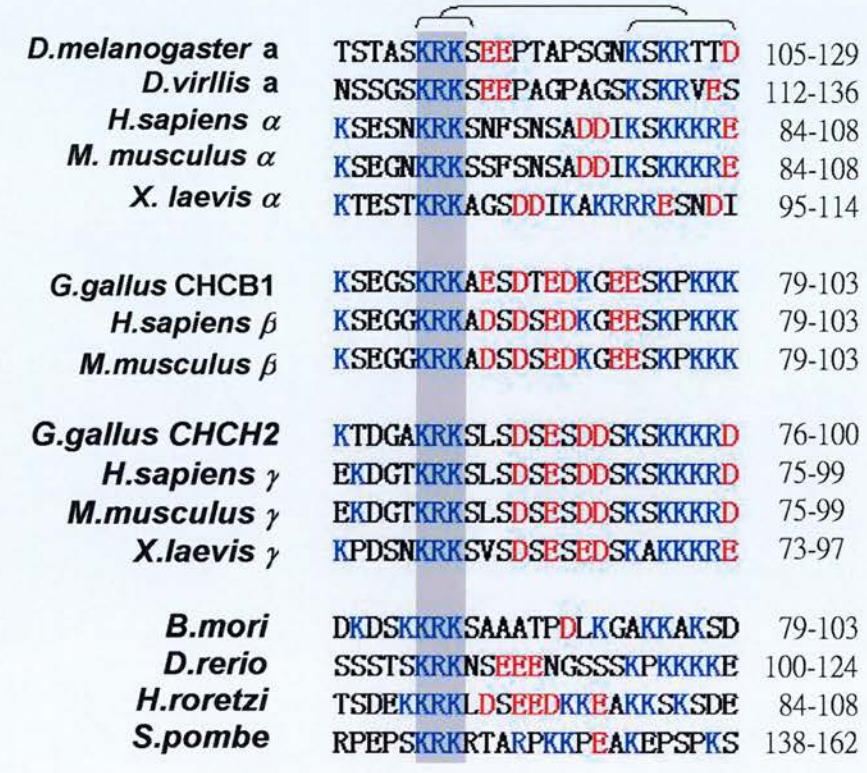

(Derived from Smothers and Henikoff, 2001)

Figure 8-2 An invariant sequences within the block is shaded and a region that conforms to a bipartite NLS is indicated by brackets. *The colour is used to discriminate amino acids based on the chemistry side chain (i.e., blue = basic and red =acidic)*

Despite these data, a role for the hinge in animal HP1 proteins beyond that of a connector for chromo domains remains speculative. In my finding, the hinge regions of *x*HP1α and *x*HP1γ display strikingly different activities in DNA and chromatin binding. Although the KRK blocks are conserved in the hinge regions of both *x*HP1α and *x*HP1γ, the spacers in the hinge of *x*HP1α have more neutral amino acids than acidic amino acids. In fact, there are four acidic amino acids (D or E; pKa = 4.4) in the spacer of HP1γ on average rather than two in the HP1α. It could be this difference in the spacer contributes to an increase of positive charge in the hinge, which may make HP1α accessible to interact with the DNA and chromatin. Interestingly, HP1β has a basic (K) and four acidic amino acids in the spacer; in addition, another two acidic residues follow the spacer and right before the 'KPKKK' block of the NLS. This prototype of the spacer is in the middle between HP1α and HP1γ. This may be functionally reflected to the spatial pattern of HP1α, HP1β and HP1γ in cell. In mouse cells, heterochromatin enriched in HP1α and HP1β is separated from less well-characterised nuclear regions enriched in HP1γ, which may correspond to euchromatin (Horsley *et al.* 1996). More diverse spatial patterns are evident in human cells, where each HP1 homologue targets distinct heterochromatin domains (Minc et al., 1999). Properties of the hinge may help explain distinct localisation patterns observed among different HP1 homologues. The chromo domains of HP1α, HP1β and HP1γ are almost indistinguishable, suggesting that interactions with these modules alone would be redundant unless features outside of the chromo domains help determine function. The hinge sequences among all of these homologues differ in their length and composition and might therefore function to discriminate these proteins *in vivo*. There is no data available concerning the biochemical properties of HP1β. It would be essential to make an investigation of HP1β by means of DNA and chromatin interacting.

8.4 HP1 and chromatin folding

Distinct levels of chromatin organisation are dependent on the dynamic higher order structuring of nucleosomes, which represent the basic repeating unit of chromatin. In each nucleosome, roughly two superhelical turns of DNA wrap around an octamer of core histone proteins forms by four histone partners: an H3-H4 tetramer and two H2A-H2B dimers (Luger et al., 1997). Histones are small basic proteins consisting of a globular domain and a more flexible and charged N-terminus (histone tails) that protrudes from the nucleosome. It remains unclear how nucleosomal arrays containing linker histone (H1) twist and fold this chromatin fibre into increasingly more compacted filaments to defines high-order structures.

Recently much attention has been drawn to the interaction between HP1 and methylated histone H3. Two independent research groups have recently shown that the chromo domain, but not the chromo shadow domain, of HP1 and Swi6 preferentially bind to methylated H3 Lys9 *in vitro* (Lachner et al., 2001; Bannister et al., 2001). The chromo domain of HP1β was selective for the H3 Lys9-methyl modification, as demonstrated by the lack of binding to an H3 unmodified or H3 Lys4-methyl peptide (Bannister et al., 2001). Interestingly, HP1 chromo domain binding affinity was significantly less than that of the full-length HP1, suggesting that native HP1 (or an HP1 dimer) is required for high-affinity binding *in vivo* (Lachner et al., 2001; Bannister et al., 2001). Therefore, chromo-domain containing proteins, such as HP1 and Swi6, are predicted to bind to the H3 Lys9-methyl modification catalysed by the Su(var)3-9 family of hitone methyltranferases (HMTs) in order to establish silent regions of heterochromatin (Figure 8-3).

However, my results differ from this model. I have demonstrated that the hinge region of HP1α, but not HP1γ has a chromatin-binding activity and using western-

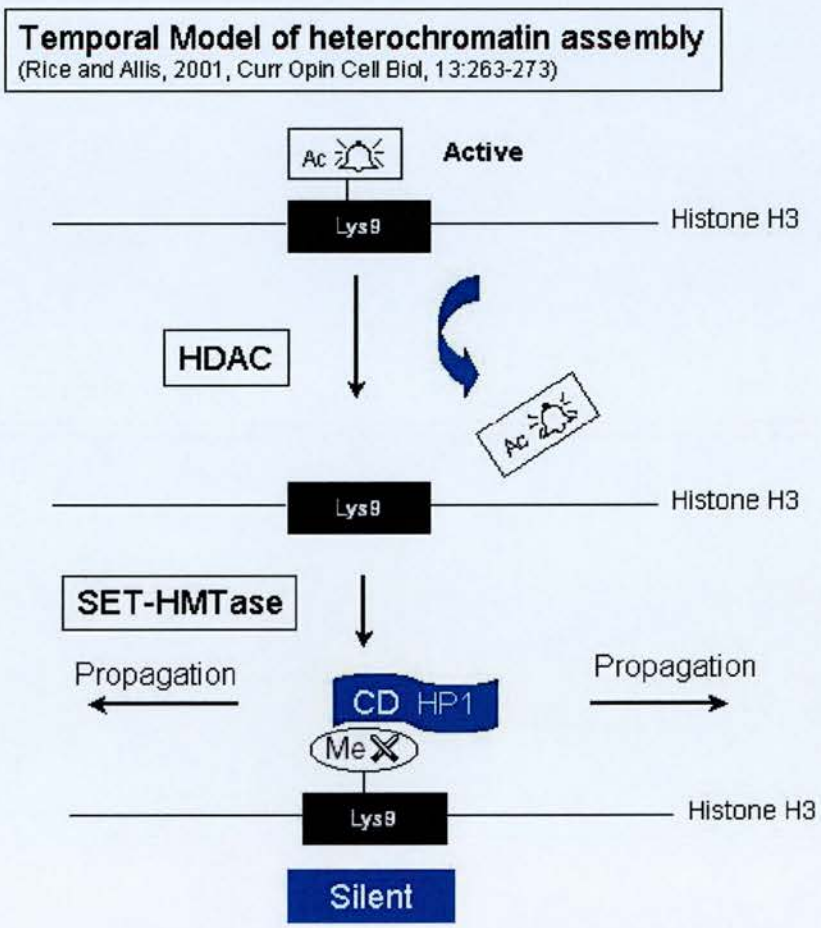

Figure 8-3 One proposed temporal pathway leading to the establishment of transcriptionally silent heterochromatic regions with regard to the covalent modifications in the histone H3 tail.
The acetyl group on H3 Lys9, a modification often associated with transcriptionally active regions, is removed by an HDAC prior to methylation by an HMT. The CD of HP1 selectively recognizes and binds to the H3 Lys9-methyl modification resulting in the self-assembly and propagation of heterochromatin and transcriptional silencing.

blotting, I show that HP1α interact specifically with histone H3 and linker histone H1, but not H5. In addition, HP1α shows an intrinsic chromatin binding activity to tailed or tailless chromatin. These findings are supported by a recent report (Nielsen et al. 2001). They show that all three mammalian HP1s bind to tailed and tailless nucleosomes *in vitro* and specifically interacts with the histone-fold domain of histone H3, but not the H3 tails. Moreover, HP1α binds to histone H3 and H1 through its chromo domain and hinge region respectively. Therefore, the model in Figure 8-3 may over-simplify what role HP1 may play in chromatin folding and compaction. Especially while the linker histone interacts with HP1α, it supports the notion that HP1 acts at a hub of silencing chromatin mechanisms, which are required to maintain the higher order structure and the appearance of heterochromatin. Indeed, a more intriguing story is ahead of us and waited to be discovered.

8.5 Developmental role for Heterochromatin

Heterochromatin-mediated silencing is developmentally regulated in *Drosophila.* The best-characterisation example is heterochromatic PEV in *Drosophila.* Two developmental stages for the regulation of heterochromatic silencing have been proposed: (1) the initiation of variegated silencing in cellularised, gastulating embryos and (2) the relaxation of silencing at the onset of terminal differentiation in imaginal tissues (Lu et al., 1998). In development of *Drosophila*, cytological visible heterochromatin first appears in the end of syncytial blastoderm embryos at approximately 1.5 hours of embryogenesis (Vlassova et al. 1991). Establishment of variegated silencing of heat-shock lacZ (***HS-lacZ***) at the end of the blastoderm stage coincides with G_2 of the 14^{th} cell cycle (Foe et al., 1993). During the interphase of the 14^{th} cell cycle, heterochromatin undergoes a rapid compaction and remains consistently

condensed thereafter (Foe et al., 1993; Hiraoka et al., 1993). Also beginning in the 14th cell cycle, heterochromatin is replicated progressively later during subsequent S phase (Edgar and O'Farrell, 1990, Foe et al., 1993). It is proposed that the initiation of heterochromatic PEV, beginning at the end of blastoderm stage. This reflects the coincidences of the silencing of ***HS-lacZ*** being initiated and the functional maturation of heterochromatin (Lu et al., 1998).

In addition, the observation linking development repression to heterochromatic associations in lymphocyte development (Brown et al., 1997) suggests that differentiation-dependent remodelling of heterochromatin may have wider implications in the maintenance of developmental silencing. This silencing effect has been shown to be mediated in part by heterochromatin–associated protein, of which the best characterised is HP1. Direct evidence that HP1 is involved in gene silencing is from the experiment in which the levels of HP1 were modulated. Mutations in the gene encoding HP1 are homozygous lethal in *Drosophila* (Eissenberg et al., 1990), HP1 heterozygotes show a loss of silencing of transgenes at centric localisation, which correlates with a more 'open' (euchromatic-like) chromatin structure (Cryderman et al., 1998). In contrast, HP1 overexpression leads to an increase in gene silencing (Eissenberg et al., 1990, 1992). In mice, increased silencing of a centric transgene was observed upon overexpression of a mouse HP1-like protein M31(Festenstein et al., 1999).

In *Xenopus*, the transcription is activated at 13th cell cycles. At this stage, the mid-blastula transition (MBT) occurs with a generally activation of gene expression. It is still unknown whether heterochromatin maturation in *Xenopus* is coincident with the onset of transcription, the equivalent with what happens in *Drosophila*. Nevertheless, in my data both the depletion and overexpression experiments clearly show that *x*HP1s are essential for early development after the MBT. Moreover, when embryos overexpressed

*x*HP1α and *x*HP1γ, or both *x*HP1 α and *x*HP1γ together, these embryos also incorporated a significantly higher level of ^{32}S-UTP after MBT. This suggests that frog may have the same programming of heterochromatin formation with fruit fly during the development.

As discussed before, *x*HP1α may be functionally essential for neural development. This vision is supported by the previous studies in another chromo-domain containing protein, *x*Polycomb. The transcripts of *x*Polycomb are expressed in a pattern that is almost identical with *x*HP1α. (Figure 8-4) (Reijnen et al., 1995). However, the expression also has been found in the somites via carefully examining the sections of embryos hybridized with *x*Polycomb. As the similarity of expression pattern and the common feature of chromo-domain protein families, it cannot be excluded that *x*HP1α could also involve in somite, notochord and muscle development, which are derived from mesoderm cells during early development. In fact, *x*HP1α also share a overlapping expressing pattern with a mesoderm marker, *Xenopus Brachyury* (Xbra) in gastrulation (Conlon et al., 1996) (Figure 8-5, A&B). Strikingly, the overexpressing and depleting *x*HP1α in *Xenopus* embryo display a truncated axis, this phenotype is similar to that with inhibition of Xbra function. (Conlon et al., 1996) (Figure 8-5, C). Taken together, the HP1 protein family may be involved in the progress of varied germ layers during early development. Although this speculation is yet conclusive, HP1might play as a global suppresser or regulator in gene expression during early development.

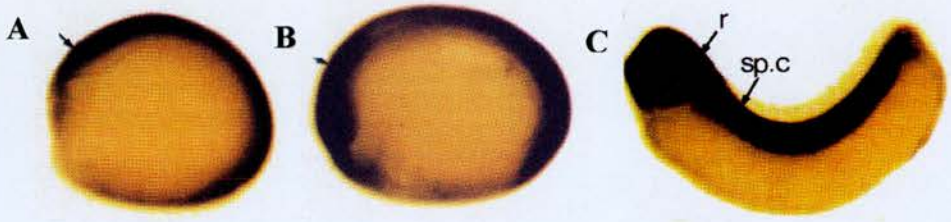

(Derived from Reijnen et al., 1995)

Figure 8-4 Localisation of xPolycomb transcripts during Xenopus early development by whole mount in situ hybridization.

(A) Stage 15, early neurula, (B) Stage 19 late neurula, (C) Stage 28 tailbud.

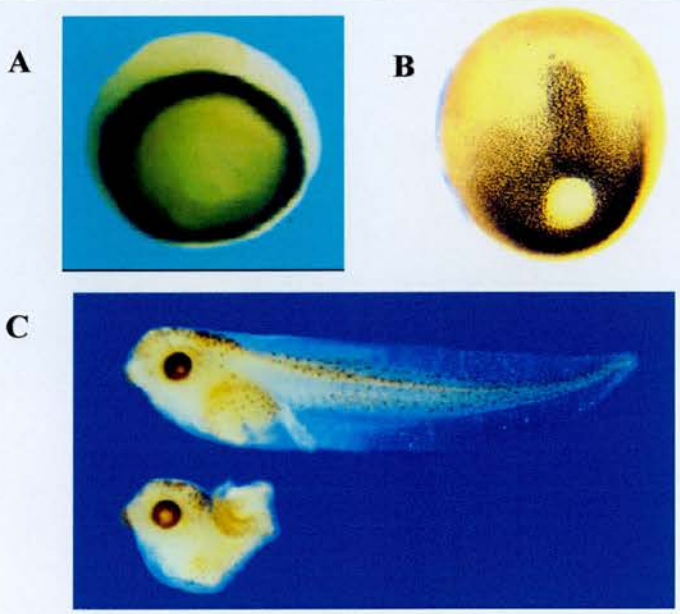

(Derived from Conlon et al., 1996)

Figure 8-5 Brachyury expression during Xenopus gastrulation.

(A) Before gastrulation, the expression of Brachyury (dark stain) marks the future mesoderms. (B) As gastrulation proceeds, the mesoderm that will form notochord converges and extends along the midkine and only notochord cells continue to express Brachyury.(C)Inhibition of Brachyury function leads to a loss of posterior and axial mesodermal structures. Control Xenopus tadpole embryo shown at top and corresponding embryo injected with a construct that interferes with Brachyury function shown at bottom of panel.

8.6 HP1 and transcription regulation

Recent reports broaden our comprehension of HP1-mediated regulation of gene expression. HP1α protein levels are significantly depleted in metastatic breast cancer cells (Kirschmann et al., 2000). Despite the presence of normal HP1β and HP1γ protein level, an increase in HP1α expression alone eliminates their invasive and metastatic properties. HP1 is also involved with the repressive function of the retinoblastoma (Rb) protein (Nielsen et al., 2001). Rb associates wit SUV39H1 and HP1 *in vivo* and SUV39H1 cooperate with Rb to repress the cyclin E promoter.

HP1 is found associated with a number of transcriptional repressors, suggesting that it may have a role in repressing other promoters. Thus, my results support the role of HP1 beyond heterochromatic gene silencing to a more general function in regulating gene transcription. A recent report shows that *Drosophila* HP1 normally represses the expression of four euchromatic genes in a dosage-dependent manner (Hwang et al. 2001). The repressive effect of HP1 is decreased by mutation in *Su(var)3-9* and *Su(var)2-1*, which is correlated with histone H4 deacetylation. These data provide genetic evidence that an HP1-family protein repress the expression of euchromatic genes in a metazoan, and that histone modifiers cooperate with HP1 in euchromatic gene expression. The model in Figure 8-6 summarises the prediction that HP1 acts as an essential player in the dynamic organisation of nuclear architecture. It is possible that HP1 acts at a hub of silencing chromatin mechanisms, which are required to maintain the higher order structure. More importantly, HP1 is key for transcription regulation.

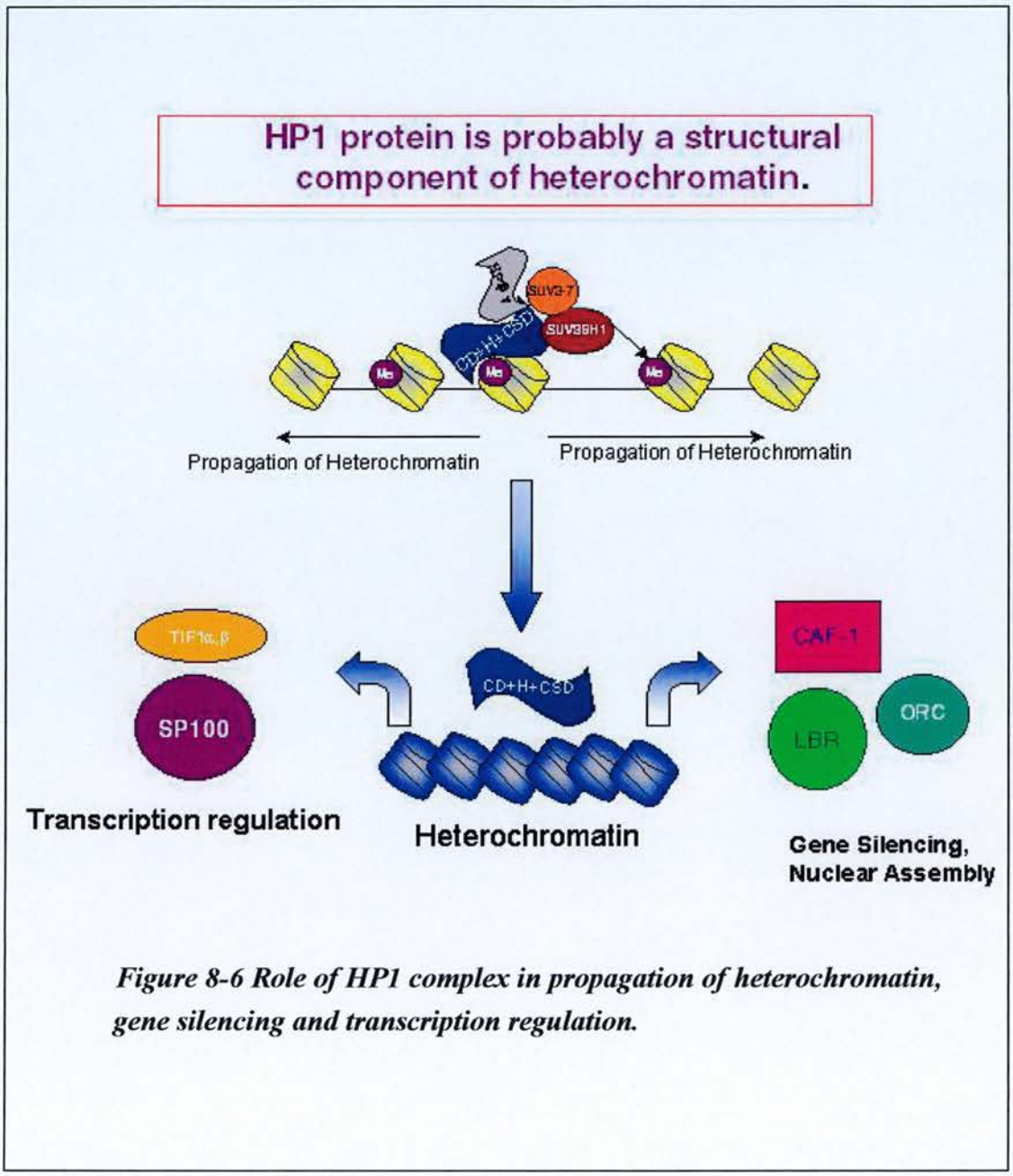

Figure 8-6 Role of HP1 complex in propagation of heterochromatin, gene silencing and transcription regulation.

8.7 Conclusion and subjects for future investigation

A fuller understanding of heterochromatin function and the mechanism of its formation are likely to have important consequences for human health, especially cancer. Although recent discoveries help us to understand more the formation of heterochromatin, the correlation between heterochromatin regulation in gene expression and cancers is poorly understood. The study indicates that HP1 is down regulated in invasive breast cancer cell line, giving the link between heterochromatin and tumorigenesis (Kirschmann et al., 2000). HP1 interacts with three categories of proteins, including transcription factors (Le Douarin et al., 1996; Ryan et al., 1999), nuclear assembly factors (Ye et al., 1997; Ainsztein et al., 1998; Murzina et al., 1999; Pak et al., 1997) and the other components of heterochromatin (Aagaard et al., 1999; Cleard et al., 1997; Le Douarin et al., 1996; Ye et al., 1997). There are many implications in those interactions At least, that means heterochromatin is very active in gene expression regulation and post cell-division nuclear assembly.

The HP1 family of proteins represents the best-characterized heterochromatin -associated non-histone chromosomal protein family in the eukaryote. Its evolutionary conservation suggests a fundamental role for HP1 proteins in nuclear organization and a highly conserved set of macromolecular interactions. Future work on HP1 and its partners will be directed at defining its roles as a subunit of heterochromatin, as a cofactor in gene regulation, and as an essential player in the dynamic organization of nuclear architecture. It will be also important to fully understand the HP1/heterochromatin-mediated transcription regulation and identify the affected genes, which are regulated. This will be the subject of future investigations to reveal whether there is a pattern of HP1-related gene expression. Key to the achievement of these goals will be the application of genetic and developmental assays to test the functional

significance of cytological and biochemical correlations.

References

Aagaard,L., Laible,G., Selenko,P., Schmid,M., Dorn,R., Schotta,G., Kuhfittig,S., Wolf,A., Lebersorger,A., Singh,P.B., Reuter,G., and Jenuwein,T. (1999). Functional mammalian homologues of the Drosophila PEV-modifier Su(var)3- 9 encode centromere-associated proteins which complex with the heterochromatin component M31. EMBO J. *18*, 1923-1938.

Aasland,R. and Stewart,A.F. (1995). The chromo shadow domain, a second chromo domain in heterochromatin- binding protein 1, HP1. Nucleic Acids Res. *23*, 3168-3174.

Ainsztein,A.M., Kandels-Lewis,S.E., Mackay,A.M., and Earnshaw,W.C. (1998). INCENP centromere and spindle targeting: identification of essential conserved motifs and involvement of heterochromatin protein HP1. J. Cell Biol. *143*, 1763-1774.

Akam,M. (1987). The molecular basis for metameric pattern in the Drosophila embryo. Development *101*, 1-22.

Allan,J., Cowling,G.J., Harborne,N., Cattini,P., Craigie,R., and Gould,H. (1981). Regulation of the higher-order structure of chromatin by histones H1 and H5. J. Cell Biol. *90*, 279-288.

Allan,J., Harborne,N., Rau,D.C., and Gould,H. (1982). Participation of core histone "tails" in the stabilization of the chromatin solenoid. J. Cell Biol. *93*, 285-297.

Allan,J., Hartman,P.G., Crane-Robinson,C., and Aviles,F.X. (1980). The structure of histone H1 and its location in chromatin. Nature *288*, 675-679.

Allan,J., Mitchell,T., Harborne,N., Bohm,L., and Crane-Robinson,C. (1986). Roles of H1 domains in determining higher order chromatin structure and H1 location. J. Mol. Biol. *187*, 591-601.

Anderson,M.J., Shi,Z.Q., and Zackson,S.L. (1997). Nerve-induced disruption and reformation of beta1-integrin aggregates during development of the neuromuscular junction. Mech. Dev. *67*, 125-139.

Andrulis,E.D., Neiman,A.M., Zappulla,D.C., and Sternglanz,R. (1998). Perinuclear localization of chromatin facilitates transcriptional silencing. Nature *394*, 592-595.

Arents,G., Burlingame,R.W., Wang,B.C., Love,W.E., and Moudrianakis,E.N. (1991). The nucleosomal core histone octamer at 3.1 A resolution: a tripartite protein assembly and a left-handed superhelix. Proc. Natl. Acad. Sci. U. S. A *88*, 10148-10152.

Baksa,K., Morawietz,H., Dombradi,V., Axton,M., Taubert,H., Szabo,G., Torok,I., Udvardy,A., Gyurkovics,H., Szoor,B., and . (1993). Mutations in the protein phosphatase 1 gene at 87B can differentially affect suppression of position-effect variegation and mitosis in Drosophila melanogaster. Genetics *135*, 117-125.

Ball,L.J., Murzina,N.V., Broadhurst,R.W., Raine,A.R., Archer,S.J., Stott,F.J., Murzin,A.G., Singh,P.B., Domaille,P.J., and Laue,E.D. (1997). Structure of the chromatin binding (chromo) domain from mouse modifier protein 1. EMBO J. *16*, 2473-2481.

Bannister,A.J., Zegerman,P., Partridge,J.F., Miska,E.A., Thomas,J.O., Allshire,R.C., and Kouzarides,T. (2001). Selective recognition of methylated lysine 9 on histone H3 by the HP1 chromo domain. Nature *410*, 120-124.

Bhadra,U. and Birchler,J.A. (1996). Characterization of a sex-influenced modifier of gene expression and suppressor of position-effect variegation in Drosophila. Mol. Gen. Genet. *250*, 601-613.

Birchler,J.A., Bhadra,U., Rainbow,L., Linsk,R., and Nguyen-Huynh,A.T. (1994). Weakener of white (Wow), a gene that modifies the expression of the white eye color locus and that suppresses position effect variegation in Drosophila melanogaster. Genetics *137*, 1057-1070.

Brasher,S.V., Smith,B.O., Fogh,R.H., Nietlispach,D., Thiru,A., Nielsen,P.R., Broadhurst,R.W., Ball,L.J., Murzina,N.V., and Laue,E.D. (2000). The structure of

mouse HP1 suggests a unique mode of single peptide recognition by the shadow chromo domain dimer. EMBO J. *19*, 1587-1597.

Braunstein,M., Sobel,R.E., Allis,C.D., Turner,B.M., and Broach,J.R. (1996). Efficient transcriptional silencing in Saccharomyces cerevisiae requires a heterochromatin histone acetylation pattern. Mol. Cell Biol. *16*, 4349-4356.

Brown,K.E., Guest,S.S., Smale,S.T., Hahm,K., Merkenschlager,M., and Fisher,A.G. (1997b). Association of transcriptionally silent genes with Ikaros complexes at centromeric heterochromatin. Cell *91*, 845-854.

Brown,K.E., Guest,S.S., Smale,S.T., Hahm,K., Merkenschlager,M., and Fisher,A.G. (1997a). Association of transcriptionally silent genes with Ikaros complexes at centromeric heterochromatin. Cell *91*, 845-854.

Carruthers,L.M., Bednar,J., Woodcock,C.L., and Hansen,J.C. (1998). Linker histones stabilize the intrinsic salt-dependent folding of nucleosomal arrays: mechanistic ramifications for higher-order chromatin folding. Biochemistry *37*, 14776-14787.

Cary,P.D., Moss,T., and Bradbury,E.M. (1978). High-resolution proton-magnetic-resonance studies of chromatin core particles. Eur. J. Biochem. *89*, 475-482.

Chevillard,C., Reik,W., McDermott,M., Fontes,M., Mattei,M.G., and Singh,P.B. (1993). Chromosomal localization of human homologs of the Drosophila heterochromatin protein 1 (HP1) gene. Mamm. Genome *4*, 124-126.

Clark,R.F. and Elgin,S.C. (1992). Heterochromatin protein 1, a known suppressor of position-effect variegation, is highly conserved in Drosophila. Nucleic Acids Res. *20*, 6067-6074.

Cleard,F., Delattre,M., and Spierer,P. (1997). SU(VAR)3-7, a Drosophila heterochromatin-associated protein and companion of HP1 in the genomic silencing of position-effect variegation. EMBO J. *16*, 5280-5288.

Clegg,N.J., Honda,B.M., Whitehead,I.P., Grigliatti,T.A., Wakimoto,B., Brock,H.W., Lloyd,V.K., and Sinclair,D.A. (1998). Suppressors of position-effect variegation in Drosophila melanogaster affect expression of the heterochromatic gene light in the absence of a chromosome rearrangement. Genome *41*, 495-503.

Conlon,F.L., Sedgwick,S.G., Weston,K.M., and Smith,J.C. (1996). Inhibition of Xbra transcription activation causes defects in mesodermal patterning and reveals autoregulation of Xbra in dorsal mesoderm. Development *122*, 2427-2435.

Cowell,I.G. and Austin,C.A. (1997). Self-association of chromo domain peptides. Biochim. Biophys. Acta *1337*, 198-206.

Cowieson,N.P., Partridge,J.F., Allshire,R.C., and McLaughlin,P.J. (2000). Dimerisation of a chromo shadow domain and distinctions from the chromodomain as revealed by structural analysis. Curr. Biol. *10*, 517-525.

Cross,S.H., Charlton,J.A., Nan,X., and Bird,A.P. (1994). Purification of CpG islands using a methylated DNA binding column. Nat. Genet. *6*, 236-244.

Cryderman,D.E., Cuaycong,M.H., Elgin,S.C., and Wallrath,L.L. (1998). Characterization of sequences associated with position-effect variegation at pericentric sites in Drosophila heterochromatin. Chromosoma *107*, 277-285.

Csink,A.K., Linsk,R., and Birchler,J.A. (1994). The Lighten up (Lip) gene of Drosophila melanogaster, a modifier of retroelement expression, position effect variegation and white locus insertion alleles. Genetics *138*, 153-163.

Csink,A.K. and Henikoff,S. (1998). Something from nothing: the evolution and utility of satellite repeats. Trends Genet. *14*, 200-204.

De Rubertis,F., Kadosh,D., Henchoz,S., Pauli,D., Reuter,G., Struhl,K., and Spierer,P. (1996). The histone deacetylase RPD3 counteracts genomic silencing in Drosophila and yeast. Nature *384*, 589-591.

DeCamillis,M., Cheng,N.S., Pierre,D., and Brock,H.W. (1992). The polyhomeotic gene of Drosophila encodes a chromatin protein that shares polytene chromosome-binding sites with Polycomb. Genes Dev. *6*, 223-232.

Dillin,A. and Rine,J. (1997). Separable functions of ORC5 in replication initiation and silencing in Saccharomyces cerevisiae. Genetics *147*, 1053-1062.

Dorer,D.R. (1997). Do transgene arrays form heterochromatin in vertebrates? Transgenic Res. *6*, 3-10.

Dorer,D.R. and Henikoff,S. (1997). Transgene repeat arrays interact with distant heterochromatin and cause silencing in cis and trans. Genetics *147*, 1181-1190.

Dorer,D.R. and Henikoff,S. (1994). Expansions of transgene repeats cause heterochromatin formation and gene silencing in Drosophila. Cell *77*, 993-1002.

du,S.D., Cancilla,M.R., Earle,E., Mao,J.I., Saffery,R., Tainton,K.M., Kalitsis,P., Martyn,J., Barry,A.E., and Choo,K.H. (1997). A functional neo-centromere formed through activation of a latent human centromere and consisting of non-alpha-satellite DNA. Nat. Genet. *16*, 144-153.

Eagleson,G.W. and Harris,W.A. (1990). Mapping of the presumptive brain regions in the neural plate of Xenopus laevis. J. Neurobiol. *21*, 427-440.

Eberl,D.F., Duyf,B.J., and Hilliker,A.J. (1993). The role of heterochromatin in the expression of a heterochromatic gene, the rolled locus of Drosophila melanogaster. Genetics *134*, 277-292.

Eberl,D.F., Lorenz,L.J., Melnick,M.B., Sood,V., Lasko,P., and Perrimon,N. (1997). A new enhancer of position-effect variegation in Drosophila melanogaster encodes a putative RNA helicase that binds chromosomes and is regulated by the cell cycle. Genetics *146*, 951-963.

Edgar,B.A. and Schubiger,G. (1986). Parameters controlling transcriptional activation during early Drosophila development. Cell *44*, 871-877.

Edgar,B.A. and O'Farrell,P.H. (1990). The three postblastoderm cell cycles of Drosophila embryogenesis are regulated in G2 by string. Cell *62*, 469-480.

Edmondson,D.G., Smith,M.M., and Roth,S.Y. (1996). Repression domain of the yeast global repressor Tup1 interacts directly with histones H3 and H4. Genes Dev. *10*, 1247-1259.

Edmondson,S.P., Qiu,L., and Shriver,J.W. (1995). Solution structure of the DNA-binding protein Sac7d from the hyperthermophile Sulfolobus acidocaldarius. Biochemistry *34*, 13289-13304.

Ehrenhofer-Murray,A.E., Gossen,M., Pak,D.T., Botchan,M.R., and Rine,J. (1995). Separation of origin recognition complex functions by cross-species complementation. Science *270*, 1671-1674.

Eissenberg,J.C. and Elgin,S.C. (2000). The HP1 protein family: getting a grip on chromatin. Curr. Opin. Genet. Dev. *10*, 204-210.

Eissenberg,J.C. and Hartnett,T. (1993). A heat shock-activated cDNA rescues the recessive lethality of mutations in the heterochromatin-associated protein HP1 of Drosophila melanogaster. Mol. Gen. Genet. *240*, 333-338.

Eissenberg,J.C., James,T.C., Foster-Hartnett,D.M., Hartnett,T., Ngan,V., and Elgin,S.C. (1990). Mutation in a heterochromatin-specific chromosomal protein is associated with suppression of position-effect variegation in Drosophila melanogaster. Proc. Natl. Acad. Sci. U. S. A *87*, 9923-9927.

Eissenberg,J.C., Morris,G.D., Reuter,G., and Hartnett,T. (1992). The heterochromatin-associated protein HP-1 is an essential protein in Drosophila with dosage-dependent effects on position-effect variegation. Genetics *131*, 345-352.

Ekwall,K., Javerzat,J.P., Lorentz,A., Schmidt,H., Cranston,G., and Allshire,R. (1995). The chromodomain protein Swi6: a key component at fission yeast centromeres. Science *269*, 1429-1431.

Ekwall,K., Nimmo,E.R., Javerzat,J.P., Borgstrom,B., Egel,R., Cranston,G., and Allshire,R. (1996). Mutations in the fission yeast silencing factors clr4+ and rik1+ disrupt the localisation of the chromo domain protein Swi6p and impair centromere function. J. Cell Sci. *109 (Pt 11)*, 2637-2648.

Ekwall,K., Olsson,T., Turner,B.M., Cranston,G., and Allshire,R.C. (1997). Transient inhibition of histone deacetylation alters the structural and functional imprint at fission yeast centromeres. Cell *91*, 1021-1032.

Epstein,H., James,T.C., and Singh,P.B. (1992). Cloning and expression of Drosophila HP1 homologs from a mealybug, Planococcus citri. J. Cell Sci. *101 (Pt 2)*, 463-474.

Fauvarque,M.O. and Dura,J.M. (1993). polyhomeotic regulatory sequences induce developmental regulator- dependent variegation and targeted P-element insertions in Drosophila. Genes Dev. *7*, 1508-1520.

Felsenfeld,G. (1996). Chromatin unfolds. Cell *86*, 13-19.

Festenstein,R., Sharghi-Namini,S., Fox,M., Roderick,K., Tolaini,M., Norton,T., Saveliev,A., Kioussis,D., and Singh,P. (1999). Heterochromatin protein 1 modifies mammalian PEV in a dose- and chromosomal-context-dependent manner. Nat. Genet. *23*, 457-461.

Festenstein,R., Tolaini,M., Corbella,P., Mamalaki,C., Parrington,J., Fox,M., Miliou,A., Jones,M., and Kioussis,D. (1996). Locus control region function and heterochromatin-induced position effect variegation. Science *271*, 1123-1125.

Fletcher,T.M. and Hansen,J.C. (1995). Core histone tail domains mediate oligonucleosome folding and nucleosomal DNA organization through distinct molecular mechanisms. J. Biol. Chem. *270*, 25359-25362.

Fox,C.A., Ehrenhofer-Murray,A.E., Loo,S., and Rine,J. (1997). The origin recognition complex, SIR1, and the S phase requirement for silencing. Science *276*, 1547-1551.

Friedman,J.R., Fredericks,W.J., Jensen,D.E., Speicher,D.W., Huang,X.P., Neilson,E.G., and Rauscher,F.J., III (1996). KAP-1, a novel corepressor for the highly conserved KRAB repression domain. Genes Dev. *10*, 2067-2078.

Garcia-Ramirez,M., Dong,F., and Ausio,J. (1992). Role of the histone "tails" in the folding of oligonucleosomes depleted of histone H1. J. Biol. Chem. *267*, 19587-19595.

Garrick,D., Fiering,S., Martin,D.I., and Whitelaw,E. (1998). Repeat-induced gene silencing in mammals. Nat. Genet. *18*, 56-59.

Gerasimova,T.I., Gdula,D.A., Gerasimov,D.V., Simonova,O., and Corces,V.G. (1995). A Drosophila protein that imparts directionality on a chromatin insulator is an enhancer of position-effect variegation. Cell *82*, 587-597.

Gindhart,J.G., Jr. and Kaufman,T.C. (1995). Identification of Polycomb and trithorax group responsive elements in the regulatory region of the Drosophila homeotic gene Sex combs reduced. Genetics *139*, 797-814.

Gottschling,D.E., Aparicio,O.M., Billington,B.L., and Zakian,V.A. (1990). Position effect at S. cerevisiae telomeres: reversible repression of Pol II transcription. Cell *63*, 751-762.

Granok,H., Leibovitch,B.A., Shaffer,C.D., and Elgin,S.C. (1995). Chromatin. Ga-ga over GAGA factor. Curr. Biol. *5*, 238-241.

Grigliatti,T. (1991). Position-effect variegation--an assay for nonhistone chromosomal proteins and chromatin assembly and modifying factors. Methods Cell Biol. *35*, 587-627.

Grunstein,M. (1990). Histone function in transcription. Annu. Rev. Cell Biol. *6*, 643-678.

Grunstein,M. (1997). Histone acetylation in chromatin structure and transcription. Nature *389*, 349-352.

Gurdon,J.B. and Woodland,H.R. (1968). The cytoplasmic control of nuclear activity in animal development. Biol. Rev. Camb. Philos. Soc. *43*, 233-267.

Guthrie,S., Turin,L., and Warner,A. (1988). Patterns of junctional communication during development of the early amphibian embryo. Development *103*, 769-783.

Hamvas,R.M., Reik,W., Gaunt,S.J., Brown,S.D., and Singh,P.B. (1992). Mapping of a mouse homolog of a heterochromatin protein gene the X chromosome. Mamm. Genome *2*, 72-75.

Hansen,J.C., Ausio,J., Stanik,V.H., and van Holde,K.E. (1989). Homogeneous reconstituted oligonucleosomes, evidence for salt-dependent folding in the absence of histone H1. Biochemistry *28*, 9129-9136.

Hansen,J.C., Tse,C., and Wolffe,A.P. (1998). Structure and function of the core histone N-termini: more than meets the eye. Biochemistry *37*, 17637-17641.

Harrison,J., Molloy,P.L., and Clark,S.J. (1994). Direct cloning of polymerase chain reaction products in an XcmI T- vector. Anal. Biochem. *216*, 235-236.

Hazelrigg,T., Levis,R., and Rubin,G.M. (1984). Transformation of white locus DNA in drosophila: dosage compensation, zeste interaction, and position effects. Cell *36*, 469-481.

Hearn,M.G., Hedrick,A., Grigliatti,T.A., and Wakimoto,B.T. (1991). The effect of modifiers of position-effect variegation on the variegation of heterochromatic genes of Drosophila melanogaster. Genetics *128*, 785-797.

Hecht,A., Laroche,T., Strahl-Bolsinger,S., Gasser,S.M., and Grunstein,M. (1995). Histone H3 and H4 N-termini interact with SIR3 and SIR4 proteins: a molecular model for the formation of heterochromatin in yeast. Cell *80*, 583-592.

Henchoz,S., De Rubertis,F., Pauli,D., and Spierer,P. (1996). The dose of a putative ubiquitin-specific protease affects position- effect variegation in Drosophila melanogaster. Mol. Cell Biol. *16*, 5717-5725.

Henderson,D.S., Banga,S.S., Grigliatti,T.A., and Boyd,J.B. (1994). Mutagen sensitivity and suppression of position-effect variegation result from mutations in mus209, the Drosophila gene encoding PCNA. EMBO J. *13*, 1450-1459.

Henikoff,S. (1990). Position-effect variegation after 60 years. Trends Genet. *6*, 422-426.

Henikoff,S. (1997). Nuclear organization and gene expression: homologous pairing and long- range interactions. Curr. Opin. Cell Biol. *9*, 388-395.

Hiraoka,Y., Dernburg,A.F., Parmelee,S.J., Rykowski,M.C., Agard,D.A., and Sedat,J.W. (1993). The onset of homologous chromosome pairing during Drosophila melanogaster embryogenesis. J. Cell Biol. *120*, 591-600.

Horsley,D., Hutchings,A., Butcher,G.W., and Singh,P.B. (1996). M32, a murine homologue of Drosophila heterochromatin protein 1 (HP1), localises to euchromatin within interphase nuclei and is largely excluded from constitutive heterochromatin. Cytogenet. Cell Genet. *73*, 308-311.

Huang,D.W., Fanti,L., Pak,D.T., Botchan,M.R., Pimpinelli,S., and Kellum,R. (1998). Distinct cytoplasmic and nuclear fractions of Drosophila heterochromatin protein 1: their phosphorylation levels and associations with origin recognition complex proteins. J. Cell Biol. *142*, 307-318.

Huang,H., Smothers,J.F., Wiley,E.A., and Allis,C.D. (1999b). A nonessential HP1-like protein affects starvation-induced assembly of condensed chromatin and gene expression in macronuclei of Tetrahymena thermophila. Mol. Cell Biol. *19*, 3624-3634.

Huang,H., Smothers,J.F., Wiley,E.A., and Allis,C.D. (1999a). A nonessential HP1-like protein affects starvation-induced assembly of condensed chromatin and gene expression in macronuclei of Tetrahymena thermophila. Mol. Cell Biol. *19*, 3624-3634.

Hwang,K.K., Eissenberg,J.C., and Worman,H.J. (2001). Transcriptional repression of euchromatic genes by Drosophila heterochromatin protein 1 and histone modifiers. Proc. Natl. Acad. Sci. U. S. A *98*, 11423-11427.

Ivanova,A.V., Bonaduce,M.J., Ivanov,S.V., and Klar,A.J. (1998). The chromo and SET domains of the Clr4 protein are essential for silencing in fission yeast. Nat. Genet. *19*, 192-195.

James,T.C., Eissenberg,J.C., Craig,C., Dietrich,V., Hobson,A., and Elgin,S.C. (1989). Distribution patterns of HP1, a heterochromatin-associated nonhistone chromosomal protein of Drosophila. Eur. J. Cell Biol. *50*, 170-180.

James,T.C. and Elgin,S.C. (1986). Identification of a nonhistone chromosomal protein associated with heterochromatin in Drosophila melanogaster and its gene. Mol. Cell Biol. *6*, 3862-3872.

Jenuwein,T., Laible,G., Dorn,R., and Reuter,G. (1998). SET domain proteins modulate chromatin domains in eu- and heterochromatin. Cell Mol. Life Sci. *54*, 80-93.

Jones,R.S. and Gelbart,W.M. (1993). The Drosophila Polycomb-group gene Enhancer of zeste contains a region with sequence similarity to trithorax. Mol. Cell Biol. *13*, 6357-6366.

Judd,B.H. (1995). Mutations of zeste that mediate transvection are recessive enhancers of position-effect variegation in Drosophila melanogaster. Genetics *141*, 245-253.

Karpen,G.H. (1994). Position-effect variegation and the new biology of heterochromatin. Curr. Opin. Genet. Dev. *4*, 281-291.

Karpen,G.H. and Allshire,R.C. (1997). The case for epigenetic effects on centromere identity and function. Trends Genet. *13*, 489-496.

Kaszas,E. and Birchler,J.A. (1998). Meiotic transmission rates correlate with physical features of rearranged centromeres in maize. Genetics *150*, 1683-1692.

Kellum,R. and Alberts,B.M. (1995). Heterochromatin protein 1 is required for correct chromosome segregation in Drosophila embryos. J. Cell Sci. *108 (Pt 4)*, 1419-1431.

Kellum,R., Raff,J.W., and Alberts,B.M. (1995). Heterochromatin protein 1 distribution during development and during the cell cycle in Drosophila embryos. J. Cell Sci. *108 (Pt 4)*, 1407-1418.

Kellum,R. and Schedl,P. (1991). A position-effect assay for boundaries of higher order chromosomal domains. Cell *64*, 941-950.

Kirschmann,D.A., Lininger,R.A., Gardner,L.M., Seftor,E.A., Odero,V.A., Ainsztein,A.M., Earnshaw,W.C., Wallrath,L.L., and Hendrix,M.J. (2000). Down-regulation of HP1Hsalpha expression is associated with the metastatic phenotype in breast cancer. Cancer Res. *60*, 3359-3363.

Koonin,E.V., Zhou,S., and Lucchesi,J.C. (1995). The chromo superfamily: new members, duplication of the chromo domain and possible role in delivering transcription regulators to chromatin. Nucleic Acids Res. *23*, 4229-4233.

Kornberg,R.D. (1977). Structure of chromatin. Annu. Rev. Biochem. *46*, 931-954.

Krieg,P.A. and Melton,D.A. (1987). An enhancer responsible for activating transcription at the midblastula transition in Xenopus development. Proc. Natl. Acad. Sci. U. S. A *84*, 2331-2335.

Lachner,M., O'Carroll,D., Rea,S., Mechtler,K., and Jenuwein,T. (2001). Methylation of histone H3 lysine 9 creates a binding site for HP1 proteins. Nature *410*, 116-120.

Larsson,J., Zhang,J., and Rasmuson-Lestander,A. (1996). Mutations in the Drosophila melanogaster gene encoding S- adenosylmethionine synthetase [corrected] suppress position-effect variegation. Genetics *143*, 887-896.

Latinkic,B.V. and Smith,J.C. (1999). Goosecoid and mix.1 repress Brachyury expression and are required for head formation in Xenopus. Development *126*, 1769-1779.

Laurent,A.M., Puechberty,J., Prades,C., Gimenez,S., and Roizes,G. (1997). Site-specific retrotransposition of L1 elements within human alphoid satellite sequences. Genomics *46*, 127-132.

Le Douarin,B., Nielsen,A.L., Garnier,J.M., Ichinose,H., Jeanmougin,F., Losson,R., and Chambon,P. (1996). A possible involvement of TIF1 alpha and TIF1 beta in the epigenetic control of transcription by nuclear receptors. EMBO J. *15*, 6701-6715.

Lechner,M.S., Begg,G.E., Speicher,D.W., and Rauscher,F.J., III (2000). Molecular determinants for targeting heterochromatin protein 1-mediated gene silencing: direct chromoshadow domain-KAP-1 corepressor interaction is essential. Mol. Cell Biol. *20*, 6449-6465.

Locke,J., Kotarski,M.A., and Tartof,K.D. (1988). Dosage-dependent modifiers of position effect variegation in Drosophila and a mass action model that explains their effect. Genetics *120*, 181-198.

Lohe,A.R., Hilliker,A.J., and Roberts,P.A. (1993). Mapping simple repeated DNA sequences in heterochromatin of Drosophila melanogaster. Genetics *134*, 1149-1174.

Lorentz,A., Ostermann,K., Fleck,O., and Schmidt,H. (1994). Switching gene swi6, involved in repression of silent mating-type loci in fission yeast, encodes a homologue of chromatin-associated proteins from Drosophila and mammals. Gene *143*, 139-143.

Lu,B.Y., Ma,J., and Eissenberg,J.C. (1998). Developmental regulation of heterochromatin-mediated gene silencing in Drosophila. Development *125*, 2223-2234.

Luger,K., Mader,A.W., Richmond,R.K., Sargent,D.F., and Richmond,T.J. (1997a). Crystal structure of the nucleosome core particle at 2.8 A resolution. Nature *389*, 251-260.

Luger,K., Mader,A.W., Richmond,R.K., Sargent,D.F., and Richmond,T.J. (1997b). Crystal structure of the nucleosome core particle at 2.8 A resolution. Nature *389*, 251-260.

Luger,K. and Richmond,T.J. (1998). The histone tails of the nucleosome. Curr. Opin. Genet. Dev. *8*, 140-146.

Margolin,J.F., Friedman,J.R., Meyer,W.K., Vissing,H., Thiesen,H.J., and Rauscher,F.J., III (1994). Kruppel-associated boxes are potent transcriptional repression domains. Proc. Natl. Acad. Sci. U. S. A *91* , 4509-4513.

Matzke,M.A. and Matzke,A.J. (1998). Epigenetic silencing of plant transgenes as a consequence of diverse cellular defence responses. Cell Mol. Life Sci. *54*, 94-103.

McCarroll,R.M. and Fangman,W.L. (1988). Time of replication of yeast centromeres and telomeres. Cell *54*, 505-513.

McGhee,J.D. and Felsenfeld,G. (1980). Nucleosome structure. Annu. Rev. Biochem. *49*, 1115-1156.

Messmer,S., Franke,A., and Paro,R. (1992). Analysis of the functional role of the Polycomb chromo domain in Drosophila melanogaster. Genes Dev. *6*, 1241-1254.

Migeon,B.R. (1994). X-chromosome inactivation: molecular mechanisms and genetic consequences. Trends Genet. *10*, 230-235.

Milot,E., Strouboulis,J., Trimborn,T., Wijgerde,M., de Boer,E., Langeveld,A., Tan-Un,K., Vergeer,W., Yannoutsos,N., Grosveld,F., and Fraser,P. (1996). Heterochromatin effects on the frequency and duration of LCR-mediated gene transcription. Cell *87*, 105-114.

Minc,E., Allory,Y., Worman,H.J., Courvalin,J.C., and Buendia,B. (1999). Localization and phosphorylation of HP1 proteins during the cell cycle in mammalian cells. Chromosoma *108*, 220-234.

Minc,E., Courvalin,J.C., and Buendia,B. (2000). HP1gamma associates with euchromatin and heterochromatin in mammalian nuclei and chromosomes. Cytogenet. Cell Genet. *90*, 279-284.

Moehrle,A. and Paro,R. (1994). Spreading the silence: epigenetic transcriptional regulation during Drosophila development. Dev. Genet. *15*, 478-484.

Moore,S.C. and Ausio,J. (1997). Major role of the histones H3-H4 in the folding of the chromatin fiber. Biochem. Biophys. Res. Commun. *230*, 136-139.

Muller HJ (1930) Types of visible variations induced by X-rays in *Drosophila*

Murzina,N., Verreault,A., Laue,E., and Stillman,B. (1999). Heterochromatin dynamics in mouse cells: interaction between chromatin assembly factor 1 and HP1 proteins. Mol. Cell *4*, 529-540.

Newport,J. and Kirschner,M. (1982). A major developmental transition in early Xenopus embryos: II. Control of the onset of transcription. Cell *30*, 687-696.

Nielsen,A.L., Ortiz,J.A., You,J., Oulad-Abdelghani,M., Khechumian,R., Gansmuller,A., Chambon,P., and Losson,R. (1999). Interaction with members of the heterochromatin protein 1 (HP1) family and histone deacetylation are differentially involved in transcriptional silencing by members of the TIF1 family. EMBO J. *18*, 6385-6395.

Nielsen,A.L., Oulad-Abdelghani,M., Ortiz,J.A., Remboutsika,E., Chambon,P., and Losson,R. (2001a). Heterochromatin formation in mammalian cells: interaction between histones and HP1 proteins. Mol. Cell *7*, 729-739.

Nielsen,S.J., Schneider,R., Bauer,U.M., Bannister,A.J., Morrison,A., O'Carroll,D., Firestein,R., Cleary,M., Jenuwein,T., Herrera,R.E., and Kouzarides,T. (2001b). Rb targets histone H3 methylation and HP1 to promoters. Nature *412*, 561-565.

Pak,D.T., Pflumm,M., Chesnokov,I., Huang,D.W., Kellum,R., Marr,J., Romanowski,P., and Botchan,M.R. (1997). Association of the origin recognition complex with heterochromatin and HP1 in higher eukaryotes. Cell *91*, 311-323.

Paranjape,S.M., Kamakaka,R.T., and Kadonaga,J.T. (1994). Role of chromatin structure in the regulation of transcription by RNA polymerase II. Annu. Rev. Biochem. *63*, 265-297.

Paro,R. and Hogness,D.S. (1991). The Polycomb protein shares a homologous domain with a heterochromatin- associated protein of Drosophila. Proc. Natl. Acad. Sci. U. S. A *88*, 263-267.

Partridge,J.F., Borgstrom,B., and Allshire,R.C. (2000). Distinct protein interaction domains and protein spreading in a complex centromere. Genes Dev. *14*, 783-791.

Platero,J.S., Hartnett,T., and Eissenberg,J.C. (1995). Functional analysis of the chromo domain of HP1. EMBO J. *14*, 3977-3986.

Platero,J.S., Sharp,E.J., Adler,P.N., and Eissenberg,J.C. (1996). In vivo assay for protein-protein interactions using Drosophila chromosomes. Chromosoma *104*, 393-404.

Polach,K.J. and Widom,J. (1996). A model for the cooperative binding of eukaryotic regulatory proteins to nucleosomal target sites. J. Mol. Biol. *258*, 800-812.

Powers,J.A. and Eissenberg,J.C. (1993). Overlapping domains of the heterochromatin-associated protein HP1 mediate nuclear localization and heterochromatin binding. J. Cell Biol. *120*, 291-299.

Pyrpasopoulou,A., Meier,J., Maison,C., Simos,G., and Georgatos,S.D. (1996). The lamin B receptor (LBR) provides essential chromatin docking sites at the nuclear envelope. EMBO J. *15*, 7108-7119.

Rastelli,L., Chan,C.S., and Pirrotta,V. (1993). Related chromosome binding sites for zeste, suppressors of zeste and Polycomb group proteins in Drosophila and their dependence on Enhancer of zeste function. EMBO J. *12*, 1513-1522.

Rea,S., Eisenhaber,F., O'Carroll,D., Strahl,B.D., Sun,Z.W., Schmid,M., Opravil,S., Mechtler,K., Ponting,C.P., Allis,C.D., and Jenuwein,T. (2000). Regulation of chromatin structure by site-specific histone H3 methyltransferases. Nature *406*, 593-599.

Reijnen,M.J., Hamer,K.M., den Blaauwen,J.L., Lambrechts,C., Schoneveld,I., van Driel,R., and Otte,A.P. (1995). Polycomb and bmi-1 homologs are expressed in overlapping patterns in Xenopus embryos and are able to interact with each other. Mech. Dev. *53*, 35-46.

Reuter,G., Dorn,R., and Hoffmann,H.J. (1982a). Butyrate sensitive suppressor of position-effect variegation mutations in Drosophila melanogaster. Mol. Gen. Genet. *188*, 480-485.

Reuter,G. and Spierer,P. (1992). Position effect variegation and chromatin proteins. Bioessays *14*, 605-612.

Reuter,G., Werner,W., and Hoffmann,H.J. (1982b). Mutants affecting position-effect heterochromatinization in Drosophila melanogaster. Chromosoma *85*, 539-551.

Reuter,G. and Wolff,I. (1981). Isolation of dominant suppressor mutations for position-effect variegation in Drosophila melanogaster. Mol. Gen. Genet. *182*, 516-519.

Round,E.K., Flowers,S.K., and Richards,E.J. (1997). Arabidopsis thaliana centromere regions: genetic map positions and repetitive DNA structure. Genome Res. *7*, 1045-1053.

Ryan,R.F., Schultz,D.C., Ayyanathan,K., Singh,P.B., Friedman,J.R., Fredericks,W.J., and Rauscher,F.J., III (1999a). KAP-1 corepressor protein interacts and colocalizes with heterochromatic and euchromatic HP1 proteins: a potential role for Kruppel-associated box-zinc finger proteins in heterochromatin-mediated gene silencing. Mol. Cell Biol. *19*, 4366-4378.

Ryan,R.F., Schultz,D.C., Ayyanathan,K., Singh,P.B., Friedman,J.R., Fredericks,W.J., and Rauscher,F.J., III (1999b). KAP-1 corepressor protein interacts and colocalizes with heterochromatic and euchromatic HP1 proteins: a potential role for Kruppel-associated box-zinc finger proteins in heterochromatin-mediated gene silencing. Mol. Cell Biol. *19*, 4366-4378.

Sabl,J.F. and Henikoff,S. (1996). Copy number and orientation determine the susceptibility of a gene to silencing by nearby heterochromatin in Drosophila. Genetics *142*, 447-458.

Sankaranarayanan,K. (1979). The role of non-disjunction in aneuploidy in man. An overview. Mutat. Res. *61*, 1-28.

Saunders,W.S., Chue,C., Goebl,M., Craig,C., Clark,R.F., Powers,J.A., Eissenberg,J.C., Elgin,S.C., Rothfield,N.F., and Earnshaw,W.C. (1993). Molecular cloning of a human homologue of Drosophila heterochromatin protein HP1 using

anti-centromere autoantibodies with anti-chromo specificity. J. Cell Sci. *104 (Pt 2)*, 573-582.

Schild,C., Claret,F.X., Wahli,W., and Wolffe,A.P. (1993). A nucleosome-dependent static loop potentiates estrogen-regulated transcription from the Xenopus vitellogenin B1 promoter in vitro. EMBO J. *12*, 423-433.

Schwarz,P.M. and Hansen,J.C. (1994). Formation and stability of higher order chromatin structures. Contributions of the histone octamer. J. Biol. Chem. *269*, 16284-16289.

Seeler,J.S., Marchio,A., Sitterlin,D., Transy,C., and Dejean,A. (1998). Interaction of SP100 with HP1 proteins: a link between the promyelocytic leukemia-associated nuclear bodies and the chromatin compartment. Proc. Natl. Acad. Sci. U. S. A *95*, 7316-7321.

Seum,C., Spierer,A., Pauli,D., Szidonya,J., Reuter,G., and Spierer,P. (1996). Position-effect variegation in Drosophila depends on dose of the gene encoding the E2F transcriptional activator and cell cycle regulator. Development *122*, 1949-1956.

Sinclair,D.A., Lloyd,V.K., and Grigliatti,T.A. (1989). Characterization of mutations that enhance position-effect variegation in Drosophila melanogaster. Mol. Gen. Genet. *216*, 328-333.

Singh,P.B., Miller,J.R., Pearce,J., Kothary,R., Burton,R.D., Paro,R., James,T.C., and Gaunt,S.J. (1991). A sequence motif found in a Drosophila heterochromatin protein is conserved in animals and plants. Nucleic Acids Res. *19*, 789-794.

Smothers,J.F. and Henikoff,S. (2000). The HP1 chromo shadow domain binds a consensus peptide pentamer. Curr. Biol. *10*, 27-30.

Smothers,J.F. and Henikoff,S. (2001). The hinge and chromo shadow domain impart distinct targeting of HP1- like proteins. Mol. Cell Biol. *21*, 2555-2569.

Spradling,A.C. and Karpen,G.H. (1990). Sixty years of mystery. Genetics *126*, 779-784.

Stassen,M.J., Bailey,D., Nelson,S., Chinwalla,V., and Harte,P.J. (1995). The Drosophila trithorax proteins contain a novel variant of the nuclear receptor type DNA binding domain and an ancient conserved motif found in other chromosomal proteins. Mech. Dev. *52*, 209-223.

Steinbeisser,H., Fainsod,A., Niehrs,C., Sasai,Y., and De Robertis,E.M. (1995). The role of gsc and BMP-4 in dorsal-ventral patterning of the marginal zone in Xenopus: a loss-of-function study using antisense RNA. EMBO J. *14*, 5230-5243.

Steiner,N.C. and Clarke,L. (1994). A novel epigenetic effect can alter centromere function in fission yeast. Cell *79*, 865-874.

Stokes,D.G., Tartof,K.D., and Perry,R.P. (1996). CHD1 is concentrated in interbands and puffed regions of Drosophila polytene chromosomes. Proc. Natl. Acad. Sci. U. S. A *93*, 7137-7142.

Sugimoto,K., Yamada,T., Muro,Y., and Himeno,M. (1996). Human homolog of Drosophila heterochromatin-associated protein 1 (HP1) is a DNA-binding protein which possesses a DNA-binding motif with weak similarity to that of human centromere protein C (CENP-C). J. Biochem. (Tokyo) *120*, 153-159.

Sullivan,K.F., Hechenberger,M., and Masri,K. (1994). Human CENP-A contains a histone H3 related histone fold domain that is required for targeting to the centromere. J. Cell Biol. *127*, 581-592.

Sun,X., Wahlstrom,J., and Karpen,G. (1997). Molecular structure of a functional Drosophila centromere. Cell *91*, 1007-1019.

Talbert,P.B., LeCiel,C.D., and Henikoff,S. (1994). Modification of the Drosophila heterochromatic mutation brownDominant by linkage alterations. Genetics *136*, 559-571.

Thoma,F. and Koller,T. (1977). Influence of histone H1 on chromatin structure. Cell *12*, 101-107.

Thoma,F., Koller,T., and Klug,A. (1979). Involvement of histone H1 in the organization of the nucleosome and of the salt-dependent superstructures of chromatin. J. Cell Biol. *83*, 403-427.

Truss,M., Bartsch,J., Schelbert,A., Hache,R.J., and Beato,M. (1995). Hormone induces binding of receptors and transcription factors to a rearranged nucleosome on the MMTV promoter in vivo. EMBO J. *14*, 1737-1751.

Tschiersch,B., Hofmann,A., Krauss,V., Dorn,R., Korge,G., and Reuter,G. (1994). The protein encoded by the Drosophila position-effect variegation suppressor gene Su(var)3-9 combines domains of antagonistic regulators of homeotic gene complexes.

Tse,C. and Hansen,J.C. (1997). Hybrid trypsinized nucleosomal arrays: identification of multiple functional roles of the H2A/H2B and H3/H4 N-termini in chromatin fiber compaction. Biochemistry *36*, 11381-11388.

Tyler-Smith,C., Gimelli,G., Giglio,S., Floridia,G., Pandya,A., Terzoli,G., Warburton,P.E., Earnshaw,W.C., and Zuffardi,O. (1999). Transmission of a fully functional human neocentromere through three generations. Am. J. Hum. Genet. *64*, 1440-1444.

van Steensel,B. and Henikoff,S. (2000). Identification of in vivo DNA targets of chromatin proteins using tethered dam methyltransferase. Nat. Biotechnol. *18*, 424-428.

Vlassova,I.E., Graphodatsky,A.S., Belyaeva,E.S., and Zhimulev,I.F. (1991). Constitutive heterochromatin in early embryogenesis of Drosophila melanogaster. Mol. Gen. Genet. *229*, 316-318.

Wade,P.A., Jones,P.L., Vermaak,D., and Wolffe,A.P. (1998). A multiple subunit Mi-2 histone deacetylase from Xenopus laevis cofractionates with an associated Snf2 superfamily ATPase. Curr. Biol. *8*, 843-846.

Wakimoto,B.T. (1998). Beyond the nucleosome: epigenetic aspects of position-effect variegation in Drosophila. Cell *93*, 321-324.

Wakimoto,B.T. and Hearn,M.G. (1990). The effects of chromosome rearrangements on the expression of heterochromatic genes in chromosome 2L of Drosophila melanogaster. Genetics *125*, 141-154.

Wallrath,L.L. (1998). Unfolding the mysteries of heterochromatin. Curr. Opin. Genet. Dev. *8*, 147-153.

Wallrath,L.L. and Elgin,S.C. (1995). Position effect variegation in Drosophila is associated with an altered chromatin structure. Genes Dev. *9*, 1263-1277.

Wallrath,L.L., Lu,Q., Granok,H., and Elgin,S.C. (1994). Architectural variations of inducible eukaryotic promoters: preset and remodeling chromatin structures. Bioessays *16*, 165-170.

Wang,G., Ma,A., Chow,C.M., Horsley,D., Brown,N.R., Cowell,I.G., and Singh,P.B. (2000). Conservation of heterochromatin protein 1 function. Mol. Cell Biol. *20*, 6970-6983.

Wasylyk,B. and Chambon,P. (1979). Transcription by eukaryotic RNA polymerases A and B of chromatin assembled in vitro. Eur. J. Biochem. *98*, 317-327.

Weiler,K.S. and Wakimoto,B.T. (1995). Heterochromatin and gene expression in Drosophila. Annu. Rev. Genet. *29*, 577-605.

Willard,H.F. (1998). Centromeres: the missing link in the development of human artificial chromosomes. Curr. Opin. Genet. Dev. *8*, 219-225.

Wines,D.R. and Henikoff,S. (1992). Somatic instability of a Drosophila chromosome. Genetics *131*, 683-691.

Wolffe,A.P. and Hayes,J.J. (1999). Chromatin disruption and modification. Nucleic Acids Res. *27*, 711-720.

Woodage,T., Basrai,M.A., Baxevanis,A.D., Hieter,P., and Collins,F.S. (1997). Characterization of the CHD family of proteins. Proc. Natl. Acad. Sci. U. S. A *94*, 11472-11477.

Wreggett,K.A., Hill,F., James,P.S., Hutchings,A., Butcher,G.W., and Singh,P.B. (1994). A mammalian homologue of Drosophila heterochromatin protein 1 (HP1) is a component of constitutive heterochromatin. Cytogenet. Cell Genet. *66*, 99-103.

Wustmann,G., Szidonya,J., Taubert,H., and Reuter,G. (1989). The genetics of position-effect variegation modifying loci in Drosophila melanogaster. Mol. Gen. Genet. *217*, 520-527.

Yamada,T., Fukuda,R., Himeno,M., and Sugimoto,K. (1999). Functional domain structure of human heterochromatin protein HP1(Hsalpha): involvement of internal DNA-binding and C-terminal self- association domains in the formation of discrete dots in interphase nuclei. J. Biochem. (Tokyo) *125*, 832-837.

Yamaguchi,K., Hidema,S., and Mizuno,S. (1998). Chicken chromobox proteins: cDNA cloning of CHCB1, -2, -3 and their relation to W-heterochromatin. Exp. Cell Res. *242*, 303-314.

Ye,Q., Callebaut,I., Pezhman,A., Courvalin,J.C., and Worman,H.J. (1997). Domain-specific interactions of human HP1-type chromodomain proteins and inner nuclear membrane protein LBR. J. Biol. Chem. *272*, 14983-14989.

Ye,Q. and Worman,H.J. (1996). Interaction between an integral protein of the nuclear envelope inner membrane and human chromodomain proteins homologous to Drosophila HP1. J. Biol. Chem. *271*, 14653-14656.

Zhao,T. and Eissenberg,J.C. (1999). Phosphorylation of heterochromatin protein 1 by casein kinase II is required for efficient heterochromatin binding in Drosophila. J. Biol. Chem. *274*, 15095-15100.

Zhao,T., Heyduk,T., Allis,C.D., and Eissenberg,J.C. (2000). Heterochromatin protein 1 binds to nucleosomes and DNA in vitro. J. Biol. Chem. *275*, 28332-28338.

Zink,B. and Paro,R. (1989). In vivo binding pattern of a trans-regulator of homoeotic genes in Drosophila melanogaster. Nature *337*, 468-471.

References (Book)

1. van Holde, K.E., 1998 Chromatin (Springer, New York).

2. Wolffe, A.P., 1995 Chromatin Structure and Function (Academic, London), 2nd Ed.

3. Hansen, J.C., 1997 Chemtracts: Biochem. Mol. Biol. 11, 56-69

4. Wasten, JD, Gilman, M., Wilkowski,J. and Zoller, M 1992 Recombinant DNA 2nd e.d.

5. Wolpert, L., Beddington, R., Brockes, J., Jessell, T., Lawrence P., and Meyerowitz, E. 1998 Principle of Development